V. P. Begishev
A. Ya. Malkin

Reactive Processing of Polymers

ChemTec Publishing

ISBN 1-895198-20-8

Printed in Canada

ChemTec Publishing
38 Earswick Drive
Toronto-Scarborough
Ontario M1E 1C6
Canada

Canadian Cataloguing in Publication Data

Begishev V. P.
Reactive processing of polymers

Includes bibliographical references and index.
ISBN 1-895198-20-8

1. Plastics--Molding. I. Malkin, Alexander Yakovlevich
II. Title

TP1150.B44 1999 668.4'12 C99-900308-9

PREFACE

Modern technologies of large-scale production processes are based on the strategy of a multistage approach to the final product. This is the historical course of development of the metallurgical industry: first, iron-ore is transformed into cast iron, then the latter is converted into steel of different types; this steel is then rolled and the final article only at the last stage by machining the rolled profiles. The same general approach is used in the building materials and construction industries. This is also true for polymeric materials. A monomer is first converted into a polymer; then raw material in the form of granules or powder is prepared by compounding of the polymer with various additives. Only after that is the polymeric material processed into a final article by extrusion, injection molding or other processing methods. The heart of this multistage process consists primarily in the separation in place and time of consecutive processing steps in passing from ore to the final article.

This approach has a great advantage of flexibility. It eliminates the necessity for rigid connection and correspondence between the various units for producing raw materials and final products, and allows for the storage of intermediate products and easy variation of the type of final articles, depending on changing demand. However, this strategy also has some obvious disadvantages. It requires repeated cooling-heating operations at different stages of the overall process and this increases energy consumption. Also, a complete cycle of the whole process - from a raw materials to an end product - is long and may require transportation and storage of intermediate products.

This is why the idea of decreasing the number of process stages has been proposed with the goal of excluding some intermediate operations and obtaining a final product directly from the raw material. The advantages of this approach are obvious: a decrease in net energy consumption, a shortened production cycle, exclusion of transportation between separate stages of a process, and reduction in wastes. The latter is especially important for ecological reasons. All this is a direct consequence of fewer processing operations. In addition, direct processing of raw materials into articles allows us to produce very large items, which are impossible or at least very difficult and expensive to make by traditional methods. This is especially true for articles of complicated configuration; application of a traditional technology is usually accompanied by a generation of large amounts of wastes.

Energy consumption and ecological and economic factors determine an expediency and sometimes a technical necessity to decrease the number of process operations and to change to processes in which several stages, previously quite separate, are combined or superimposed in a single process. At present this approach is only a tendency which does not exclude the traditional course of industrial development. Nevertheless, the tendency is seen quite clearly in the increasing volume of products produced by such integrated production process and in the share of total production from these processes.

This general tendency is also observed in the polymer industry . In this case it is realized in the form of reactive (or chemical) processing. Its essence consists in carrying out chemical reacting, resulted in synthesis of the final molecular structure of a material, simultaneously with processing of

this material, thus forming and shaping the final article in a mold. Of course, filling a mold can be combined with additional operations, such as inserting fillers or other functional components into a composition.

The current stage of development of reactive processing can be traced back to the technology of processing thermosetting oligomeric resins, which appeared in the early years of a polymer industry, about a century ago. In both cases, shaping of an article occurs simultaneously with formation of a chemical (polymeric) molecular structure of the final material. Reactive technology can be treated as a modern step (or a new stage) in a development of processing of reactive monomers and thermosetting oligomers. Meanwhile, reactive (chemical) processing, or reactive molding, is characterized by some special features. None of them is unique or obligatory, and all could be met in other situations, but their sum creates the distinctive features of modern reactive processing of monomers and/or oligomers, which allow us to treat it as a new technological approach to polymer processing.

These features are as follows:

- *low viscosity of initial raw materials*; this permits the use of low or moderate injection pressures to fill molds of large sizes and complex configuration quickly and completely; the weight and size of an article are practically unlimited in contrast to traditional processes;
- *high reaction rates*, leading to synthesis of high-molecular-weight polymeric products; this allows us to shorten the process cycle from tens of minutes down to several seconds and to achieve a reaction in mild processing conditions (i.e., low temperatures and pressures);
- *absence of by-products in polymer synthesis*; this makes the production process simpler, improves the quality of a product, and favors environmental protection;
- *regularity of chemical structure of the final polymeric product;* reactive processing very often leads to synthesis of a thermoplastic material composed of linear macromolecular chains; these may crystallize to yield materials belonging to the class of engineering plastics with high breaking stresses and impact strength;
- *easy possibility for varying the properties of the final product;* this is realized by simple changes in the composition of the reactive materials used (by varying the chemical nature of the monomers and oligomers, adding comonomers and modifiers and so on) and/or by introducing different functional additives into the reactive charge during processing.

However, it is obvious that the evident advantages of the reactive processing method - low energy consumption, high processing rates, mild processing parameters - can be realized only if some principal technical and plant peculiarities of the process are taken into account. Some special problems appear in large-scale industrial applications of the reactive processing method. The most evident problems, which must be solved during laboratory development stage, are:

- *choice of reagents* (monomers, oligomers, content of a reactive mass), to give a final product with the necessary performance characteristics and to provide a technological process with the required rate and without by-products;
- *solving a complex of kinetic, rheological, hydrodynamic, thermal and mechanical problems*, modelling the main stages of the process, such as filling the mold, polymer synthesis, cooling of an article in the mold and so on.

- *choice of process equipment*, to provide the required production rate for satisfactory results.

This book attempts to answer some of the questions listed above. The method of choice in the search for answers is modelling the principal stages of the technological process on the basis of laboratory investigations of the fundamental chemical and physical phenomena leading to formation of the final product (article).

Finally, it is our pleasure to acknowledge Dr. Yu. B. Lavochnik for his technical assistance in preparing the manuscript; he also took part in gathering published papers and in discussing the material related to Sections 4.5 and 4.9 of the book.

At last it is our special pleasure to express our gratitude to Mrs. K. Olson who courted out on uneasy job of English editing the manuscript and made the text much more English-like than it was written by the authors.

A. Ya. Malkin
B. P. Beghishev
December, 1998

Table of Contents

1

THE METHOD OF REACTIVE PROCESSING

1.1 INTRODUCTION

Reactive processing of polymers is based on the use of low-melting-point solid or liquid raw materials or premixes to form articles of the required by the usual polymerization process shape simultaneous transformation into linear, branched or network polymers and/or solidification at moderate temperatures (as a rule, up to 200°C) and pressure.

The general principles of the method for processing thermosetting resins were proposed and developed in the beginning of the 20th century for phenol-formaldehyde, carbamide, glyptal and other oligomeric products. These compounds transform into polymers by a polycondensation mechanism with removal of low-molecular-weight, volatile products appearing during synthesis. Subsequent efforts were devoted to finding other polymerization reactions using different initial substances, especially those that occur without the formation of by-products. The other problems which had to be solved were: increasing article size, reduction of shrinkage, and removal of residual stresses.

Oligomeric products of the class of thermosetting compounds, such as unsaturated polyester resins, epoxy oligomers, allyl monomers, urethane-forming oligomers, oligo(ester acrylates) etc., are widely used in this technology. The articles made of thermoplastics - polyamides, acrylate resins, polyurethanes, and some copolymers - are also produced by the reactive processing method. Using a wide variety of initial reactants allows us to produce high-quality goods by different processes. Thus, along with batch polymerization in stationary molds, centrifugal and rotational processes in tubular reactors, shear continuous reactors,and front-spreading operating conditions are used.

During the first half of the 1970s, processing of liquid reactants into various articles by injection molding – the so-called RIM-process (reaction injection molding) – was implemented. This process allows the production of goods of different sizes and complicated configurations at low energy consumption (because of the low viscosity of the initial liquid reactants) and the low weight of the metallic equipment.

The choice of monomers, oligomers or their mixtures, catalysts and initiators, and other components of a product depends on a number of factors:

(i) The properties and required use of the product

(ii) The process technology and its features

(iii) The safety of the process

(iv) The economics of the process

A great number of works dedicated to polymerization processes and oligomer curing have been published. In this book, we will pay attention only to the main characteristics of reactive processing technology in the absence of by-products.

1.2 LACTAM POLYMERIZATION

An example of reactive processing is acid-ion activated lactam polymerization catalyzed by basic reagents. Thermoplastic engineering polymers are produced as a result of this reaction, and these materials are widely used in many technologies. Polymers, copolymers, and reinforced compositions based on ε-caprolactam $[-HN(CH_2)_5CO-]_n$ and ω-dodecalactam $[-HN(CH_2)_{11}CO-]_n$ have many applications. One of the peculiarities of acid-ion lactam polymerization is that there is no chain termination stage. If the inhibiting effect of admixtures and other factors causing termination are excluded, it is possible to obtain polymeric products with sufficiently high degrees of polymerization.

A large number of compounds used as catalysts in acid-ion lactam polymerization are known. These include alkalis, alkali-earth metals, hydrates, Grignard reagents, lithium oxide, various hydroxides and carbonates, sulfates, halides, sodium zincate, alkaline salts of different acids, i.e., compounds that cause the formation of lactam acid ion in the reactive medium. The mechanism of polymerization in the presence of sodium-lactam– salt compounds is largely known.

During a study of the ε-caprolactam polymerization mechanism in isothermal conditions,[1,2] it was found that there was a distinct induction period at the beginning of the process when sodium caprolactam salt was used as a catalyst. The addition of the necessary quantity of an activator into the reactive mixture leads to a reduction of the induction period and thus allows us to regulate the process rate.

A large number of inorganic compounds can be used as the activators of acid-ion (anionic) activated lactam polymerization . The activator in anionic activated lactam polymerization not only increases the process rate, but also changes the structure and functionality of a polymer formed, and, as a result an activator can regulate the properties of the end-product.[1]

In the presence of an activator, for example, an alkyl-amide, polymerization begins with a high reaction rate between molecules of the activator and the catalyst.

Except for lactam n-acyl derivatives, compounds such as esters, anhydrides and halogen anhydrides of carboxylic acids, which can activate lactam polymerization, can also be used as activators (promoters).

Polycaproamide (PA-6), which is synthesized from ε-caprolactam in the presence of catalysts such as sodium-ε-caprolactam or magnesium bromide-caprolactam (obtained by the reaction of

Grignard reagent with caprolactam) is widely used in technological practice. Compounds of the carbamoyl caprolactam class, for example, 2,4-toluylene bis(carbamoyl) caprolactam and acetyl caprolactam, are used as activators.

New reactive systems for synthesizing polyamides, with high impact strength and low molding shrinkage have recently been investigated. The latter attribute appeared to be very important, as it allowed the development of reactive molding processes for such compositions. This approach was implemented by the application of polymer activators containing isocyanate, acyllactam, chloranhydride, and other groups. For this purpose, block copolymers of A-B-A structure were synthesized. In this case, the two outer blocks A are polyamides and the inner block B is another polymer.[2] Polyethers and polyesters, liquid rubbers, polystyrene, epoxy resins, polysiloxane, and other polyamides may be used to form the central block. By changing the polymer composition and the ratio of macromolecular activator and lactam, the properties of the block copolymers may be varied.

The examples of two recipes used for the RIM-technology are listed below:[3] the A and B compositions are mixed during processing in the ratio 1:1.

Composition A	Composition B
Caprolactam 60%	Caprolactam 99%
Polypropylene acyl 40%	MgBr-lactam 1%
Caprolactam 60%	Caprolactam 99%
Macro(diisocyanate) based on 2,4-toluylene isocyanate 40%	Na-lactam 1%

A peculiarity of the anionic activated polymerization process for ε-caprolactam is that it proceeds at temperatures below the polymer melting point. This leads to superposition of the polymerization process and crystallization of the newly synthesized polymer.

Products of acid-ion activated polymerization of ω-dodecalactam (PA-12) are characterized by a higher chemical resistance, improved low-temperature toughness, and low water absorption. Caprolactam and dodecalactam copolymers are very important for various technical applications. Polymers produced by the anionic activated process using other lactams have no practical application as yet.

Articles made from polyamides synthesized by the reactive processing method are widely used as engineering materials in the automotive industry, ship-building, electrical engineering, the light and chemical industries, and other applications.

Properties of typical grades of PA-6 produced by the anionic activated polymerization (AAPL) method in the form of blocks, slabs, rods, pipes, and plates are shown in Table 1.1.

In comparison with other thermoplastics, polyamides have superior mechanical properties, vibration and chemical resistance, and high dielectric properties. The superior antifrictional characteristics of cast PA-6 allow us to use it for bearings instead of bronze, cast iron, steel, babbit, reinforced phenolic compounds, and other materials.

Table 1.1. Properties of some unfilled plastics produced by free casting compared with PA-6

	PA-6	PMMA	Epoxy*	Epoxy**	U-PEST***	OEA****
σ_b, MPa	90-96	60-80	40-60	50-80	5-60	30-50
τ_b, MPa	80-100	100-130	100-150	120-130	25-100	70-90
ε, %	6-20	2-4	1.6-2.0	4-7	2-400	-
E, GPa	2.0-2.3	2.4-3.5	-	-	-	-
A, kJ/m^2	5-10	7-20	10-20	15-20	2-10	7-20
T_g, °C	40-50	115-120	-	115-120	-	-
T_m, °C	220-225	-	-	-	-	-
ρ, g/cm^3	1.15-1.16	1.18-1.20	1.0-1.1	1.1-1.2	1.1-1.4	1.2-1.3
Σ, MV/m	20-23	30-45	20-25	-	14-23	20-40
$\alpha \times 10^5$ K^{-1}	9.8	8	-	-	10-20	-
w, %	6-7	0.3-0.5	0.05-0.1	0.01-0.04	0.5-3	-

*Curing agent - amines; **Curing agent - acid anhydrides; ***Unsaturated polyesters; ****Oligoester acrylates

The following symbols are used in Table 1.1: σ_b is the strength limit in extension; τ_b is the strength limit in bending; ε is elongation at break; E is the modulus of elasticity in extension (Young modulus); A is impact strength; T_g is glass transition temperature; T_m is melting point; ρ is density; Σ is electrical strength; α is thermal coefficient of linear expansion; w is maximal water absorption.

1.3 POLYMERIZATION OF MONOMERS AND OLIGOMERS WITH DOUBLE BONDS

Monomers containing double bonds, which can be transformed into massive items by free radical polymerization, are widely used.

Vinyl monomers are important members of this group of products, particularly, methyl and butyl methacrylates, which polymerize into useful thermoplastic materials:

poly(methyl methacrylate) (PMMA): $[-CH_2-C(CH_3)(COOCH_3)-]_n$

poly(butyl methacrylate) (PBMA): $[-CH_2-C(CH_3)(COOC_4H_9)-]_n$

Mixtures of methyl methacrylate and methacrylic acid or butyl methacrylate are also used. Polymer-monomer mixtures are often used in the production process. This allows reduction of the total exothermic effect of the process, shrinkage, and production time. These mixtures are obtained by two methods:

dissolution of polymer powder in a monomer

monomer polymerization until the desired degree of conversion is achieved.

Organic peroxides: acyl peroxides (benzoyl, acetyl, lauryl peroxides, etc), alkyl peroxides, hydroperoxides, etc. are used as polymerization initiators. Azocompounds (for example, α,α'-azobis(isobutyronitrile), initiator mixtures, redox systems, etc. are also widely used as initiators. In

some cases, activators – compounds, that are reductants and form redox systems, for example, dimethylaniline and cobalt naphthenate – are used to accelerate the process and to realize it without heat added.

Free radical polymerization of vinyl monomers is accompanied by the production of a large quantity of heat (in the case of PMMA - 54.5 KJ/mol). In the production of glass sheet from amorphous organic polymers, this heat output can be dissipated with coolants. However, this method is ineffective for large articles. The greatest heat output occurs during gelation. It increases the polymerization rate due to a reduction in the chain termination rate.[4] By influencing this important effect of radical polymerization, the process rate as a whole and the heat output rate can be regulated. This can be achieved by means of autoregulators: halogen alkanes, allyl halogen derivatives, polynitroalkanes, and hydrazine derivatives. Photopolymerization in the presence of photosensitizers, for example, diacetyl and autoregulators, is used in order to obtain especially large articles. Along with the block periodic method of monomer processing, continuous methods for bulk poly(methyl methacrylate) production have been developed: for example, this can be carried out by extrusion.

The important feature of polymers based on vinyl monomers is their transparency in the visible part of the spectrum. This is why the most important articles produced from these materials are organic glasses, which are used in the aircraft, automobile and ship-building industries as engineering materials, and also in civil engineering, and the optical, chemical, food industries, etc. The main technical characteristics of poly(methyl methacrylate) are given in Table 1.1.

Mixtures of liquid vinyl monomers and polymer powders serve as a basis for a special group of engineering materials. Vinyl acetate and acrylonitrile monomers are injected into polymer powders to accelerate swelling and gel formation. Styrene is added to improved the molding characteristics of reactive mixtures. Polystyrene, poly(vinyl acetate), poly(vinyl chloride), etc. are the most commonly used polymer powders.

Optically transparent materials with different properties are synthesized from monomers containing the allyl group $CH_2=CH-CH_2-$. Allyl monomers and their mixtures with other monomers are polymerized in the presence of radical initiators, which break down into radicals during thermolysis or under the influence of ultraviolet or ionizing rays. Such allyl monomers as diethylene glycol bisallyl carbonate, diallylphthalate, triallylcyanurate, and others are widely used.

The nonisothermal character of the process caused by intensive heat output and the resulting heterogeneity of the end-product are fundamental problems in monomer polymerization, especially during the processing of large articles. One of the methods used for regulating heat output in block polymerization consists in changing the starting reactants from monomer compounds to oligomers . Thus, oligo(ester acrylates) (OEA), which are oligomers belonging to the class of esters and ethers with end or regularly repeating acryl groups are of interest for use in reactive processing of large articles. Their general formula is

$$CH_2=C(X)-CO-O-R-O-(-CO-R'-CO-R-O-)_n-CO-C(X)=CH_2,$$

where R is the glycol or polyol residue; R' is the dibasic carboxylic acid residue; X = H, CH_3, halogen.

The main oligoester chain of these compounds may also include fragments of urethanes, sulfoesters, amides, and others. Along with the end-acryl groups, they may contain other reactive groups, such as carboxylic, allyl, hydroxylic, etc.

By varying the double bonds in OEA synthesis, materials with different characteristics can be produced (an example can be found in Table 1.1). Homopolymerization of OEA proceeds at high rates without the use of volatile monomers. Three-dimensional polymerization of OEA is initiated by radical and ionic initiators. Some widely used systems are: peroxides, i.e., tertiary amine and hydrogen peroxides; organic salts metals with variable valence. OEA is used in the varnish and dye industries for production of film-forming compounds and tape dyes; in binders for glass-reinforced plastics, glues, and molding materials; for the modifying thermoplastics, rubbers, fibers, and films; and for electroinsulating filled compounds.

The integrity of articles formed from three-dimensional polymers of OEA is strongly influenced by the residual stresses appearing during processing. With other parameters being equal, the larger the article size and the greater the oligomer chain rigidity, which impedes stress relaxation, the greater the probability of fracturing and premature failure of the article. The appearance of high residual stresses during processing is one of the main difficulties in the production of large articles from OEA.

1.4 CURING OF UNSATURATED POLYESTER RESINS

Unsaturated liquid polyester resins – oligo(ester maleates), and especially oligo(ester maleate fumarates) – OEMF, are stable in storage for months and sometimes years at normal temperature. Their general formula is:

$$H\text{-}[(\text{-OR'OCOCH=CHCO-})_x(\text{-OR'OCOR"C-})_y]_n\text{-OH}.$$

where R' and R" are the residues of glycols and dibasic unsaturated acids.

Maleic and phthalic anhydrides and fumaric acid are mainly used for polyester resin synthesis. However, dihydric alcohols such as ethylene and propylene glycols, diethylene, dipropylene, triethylene and neopentyl glycols, and hydrided or oxypropylened diphenylolpropane are also used.[5-7] Different combinations of dibasic acids with diols allow us to vary the composition and properties of the resulting polyester resins over a wide range.

Resin solidification (curing) occurs by a free radical addition mechanism at the double bonds. That is why no by-products are formed. Curing compositions based on polyester resins contain a large number of different components (resins, initiators, accelerators, monomers, oligomers, fillers, etc), which may have various chemical structures, and may be used in various proportions.

The best materials are produced by curing unsaturated polyester during copolymerization with different types of unsaturated monomers and oligomers, such as styrene and its derivatives, methyl methacrylate, vinylacetate, sulfone-type compounds, allyl esters, and oligo(ester acrylates).[5]

The most widely used initiators for curing unsaturated resins are peroxide compounds, which form free radicals on thermal breakdown, or redox systems. Duration of the process, lifetime of ini-

tial reactant mixtures, rate and extent of copolymerization, and mechanical properties of the cured copolymer all depend on the initiation system used. Accelerators are also employed to increase curing rates by promoting peroxide breakdown in the initial stage of the process. Heavy metal salts of aliphatic acids (for example, cobalt naphthenates) are also widely used for curing polyester resins. The curing process for three-dimensional copolymerization of mixtures of unsaturated resins may be initiated by ultraviolet[8] or high-energy radiation.

Two typical recipes (in weight proportions) for polyester resin-based materials are listed below (I is a filled composite for radio and electrotechnical equipment, which can also be used for sheet and rod production; II is a composite recommended for coating).

I.	Resin consisting of a long-chain glycol dissolved styrene - the binder	100
	Benzoyl peroxide (50% solution in dibutyl phthalate) - an initiator	0.5-2
	Dimethylaniline (10% solution in styrene) - the accelerator	0.5-3
II.	Resin consisting of a short-chain glycol dissolved styrene - the binder	100
	Methylethyl ketone (50% solution) - the initiator	1-2
	Cobalt naphthenate (styrene solution) - the accelerator	1-3
	Aerosil - a thixotropic additive	1-3

Two-component systems are used for reactive processing: the first component may be an unsaturated polyester, containing an initiator and 30% monomer; the second may be the same mixture but with the addition of copolymerization accelerators. The polymerization rate is increased if heated molds are used.

Plastics with different properties, ranging from brittle to highly elastic (see Table 1.1), may be produced from unsaturated polyester resins. It is often advantageous to load a composition with powder and reinforcing fillers, such as alumina, silica, calcium carbonate, fiberglass, etc. Fillers increase material strength and decrease shrinkage and costs. Thermoplastics, such as polyurethanes or butadiene-styrene copolymers, are added to unsaturated polyester resins in order to decrease the shrinkage of articles during processing and to increase their impact strength at the same time. It may also be useful to introduce a flexible thermoplastic block into a polyester resin during synthesis.[9]

1.5 CURING OF EPOXY RESINS

Transformation of epoxy resins, which are viscous liquids or thermoplastic solids, into network polymers is a result of interaction with alkali or acid substances by means of to polyaddition and ionic polymerization mechanisms.[10] A resin solidified by to the polyaddition mechanism, is a block copolymer consisting of alternating blocks of resin and a hardener or curing agent. A resin solidified by the ionic mechanism is a homopolymer. Molecules of both resin and hardener contain more than one active group. That is why block copolymer formation is a result of multiple reactions between an epoxy resin and a curing agent.[11]

Epoxy resins are solidified by the polyaddition mechanism by primary and secondary amides di- and polyamides, polybasic acids and their anhydrides, monomer and oligomer isocyanates, poly-

hydric alcohols, phenol-formaldehyde resins of novolac and resol types, etc. In the ionic polymerization mechanism, epoxy resins are solidified by tertiary amines, aminophenols and their salts, Lewis acids and their amine complexes, etc. Photoinitiated catalytic acid ion polymerization is widely used to solidify low-temperature coatings.

Depending on the type of curing agent, epoxy resins interact with it at room or higher temperatures. In the first case, when aliphatic amines are used as curing agents, self-heating occurs. Together with low heat conductivity, this phenomenon complicates the production of large size articles with desirable properties. As a result of temperature variations during the reaction, complicated physical liquid-to-glass transitions typically occur during the processes of curing of epoxy resins.[12]

Depending on the nature and proportions of the initial components and the technological peculiarities of the polymerization process, it is possible to produce epoxy resins of different compositions and molecular weights. Products can contain different contents of active groups; for example, epoxy or glycidol and epoxydian, cycloaliphatic, nitrogenated, halogenated, and epoxy novolac resins can also be produced from resorcin and its derivatives. Similarly, aliphatic resins can be formed from di- and polyols, diglycil ethers, etc.

Epoxy resin-based compounds are used in many industries as binders for reinforced plastics, engineering glues, putties, pastes, coatings, and cast articles. Materials based on epoxy resins are widely used for their high chemical resistance, solvent resistance, high adhesion to some materials, and their good mechanical and excellent electrical properties. There is a large amount of data on epoxy resins, curing agents, fillers and modifiers, and their applications in different industries.[12]

Typical recipes of compositions, widely used in the electrical industry and in the production of reinforced plastics, are given in Table 1.2, while the basic properties of epoxy plastics cured by amine and anhydride hardeners can be found in Table 1.1.

Epoxy resins are an important class of polymers used for reactive processing. However, it is rather difficult to find a formulation which provides sufficiently high process rates to be useful in the modern processing equipment used for the RIM-process.

1.6 CURING OF PHENOLIC-BASED COMPOSITIONS

Processing of phenol-aldehyde oligomers into various articles is based on a polycondensation reaction which leads to solidification of the material at temperatures below 200°C and pressures exceeding 10 MPa. The process is accompanied by volatile product formation. However, phenol-formaldehyde resins of the resol type can be cast without additional pressure and heat. The raw molding reactants contain different organic and mineral fillers and other additives in addition to the basic resin.

The strength of articles based on phenolic compositions and solidified without additional pressure and heat supply is 2-4 times lower than the strength of thermally solidified resins; this limits their applications as engineering materials. One of the primary causes of material strength decrease is pore formation due to volatilization of water and formaldehyde during polycondensation. Different water adsorbents (calcium carbonate, clay, silicates, methasilicates, zeolites, etc.) should be

Table 1.2. Examples of epoxy formulations

Component	Contents, weight proportions	Curing temperature, °C	Type	Main fields of application
I				
Dian resin	100	140-150	binder	Electro-insulating
phthalic anhydride	35		curing agent	Molding compound
quartz, powdered	200		filler	
II				
Dian resin, modified by aliphatic epoxy resin	100	140-150	binder	Binder for reinforced plastics
triethanol-amine titanate	8-11		curing agent	
III				
Dian resin	100	20	binder	Molding compound
polyethylene	20		curing agent	Binder for reinforced plastics
polyamine	25			
dibutyl phthalate	20		plasticizer	

incorporated into the molding compounds to eliminate pores. Increasing resin hydrophilicity, application of special catalytic systems, adding fillers, and treating their surfaces by special physical and chemical methods lead to improved strength in the final products. Casting of engineering materials based on phenol-formaldehyde resins with various mineral fillers is widespread. The use of resol casting resins permits the production of thick heat-resistant and even fireproof coatings, with good electrical insulating properties, and chemical resistance.

1.7 SYNTHESIS OF POLYURETHANE COMPOUNDS

Urethane-containing polymers -NH-(CO)O- are usually synthesized from esters and/or ethers with hydroxyl groups on their chain ends, diisocyanates, and other polyfunctional compounds that contain a mobile hydrogen atom. If there are only two reactive groups in starting compounds, then linear polyurethanes are synthesized; if there are more than two groups, then three-dimensional structures are obtained. Aggregates of stiff blocks (domains) are formed in the final products because of intensive intermolecular interaction resulting from microphase separation.

These domains are connected by hydrogen bonds, which act as knots or crosslinking centers to create flexible blocks.[13] Microphase separation and the appearance of domain structure are considered to be the main factors, which determine the unique properties of this class of polymers.

Mono- and two-stage methods are used to produce articles from polyurethane-containing materials.[14] In the two-stage method, prepolymers, e.g.macro(diisocyanates), are synthesized by the reaction of polyesters containing end-hydroxy groups (polyols) with diisocyanates:

$$HO\text{-}R\text{-}OH + 2OCN\text{-}R_1\text{-}CNO \rightarrow OCN\text{-}R_1\text{-}NH(CO)\text{-}R\text{-}O(CO)NH\text{-}R_1\text{-}NCO$$

Low-molecular-weight glycols or diamines are used for further propagation of prepolymer molecules and for crosslinking the chains:

$$2OCN\text{-}R_1\text{-}NH(CO)\text{-}R\text{-}O(CO)NH\text{-}R_1\text{-}NCO + HO\text{-}R_2\text{-}OH \rightarrow [OCN\text{-}R_1\text{-}NH(CO)O\text{-}R\text{-}O(CO)NH\text{-}R_1\text{-}NH(CO)\text{-}R_2\text{-}]_2$$

The reagent ratio in the reactive mixture is selected so that there is a small surplus of isocyanate groups.

Curing of the prepolymer occurs at temperatures $\geq 80^{\circ}C$. If glycols are used for curing, a network of allophanate knots leading to branching is formed. If the chains contain urea groups as a result of their interaction with surplus end NCO-groups, then biuret knots lead to branching. Allophanate and biuret structures are not stable formations; therefore tri-functional agent is often added to the initial mixture to increase the number of stable crosslinking urethane bonds. The curing rate is regulated by organic derivatives of two- and four- valent tin, amines, etc. The use of catalysts in the one-stage method of polyurethane synthesis is particularly important, because it is necessary to follow a definite order when introducing reagents into a reaction.

One of the most widespread methods of preparing linear elastomeric polyurethanes is to use a mixture of macrodiisocyanate prepolymer and methylene bischloraniline ("Diamet X"). Minimal sensitivity to moisture, a short curing cycle and good properties of the end product are characteristic of this method. Prepolymer is synthesized from 2,4-toluylene diisocyanate (TDI) and poly(tetramethylene glycol) or polyester polyol at a 2:1 mole ratio of TDI to polyol. In such a prepolymer, the majority of free isocyanate groups are in position 6, which makes it less chemically active and provides high stability. In this case, it is possible to produce a ready-to-use prepolymer, so that the whole process consists of adding Diamet X, which is used as a chain propagator and curing agent in poly(urethane urea) elastomer formation. The presence of chlorine atoms in position 3,3' also diminishes amine group activity in Diamet X and slows the reaction rate. A combination of elastic polyester and rigid carbamide segments and the resulting, microphase separation guarantee rubber elasticity and unique mechanical properties in the end-product even at low temperatures. Poly(tetramethylene glycol) segments provide good resistance to hydrolysis. When oil, gasoline and solvent resistance is necessary, polyester-based compounds are used as additives. The principal disadvantage of Diamet X is its toxicity. The use of mixtures containing diphenylmethane diisocyanate (MDI) instead of TDI is the most common way of dealing with this problem. A possible new approach to

Table 1.3. Properties of some elastomers based on of reactive oligomers compared with polyurethanes

Property	PU-I	PU-II	Hydrocarbonate oligomer	Thiokol	Silicone organic oligomer
σ_b, MPa	40-50	50-60	2.0-8.0	14-20	4.0-7.0
ε, %	500	600	500-1000	150-300	500
E, MPa	13-15	6-7	0.5-3	-	-
ε_r, %	10-12	5-7	3-5	6-10	6-8
H_S	90-94	60-80	30-40	20-40	40-60
ε_{el}, %	35-38	25-28	-	-	-
T_g, °C	-35 to -40	-25 to -30	-60 to -80	-40 to -50	< -80

The following symbols are used in Table 1.3: σ_b is strength limit in extension; ε is deformation at break; E is modulus of elasticity; ε_r is residual deformation (after elastic recoil); H_b is Shore hardness; ε_{el} is rebound elasticity; T_g is glass transition temperature

elastomer production is to use a prepolymer synthesized from polyester and excess diphenylmethane diisocyanate (pseudo-polymer). This allows us to use reactive processing technology, because it is possible to use components in near 1:1 proportions, to select those with similar viscosities, and to vary their reactivity over a wide range by using catalysts. In this case the initial reaction is between part of the polyol and the isocyanate, as the latter is present in excess of 2:1 ratio. The rest of the polyol together with the extender (1,4-butane diol or 3,5-diethyl toluylene diamine), are added during mixing. Other additives are dispersed or dissolved in other components according to their chemical nature. This approach provides extensive possibilities for synthesizing elastomers with a wide range of physical and chemical properties. These possibilities arise for same reasons as those given for poly(ester urethaneureas).

Esters and ethers based on poly(tetramethylene glycol) and propylene oxide or a combination of propylene and ethylene oxides commonly are used in reactive processing. The chemistry of leading to polyurethane formation, has been analyzed in many publications;[15-17] however, the practical problems of processing real initial oligomers and molding compounds based on them into articles for different applications have received less attention.

The properties of some polyurethane elastomers, used as such as elastic damping components in engineering applications (e.g., in sheet stamping operations and for coating of press and other rolls of paper-making equipment[18]) are shown in Table 1.3.

The two elastomeric polyurethanes listed in Table 1.3, are synthesized in the following way: PU-I is the reaction product of a prepolymer based on poly(tetramethylene glycol) ether and 2,4-toluylene diisocyanate; (this product is analogous to "Adiprenyl-167", Du Pont, USA); PU-II is the

reaction product of a prepolymer based on poly(ethylene glycol adipate) ester with 2,4-toluylene diisocyanate cured with a mixture of diethylene glycol and glycerin.

Among the new being consider for reactive processing into polyurethane-based materials, the so-called polyester amines, in combination with chain extenders, which also contain amine groups, are especially promising.[19] Using these materials allows the synthesis of polymers with polyurea instead of polyurethane bonds. This results in materials with improved impact strength and lower water absorption.

1.8 CURING OF LIQUID RUBBERS AND OLIGOMERS WITH FUNCTIONAL GROUPS

The synthetic rubber industry is now producing a great number of low-molecular-weight rubbers that are liquids in the processing temperature range. The low viscosity of such rubbers allows us to cast articles of any form and to produce rubber mixtures or glues using the reactive (chemical) molding method. Liquid rubbers synthesized by diene polymerization or copolymerization of dienes and vinyl monomers form a large group of materials with many applications. Hydrocarbon oligomers containing functional groups (OH, COOH, SH, NCO, epoxy, acrylate, etc.) are widely used. Liquid rubbers can be improved by incorporating plasticizers and active fillers (carbon black, aerosil, etc). Polymers with different structures and, therefore, with a range of properties from elastomers to high impact plastics, may be synthesized from a liquid rubber base.

Vulcanization by the traditional curing methods utilized in the rubber industry is based on sulfur or sulphur-containing compounds and is also the most widely applied technique for curing liquid rubbers containing macromolecules with double bonds. Chinons, peroxides, phenol formaldehyde resins, and other compounds are often used for curing liquid rubbers as an alternative sulfur vulcanization.

Oligomers with functional groups are vulcanized by chemical interaction of these groups with curing agents. The properties of the final product essentially depends on the nature and location of the functional groups in the macromolecule and the oligomer's molecular weight distribution. Various compounds are used for curing, depending on the chemical structure of the end-groups. Hydroxyl-containing oligo(butane dienes) are cured by the conventional methods used in polyurethane chemistry to synthesize oligo(diene urethane). In this case, the one-stage method of curing by mixtures of polyols, diisocyanates, and curing catalysts is used. Curing systems, consisting of a mixture of polyhydric alcohols and diamines are also widely employed to provide high-strength vulcanized products. Two-stage elastomer production, including the isocyanate reaction for polymer formation, is also used. hydroxyl carbonate polyurethane and urea-urethane elastomers have important advantages (compared to polyurethanes based on esters and ethers): they are freeze resistant, hydrolysis-resistant, and compatible with fillers and plasticizers, although they typically have lower strength than polyurethanes (see Table 1.3.). Besides functional end groups, butadiene oligomers contain double bonds, which can also react during curing. This allows the use of combined curing systems that involve both functional end groups and double bonds.

Oligo(diene urethane) with epoxy, acrylate, halogen-containing, hydrazine and other end-groups are used to avoid the disadvantages (moisture sensitivity, toxicity, etc,) typical of curing systems containing diisocyanates. In this case, curing systems appropriate to each type of functional group, are used. This allows us to synthesize a variety of polymers of with the desired range of properties. In addition, the potential for using rubber combinations with various additives, for example, oligo(diene urethanes) with epoxy groups in a composition with epoxy resins poly(diene urethane acrylates), with styrene and so on, is promising. Epoxy resins combined with catalysts (for example tertiary amines) are used for curing bifunctional carboxyl containing oligomers. Liquid rubbers are used to produce hermetic seals for artificial leathers and films and to modify tire rubbers, pneumatic tires, plastic concrete, coatings, etc.

1.9 CURING OF POLYSULPHIDE OLIGOMERS (THIOKOLS)

Liquid polysulphide oligomers (thiokols) $X[-R-S_m-]_mX$ (where R is an aliphatic radical, m = 2 or 4, and X is an SH or OH-group) are cured by two possible mechanisms: oxidation of sulphohydryl end-groups by inorganic oxides (MnO_2, PbO_2), metal peroxides, hydrogen peroxides, n-chinonedioxime, nitrobenzene, and other compounds, and by interaction with different reactive compounds, such as macro(isocyanates), unsaturated compounds, and epoxy oligomers, in the presence of an amine-type activator.[20] Curing systems containing compounds of both types, for example, manganese dioxide, epoxy resin, and diphenyl guanidine, are widespread in technological practice. Thiokols are cured at temperatures of 5-30°C, practically without shrinkage, resulting in elastomer production (see Table 1.3).

The main application of polysulphide compounds is in seals and glues, e.g., gaskets with high gasoline- and oil-resistance due to a high content of disulphide fragments in the polymer chain. Sealers based on thiokols are primarily used in housing, machinery, road building, aircraft and shipbuilding, space technology, etc. An important limitation on increasing thiokol production is the large amount of waste produced and the difficulty of eliminating harmful admixtures from the products.

1.10 CURING OF SILICONE ORGANIC OLIGOMERS

Curing of the majority of reactive silicone-organic oligomers $(-[-R_2SiO-]_n-)$, usually, occurs by a polyaddition (condensation) reaction at room temperature in one and two-component compositions. One-component systems that contain an oligomer plus alkoxy silanes or acetoxy silanes are cured by moist air. Curing of two-component systems occurs by interaction of the oligomer with alkoxy silanes under the influence of a catalyst, i.e., tin-containing compounds, or by neutral cure process. In both cases, the formation of low-molecular-weight substances (acid, alcohol) occurs as a result of the reaction. If these low-molecular-weight substances remain in the polymer, they have an adverse effect on its properties and performance.

Composites cured by the polyaddition mechanism are especially interesting for reactive molding, because by-products are not formed and there is no appreciable shrinkage during the reaction. This is the principal difference between polyaddition and polycondensation.

The possibility poly(organo siloxanes) without by-product formation has expanded the areas of application of silicone organic polymeric materials; in particular, this has allowed the production of various articles by the reactive processing method. If there are vinyl groups in side-chains, then organo-siloxanes are cured by conventional free radical polymerization. Bifunctional hydroxyl-containing oligomers are cured by methods used in polyurethane chemistry. Silicone organic oligomers containing spirane groups, which transform into three-dimensional polymers by cyclic reactions under the influence of hydroxyl silane ions, are of growing interest. It has been suggested that linear di(hydroxyl organosiloxanes) could be vulcanized by catalytic polymerization methods. The high molecular weight (not less than 10^4) of di(hydroxyl organosilanes) is their most important feature, since they provide necessary level of physical and mechanical properties (see Table 1.3).

A reinforcing filler, for example, highly dispersed silicon dioxide, is added to the mixture to produce vulcanizated material with improved strength. Cast silicone organic composites are widely used in electrical and electronic devices, in medicine, in the aircraft industry, etc., due to their ease of processing and the advantageous physical and chemical properties of the cured materials.

1.11 PROCESSING OF OLIGOMER-MONOMER MIXTURES

One of the principal features of the compounds discussed above is their ability to be transformed into final products and/or articles from mixtures of almost any composition, even those whose components have little compatibility. The use of oligomers and monomers of various chemical structures expands the assortment of materials and articles that can be produced by combining different components. The interest in so-called hybrid binders, interpenetrating networks, polymer-oligomer systems, and other possible reactive components has increased during recent years.

There are several techniques for producing polymer mixtures for further processing into articles by the reactive (chemical) molding methods: simultaneous formation of two polymeric systems with mutual entanglement of their chains and the appearance of so-called interpenetrating networks; synthesis of the second polymer within an expanded network of the initial polymer; incorporation of oligomers into a polymer matrix as a "temporary" plasticizer followed by polymerization.

Block-copolymers based on polycaproamide and oligomer activators, composites based on polyester resins with unsaturated monomers and oligomers, and oligo(diene epoxy urethanes) with epoxy resins have already been mentioned. Combinations of epoxy resins with reactive silicone organic oligomers, poly(vinyl chloride) with oligo(ester acrylates), polyurethanes with vinyl monomers, composites consisting of unsaturated esters and oligoesters, and many others are also used for different applications. Problems in the reactive molding of oligomer-monomer mixtures are caused by their complexity; the various components in these systems have different reactivities, resulting in different rates for chemical and physical processes. The most promising method of forming articles from these mixtures is reactive processing.

1.12 PROCESSING OF FILLED COMPOSITES

The incorporation of different fillers, which essentially change the physical, mechanical and thermal properties of a composite, into a polymeric matrix is one of the main methods for modifying material properties. There are various methods for preparing filled polymeric composites. One of them is the so-called "polymerization filling", when a filler is inserted into a composites at the polymer synthesis stage. This method has been actively developed, especially in the last twenty years.[21] Implementation of this process is based on the principles of reactive (chemical) processing; this is due to the simplicity of both the process itself and the processing equipment, although the presence of a filler adds some special features to the process. A filler influences not only the properties of the final product, but also the processing of the initial components. For example, fillers used in composites based on unsaturated polyester resins make it possible to polymerize a monomer at higher temperatures, the heat of reaction is reduced and hence, the articles produced have less tendency to crack.

Some new problems arise in processing filled composites. One of these is sedimentation instability of the initial reactive mixtures, especially if the viscosity of the monomer (or oligomer) is low; an example is anionic activated polymerization of lactams in the presence of various solid fillers (talc, graphites, molybdenum disulphide, metal oxides). In this case, it is necessary to know the dispersion of the filler and its ability to absorb lactams. Sedimentation of filler particles in the polymerizing mass can be prevented by adding a special thickening agent, which increases the initial viscosity of the reactive medium. For example, aluminum naphthenate, aerosil, or a polymer soluble in the monomer or oligomer can be used as these thickening agents. However, it may be difficult to achieve adequate dispersion of the filler in an oligomer if the viscosity of the reactive medium is too high. One way to solve this problem consists in preliminary mixing of the filler with a small amount of an oligomer and then using this thick paste in further operations. Fillers play an important role as dyestuffs and pigments, oxidation stabilizers, ultraviolet absorbers, etc.

Filled composites consisting of a polymer binder and various reinforcing organic and inorganic fibers are of special importance in different applications.[22] Reinforcing fibers (made of glass, carbon and graphite, boron, organic fibers, etc.) are now used in combination with practically all the above mentioned binders to produce composite materials and articles made from them for almost all branches of industry.

Finally, oligomers in reactive processing to produce foamed plastics and elastomers for various industrial purposes. These materials have many of the valuable properties of conventional polymers, with the addition of low density and high heat, electrical, and sound insulation characteristics.[23]

Reactive (chemical) processing of monomers and oligomers is now developing rapidly. New initial reactants, which can be processed without significant shrinkage, residual stresses, or volatile product formation are part of modern technology. These processes produce thermoplastics or thermoset plastics with the necessary range of performance characteristics. One of the newest examples of materials produced by reactive processing is a system based on polymerization of a bifunctional monomer - dicyclopentadiene - with a Ziegler-Natta catalyst. This system was developed especially

for reactive processing technology. As a result, a new, highly cured engineering plastic with high performance characteristics was obtained.[24] Another example of a new material is the urethane-isocyanurate system.[25] High-temperature engineering plastics based on cyclic oligomers, oligoimides, polyimides, etc. are also processed into articles of various types by reactive molding. Direct transition from a liquid state into articles or structural engineering components is also used with inorganic reactants, for example, in the production of ceramics articles.[26]

2

MODELLING

2.1 OBJECTIVES OF MATHEMATICAL MODELLING

Reaction (or chemical) molding of articles makes it possible to obtain both bulky semi-finished items with simple shapes (in the form of rectangular plates, cylindrical blocks, tubes and shells) and complex-shaped parts. The process comprises a number of different chemical and physical phenomena and is therefore rather complicated. Commercial realization of the process, as with any chemical process, comprises plant design and establishing controlled process variables. As usual, a central problem to be solved is the extension of laboratory investigation results to a much larger scale. Here, one can follow the conventional path by gradually scaling up from laboratory prototypes weighing tens of grams to industrial items weighing hundreds of kilograms (1:10,000 increase in scaling). This is a lengthy and expensive process, which is why it is desirable to eliminate the intermediate steps and achieve the final result by a faster method.

It is clear that this method cannot be based on the use of similarity parameters since reactive molding in common with other chemical engineering processes, involves nonlinear phenomena that result in the invalidity of similarity conditions as geometric, chemical, and thermal parameters.

A universal method of handling the problem is mathematical modelling, i.e., a quantitative description by means of a set of equations of the whole complex of interrelated chemical, physical, fluiddynamic, and thermal processes taking place concurrently or consecutively in a reactor. Constants of these equations are determined in laboratory experiments. If the range of determining factors (reactive mass compositions, temperature, reaction rates, and so on) in an actual process lie within or only slightly outside the limits studied in laboratory experiments, the solution of the determining set of equations provides a reliable idea of the process operation.

This approach, taken to its logical conclusion, makes it possible to achieve two main goals: first, to optimize the process so as to provide the maximum possible throughput at minimum cost, and, second, to ensure the required quality level of the final products. Development of a deterministic mathematical model of a process requires an adequate representation of its main constituent stages. This always involves an internal contradiction: on the one hand, it is desirable to describe all

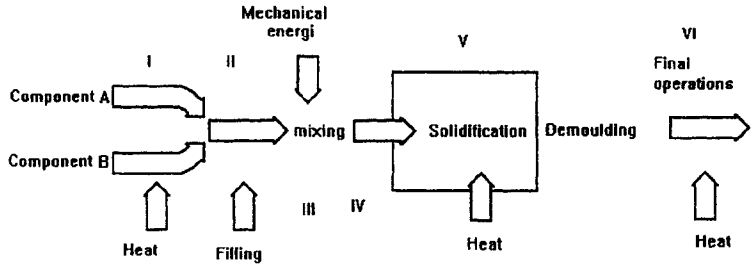

Figure 2.1. Scheme of two-component reactive processing.

the process elements as closely, fully, and accurately as possible, and on the other hand, the greater the detail, the more effort, time, and funds are required and the less worthwhile (in terms of the final result) the model becomes. The choice of an optimum compromise or a reasonable tradeoff is dictated by the ultimate goal and sometimes has no unique solution. That is why in developing a mathematical model of a process there is always room for a creative and intuitive approach; i.e., as in any serious undertaking, success results from an alliance between science (design) and art (experience and qualitative assessments).

The starting point in developing a mathematical model is breaking up a process into its main stages (elements) and treating each one as an independent subject for mathematical modelling. Let us consider this approach for a classical two-stream chemical molding flow sheet. The following basic stages can be distinguished in this flow-sheet (Fig. 2.1): charging and heating of the feed reactants (I); addition of agents, such as fillers (II); mixing of components to obtain a reactive mass (III); reactive mass moves (flows) through channels, valves, etc. (IV); mold filling and polymerization (V); discharge and heat treatment (VI).

Consideration of these stages makes it possible to review a number of problems, some quite trivial and solvable by standard engineering methods and other, more general physical and chemical problems calling for separate analyses. Process stages I, and to some extent II and III, are among the ordinary technical problems, although they also require a substantiated design. However, from stage IV on, problems arise that are specific to reactive processing (or chemical molding). Thus, for stage IV, a new problem, which has been given virtually no consideration in chemical engineering, turns out to be the flow of a fluid with changing rheological properties. This involves evaluating changes in the reacting fluid of a molecular flow characteristics in a nonuniform hydrodynamic field. For stage V, it is necessary to consider the macrokinetic problem of polymerization under nonisothermal conditions. A rigorous method for describing such polymerization processes has to be developed to deal with this situation. It is also important that polymerization is very often accompanied by crystal-

lization of the newly formed product, which significantly complicates the process under discussion and, consequently, its quantitative description.

For stage VI, the analysis of inherent (or residual) stresses resulting from nonuniform cooling and heat treatment of final articles appears to be critical. Thus, stages IV to VI should be the subject of mathematical modelling specific to reactive processing (chemical molding processes).

It should be emphasized that in all these cases, combined or superimposed phenomena must be dealt with, viz.: for stage IV, fluiddynamics, kinetics of polymerization, and rheokinetic changes caused by chemical reactions; for stage V, polymerization kinetics, crystallization kinetics and heat transfer effects; a thermomechanical problem in combination with crystallization kinetics. Construction of a mathematical model requires simultaneous solution of a set of equations in order to describe these related phenomena.

2.2 KINETICS OF POLYMER SYNTHESIS (GENERAL)

In building mathematical models of product formation in a mold it is possible to treat a polymeric material as motionless (or quasi-solid), because the viscosity grows very rapidly with the formation of a linear or network polymer; thus, hydrodynamic phenomena can be neglected. In this situation, the polymerization process itself becomes the most important factor, and it is worth noting that the process occurs in nonisothermal conditions.

A complete description of the process must consist of kinetic equations for all components of the reactive mass, including all fractions of different molecular weights and intermediate and by-products as well. Such an "exact" approach is usually superfluous for modelling any real process and should not be applied, because excessive detail actually prevents achievement of the final goal due to overcomplicating of the analysis. Therefore, why correct (necessary and sufficient) choice of the parameters for quantitative estimation is of primary importance in mathematical models of a technological process.

On these lines, two approaches can be proposed. The first can be applied to the synthesis of linear polymers. In this case, the degree of conversion of a monomer can be chosen as a determining factor. This degree of conversion, β, is expressed as the proportion of a monomer included in macromolecular chains:

$$\beta = \frac{[M]_0 - [M]}{[M]_0} \qquad [2.1]$$

where $[M]_0$ and $[M]$ are the initial and current (not yet incorporated into polymeric chains at t concentrations of a monomer, respectively.

It is evident that at $t = 0, \beta = 0$, and after the sufficiently long time, some equilibrium (residual) concentration of the monomer in the reactive medium is maintained. In any practical situation important for technological applications this residual concentration is much less than $[M]_0$ and we can assume that $\beta = 1$ at $t \to \infty$.

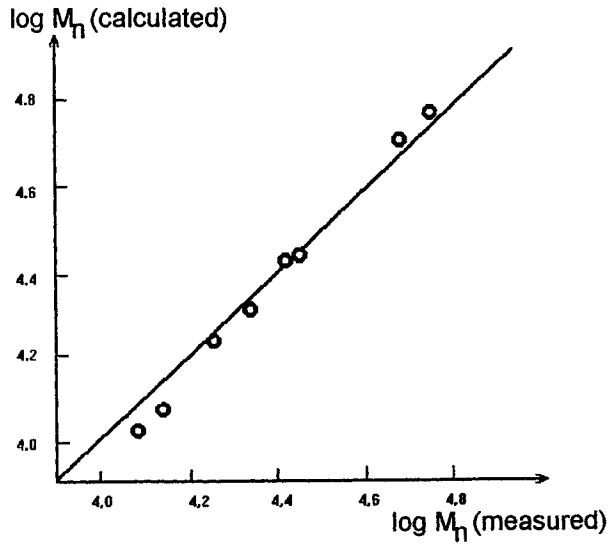

Figure 2.2. Correlation between molecular weights in synthesis of polydodecanamide (PA-12), calculated by concentration of active centers of polymerization (I) and measured by intrinsic viscosity (II).

Now we can assume that a polymerization reaction starts at active centers, and that their initial concentration is [A] mol%. Then we can calculate the number-averaged degree of polymerization in the end product as follows

$$N_n = \frac{100}{[A]} \qquad [2.2]$$

This means that the number-averaged molecular weight at any current time t can be expressed as

$$M_n(t) = \frac{100 M_0 \beta}{[A]} \qquad [2.3]$$

The molecular weight of the end-product can be calculated as

$$M_n(\infty) = \frac{100 M_0}{[A]} \qquad [2.4]$$

where M_0 is the molecular weight of a monomer.

Values of both parameters, β and M_n, are generalized characteristics of any polymerization process; therefore, it is reasonable to construct a mathematical model of the kinetics for the parameter β; and then calculate M_n from β with Eq. (2.3).

An example illustrating the application of Eq. (2.4) for calculating M_n is shown in Fig. 2.2.[27] The position of the line at 45^0 reflects the exact equality of the M_n values calculated from the concentration of active centers and those determined by measurement of intrinsic viscosity, [η]. Bearing in mind possible experimental errors and the accuracy of the equation relating [η] and M_n, we can conclude that the correspondence between the two series of M_n values is satisfactory.

The second method of characterizing the "chemical" order of a reaction is by the concentration of reactive groups, [R]. This method is most applicable to reactive oligomers that polymerize into both linear and three-dimensional polymers. Let the initial concentration be $[R]_0$ and the final one be $[R]_\infty$. Then the "chemical" degree of conversion β_{ch} is

$$\beta_{ch} = \frac{[R]_0 - [R]}{[R]_0 - [R]_\infty} \qquad [2.5]$$

where $[R]_\infty$ is the concentration of reactive groups in the end-product.

It is evident that in this case, as in the former one, that at $t = 0$ (at the beginning of the process), $\beta_{ch} = 0$ and at $t \to \infty$ (finish of the process) $\beta_{ch} = 1$.

Analytical monitoring of a polymerization process (during synthesis of either linear or three-dimensional polymers) by purely chemical methods is often inconvenient or too slow and laborious. Therefore the use of various physical methods for this purpose has became popular. All these methods are based on measuring different physical properties of a reactive medium. The most important of these are thermal (or calorimetric) and mechanical methods.

The thermal method consists of measuring the rate of heat output dq/dt as a function of time t in the course of a reaction. In this case, it is assumed that the quantity of heat dq is proportional to the change in the degree of conversion dβ. According to this formulation, the actual nature of the reactions occurring in the material is not a concern; however it is assumed that the total output Q corresponds to completion of the polymer formation process; i.e., it corresponds to $\beta = 1$. Therefore, the main expression for the "calorimetric" degree of conversion β_c becomes

$$\frac{d\beta_c}{dt} = \frac{1}{Q}\frac{dq}{dt} \qquad [2.6]$$

or

$$\beta_c = \frac{1}{Q}\int_0^t \frac{dq}{dt}dt \qquad [2.7]$$

This thermometric method, which consists of measuring the temperature of a reactive medium in an adiabatic polymerization process T(t), is quite close to the calorimetric method. If we assume that the product of specific heat and density, $C_p\rho$, does not depend on temperature and the degree of conversion (this assumption is quite realistic), then it is possible to relate changes in temperature dT to heat output dq:

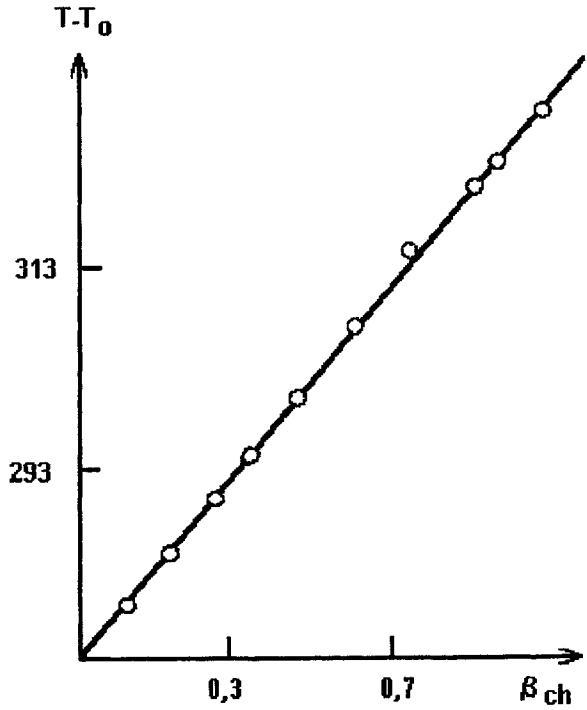

Figure 2.3. Correspondence between "chemical" degree of conversion and the degree of conversion, found by a calorimetric method proportional to the temperature difference.

$$dT = \frac{1}{C_p \rho} dq \qquad [2.8]$$

Then the "thermal" degree of conversion β_{th} can be calculated as

$$\beta_{th} = \frac{T - T_0}{\Delta T_{max}} \qquad [2.9]$$

where T_0 is the initial temperature of a reactive medium and T_{max} is the maximum (adiabatic) increase in temperature due to heat output in the course of polymerization.

It might be expected that β_c should be close to β_{th}, although there is no *a priori* knowledge of the accuracy of the equality $\beta_c = \beta_{th}$. An example confirming the direct correspondence between β_c and β_{th} is shown in Fig. 2.3.[28] It is evident that variation of the factor $C_p\rho$ is negligible for the example shown in Fig. 2.3.

The mechanical method of monitoring chemical reactions is based on measuring the viscosity or the elastic modulus of a reactive mass. Naturally, the viscometric method relates to liquid systems, while the elastic modulus method is valid primarily for solids (viscoelastic or elastic materials). However, there is an important difference between these two methods. Viscosity and its rate of change are not direct measures of a chemical reaction, because there are no linear or other simple relationships between viscosity and molecular weight, degree of branching, and other structural parameters of a newly formed polymer. Therefore, changes in viscosity reflect chemical transformations but cannot be related to them in a simple manner; correlations between changes in viscosity and the kinetics of a chemical reaction must always be determined independently. Meanwhile, it is reasonable to assume that in many cases there is a linear relation between the modulus of elasticity and the degree of curing (the reciprocal of the average length of a molecular chain between adjacent crosslinking chemical bonds). The main equation for establishing the correspondence between the molecular weight of a chain between crosslinking, M_c, and the modulus of elasticity G' is as follows:

$$G' = f\frac{\rho RT}{M_c} \qquad [2.10]$$

where f is the so-called front-factor, with a value close to 1; ρ is the density; R is the universal constant; T is the temperature in K. Strictly speaking, the modulus value in this equation should be the equilibrium modulus, but for cured polymers in the low-frequency range (to be more exact - in the plateau range), the modulus does not depend on frequency. Therefore Eq. (2.10) is also applicable if the low-frequency dynamic modulus is used instead of the equilibrium modulus.

It is also possible to introduce the idea of the "rheological" degree of conversion $\beta_{rh,\,l}$ which allows the curing process to be monitored. This is

$$\beta_{rh} = \frac{G'(t)}{G_{\infty,20}} \qquad [2.11]$$

where G'(t) is the current value of the dynamic modulus at time t; $G'_{\infty,\,20}$ is the value of the dynamic modulus for the end state of the material at 20°C. $G'_{\infty,\,20}$ is not equal to the final value of the modulus reached as a result of isothermal curing at an arbitrary temperature T; use of this reference value of the modulus at a fixed temperature is convenient for practical applications.

Other estimates of the degree of conversion in curing of reactive polymeric systems are also possible but they have much narrower areas of application. To construct a mathematical model, it is necessary to relate the inherent characteristics of the reactive mass (molecular weight, molecular weight distribution, degree and character of branching, topology of the forming network, and so on) to the process parameters (temperature, geometrical shape of the reactor or article, pressure, hydrodynamic situation) and the properties of an end-product.

2.3 KINETIC MODELS OF LACTAM POLYMERIZATION

2.3.1 GENERAL KINETIC EQUATION

Polymerization of lactams in reactive processing proceeds with the involvement of a catalyst and direct or indirect activators. A mathematical model of the process must be a kinetic equation relating the rate of conversion of a monomer to a polymer to the reagent concentrations and temperature. The general form of the model is

$$\frac{d\beta}{dt} = k_0 f(\beta) e^{-U/RT} \qquad [2.12]$$

where $f(\beta)$ is a kinetic function whose form depends on the nature of the polymerizing monomer; U is the apparent activation energy; k_0 is a constant related to the initial reaction rate. It is convenient to impose the conditions $f(0) = 1$ and $f(1) = 0$ on the kinetic function. These conditions correspond to the starting and end-points of the reaction; thus, the initial reaction rate has the following value:

$$K = k_0 e^{-U/RT_0}$$

where T_0 is the initial temperature of the reaction mass.

The second limitation imposed on the function $f(\beta)$ means that the reaction rate decreases to zero at completion, when all reactive groups (at $\beta = 1$) are exhausted. Since the structure of the kinetic function $f(\beta)$ depends on the type of monomer, it is reasonable to discuss the kinetics of polymerization of the main lactams separately.

2.3.2 ISOTHERMAL POLYMERIZATION OF ε-CAPROLACTAM

The use of various thermal methods to investigate ε-caprolactam polymerization allowed us to determine the expression for the kinetic function $f(\beta)$ for this monomer:[29-32]

$$f(\beta) = (1 - \beta)(1 + c_0\beta) \qquad [2.13]$$

This function corresponds to the first order kinetic equation (first term on the right-hand side of the equation) and also reflects the effect of self-acceleration (second term on the right-hand side of the equation); the quantitative measure of this effect is the constant c_0. Thus the reaction rate is determined by two independent constants c_0 and K. The fit of this equation to experimental data is illustrated in Fig. 2.4. The effect of self-acceleration in anionic polymerization of ε-caprolactam was also discussed in other publications.[33-35] The kinetic equation of isothermal polymerization based on Eq. (2.13) can be written as

$$\frac{d\beta}{dt} = K_0(1 - \beta)(1 + c_0\beta) \qquad [2.14]$$

where K_0 is the initial reaction rate at the polymerization temperature T_0. The integral of this equation is

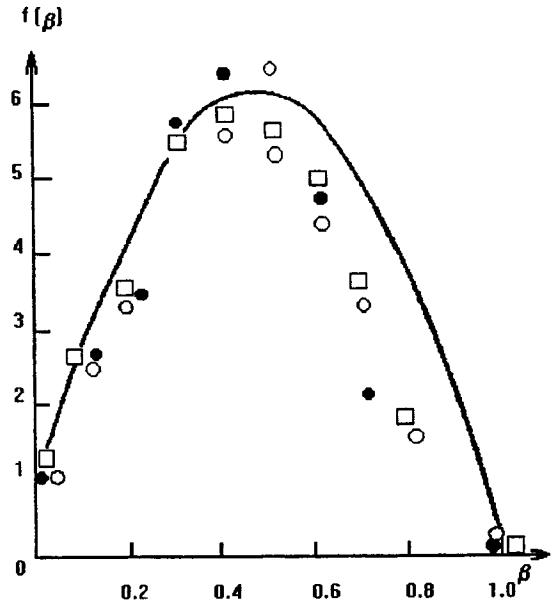

Figure 2.4. Comparison of the kinetic function, calculated as $f(\beta) = (1 - \beta)(1 + c_0\beta)$, and experimental data obtained by adiabatic polymerization at different initial temperatures: 151°C (○); 159°C (●); 170°C (□). Concentrations of the activator and catalyst are [A] = [C] = 4.45×10^{-2} mol^{-1}.

$$\beta = 1 - \frac{c_0 + 1}{e^{(1 + c_0)K_0 t} + c_0} \qquad [2.15]$$

This integral function is shown in Fig. 2.5 a. This type of kinetic curve can be treated as a description of a reaction with an apparent induction period t_i. The method of estimating this apparent induction period is also shown in Fig. 2.5. The influence of the constant c_0 on the form of the integral kinetic curve is illustrated in Fig. 2.5 b, where a dimensionless parameter (K_0t) is used as the argument. At $c_0=0$ an apparent induction period is absent (in this case we are dealing with a standard first-order reaction), but with increasing c_0 an apparent induction period appears and becomes longer. At the same time the slope of the main (central) part of the dependence of K_{0t} on c_0 also increases.

Experiments have confirmed that the pre-exponential factor K_0 and the constant c_0, which characterizes the self-acceleration effect, both depend on the concentration of the catalytic complex, i.e., on the concentrations of the catalyst [C] and the activator [A]. On the basis of purely chemical

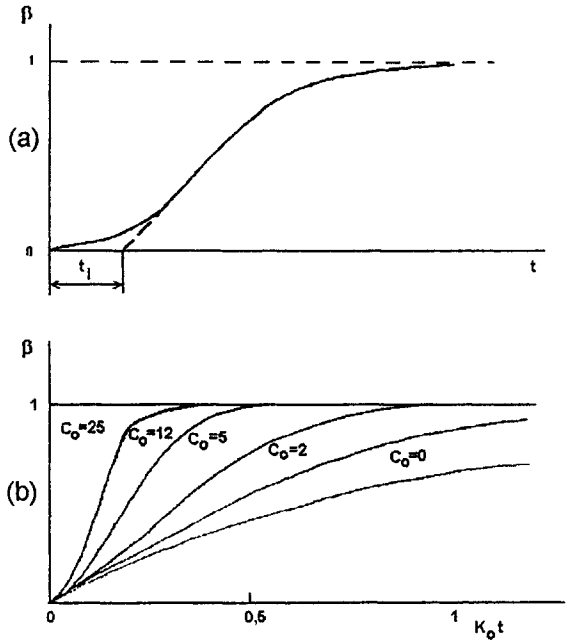

Figure 2.5. Typical pattern of the β(t) dependence in anionic activated polymerization of ε-caprolactam at 170°C (a) and the influence of the constant c_0 (marked on the curves) on the reaction rate (b). The apparent "induction period" is also shown.

arguments, it seems reasonable to have equal concentrations of both components, although some deviation from strict equality is permissible (and sometimes even desirable) in real technological processes. However, the relationships discussed below are correct if the following equality is maintained:

$$[A] = [C]f \qquad [2.16]$$

where f is the functionality of the activator; it is assumed that every molecule of the catalyst has only one functional group. By maintaining this condition, the following dependencies of the kinetic constants on the product [C][A] were found:

$$K = k\frac{[C][A]}{[M]_0} \qquad [2.17]$$

$$c_0 = m\frac{1}{([C][A])^{1/2}} \qquad [2.18]$$

where k and m are empirical constants depending on the nature of the catalytic system.

Table 2.1. Efficiency of different catalytic systems in anionic activated polymerization of ε-caprolactam[31]

Activator	f	$k \times 10^{-10}$, l/mol min	m, mol/min
N-acetyl CL	1	0.77	0.93
Phenylcarbamoyl CL	1	2.22	0.36
2,4-toluene-biscarbomoyl CL	2	2.70	0.70
4,4-diphenylmethane-biscarbomoyl CL	2	6.70	0.16
Hexamethylene-biscarbomoyl CL	2	10.0	0.03

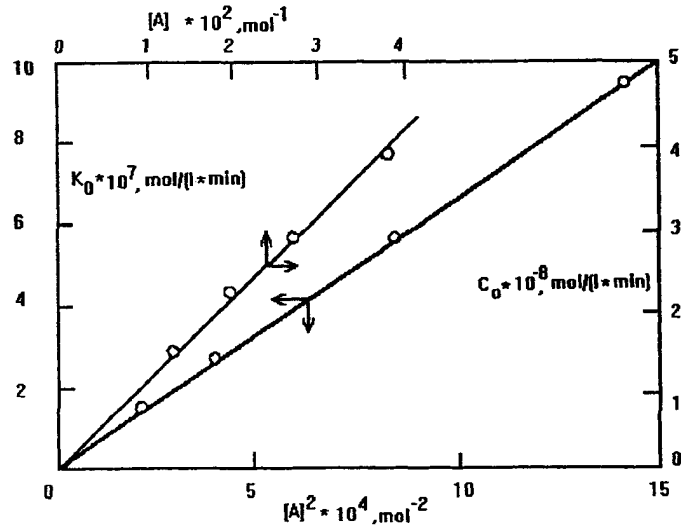

Figure 2.6. Dependencies of kinetic constants on the catalyst concentration in anionic activated polymerization of ε-caprolactam; concentrations of the activator and the catalyst are equal [A] = [C].

The adequacy of these relationships can be seen from Fig. 2.6, where a coordinate system linearizing these equations was chosen. On the basis of Eqs (2.13), (2.17) and (2.18), it is possible to formulate the final equation of the kinetic model for anionic polymerization of ε-caprolactam:

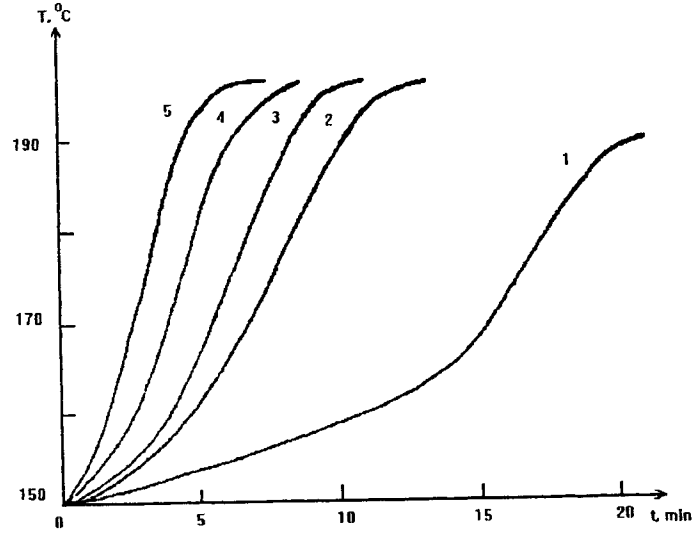

Figure 2.7. Influence of different catalytic systems on the rate of anionic activated polymerization of ε-caprolactam in an adiabatic regime. Numbers on the curves correspond to numbers in the list in Table 2.1.

$$\frac{d\beta}{dt} = k\frac{[C][A]}{[M]_0}(1-\beta)\left[1+\frac{m}{[C][A])^{1/2}}\beta\right]e^{-U/RT} \qquad [2.19]$$

The value of the initial concentration of a monomer $[M]_0$ is introduced in Eq. (2.19) in order to express the constant k in the units of the reaction rate [l/(mol min)]; the coefficient m is expressed in (mol/l). Eq. (2.19) demonstrates that the reaction rate is of second order in the concentration of the catalyst.

The single form of the kinetic equation for anionic polymerization of ε-caprolactam allows us to make quantitative comparison of different catalytic systems using the constants k and m. Such a comparison is represented in Table 2.1. Data reproduced in this table were obtained for the catalyst, Na-caprolactam. Activators from the class of carbamoyl caprolactams (CL) are compared. They are listed in the order of increasing values of k.

It is interesting to note the following rule applying to a homologous series of activators: the higher the initial reaction rate (higher values of k) the smaller the effect of self-acceleration (lower values of m). A typical example demonstrating the pattern of kinetic curves for the systems with different activators listed in Table 2.1 is shown in Fig. 2.7.

It is instructive to compare numerical values of the constant c_0 in Eq. (2.13) for some real systems. For example, if N-acetyl caprolactam is used as an activator, increasing concentrations within

the range of standard formulations, the values of c_0 can vary from 25 to 8.[29] Some other examples are listed below:

Catalyst	c_0	Reference
Na-hexamethylene diisocyanate	6.4	8
Na-hexamethylene diisocyanate-propylene	6.4	8
Na-phenyl diisocyanate	5	9

Thus, in all investigated cases, anionic activated polymerization of ε-caprolactam proceeds with strong self-acceleration. This phenomenon occurs in isothermal conditions and is not related to the increase in temperature due to the exothermal nature of the polymerization reaction. The latter also results in an increase in the reaction rate, but as a rule, it is weaker than self-acceleration due to chemical reasons.

The treatment of kinetic effects in anionic polymerization of ε-caprolactam in terms of self-acceleration is now quite conventional; thus it is considered incorrect to use first- or second- order kinetic equations to describe the kinetics of this reaction, although this was attempted in some early publications. However, the analytical representation of the kinetic function $f(\beta)$ need not be like Eq. (2.14). For example, the same qualitative effect was observed in one publication,[36] which was described in other publications as self-acceleration. A different kinetic function was derived from the proposed set of elementary reactions:

$$f(\beta) = k\frac{1-\beta}{1+c\beta} \qquad [2.20]$$

For low degrees of conversion Eq. (2.20) is the same as Eq. (2.13), because if $c\beta << 1$, then

$$(1-c\beta)^{-1} \approx 1 + c\beta$$

However, if the full range of conversions is of interest, then Eq. (2.20) shows that the constant of self-acceleration c_0 depends on β.

The quantitative discrepancy between the functions represented by Eqs. (2.13) and (2.20) is not large and therefore either one may be used for mathematical modelling of chemical processing. However, experimental data can be better fitted by one or the other equation, since the choice depends on the reactive system under discussion.

Analysis of the non-isothermal polymerization of ε-caprolactam is based on the equations for isothermal polymerization discussed above. At the same time, it is also important to estimate the effect of non-isothermal phenomena on polymerization, because in any real situation, it is impossible to avoid exothermal effects. First of all, let us estimate what temperature increase can be expected and how it influences the kinetics of reaction. It is reasonable to assume that the reaction proceeds under adiabatic conditions as is true for many large articles produced by chemical processing. The total energy produced in transforming ε-caprolactam into polyamide-6 is well known. According to the experimental data of many authors, it is close to 125 - 130 J/cm^3. If the reaction takes place under adiabatic conditions, the result is an increase in temperature of up to 50 - 52°C; this is the maximum possible temperature increase T_{max}. In order to estimate the kinetic effect of this increase

it is convenient to linearize the exponential term in Eq. (2.12). If we let the reaction start at temperature T_0, it is easy to prove that

$$k_0 e^{-U/RT_0} \approx K_0(1 + n\beta) \qquad [2.21]$$

where

$$K_0 = k_0 e^{-U/RT_0}$$

and

$$n = \frac{U\Delta T_{max}}{RT_0^2}$$

The last factor reflects the role of the non-isothermal effect on the kinetics of the process. The complete kinetic equation for non-isothermal polymerization can be written as

$$\frac{d\beta}{dt} = K_0(-\beta)(1 + c_0\beta)(1 + n\beta) \qquad [2.22]$$

We see that an increase in temperature leads to self-acceleration (as expected), but it is important to compare the two accelerating effects, of the reaction (factor c_0) and the other due to the increase in temperature (factor n). The following are reasonable values of the constants: $U \approx 70$ kJ/mol, $T_0 = 433$K and $\Delta T_{max} \approx 50$K, which give $n \approx 2.3$. According to the experimental data cited above, the value of the self-acceleration constant c_0 in ε-caprolactam polymerization is usually considerably larger; i.e., the acceleration due to "inherent" causes is greater than that due to non-isothermal effects. Nevertheless, it would be erroneous to ignore the latter factor completely if we are interested in a quantitatively correct interpretation of the experimental data and adequate modelling of a real process.

2.3.3 POLYMERIZATION OF ω-DODECALACTAM

The polymerization kinetics of ω-dodecalactam in chemical processing has been investigated in a more limited number of publications in comparison with ε-caprolactam. It is not really possible to compare different data; therefore only the results of Ref.[37] will be discussed below. It was shown that up to a degree of conversion $\beta \approx 0.7$, the kinetics of anionic activated polymerization of ω-dodecalactam is described by the first-order equation:

$$\frac{d\beta}{dt} = k_0(1 - \beta)e^{-U/RT} \qquad [2.23]$$

or in isothermal conditions at temperature T_0:

$$\frac{d\beta}{dt} = K_0(1 - \beta) \qquad [2.24]$$

where

$$K_0 = k_0 e^{-U/RT_0}$$

is the initial reaction rate.

However, this equation is of limited value because investigations of the deep conversion stage showed that activation energy changes appreciably. In the initial part of the process, at $\beta < 0.35$, $U = 50$ kJ/mol, but in the conversion range $0.35 < \beta < 0.8$, it appears that the dependence $U(\beta)$ is described by the formula:

$$U(\beta) = 50 + 80(\beta - 0.35) \text{ kJ} / \text{mol} \qquad [2.25]$$

Experimentally the increase in activation energy is quite evident, but the cause of this increase is not clear. It can be argued that the increase in activation energy is related to a strong increase in viscosity of the reactive medium or to phase separation in the reactive mass when a newly formed polymer precipitates from a solution and forms colloid particles. The experimental data described by Eqs. (2.23) - (2.25) can also be treated in ways other than those used in the original publication. For example, it is possible to linearize the exponential factor in Eq. (2.23), as was done above for other purposes. Then for the range of β from 0.35 to 0.8 we can write:

$$e^{-U/RT} = e^{-(U_0 - 80\beta)/RT} \approx e^{-U_0/RT_0}\left[1 - \frac{80}{RT_0}\beta\right]$$

The kinetic equation can then be rewritten in the following manner:

$$\frac{d\beta}{dt} = k_0(1-\beta)(1-\xi\beta)e^{-U_0/RT} \qquad [2.26]$$

where the factor $\xi = 80/RT_0$ represents the effect of deceleration on the polymerization reaction; this effect is quite pronounced due to the high value of ξ. In essence, this interpretation is equivalent to an increase in the activation energy of the reaction.

It is worth emphasizing that deceleration in anionic activation polymerization of ω-dodecalactam is the reverse of self-acceleration in ε-caprolactam polymerization.

Non-isothermal acceleration due to the enthalpy of the ω-dodecalactam polymerization reaction is much less than that of ε-caprolactam polymerization. Indeed, the total heat effect in polymerization of ω-dodecalactam is ≈43 J/g, and it results in a maximum increase in temperature in adiabatic conditions of 18 - 20°C (2.5 times less than for ε-caprolactam).

The rate of polymer synthesis in ω-dodecalactam polymerization is proportional to the first power of the catalyst concentration (in contrast to ε-caprolactam, where the rate is second-order in the catalyst concentration when the concentrations of an activator and the catalyst are equal). If the system Na-caprolactam/Na-acetyl ε-caprolactam is used in equimolar ratio as the catalyst/activator mixture and the range of concentrations is [C] = 0.35 - 1.5 mol% (or 0.0175 - 0.075 mol/l), the dependence of the constant k_0 on [C] is as follows:

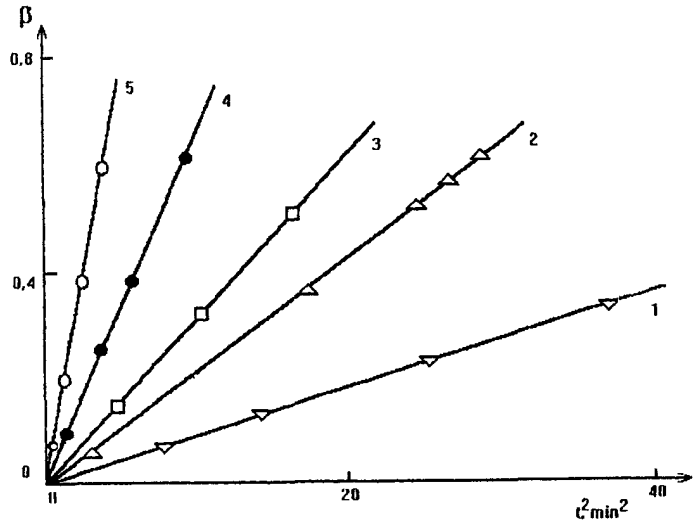

Figure 2.8. Dependencies β(t) in polymerization of ω-dodecalactam, initiated by an indirect activator, N-acetyl diphenylamine. Catalyst: Na. Initial temperature: 180°C. Concentration of the activator [A]: 0.5 mol% (curve 1); 0.75 mol% (curve 2); 1.0 mol% (curve 3); 1.25 mol % (curve 4); 1.5 mol% (curve 5).

$$k_0 = 2.9 \times 10^5 [C] \text{ min}^{-1} \qquad [2.27a]$$

if [C] is expressed in mol%

$$k_0 = 5.6 \times 10^6 [C] \text{ min}^{-1} \qquad [2.27b]$$

and if [C] is expressed in mol/l. This range of concentration covers the whole range used in practice.

There is one especially interesting version of the anionic polymerization of ω-dodecalactam, that uses activators for indirect action.[38] In some technological applications related to chemical processing it may be desirable not to start the reaction at the beginning of the process. Then an activator need not be present in an initial reactive medium but may be synthesized directly from some compounds during the process. In this case, it is necessary to take into account two independent sequential reactions that proceed with comparable rates: formation of active centers for polymerization due to the reaction of the indirect activator and anionic lactam chains propagation. Let the rate constant of the first reaction be k_a and the second one be k_p; then the dependence of the degree of conversion on time in the initial stage of the process is described by the equation:[39]

$$\beta = \frac{1}{2} k_a k_p [A]_0^2 t^2 \qquad [2.28]$$

where $[A]_0$ is the initial (at $t = 0$) concentration of an indirect activator.

An example illustrating the validity of this equation is shown in Fig. 2.8: experimental data are fitted to a straight line in the coordinates β-vs-t^2. Experiments also confirm the validity of Eq. (2.28) for predicting dependence of β on $[A]^2_0$.

Eq. (2.28) is valid for initial part of the reaction. It is also possible to obtain a formula for the whole range of $\beta(t)$. This formula is as follows:[40]

$$\ln(1 - \beta) = - k_p [A]_0 t + \frac{k_p}{k_a} \ln(1 + k_a [A]_0 t) \qquad [2.29]$$

It is easy to show that for small t values, Eq. (2.29) transforms to Eq. (2.28). However, it is interesting to follow the pattern of $\beta(t)$ dependence for the full range of β, from which it can be seen this dependence looks like a kinetic curve with self-acceleration. Thus the phenomenon of self-acceleration, which is observed in some cases, may be treated as a consequence of a two-stage polymerization reaction if the rate constants of both stages have values of the same order. The reaction rate at the initiation stage can be limited by various factors, and in this case, classification of activators as direct or indirect becomes meaningless.[41]

Na-caprolactam is widely used as a catalyst in ω-dodecalactam polymerization. In fact, this means that a copolymer of both lactams enriched in dodecalactam blocks is produced. Synthesis of copolymers of both lactams with different ratios of monomers is used in chemical processing, since varying the ratios of the monomers makes it possible to govern the mechanical properties and melting temperature of the final product and to create a range of products for different applications. In particular, a copolymer in the middle range of monomer ratios is a low-crystalline product with high impact resistance and represents a new engineering material in comparison with both homopolymers. However, practically nothing is known about the kinetics of copolymerization of different lactams.

2.3.4 SYNTHESIS OF POLYBUTENAMIDE

The kinetics of α-pyrrolidine polymerization has been investigated only qualitatively.[42] Nevertheless, it is clear that the nature of the activator (using the catalyst Na-α-pyrrolidine) greatly influences the kinetics of polymerization. For example the presence of Si-C or Sn-Cl groups causes a decrease in the polymerization rate.

A quantitative kinetic model of the polymerization of α-pyrrolidine and cyclo(ethyl urea) showed,[43] that two effects occur: the existence of two stages in the initiation reaction and the absence of an induction period and self-acceleration in α-pyrrolidine polymerization. It was also apparent that to construct a satisfactory kinetic model of polymerization, it was necessary to introduce a proton exchange reaction and to take into consideration the ratio of direct and reverse reactions. As a result of these complications, a complete mathematical model appears to be rather difficult and the final relationships can be obtained only by computer methods. Therefore, in contrast to the kinetic equations for polymerization of ε-caprolactam and ω-dodecalactam discussed above, an expression

for the time dependence $\beta(t)$ applicable to polybutenamide synthesis cannot be written in analytical form.

2.4 KINETIC MODELS OF POLYURETHANE SYNTHESIS

Modern technological practice, particularly the various types of chemical processing, use a great variety of formulations for the synthesis of polyurethanes. Therefore it is nearly impossible to create a general kinetic model which would be valid for various polymerizing systems. However, the same general approach to creating such models can be used for different cases. Therefore, it is useful to demonstrate the method used to construct a model and its characteristic kinetic equations for some typical cases.

The most comprehensive kinetic model for the synthesis of polyurethanes was developed by Macosko and his team.[44-46] In all cases the heart of the model is the degree of conversion, β, which is defined for polyurethane synthesis as

$$\beta = \frac{[R]_0 - [R]}{[R]_0}$$

where $[R]_0$, as before, is the initial and [R] is the current concentration of reactive groups. In the publications cited, a system consisting of 1,6-hexamethylene diisocyanate oligomers (18.5% of NCO-groups) and ε-caprolactone-based triol was used; for this system $[R]_0 = 2.64 \times 10^3$ equiv/m^3.

The authors of the original publications mention that the kinetic equation is rather complicated but does not degenerate into an nth-order kinetic equation. However, in order to use the experimental data for practical calculations and computer simulations of a process, they can be described by the following equation:

$$\frac{d\beta}{dt} = k_0 [R]_0^m (1-\beta)^n e^{-U/RT} \qquad [2.30]$$

where $m = 0.5$ and the order of the reaction is equal to 1.5.

For the specific polymerizing system, mentioned above, $k_0 = 3.14 \times 10^8$ (time in min); U=64 kJ/mol; and the enthalpy of reaction equals 60.33 kJ/equiv.

Equations of an analogous type can be used for other polyurethane-forming systems, although the numerical values of the constants may be different, because Eq. (2.29) must be treated primarily as empirical. It is reasonable to expect that an adequate approximation for other systems would be n equal to 2 (which is typical for polyaddition reactions) and m also equals to 2. Such values of the constants m and n are valid, for example, for RIM-2200 (produced by "Union Carbide"), which consists basically of polyester and 4.4-diphenylmethane diisocyanate.[47]

The kinetics of polyurethane curing in adiabatic conditions was studied by the thermometric method (see Section 2.2) for a composition based on macro(diisocyanate) and diamine.[48] It was proved that in this case, the second-order kinetic equation was inapplicable for the range $\beta > 0.7$. By analyzing the time dependencies of temperature of the reactive medium, it was established that the

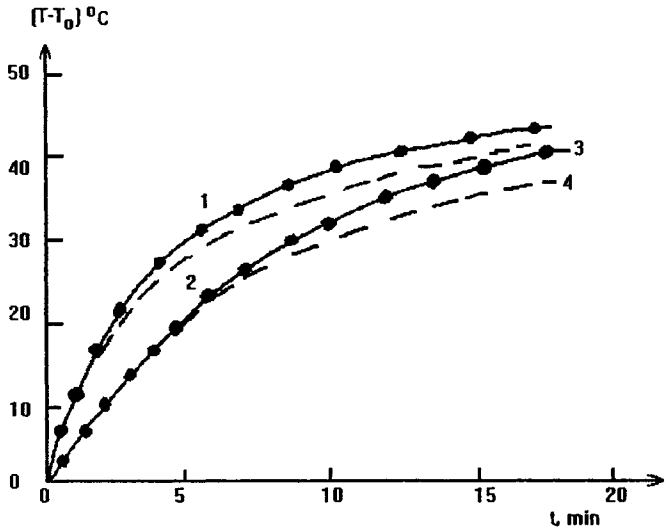

Figure 2.9. Increase in temperature during polyurethane synthesis. Initial temperature, T_0 = 90°C (curves 1 and 2) and 72°C (curves 3 and 4). Solid lines are according to a self-deceleration equation. Dotted lines correspond to the second-order kinetic equation. Points - experimental data.

experimental data could be described by a self-deceleration equation. For isothermal conditions this equation can be written as

$$\frac{d\beta}{dt} = K_0(1-\beta)(1-\xi\beta)$$

Its integral is

$$\beta = 1 + \frac{\xi - 1}{e^{(1-\xi)K_0 t} - \xi}$$

where K_0 and ξ are empirical constants.

This equation shows that at $t \to \infty$ (at the end of the process) a limiting degree of conversion $\beta_\infty = \xi^{-1}$ is reached, and this limiting value is less than 1; i.e., we have an incomplete conversion. In particular, in adiabatic conditions at $\beta \to \beta_{ad}$, the temperature T approaches the limit T_{ad} and consequently we have:

$$k_0 e^{-U/RT}(1-\beta) \to k_0 e^{-U/RT_{ad}}(1-\beta_{ad}) = \text{const}$$

and again we reach a limit of conversion which is less than 1. At $t \to \infty$, at the end of the process, the rate must decrease to zero; consequently $(1 - \xi\beta_{ad}) = 0$ and $\beta_{ad} = \xi^{-1}$.

The experimental curves in Fig. 2.9 are compared with the curves calculated according to the second-order kinetic equation for two different initial temperatures. The divergence between the pairs of curves at the final stages of the process reaches 15%, while the experimental is less than 3%. This proves that the equation is inadequate. On the other hand, a kinetic equation that takes into account the effect of self-deceleration fits the experimental data along the whole curve. Therefore, we can predict that the reaction in the system under discussion will be incomplete.

Some investigators who studied polyurethane synthesis proposed that both the forward and the reverse reactions were important. For example this approach was assumed for the formation of linear polyurethane,[49] and the following kinetic equation was derived:

$$\frac{d\beta}{dt} = k_f C_0 (1-\beta)^2 - k_r \beta \qquad [2.31]$$

where k_f is the rate constant for the forward reaction, and k_r is the rate constant for the reverse reaction.

Regardless of the detailed form of the kinetic equations describing polyurethane synthesis in chemical processing, it is possible to state that these equations are exponential and that the value of the exponents will depend on the formulation of the reactive system.

The next problem which needs to be discussed in modelling a process is the calculation of an average molecular weight, because the performance characteristics of a material depend on its molecular weight. It is well known that the average molecular weight of a polymerized product depends on the degree of conversion β, and if the chemical evolution of the reaction is known, the molecular parameters of the reactive system can be found.

As an example, the following relationship between weight average molecular weight M_w and β for a two-component reactive system can be given.[46] Let the number and weight average molecular weights of the two components be:

$$M_{n,1} = 454; \quad M_{w,1} = 810; \quad M_{n,2} = 537; \quad M_{w,2} = 715.$$

Then the weight average molecular weight of the polymerizing system as a function of the degree of conversion can be calculated from the formula[46]

$$M_w = 768 + \beta \frac{1725\beta + 1200}{1 - 2\beta^2} \qquad [2.32]$$

During synthesis of a polymer, particularly of polyurethane, gaseous products can appear. Therefore, a complete model of the process must take into account (at least in some cases) the possibility of local evaporation and condensation of a solvent or other low-molecular-weight products. Such a complex model is discussed for chemical processing of polyurethane that results in formation of integral foams in a stationary mold.[50] In essence, the model is an analysis of the effects of temperature in a closed cell containing a solvent and a monomer. An increase in temperature leads to an increase in pressure which influences the boiling temperature of the solvent and results in an increase in cell volume. The kinetics of polymerization is described by a simple second-order equation. The

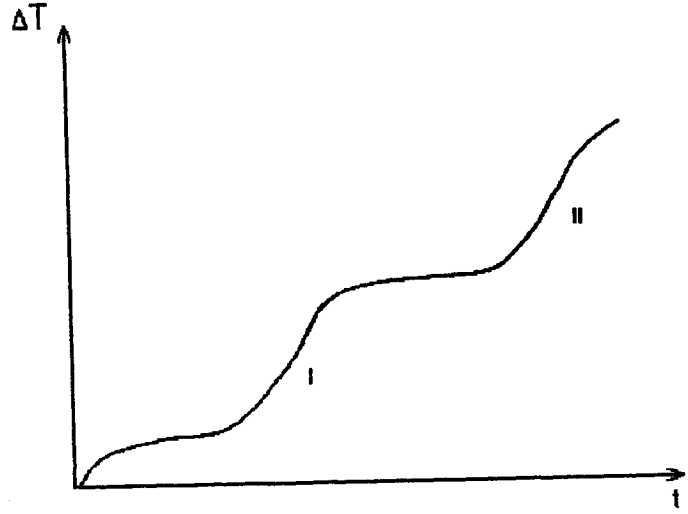

Figure 2.10. Temperature increase in adiabatic polymerization of polyurethane accompanied by the formation of interpenetrating networks in the polyurethane-unsaturated polyester system.

energy balance equation is used in its usual form, but an important new element of the model under discussion is an "equation of state" for the medium inside every cell. The complete system of equations was solved numerically, and the computer simulation allowed the authors to calculate distributions for the main factors, such as temperature, degree of conversion, and density through the volume of a cell (or a slab). It is worth mentioning that this method of calculation gives quite good estimates of time change in density with time, including the appearance of the dense crust and foam core of an article at the final stage of the process.

This model, which is discussed in detail in the publication cited, can be successfully used to analyze chemical (reactive) processing of foamed items of different sizes and shapes.

The problem of modelling polyurethane synthesis in reactive processing is similar to the related problem of the formation of interpenetrating networks in two-component systems, for example the polyurethane-unsaturated polyester mixture. This is a complicated material with a wide range of permissible ratios and corresponding variations in the properties of the end product. Formation of interpenetrating networks can occur in various chemical systems and by different mechanisms. For example, polyester is synthesized by the free-radical polymerization method, while polyurethane forms as a result of a polyaddition reaction (polycondensation). Different phenomena, such as gelation, glass transitions,and phase separation,may occur in the course of the reaction,partly due to the incompatibility of the components. Therefore, the study of the kinetics of formation of the final

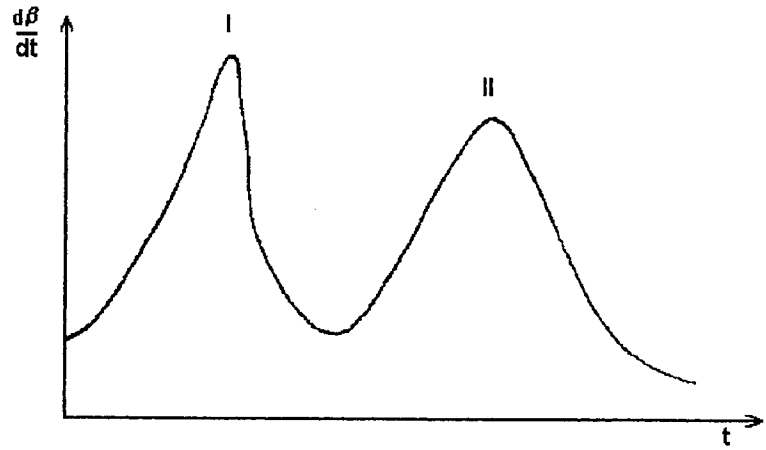

Figure 2.11. Changes in the rate of curing in the polyurethane-unsaturated polyester system.

product is perforce limited to a phenomenological approach to the final degree of conversion. However, it is quite enough for processing purposes, i.e., for choosing the appropriate temperature and time regimes. In this case, the clearest results can be obtained by thermometric or calorimetric methods. If the adiabatic temperature increase is measured as a function of time, two separate parts in the curve are clearly seen (Fig. 2.10). The first part (I) is due to polyurethane synthesis and the second (II) is related to polyester formation. The time dependence of the reaction rate can be estimated from this curve, as shown in Fig. 2.11. There are two separate maxima (I for polyurethane and II for polyester), connected with the two above-mentioned reactions. The relative heights of the maxima depend on the ratio of the components in the reactive medium.

In discussing the formation of interpenetrating networks, we may reasonably assume as a first approximation that the synthesis of each component occurs irrespective of the others, and that the kinetics of the process is determined by the concentration of one or another component. However, this is a rather rough approximation, which is more or less valid at low concentrations of the polyurethane component. As was shown before,[51] when the content of polyurethane exceeds 50%, its network begins to work as a cage, preventing polyester formation because the primary polyurethane network hampers diffusion of the ester. This means that in such systems, mutual interference of the components occurs even in the absence of chemical interactions between them.

An approach based on measuring temperature changes in adiabatic polymerization or heat effects in an isothermal reaction gives us a clear picture of the process, although the overall estimate of the process characteristics of a chosen formulation has only limited validity.

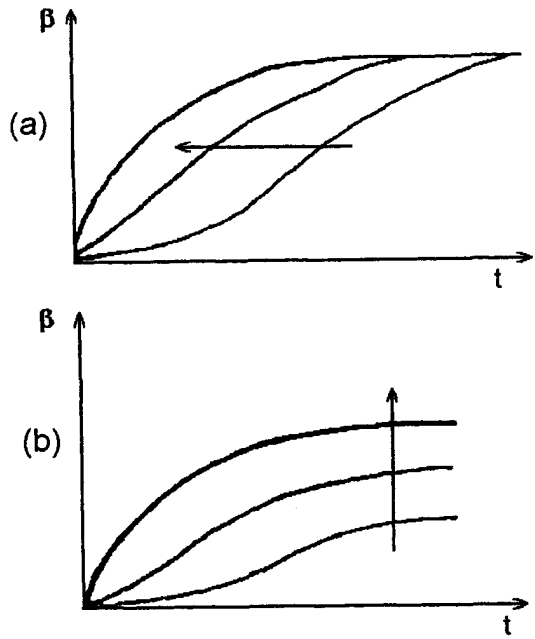

Figure 2.12. Time dependencies of the degree of conversion in epoxy resin curing for complete (a) and incomplete (b) conversion. The arrow shows the direction of the temperature increase.

2.5 KINETIC MODELS OF CURING OF EPOXY-BASED COMPOUNDS

Epoxy resins and other chemical products containing reactive epoxy groups are used in various combinations and compositions for producing engineering materials that are cured (solidified) directly in a mold during processing of finished products. All these processes are quite similar to reactive processing. A great variety of materials belong to this class of products; therefore, it is impossible to construct a general kinetic model of curing of epoxy resins, and we are only able to formulate common approaches and discuss some typical results.

The following main factors help to determine the course of the curing process for epoxy resins. First, a correlation exists between the change in concentration of the epoxy groups and the modulus of elasticity of the product. Second, at least in some cases there is a distinct correlation between the heat of reaction and the modulus of the product material. Third, measured values of the modulus of elasticity correspond to parameters of the molecular network formed during curing of epoxy resin.[52] All this means that by measuring the modulus of elasticity we obtain an adequate representation of the chemical reaction and at the same time obtain direct quantitative characteristics of the material at different stages of the process.

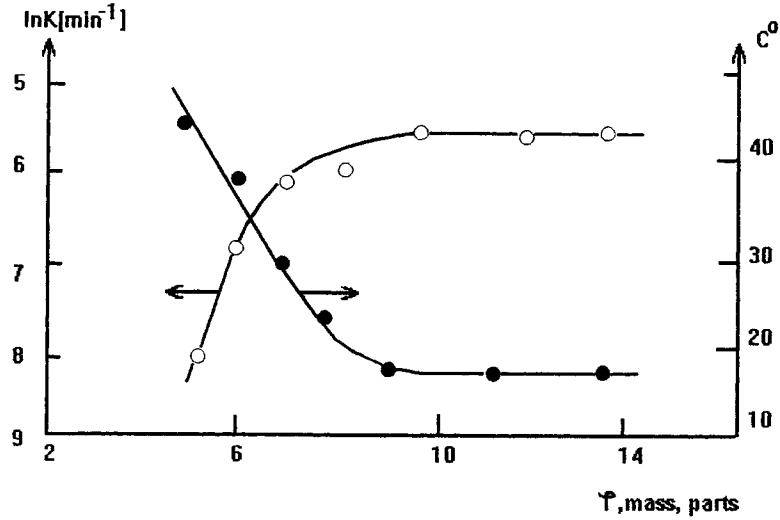

Figure 2.13. Dependencies of the rate constant of a reaction K and the constant of self-acceleration c_0 on the concentration ϕ of a curing agent (dicyandiamide).

The degree of conversion $\beta(t)$ calculated from changes in the modulus of elasticity is a measure of the "chemical" degree of transformation of epoxy-based composites, and the time derivative $d\beta/dt$ is characteristic of the reaction rate. In an analysis of the time dependencies of β for epoxy-based composites, two situations can be distinguished, which are shown in Fig. 2.12. In Fig. 2.12 the arrow shows the direction of temperature increase. In the first case, complete conversion takes place at any temperature and the limiting degree of conversion $\beta = 1$. Temperature influences the rate of the process only. In the second case, decreasing temperature not only slows the process but limits the final degree of conversion. Transition of a reactive mass to the glassy state may be the most obvious reason for incomplete conversion at low temperatures. However, the situation represented in Fig. 2.12 b, can also be observed at temperatures much higher than the glass transition temperature of the reactive mass. Therefore, it is necessary to search for other reasons for incomplete conversion, such as topological restriction.

For the case where complete conversion is reached (i.e., $\beta \rightarrow 1$ when the reaction time is sufficiently long), the following rheokinetic equation, which assumes a self-acceleration effect, is

$$\frac{d\beta}{dt} = K(1-\beta)(1 + c_0\beta) \qquad [2.33]$$

The constant K in this equation, as in some other cases discussed above, denotes the initial reaction rate. Its temperature dependence is described by the standard Arrhenius equation with activation energy U. The constant c_0 characterizing the self-acceleration does not depend on temperature but does depend on the composition of the reactive medium; in particular, such factors as the chemical structure and concentration of the curing agent, and the concentration of the catalyst and other components influence the value of c_0.

The occurrence of self-acceleration during curing of epoxy resins and epoxy-based compounds was proven by rheokinetic and calorimetric methods.[53] This phenomenon can be treated formally in terms of an induction period (when the reaction is very slow in the initial stage of a process), followed by a constant rate. However, it seems preferable to use a single kinetic equation incorporating the self-acceleration effect to describe reaction as a whole. Such a kinetic equation contains only a limited number of constants (K and c_0 in Eq. (2.33)) and allows easy and unambiguous interpretation of their dependencies on process factors.

A typical example illustrating the dependencies of K and c_0 (kinetic curves fitted by Eq. (2.33)) on concentration of the dicyandiamide curing agent Φ is shown in Fig. 2.13 for the system bisphenol A - dicyanodiamide. The dependencies $K(\Phi)$ and $c_0(\Phi)$ are opposite, although both of them become straight horizontal lines at high concentrations of the curing agent.

Values of the activation energy U for the curing of epoxy resins depend on the chemical composition of the system, although as a general rule, U lies in the range 50 - 70 kJ/mol. It is also interesting to note that the same value of activation energy is obtained when the temperature dependencies of K and gelation time t^* are compared, which proves the existence of a direct correspondence between K and t^*. The relationship beween these two parameters can be obtained from the general kinetic equation (2.33). For $t = t^*$ the degree of conversion equals β^*, and then Eq. (2.33) gives:

$$t^*K = \frac{1}{1 + c_0} \ln \frac{1 + c_0\beta^*}{1 - \beta^*} \qquad [2.34]$$

where β^* is the characteristic temperature-independent degree of conversion at the time of gelation, i.e., when a three-dimensional network has formed throughout the whole volume of the material.

Incomplete conversion must also be covered by the rheokinetic equation. A possible version of such an equation is:[54]

$$\frac{d\beta}{dt} = K(1-\beta)(1 - \xi\beta) \qquad [2.35]$$

i.e., an equation with a self-deceleration term, as was discussed above for the other case. As before, the constant characterizes the decreasing reaction rate at the final stage of the process, and the limit-

ing degree of conversion $\beta_\infty = \xi^{-1}$. It is evident that, at $\xi = 1$, Eq. (2.35) transforms to the ordinary second-order kinetic equation, and in this limiting case $\beta_\infty = 1$.

It is generally found that the constant ξ, in contrast to c_0, depends on temperature. If the temperature dependence of $\xi(T)$ is represented by the standard Arrhenius equation, then the apparent activation energy appears to be on the order of 10 kJ/mol, which is close to the activation energy of most fluid diffusion processes.

In the most general case, curing of an epoxy-based compound can be accompanied not only by self-acceleration at the beginning of the process but also simultaneous slowing of the reaction in its final stage. Therefore the complete rheokinetic equation can be written as follows:

$$\frac{d\beta}{dt} = K(1-\beta)(1 + c_0\beta)(1 - \xi\beta) \qquad [2.36]$$

Constants K and ξ have the same meaning as before and have different values for every composition.

In discussing the kinetics of epoxy-based oligomer curing, it is important to examine some general features of the influence of the reactant composition on the reaction rate. Although it is difficult to do this in a generalized way due to the numerous possible formulations, some important features can be noted. For example, let us analyze the results of a kinetic investigation of epoxy oligomer curing by m-phenyl diamine.[55] Adiabatic calorimetric measurements were made on this system. The concentration of Y epoxy groups that have reacted at time t, when the temperature has reached T(t), is given by the equation:

$$Y = \frac{C_p\rho}{Q}[T(t) - T_0] \qquad [2.37]$$

where T_0 is the initial temperature; C_p is the specific heat; ρ is heat density; Q is the heat (enthalpy) of the reaction. For the reaction under discussion Q = 0.68 kJ/mol and the term $(Q/C_p\rho) = 25.7$ (K l)/mol.

It was found that the initial reaction rate was equal to Y_0A_0, where Y_0 and A_0 are the initial concentrations of epoxy groups and m-phenyl diamine. Formation of hydroxyl groups during the reaction leads to self-acceleration. This prediction was confirmed by measurements carried out in an isothermal regime, because adiabatic conditions for a reaction lead to self-acceleration due to an increase in temperature (see above). Thus, the initial reaction rate v_0 can be expressed as

$$v_0 = \frac{Q}{C_p\rho}k_0Y_0A_0e^{-U/RT} \qquad [2.38]$$

where k_0 is constant and U is the activation energy equal to 52±2 kJ/mol.

It is interesting to note that the kinetics of this reaction can also be treated the same as this of a process with an induction period. In this approach, the activation energy calculated from the temperature dependence of the induction time is the same as that found for the initial reaction rate.

Eq. (2.38) is valid for the initial part of a reaction. However the influence of concentration on the kinetics of the reaction as a whole is not so simple, and a quantitative description of the process

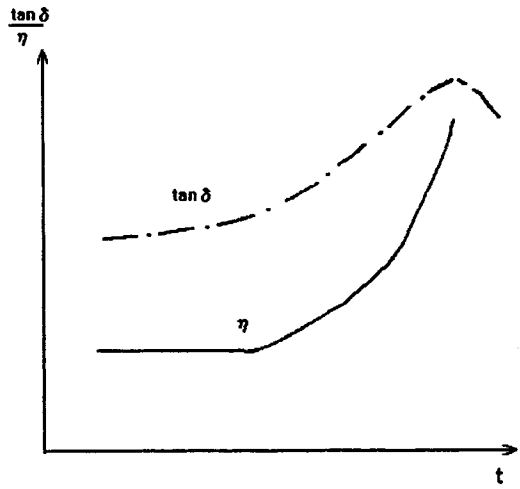

Figure 2.14. Changes in viscosity and loss tangent during a curing process.

requires the construction of a rather complicated kinetic model.[56] In particular, it was shown that the initial rate of the curing reaction increases with an increase in the molecular weight of the epoxy oligomer, but the higher the molecular weight the weaker the dependence of the initial rate on Y_0. In general, the existence of a group of catalytic and non-catalytic reactions proceeding simultaneously during curing of epoxy oligomers leads to a system of kinetic equations which cannot be replaced by a single phenomenological one-parameter equation, as is possible in some other cases.

Curing behaviors are very interesting, but in the actual practice of processing epoxy-based compounds it is also important to know how the properties of the material vary before the gel-point t^*, while flow is still possible. From this point of view, the time dependence of viscosity $\eta(t)$ is of primary interest. Numerous experimental data for $\eta(t)$ can be found in various publications, but they all relate to specific systems. Also, in some cases, monitoring of curing was carried out not by direct viscosity measurements but by following changes in the dynamic properties of the material, and by mechanical loss or dynamic viscosity measurements at fixed frequency. The viscosity was then recalculated from the experimental data, a not entirely satisfactory procedure. On the other hand, the use of a dynamic method can be especially fruitful for fast curing processes when direct viscometry

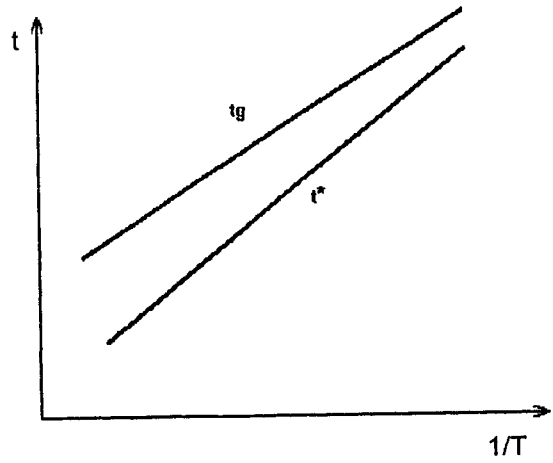

Figure 2.15. Correlation of the gel-time t^* and the time period before the glass transition t_g in epoxy resin curing. [Adapted, by permission, from O. Harran, A. Lauconard, *J. Appl. Polym. Sci.*, 32 (1986), 6058.]

cannot be applied; this is true, for example, for monitoring the curing of epoxy-based compounds, when curing is initiated by ultraviolet radiation.[57]

In some publications it has been stated that the moment of gelation is characterized by the equality $\tan\delta = 1$.[58] However, it has been proven that this criterion is not generally valid.[59] Nevertheless, monitoring of the initial stages of curing by measuring the changes in mechanical losses with time is applicable to many situations. It is worth mentioning that during the initial stage of curing of epoxy resins, as a general rule, $\tan\delta >> 1$.[60] Measuring viscosity and its changes is a very useful method for assessing the properties of epoxy resins. Three factors determine properties: the initial viscosity, the activation energy of viscous flow (which is on the order of 60 kJ/mol), and the "induction period", which is treated as the period of time during which viscosity stays practically unchanged in comparison with its initial level.

Estimates of the time period over which processing of a composite is possible, are rather arbitrary and are based on the choice of some level of viscosity, up to which the reactants can be treated as a viscous liquid. Measuring $\tan\delta$ can be useful for this purpose, because it was shown that the most rapid increase in viscosity occurs in the vicinity of values of $\tan\delta$ close to 1,[57] even if this value does not correspond to the gel-point, as illustrated in Fig. 2.14. Therefore, the position of the point corresponding to $\tan\delta = 1$ may have different meanings: in some cases it is related to gelation, in others, to the maximum increase in viscosity.

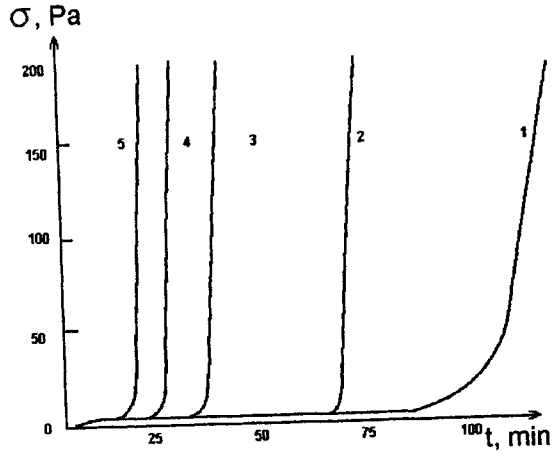

Figure 2.16. Changes in shear stress vs. time before the gel-point during curing of an unsaturated ester based composite at different temperatures: 140°C (curve 1); 150°C (curve 2); 160°C (curve 3); 170°C (curve 4); 180°C (curve 5).

As Gillham and his co-authors showed in many publications,[61,62] changes in the rheological properties of materials during curing, and of epoxy resins in particular, are controlled by two phenomena – gelation and the glass transition. Moreover, in low-temperature curing, the glass transition can occur before gelation so that that a three-dimensional network is absent from the final product. This point may seem obvious, even though it was stated that the time to gelation t^* in isothermal curing of epoxy resins is always shorter than the reaction time t_g leading to a glass transition in the material,[63] as shown in Fig. 2.15. At lower temperatures, t^* approaches t_g but invariably $t^* < t_g$, which means that gelation always proceeds a glass transition.

2.6 KINETIC MODELS OF CURING OF UNSATURATED POLYESTERS

Unsaturated polyesters - oligo(ester maleinates and fumarates) are the basis of numerous composites used for molding articles by the reactive (chemical) processing method in different technological schemes. As with other materials, rheokinetic investigations of the curing process of unsaturated polyesters have two aims: a description of the viscosity changes up to the gel-point and modelling the complete curing process.

The increase in viscosity at the initial stages of a process is related to formation of a prepolymer, i.e., a transition from a monomer (or a monomer-polymer mixture) with viscosity in the range of 0.01 - 1 Pa s to a prepolymer with viscosity 100 - 1000 Pa s. The increase in viscosity occurs almost as a jump, i.e., very sharply in a relatively short induction period. A typical example is shown

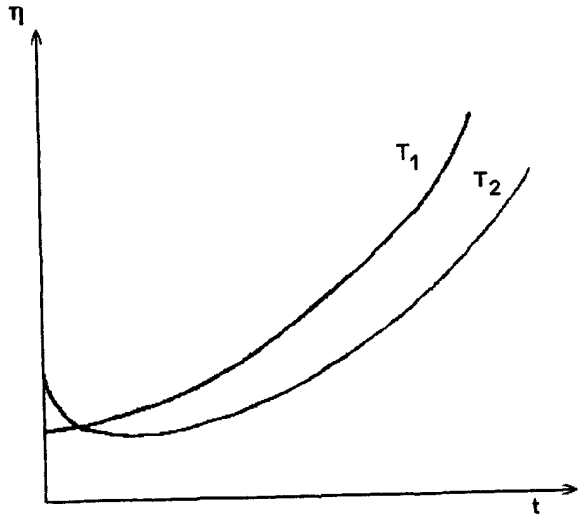

Figure 2.17. Change in viscosity in non-isothermal gelation and curing of an unsaturated polyester at different temperatures ($T_2 > T_1$).

in Fig. 2.16[64] for an ester-based composite with an initial viscosity of 2 Pa s at 30°C, where a "threshold" in the viscosity change (or shear stress at constant shear rate, as in Fig. 2.16) is clearly seen.

By taking into account this sharp increase in viscosity, we can represent the dependence $\eta(t)$ by an exponential function:

$$\eta = \eta_0 e^{t/t_0} \qquad [2.39]$$

where η_0 is the initial viscosity level, t_0 is a characteristic time constant, depending (as does η_0) on temperature; at $t << t_0$ we have $\eta \approx \eta_0$; therefore, t_0 can be treated a measure of induction period.

Using an exponential equation to describe the time dependence of the viscosity clearly represents this process adequately, and in many cases the fit to the experimental data is quite satisfactory. However, this approach does not allow us to determine the gel-point directly. The gel-point is defined as the time when the viscosity increases without limit; but according to Eq. (2.39), the viscosity is always limited (although it can be very high) at any specified time. Therefore, if order to use Eq. (2.39), in practice, it is necessary to characterize the properties of a material either by the time t_0 or by the time required to reach a certain viscosity level, for example 1000 Pa s.

The non-isothermal nature of the process is one of the most important problems in the gelation and curing of ester-based compounds, since the increase in temperature in the reaction can reach

100°C. This figure is appropriate for adiabatic polymerization, which approximates reality in reactive processing of large articles with high volume-to-surface ratios. In this case, it is impossible to remove the heat effectively and to avoid intense local temperature jumps. Therefore, it is essential to know how to calculate temperature increase for reactions proceeding in non-isothermal conditions. The time dependence of viscosity in this situation can be written as

$$\eta = \eta_0 e^{[(E/RT) + B\beta(t)]} \qquad [2.40]$$

where E is the activation energy for viscous flow; B is a constant reflecting the dependence of viscosity on the degree of conversion $\beta(t)$; η_0 is a pre-exponential factor.

To carry out further calculations, the kinetics of a reaction, i.e., $\eta(t)$ dependence, must be known. As a first approximation, let the reaction rate be constant at temperature T. Then we have a first-order kinetic equation such that

$$\beta(t) = k_0 t e^{-U/RT} \qquad [2.41]$$

where k_0 is a constant and U is the apparent activation energy of the chemical process. Then we derive the following equation for the time dependence of the viscosity:

$$\eta(t) = \eta_0 \exp\left[\frac{E}{RT} + Bk_0 t e^{-U/RT}\right] \qquad [2.42]$$

The function T = T(t) in Eq.(2.42) is determined by the heat of reaction, as discussed above (see, for example Eq. (2.9)). Experimental data confirm that such an equation is correct when there is an inherent source of heat due to an exothermal process of prepolymer formation and when temperature profile is dictated by the surroundings.[65]

Eq. (2.42) predicts that in the initial stages of the process, the viscosity of a reactive medium must decrease due to the input of the first term in the exponential (as in Fig. 2.17).Only after that does an increase in viscosity (explained by the increase in molecular weight of the prepolymer - the second term of the exponential) becomes dominant. In this case, the two curves corresponding to different initial temperatures T_1 and T_2 cross each other, because at $T_2 > T_1$ we have $\eta_{0,1} > \eta_{0,2}$ but the reaction rate is greater at T_2. Therefore,the reduction in viscosity at higher temperature resulting from the higher rate of increase in the molecular weight of the prepolymer will overcome the greater viscosity at a lower initial temperature. Experimental data confirm this prediction. This provides a means of governing the kinetics of a reaction by varying the temperature during the process: an increase in temperature during the later stages allows us to decrease the initial temperature and to shorten the induction period. Thus we can regulate the overall reaction rate as desired by varying temperature during the process.

Polyester resins are frequently used as binders in various composites. Therefore it is necessary to know the effects of solid fillers or reinforcing fibers on the properties of a material. Systematic investigations[66] that all the main effects observed when a filler is introduced into a low-viscosity matrix also occur with polyester resins. As was shown in many cases the presence of a filler leads to a

decrease in the rate of viscosity increase. Clearly this effect depends on both the content and the chemical nature of the filler, and we observe that the filler may have a double role: it can interact with the matrix and change its reactivity, and it can also form its own three-dimensional structure, thus influencing the rheological properties of a composite. If a non-active filler is used, the Newtonian flow properties of the composite remain the same as those of a polyester matrix. Introducing active fillers results in non-Newtonian properties in a composite up to the appearance of yield stress. The elasticity of the material also increases, and as a result, normal stresses (Weissenberg effect) appear and become appreciable.

Numerous experimental data clearly show[67,68] that the rheological properties of polyester-based composites can be regulated by varying the material proportions. The latter is also true for some additives that are used in very small quantities. It is to be expected that varying the proportions would change the rate of viscosity increase and limiting level of viscosity achieved during gelation. Therefore, there is a vast field for regulating both the processing properties of polyester-based compounds and the properties of the end-products.

Studies of rheokinetics over the whole range of polyester curing is based (as for other materials) on a dynamic method, i.e., on measurements of the time dependence of the dynamic modulus at a fixed frequency, from which the time dependence of the degree of conversion $\beta(t)$. The observed dependence $\beta(t)$ for polyester resins can be analyzed by an equation of the type used for other materials. Thus the following general equation was proposed for the kinetics of curing polyester and epoxy resins:[69-72]

$$\frac{d\beta}{dt} = (k_1 + k_2\beta^m)(1-\beta)^n \qquad [2.43]$$

where k_1, k_2, m and n are empirical parameters.

Although simpler power equations were used in earlier publications,[72] later investigations[67,68,74-77] confirmed that the phenomenological Eq. (2.43) corresponds much better to the numerous experimental data.

It is interesting to note the following results cited in these publications. First, the sum of the exponents $m + n = 2$ which diminishes the number of arbitrary constants. Second, m and n do not depend on temperature (changes of both constants with temperature were mentioned only in[74]). Third, while k_1 and k_2 are strongly temperature dependent functions, their ratio which characterizes the effect of self-acceleration is almost independent of temperature. This was also mentioned above in the discussion of self-accelerating kinetics equations for lactam polymerization. Values of the constants m and n according to the experimental data from several publications are listed below:

m	0.25	0.35	0.45	0.49
n	1.75	1.67	1.55	1.55
m + n	2.00	2.02	2.00	2.04
Reference	33	35	36	38

According to the results of many authors, the apparent activation energy, calculated from the temperature dependence of k_2, generally lies in the range 76±3 kJ/mol, although some other values have also been found. For example, according to,[78] $U \approx 40$ kJ/mol, although this value was found from the temperature dependence of the modulus and not from the constants of the kinetic equation at the fixed frequency.

It is quite evident that the critical value of the time to gelation t^* must depend on the temperature, because of the temperature dependence of the reaction rate. More interesting and unexpected was the finding that the critical value of the degree of conversion β^* in the curing of polyester resins also depends on temperature,[74,75] although it might be expected that β^* would be a purely topological (rather than a kinetic) parameter of a network.However it may be that the temperature dependence of β^* is explained by inhomogeneity in the formation of a network of chemical bonds during polyester curing.

The main application of interest is connected not with polyester resins themselves but with polyester-based compounds. Therefore, it is interesting to know how a filler influences the kinetics of curing. Different cases are possible, and the presence of a filler can have a strong effect on a "life time" of a material (which determines whether a material can be processed) and its rate of curing. Systematic and complete investigations of this problem are unavailable and general conclusions are a most impossible due to the great variety of fillers and mix ratios in multicomponent compositions. However, some known examples convincingly the need to consider this factor when discussing the properties of filled composites. Filling a polyester resin with small glass or phenolic spheres results in a twofold change in the lifetime of a material[79] (i.e., the time during which processing of a material is possible, because the material stays fluid). It is evident that, various effects can be expected from different interaction between the filler and the polyester binder. In principle, it is possible to use these interactions to optimize the process and performance characteristics of a material.

2.7 NON-ISOTHERMAL POLYMERIZATION IN A BATCH-PROCESS REACTOR

In current industrial practice, reactive processing carried out in non-isothermal conditions, for both inherent and other reasons, such as changes in temperature at the surface of an article during the process cycle. Inherent reasons are the existence of inner heat sources, which can be of chemical origin (enthalpy of reaction), heat of phase transition from crystallization of a newly formed polymer or heat dissipated due to the flow of a reactive mass.

Transfer of the theoretical results obtained for isothermal conditions to the non-isothermal case is rather simple; provided the temperature dependencies of the constants are known. A theoretical analysis of non-isothermal processes may be limited by thermal runaway, which is equivalent to the thermal instability already thoroughly studied for chemical reactors.[80,81] There are two limiting situations, known as the Semenov and Frank-Kamenetzky models;[80,82] these correspond to periodic ideal stirred and periodic ideal plug reactors, respectively.

Temperature and concentration gradients are absent inside an ideal stirred reactor. Mixing can be achieved by forced or free-convective movement of a material. For such a reactor the energy balance equation can be written as:

$$C_p\rho\frac{dT}{dt} = Q\rho k_0 e^{-U/RT} f(\beta) - \kappa\frac{S}{V}(T - T_{sur}) \qquad [2.44]$$

where C_p is the specific heat; ρ is the density; Q is the enthalpy of the reaction; k_0 is a pre-exponential factor; U is the apparent activation energy of the chemical reaction; κ is the heat transfer coefficient; S is the surface area of heat exchange; V is the volume of the reactive medium; T is temperature of the reactive medium; T_{sur} is the temperature of the surroundings; $f(\beta)$ is a kinetic function for an isothermal reaction. A system, described by Eq. (2.44) and first-order kinetic reaction, was analyzed.[83,84] This approach is convenient for modelling reactive processing of large slabs or articles because the polymerization regime inside these items is close to adiabatic (the Biot Number is less than 1). The complete formulation of the reactive processing model is based on the theory of an ideal plug reactor undergoing a non-stationary chemical reaction with conductive heat exchange. One possible formulation of the problem is as follows:[85]

- the reaction inside a certain volume is one-stage and irreversible;
- heat exchange in the reaction zone is by conduction;
- movement inside the reactive mass and convective transfer are absent;
- the initial reactive mass and the final product are in the same phase, i.e., the chemical reaction is not accompanied by phase transitions;
- the boundary of the volume is impermeable to the reactive material;
- heat exchange through the boundary occurs according to Newton's law;
- the parameters characterizing the physical properties of material (specific heat, density, thermal conductivity), the kinetics and thermodynamics of the chemical reaction (pre-exponential factor, apparent activation energy, enthalpy), and the process conditions (ambient temperature, pressure, shape and size of the reactive volume) do not change in the course of the process.

Based on these assumptions, the mathematical formulation for condensed media can be expressed by the following system of equations:

$$C_p\rho\frac{dT}{dt} = \lambda\left(\frac{d^2T}{dx^2} + \frac{n}{x}\frac{dT}{dx}\right) + Q\frac{d\beta}{dt} \qquad [2.45]$$

and

$$\frac{d\beta}{dt} = k_0 e^{-U/RT} f(\beta) \qquad [2.46]$$

The boundary conditions are:

at $x = 0$

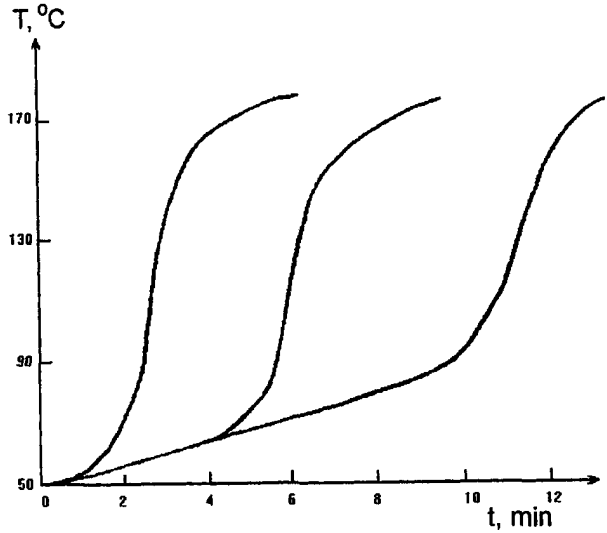

Figure 2.18. Development of temperature profiles along the length of the reactor (at three arbitrary points) vs. time during front polymerization.

$$\frac{dT}{dt} = 0$$

at x = r

$$-\lambda \frac{dT}{dx} = \kappa(T - T_{sur})$$

The initial conditions are: at t = 0, T = T_0, and $\beta = 0$. The parameter n characterizes the dimensions of the volume: for a parallel plate reactor n = 0; for a cylindrical reactor n = 1 and for a spherical reactor n = 2. In these equations, x is a space coordinate; λ is the coefficient of thermal conductivity; r is the characteristic size of the reactor; κ is the heat transfer coefficient; and T_0 is the initial temperature of the initial medium.

Analysis of the system (2.45) - (2.46) was carried out[84] for a wide range of values of parameters U and Q. It is clear that the temperature field is inhomogeneous throughout the reactor the degree of conversion is also inhomogeneous. The degree of inhomogeneity increases with an increase in the Frank-Kamenetzky criterion δ, which is a measure of the ratio of the rates of heat output and heat removal due to thermal conductivity. This parameter is given by:

$$\delta = \frac{Qk_0 Ur^2}{\lambda RT_0^2 e^{U/RT}}$$

At low values of λ polymerization proceeds with a relatively uniform distribution of temperature and degree of conversion throughout the reactive volume ("volume" polymerization regime). At high values of λ, the reaction is completed first in the outer layers of the reactive volume and then moves into the center of the reactor ("front" polymerization regime).[83,84] This process was studied in detail for radical polymerization of acrylics,[86] epoxy resins,[87] and ε-caprolactam.[88] In a front polymerization with reaction temperature T_0, the reaction will be virtaully absent below this temperature. Initially wall temperature is increased to T_0, and this "bursting" temperature is enough to initiate the reaction. Then the reaction starts, and is accompanied by heat output due to the exothermal effect. The heat flux moves along the reactor due to thermal conductivity and initiates a reaction in the adjacent layers of the reactive medium. Thus, the reaction front is moving, and the process becomes stationary with a definite time. Fig. 2.18 shows the evolution of the temperature profiles along the length of the reactor during curing of an epoxy dian oligomer by poly(ethyl polyamine).[87] It is important that the planar reaction front and the nearly complete conversion of the reactants create optimal conditions for producing articles without residual stresses.

The thermal and kinetic models discussed above are the basis for determining the processing conditions for reactive processing by ionic polymerization,[29] addition polymerization, vulcanization of rubbers and radical polymerization, although in the latter case additional assumptions of a constant initiation rate and a quasi-stationary concentration of radicals are made.[89] These models can also be used to solve optimization problems to improve the performance and properties of end-products.

2.8 NONISOTHERMAL CRYSTALLIZATION

Modelling non-isothermal crystallization is the next important step in a quantitative description of reactive processing. This is particularly important, because crystallization determines the properties of the end product. Therefore, the development the spatial distribution of crystallinity, α, and temperature, T, with time throughout the volume of the reactive medium must be calculated. It is also noteworthy that crystallization and polymerization processes may occur simultaneously. This happens when polymerization proceeds at temperatures below the melting point of the newly formed polymer. A typical example of this phenomenon is anionic-activated polymerization of ε-caprolactam, which takes place below the melting temperature of polycaproamide.

The key to modelling the crystallization process is the derivation a kinetic equation for $\alpha(t,T)$. It is possible to find different versions of this equation, including the classical Avrami equation, which allows adequate fitting of the experimental data. However, this equation is not convenient for solving processing problems. This is explained by the need to use a kinetic equation for non-isothermal conditions, which leads to a cumbersome system of interrelated differential and integral equations. The problem with the Avrami equation is that it was derived for isothermal conditions and

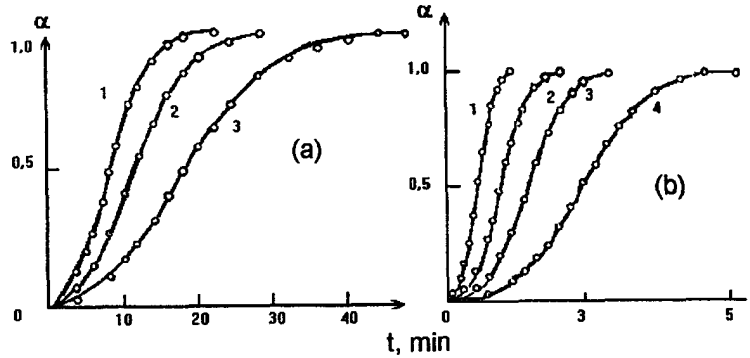

Figure 2.19. Isotherms of polycaproamide (a) and poly(ethylene terephthalate) (b) crystallization at different temperatures. a: 180°C (curve 1); 184°C (curve 2); 188°C (curve 3); b: 180°C (curve 1); 200°C (curve 2); 210°C (curve 3); 220°C (curve 4). Solid lines are calculated in accordance with Eq. (2.48); points are experimental data.

generalized to non-isothermal conditions. The Avrami equation expresses the degree of crystallinity, while the intensity of the heat output in the energy balance equation is proportional to the crystallization rate, rather than to the degree of crystallinity. A new kinetic equation was proposed,[90-92] which is written as follows:

$$\frac{d\alpha^*}{dt} = K_0(1-\alpha^*)(1+B_0\alpha^*) \qquad [2.47]$$

where α^* is the ratio of the current degree of crystallinity to its equilibrium value: $\alpha^* = \alpha(t)/\alpha_\infty$; B_0 is a constant characterizing the effect of acceleration during crystallization (analogous to the constant c_0, which characterizes self-acceleration during polymerization); K_0 is a temperature-dependent factor, which in a general, may be some non-exponential function, in contrast to the constant appearing in the kinetic equations of chemical reactions. The integral form of this equation is similar to the Avrami equation. Its analytical form is:

$$\alpha(t) = \left[1 - \frac{1+B_0}{B_0 + e^{(1+B_0)K_0 t}}\right]\alpha_\infty \qquad [2.48]$$

Isothermal curves derived from this equation are shown in Fig. 2.19. It is clear that this equation fits the experimental data. A comparison of the kinetic equation (2.48) and the Avrami equation shows[93] that any experimental data described by the Avrami equation can be approximated by Eq. (2.48) for any arbitrary set of constants. The divergence of the curves does not exceed 1% in the range $0.2 < \alpha < 1.0$ and 8% in the range $0 < \alpha < 0.2$. This means that the same experimental data (in the isothermal case) can be analyzed by both equations with practically the same reliability. Thus the choice of approximating equation depends on the goal of this procedure: if we are interested in physi-

cal treatment of results, the Avrami equation if preferable, because it includes generally accepted principles; if we are primarily interested in applying experimental results to solve non-isothermal problems, then Eq. (2.47) must be used, because it gives the crystallization rate, which is a parameter in the heat balance equations.

To applying Eq. (2.47) to non-isothermal problems, it is necessary to generalize it by introducing temperature-dependent constants. The basic approach was proposed by Ziabicki[94,95] who developed a quasi-static model of non-isothermal crystallization in the form of a kinetic rate equation:

$$\frac{d\alpha}{dt} = f(T,\alpha) \qquad [2.49]$$

The kinetic function $f(T,\alpha)$ was assumed to be a first-order equation. For a quasi-static approximation, we can write the following equation for the rate of crystallization:

$$\frac{d\alpha}{dt} = K(T)[\alpha_\infty(T) - \alpha][1 + B_0(T)\alpha] \qquad [2.50]$$

The temperature dependencies of K, α_∞ and Bo in Eq. (2.50) can be found from experimental data for the kinetics of isothermal crystallization. As a general rule, the temperature dependence of K can be represented by a double exponential function:[96]

$$K(T) = k_0 \exp\left[-\frac{E}{RT} - \frac{\psi T_m}{T(T_m - T)}\right] \qquad [2.51]$$

where E is the activation energy for mass transfer through crystal surface growing from the melt; T_m is the equilibrium melting temperature; T is the current temperature; ψ and k_0 are constants. The change in the constant B_0 with temperature is negligible in comparison with the temperature function K(T) in Eq. (2.50). Thus, the final form of the kinetic equation for crystallization is Eq. (2.50), where B_0 = const and the function K(T) is expressed by Eq. (2.51):

$$\frac{d\alpha}{dt} = k_0 \exp\left[-\frac{E}{RT} - \frac{\psi T_\infty}{T(T_m - T)}\right][\alpha_\infty(T) - \alpha](1 + B_0\alpha) \qquad [2.52]$$

Eq.(2.52) is a self-acceleration type kinetic equation for crystallization, but the temperature dependencies of constants are different. In some cases, the temperature dependence of K(T) given by Eq. (2.51) is better expressed by an alternative equation widely used in the theory of crystallization:

$$K(T) = k'_0 \exp\left[\frac{F}{T - T_g} - \frac{\xi}{T - T_m}\right] \qquad [2.53]$$

where k_0, E, and ξ are constants; T_g is the glass transition temperature, and T_m is the melting temperature. Eq.(2.53) clearly shows that the temperature dependence of the crystallization rate has a

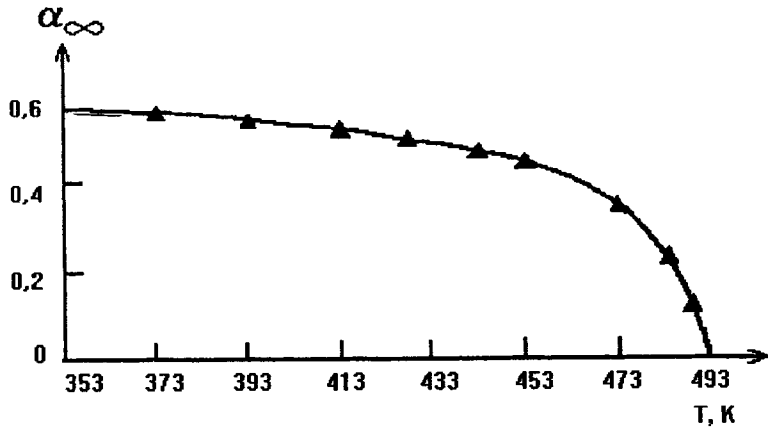

Figure 2.20. Temperature dependence of the equilibrium degree of crystallinity for polycaproamide.

bell-like shape in the interval between the glass transition and the melting point, with the crystallization rate falling to zero at $T \rightarrow T_m$ and $T \rightarrow T_g$.

By integrating Eq. (2.50) for different cooling rates, i.e., for different functions T(t), it is possible to find the time dependence of crystallinity and the rate of the crystallization process. It is also necessary to bear in mind the temperature dependence of the equilibrium degree of crystallinity, $\alpha_\infty(T)$. As an example, this dependence is shown for polycaproamide in Fig. 2.20.[97] It is evident from Eq. (2.53) that the function $\alpha(T)$ must have a maximum whose location on the temperature axis depends on the cooling rate. This is illustrated in Fig. 2.21, where values of the rate of heat output dQ/dt, proportional to $d\alpha/dt$, and degree of crystallinity α are shown as functions of temperature. It is worth mentioning that all the curves in this figure are adequately described by Eq. (2.52).

A complete solution to the problem of modelling the crystallization process requires the determination of the space-time distribution of temperature and crystallinity. These distributions can be predicted using the thermal kinetic approach formulated above with the following assumptions:

- heat exchange in the crystallizing volume is by the conduction only;
- movement of amorphous and crystalline phases and heat convection are absent due to the high viscosity of the medium;
- the boundary conditions and geometrical shape of the volume do not change during crystallization;
- the power of the inherent heat sources is proportional to the crystallization rate;
- heat exchange through the surface of the crystallizing volume proceeds according to Newton's law.

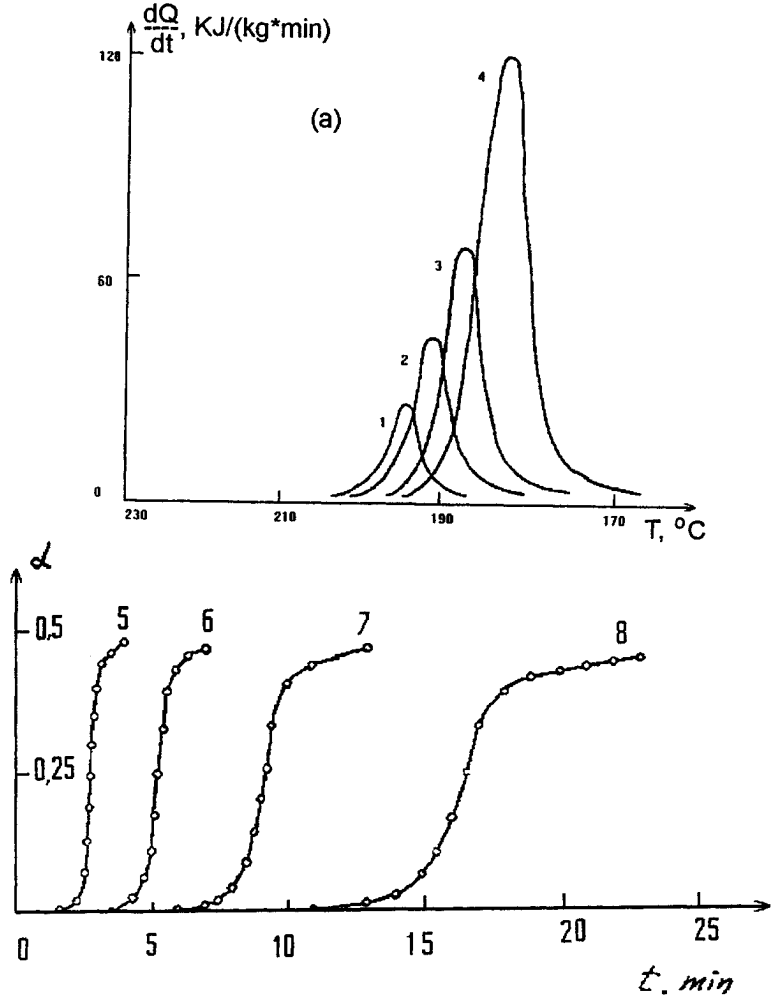

Figure 2.21. Temperature dependencies of the rate of heat output and time dependencies of the degree of crystallinity in the homogeneously cooled polycaproamide sample. The rates of linear decrease in temperature are 2 K/min (curves 1 and 8); 4 K/min (curves 2 and 7); 8 K/min (curves 3 and 6); 16 K/min (curves 4 and 5).

In this case, the differential equations describing the process of non-isothermal crystallization in a batch-process reactor configured line a plane plate can be as:

$$\frac{\partial T}{\partial t} = a\frac{\partial^2 T}{\partial z^2} + \frac{Q_c}{C_p \rho}\frac{d\alpha}{dt} \qquad [2.54]$$

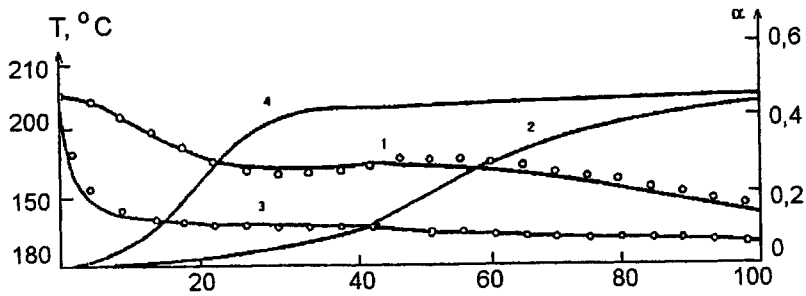

Figure 2.22. Experimental data (points) and calculated curves (solid lines) for changes in the degree of crystallinity in the center (curves 1 and 2) and at the wall (curves 3 and 4) of a plate reactor. The width of the plate is 32 mm. T_{sur} = 140°C.

where the function $\alpha(t)$ is described by Eq. (2.52) and a is the coefficient of temperature conductivity. Boundary conditions are as follows:

at t = 0:

$$T(z) = T_0 \text{ and } \alpha = 0;$$

at z = 0:

$$\frac{\partial T}{\partial z} = 0$$

at z = z_0:

$$\frac{\partial T}{\partial z} = \frac{Bi}{z_0}(T - T_{sur})$$

where T_0 is the initial temperature inside the reactor; z_0 is the half-width of the plate; Bi is the Biot Number; T_{sur} is the temperature of the surroundings; Q_c is the enthalpy of crystallization.

Experiments were carried out on the crystallization of polycaproamide slabs produced by the reactive processing method using the following values:[97-99]

T_0 = 205°C;	$a = 1\times10^{-7}$ m^2/s;	Q_c = 18.85 kJ/mol;
C_p = 2.7 J/(g K);	B_0 = 40;	α_∞ = 0.5;
$k_0 = 1.03\times10^6$ min^{-1}	E = 36 kJ/mol;	ψ = 225K.

An example illustrating the results of calculations for the dependencies T(t) and $\alpha(t)$ is shown in Fig. 2.22 for two locations: the center of the plate (z_0 = 16 mm) and its surface. Experimental points are also marked.[97,99] The evolution of the spatial distribution of the crystallinity in a plate reactor is shown in Fig. 2.23. Comparison of the calculated curves and experimental points confirms that the theoretical model is correct and that the results reflect all the main features of the real situation, including the slight curvature and the plateau in the T(t) dependence. A very pronounced inhomogene-

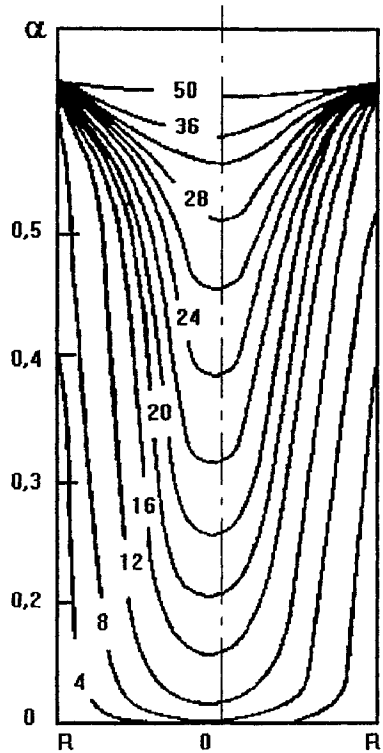

Figure 2.23. Evolution of the spatial distribution of the degree of crystallinity on cooling of a polycaproamide plate at T_{sur} = 140°C. Figures on the curves show time from the beginning of the process.

ity in the α and T values really exists, even in rather thin plates. Clearly, this inhomogeneity depends on the size and shape of the article being formed.

2.9 SUPERIMPOSED PROCESSES OF POLYMERIZATION AND CRYSTALLIZATION

In the general formulation the reactive processing model (Section 2.1), it was stressed that different phenomena occurring during a process cycle may be superimposed and that may be mutual influence between the various processes. Superposition of polymerization and crystallization is of particular importance, because it always occurs when a crystalline polymer is synthesized below its melting point. It is especially convenient to study this effect for anionic activated polymerization of ε-caprol-

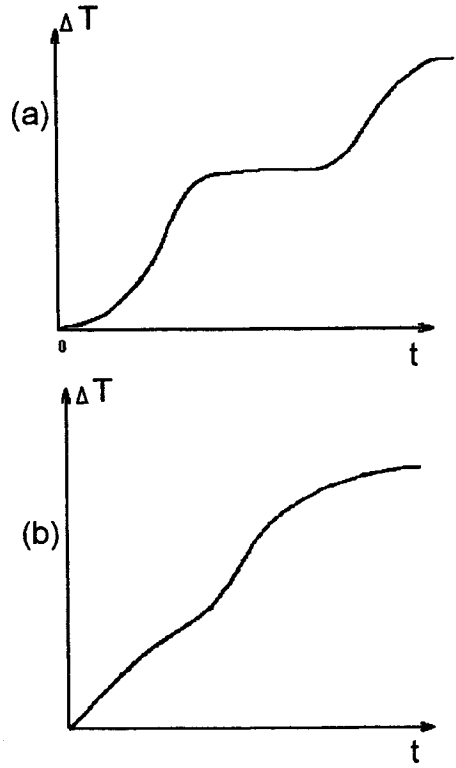

Figure 2.24. Changes in temperature in adiabatic regime of anionic polymerization of ε-caprolactam when a processes starts at low (a) or at high (b) temperature.

actam by measuring the heat output q(t) in isothermal conditions or temperature evolution T(t) in adiabatic conditions.

Two typical cases are illustrated in Fig. 2.24: the first scheme (Fig. 2.24 a) is related to high-temperature polymerization, in which newly formed polymer is molten and the processes of polymerization (part 0b of the full curve) and crystallization (part bK of the full curve) are separated in time. The second case (Fig. 2.24 b) illustrates low-temperature polymerization; in this situation crystallization starts before the full process of polymerization is completed. This is typical superposition of two kinetic processes, and the shape of the curve in Fig. 2.24 b does not allow the separation of these processes without additional information and assumptions. The net heat effect is the same in

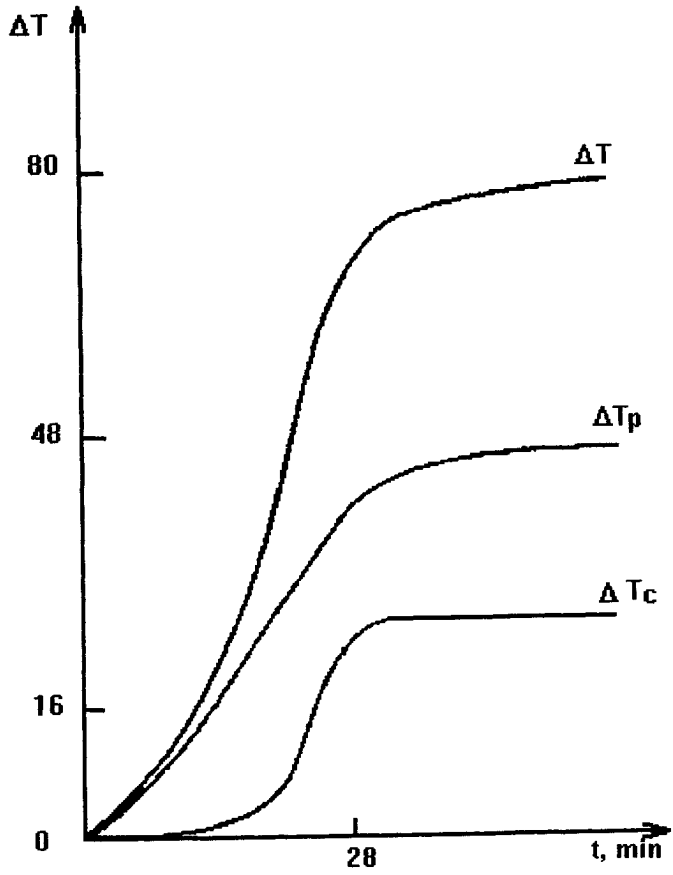

Figure 2.25. Separation of the net exothermal effect (characterized by a temperature increase ΔT) into components of polymerization ΔTp and crystallization ΔTc.

both cases and corresponds to a temperature increase of 80-82°C (the part of this temperature increase, 50-52°C, is explained by the enthalpy of polymerization).

A typical example illustrating the separation of the net heat effect ΔT into parts corresponding to polymerization ΔT_p and crystallization ΔT_c is shown in Fig. 2.25.[100] These data were obtained by direct measurement of the quantities of polymeric products formed during the reaction. This gives us the value of ΔT_p calculated from β(t) and the known value of the maximum temperature increase dur-

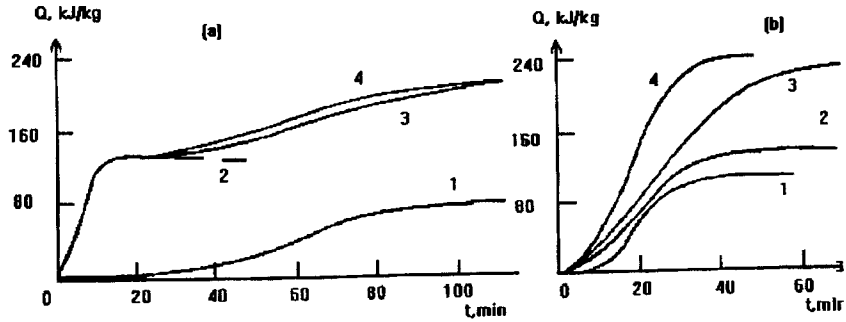

Figure 2.26. Heat effects, observed during anionic activated polymerization of ε-caprolactam at 190°C (a) and 160°C (b). Curves 1 and 2 are components related to crystallization and polymerization, respectively. Curves 3 and 4 are calculated from Eq. (2.56) and from a simple additive rule, respectively.

ing adiabatic polymerization ΔT_{max}. The value of ΔT_c was then calculated as the difference between the total value ΔT and ΔT_p.

From the experimental data shown in Fig. 2.25 and other analogous situations, it is difficult to ascertain the beginning of crystallization at the very start of the process. It is reasonable to suppose that crystallization cannot occur at the beginning of the process but only after some degree of conversion is reached[101] or the molecular weight of the product becomes high enough.[28] However, the effects at the beginning of crystallization are rather small, making it possible to formulate the following general assumptions about the superposition of the two processes: only the material that has been formed up to the current time can crystallize, and the kinetics of crystallization must be related to the polymer already existing at this time. These assumptions include the possibility of crystallization from the very beginning, but the input of the initial part of the process is small and does not significantly influence the final results.

Modelling of crystallization was discussed in Section 2.8. Now, we shall develop a model for superimposed polymerization and crystallization processes. This model is important for calculating temperature evolution during reactive processing, because an increase in temperature, regardless of its cause, influences the kinetics of both polymerization and crystallization. This concept is expressed by the following equation for the rate of heat output from the superimposed proceses:[102,103]

$$\frac{dq(t)}{dt} = Q_p \frac{d\beta(t)}{dt} + Q_c \beta(t) \frac{d\alpha(t)}{dt} \qquad [2.55]$$

where Q_p and Q_c are the enthalpies of polymerization and crystallization, respectively; β and α are the degrees of conversion in polymerization and crystallization, respectively.

The most important feature of this model is the introduction of the factor $\beta(t)$ into the second term on the right-hand side of Eq. (2.55). This factor reflects the hypothesis stated above about crys-

tallization of a newly formed polymer, an assumption that is quite different from the calculation of the net heat effect by the simple additive scheme described by the equation:

$$\frac{dq}{dt} = Q_p \frac{d\beta}{dt} + Q_c \frac{d\alpha}{dt} \qquad [2.56]$$

The validity of Eq. (2.55) is illustrated in Fig. 2.26, where calculated curves are compared with experimental data for two different temperature regimes of a superimposed process. It can be seen that for high-temperature polymerization, Eqs. (2.55) and (2.56) give similar results. This is to be expected, because we are dealing with time-separated processes; i.e., crystallization only starts when almost all of the polymer is already present. However, for low-temperature polymerization, the situation is quite different, and the curves representing Eq. (2.55) - curve 3, and (2.56) - curve 4, do not coincide. The experimental data follow curve 3, and thus we may conclude that the model represented by Eq. (2.55) is correct because it fits the experimental data. A model for superimposed processes similar to that discussed above, was also proposed.[101] In this approach, the temperature increase in a superimposed process is expressed by the following equation:

$$\frac{T - T_0}{\beta} = [M]_0 \frac{Q_p}{C_p\rho} + \frac{Q_c}{C_p\rho}\alpha \qquad [2.57]$$

where $[M]_0$ is the initial concentration of the monomer. The model, represented by Eq. (2.55), is confirmed by experimental data, but there may be other situations for which Eq. (2.57) would be more appropriate.

For modelling the temperature distribution in a cylindrical article and its evolution with time during reactive processing with only an inherent heat source, Eq. (2.55) takes the form:

$$\frac{\partial T}{\partial t} = \frac{1}{r}\frac{\partial}{\partial r}\left(ar\frac{\partial T}{\partial r}\right) + \frac{\partial}{\partial z}\left(\lambda\frac{\partial T}{\partial z}\right) + \frac{1}{C_p\rho}\frac{dq}{dt} \qquad [2.58]$$

where the standard notation is used.

In addition to these equations, it is necessary to introduce Eq.(2.22) for the kinetics of anionic activated polymerization of ε-caprolactam and Eq. (2.52) for the kinetics of crystallization. Let us write the boundary and initial conditions:

at r = R

$$-\lambda\frac{\partial T}{\partial r} = \kappa^*(T - T_{sur})$$

and at t = 0:

$$T = T_0; \quad \beta = 0; \quad \alpha = 0$$

Here κ^* is the heat transfer coefficient and T_0 is the initial temperature of the reactive medium. In computer modelling and solution of this system of equations, the following values were used:

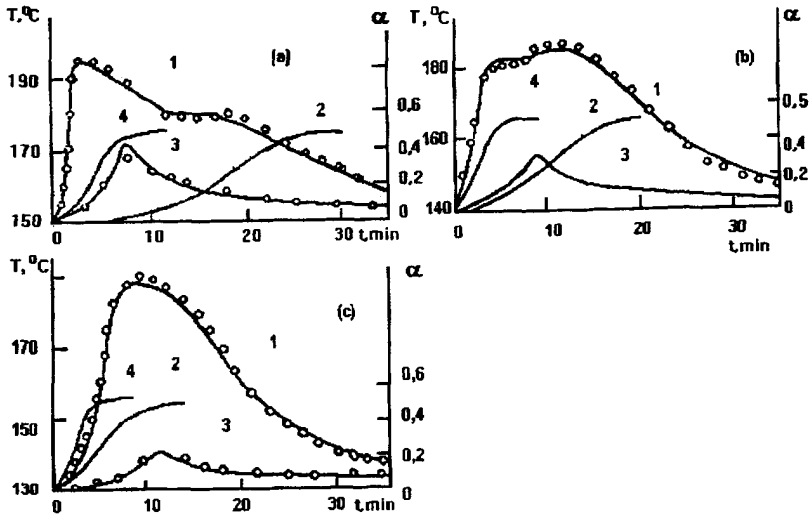

Figure 2.27. Experimental data (points) and theoretical curves (solid lines) representing changes in temperature (curves 1 and 3) and the degree of crystallinity (curves 2 and 4) during anionic activated polymerization of ε-caprolactam in a plate reactor. Width of the reactor is 32 mm; T_{sur} = 150°C (a); 140°C (b) and 130°C (c). Data are shown for the center (curves 1 and 2) and for the wall (curves 3 and 4).

Q_p = 128 kJ/mol; U = 71.2 kJ/mol; E = 35.6 kJ/mol;
$k_0 = 3.85 \times 10^4$ min^{-1}; $k = 6.3 \times 10^6$ min^{-1}; c_0 = 18;
Q_c = 18.8 kJ/mol; ψ = 225K; T_m = 501K;
R = 0.08 m; λ = 0.361 W/(m K); C_p = 3.04 J/(g K);
$\rho = 1152$ kg/m^3.

Solving this system of equations allows us to construct space-time distributions of temperature and degree of conversion for various temperature regimes in anionic-activated polymerization of ε-caprolactam (Fig. 2.27). As can be seen,there is a good correlation between theoretical results and experimental data. Specifically, the calculations correctly reflect two possible regimes of polymerization-crystallization, when either separated or superimposed processes occur. The calculations also demonstrate that differences in crystallinity between the center and the surface of the article depend on the initial temperature of the reactive medium. It has been proven that a low-temperature polymerization regime leads to near-adiabatic crystallization throughout the whole volume and improves the quality of the product by decreasing residual stresses. However, lowering the temperature below 150°C results in a rapid increase in the proportion of low-molecular-weight frac-

tions in the end-product (from the normal 1-2% to 8-16%) and synthesis of a polymer with a very broad molecular weight distribution. Therefore, this lower temperature limit must not be transgressed. Use of a high-temperature polymerization regime leads to the formation of an end-product by crystallization from the melt, analogous to injection molding. In this case, polymerization influences only the initial temperature at which cooling and crystallization begin.

This approach to modelling superimposed processes is applicable to many cases where physical transitions proceed simultaneously with polymerization. Glass transition or phase separation are typical examples of physical processes which may occur in addition to, or instead of, crystallization.

2.10 INVERSE KINETIC PROBLEMS

Let us discuss the general problem of estimating the terms in a kinetic equation for a specific process with an equation written as:

$$\frac{d\beta}{dt} = K(T)f(\beta) \qquad [2.59]$$

where K(T) is the temperature dependence of the reaction rate; f(β) is an isothermal kinetic phenomenological function. As a general rule, the temperature dependence K(T) for chemical reactions is described by the Arrhenius equation:

$$K(T) = k_0 e^{-E/RT}$$

where R is the universal gas constant; T is the temperature in K; E is the apparent activation energy; and k_0 is a pre-exponential factor. The solution depends on the kinetic function and the values of the constants in Eq. (2.59). For many relatively simple analytical forms of the kinetic function, Eq. (2.59) can be integrated, and the (βt) dependencies can be obtained in an analytical form. In all cases the initial condition $\beta(0) = 0$ must be maintained. Several versions of kinetic functions are listed below (the parameter K_i corresponds to the value of K at T_i, the temperature of isothermal polymerization).

1. Kinetic equation of the n-th order:

$$f(\beta) = (1-\beta)^n$$

and

$$\beta(t) = 1 - \frac{1}{[1 + (n-1)K_i t]^{1/(n-1)}} \qquad [2.60]$$

2. Kinetic equation with self-acceleration:

$$f(\beta) = (1-\beta)(1 + c_0\beta)$$

and

Table 2.2. Values of the constants c_0 and $c_1 = K(1 + c_0)$ in the kinetic equation for ε-caprolactam polymerization

Concentration of the catalyst [C]×10^2 mol/l	Computer method		Graphic method	
	c_0, min^{-1}	c_1	c_0, min^{-1}	c_1
3.20	0.24	12.0	0.22	10.8
4.49	0.31	9.5	0.29	10.0
6.32	0.38	5.6	0.34	6.5
8.97	0.44	3.0	0.40	3.5

$$\beta(t) = 1 - \frac{1 + c_0}{c_0 + e^{[(1+c_0)K_i t]}} \qquad [2.61]$$

This equation can be easily modified if the equilibrium degree of conversion at $T = T_i$ is equal, not to 1, but to some value $d\beta_\infty < 1$.

3. Kinetic equation with incomplete conversion:

$$f(\beta) = (1 - \beta)(1 - \xi\beta)$$

and

$$\beta(t) = 1 + \frac{\xi - 1}{e^{[(1-\xi)K_i t]} - \xi} \qquad [2.62]$$

The last two equations can be combined to describe a kinetic process with self-acceleration at the initial stage of the process and incomplete conversion at the final stage of the reaction.

The parameters in Eq. (2.59) are usually determined from the condition that some function Φ is minimized. This function can be, for example, the sum of the mean-square deviations between the experimental and calculated curves (the error function). The search for the minimum of the function Φ can be carried out by various methods, in particular by the Nelder-Mead algorithm.[103] As an example, Table 2.2 contains results of the calculation of the constants in a self-accelerating kinetic equation used to describe experimental data from anionic-activated ε-caprolactam polymerization for different catalyst concentrations. There is good correlation between the results obtained by different methods, as can be seen from Table 2.2. In order to increase the value of the experimental results, measurements have been made at different non-isothermal regimes, in which both the initial temperature and the temperature changes with time were varied.

As a typical example let us discuss the experimental data for the kinetics of polycaproamide crystallization obtained by differential scanning calorimetry.[99] The primary experimental data are

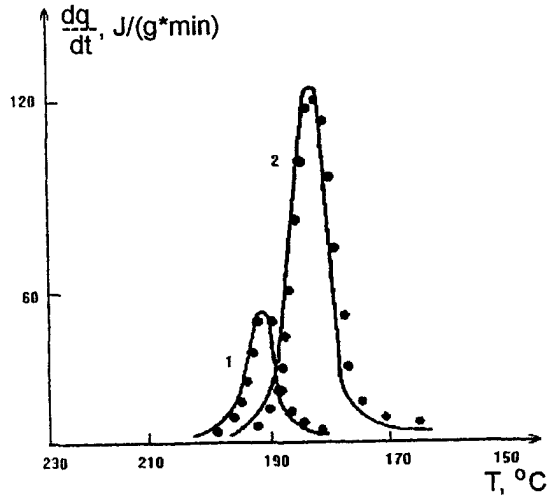

Figure 2.28. Comparison of the results obtained by solving the inverse problem (solid lines) with experimental data (points) for cooling of a polycaproamide plate with constant rate: 4 K/min (curve 1) and 16 K/min (curve 2).

the heat output rates dq/dt as functions of temperature for different temperature variations with time T(t). It is assumed that dq/dt is proportional to the crystallization rate dα/dt, i.e.:

$$\frac{dq}{dt} = Q_c \frac{d\alpha}{dt} \qquad [2.63]$$

where Q_c is the enthalpy of crystallization.

In formulating the inverse problem, we are required to find the values of the constants in the kinetic equation which will minimize the divergence between the temperature-vs.-time curves calculated from the equation and those obtained experimentally. To do this, the time dependence of the temperature is taken to be linear:

$$T(t) = T_m - a'_T t$$

where a'_T is the cooling rate and T_m is the melting point (start of crystallization). The inverse problem is solved by defining some function, Φ, which characterizes the divergence (or error) between the calculated and experimental curves. This function depends on the values of the parameters E, ψ, k_0, B_0, and Q_c,and is calculated as:

$$\Phi(\sigma_1,\ldots,\sigma_n) = \frac{1}{N}\sum_{k=1}^{N}\left[\sum_{i=1}^{m_k}\frac{\mu_{k,l}}{t_{k,l+1}-t_{k,l}}\int_{t_{k,l}}^{t_{k,l+1}}\mu_k dt\right]^{1/2} \qquad [2.64]$$

The values λ in this function are measures of the "errors". They are determined in the following manner:

$$\mu_k = \frac{\beta}{2}\left[\left(1-\frac{f_k^c}{f_k^m}\right)^2+\left(1-\frac{f_k^m}{f_k^c}\right)^2\right]+\frac{\gamma}{2}\left[\left(1-\frac{f_k^c}{f_k^m}\right)^2+\left(1-\frac{f_k^m}{f_k^c}\right)^2\right]$$

In these relationships, N is the number of independent experiments; k is the number of an experiment; m_k is the number of time intervals into which the whole process time is divided; $\mu_{k,l}$ is the "weight" corresponding to the l-th interval in the k^{th} experiment, whose sum over m_k intervals equals 1; f_k^c is the k^{th} calculated function; f_k^m is the k^{th} measured function; β and γ are "weights".

Let us introduce a characteristic temperature T_*, which is typical for the specific process being discussed (it might be the wall temperature, the initial temperature of the reactive medium, and so on). The introduction of this characteristic temperature allows us to obtain partial derivatives $\partial\Phi/\partial\sigma_i$ of the same order. Then we can formulate a convenient system of parameters to use in minimizing the function Φ. These are as follows:

$$U^* = \frac{U}{RT_*};\quad \psi_0^* = \frac{\psi_0}{R(T_m - t_*)^2};$$

$$K^* = k_0 e^{-\frac{U}{RT_*}-\frac{\psi}{R(T_m-T)}}$$

$$\beta_1 = \frac{1}{T_*};\quad \beta_2 = \frac{1}{T_m - T_*};\quad U = E + \psi_0;\quad \psi_0 = \psi R;\quad \theta = T - T_*$$

Using this system of parameters, we can rewrite Eq. (2.52), which determines the crystallization rate, as follows:

$$\frac{d\alpha}{dt} = K^*(1 + B_0\alpha)(\alpha_\infty - \alpha)\exp\left[\frac{U^*\theta}{1+\beta_1\theta}-\frac{\psi_0^*\theta}{1-\beta_2\theta}\right] \qquad [2.65]$$

with the following initial conditions: at $t = 0$ we have $\alpha = 0$ and $\theta = T_m - T_*$. Then, the following parameters must be found by minimizing the function Φ: K^*, U^*, ψ^*, Q_c, and the constant B_0, which characterizes the self-acceleration effect in polymer crystallization.

Generally speaking, with having to find so many independent constants, we cannot be sure that the solution is unambiguous. Therefore, it is preferable to find some of them by independent methods. For example, it is possible to determine the activation energy or enthalpy of polymeriza-

tion. It is also possible to estimate solutions by applying common sense and eliminating some sets of constants that are obviously unrealistic.

Fig. 2.28 shows the results of a solution of the inverse problem. The solid lines represent the calculated function dq(T)/dt with the following optimal values of the constants: U = 36.9 kJ/mol; ψ = 225K; B_0 = 42; $k_0 = 1.03\times10^6$ min^{-1} and Q_c=18.9 kJ/mol. The approach discussed above allows us to find values of the constants of a kinetic equation that provide a satisfactory fit to the experimental dq/dt curve, and to obtain results that correctly predict the shift in the maxima as a function of the cooling rate.

An analogous method for solving the inverse problem allows us to determine the constants in a kinetic equation using other experimental data; for example, the results of measurements of the T(t) dependence at different points on an article (or model sample) can be successfully used for this purpose.

2.11 CHANGES IN RHEOLOGICAL PROPERTIES OF A REACTIVE MEDIUM

2.11.1 CHANGES IN RHEOLOGICAL PROPERTIES DURING SYNTHESIS

Consideration of the changes in the rheological properties of a flowing liquid with time is one of the fundamental tools for modelling reactive processing. Changes in viscosity and in the whole complex of viscoelastic properties during polymerization and synthesis of linear polymers are consequences of the increase in molecular weight due to chain propagation and of the increase in their number in a reactive medium due to appearance of new polymeric chains. The kinetics of changes in these two determining factors depend on the overall chemistry of the process and on the kinetics of the elementary reactions. This is true until the reactive medium becomes a homogeneous (one-phase) solution. If the newly formed polymer is insoluble in the reactive medium, new effects might be expected, including such a "strange" phenomenon as inversion of the time dependence of the viscosity in spite of increase in molecular weight.[104]

Two stage can be distinguised in the curing of polyfunctional compounds form three-dimensional networks. First, growth and branching of individual macromolecules takes place. This continues up to some critical degree of conversion, at which fluidity is lost; this is the gel-point, t^*. The rheological properties of a reactive medium up to the gel-point are characterized by the viscosity, η, whose measurements provide a rheokinetic picture of the polymerization process. Second, beyond the gel-point, a network of chemical bonds extends throughout the whole volume, and the rheological properties of a material are usually characterized by its modulus of elasticity, G, because viscosity cannot be measured at this stage (formally $\eta\rightarrow\infty$). The general pattern of changes in viscosity, modulus of elasticity, and heat output during curing is shown schematically in Fig. 2.29.

The main rheokinetic problem consists of the determination of the time dependence of the degree of conversion $\beta(t)$ and the correlation between $\beta(t)$ and the changes in the rheological properties of the reactants. One possible kinetic function $\beta(t)$ was discussed in Section 2.2. In considering the rheological properties of the reactive medium, we can neglect non-Newtonian

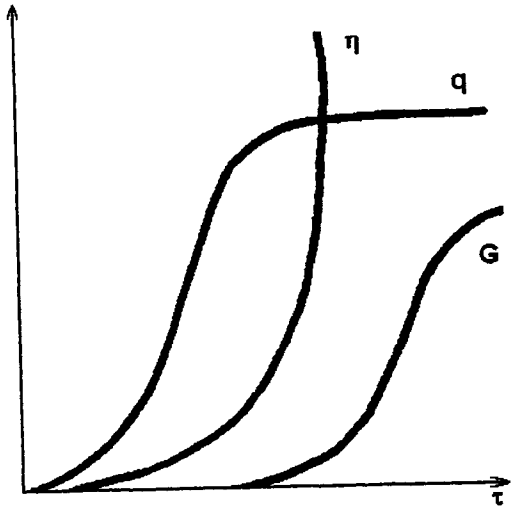

Figure 2.29. Changes in integral mechanical properties of a polymer (heat output, q, shear modulus of elasticity, G, and Poisson ratio, μ) in the process of homogeneous cooling.

effects, because, as a general rule, only relatively low-molecular-weight products are used in reactive processing. The nature of the changes in the rheological properties of a reactive medium during processing depends on its chemical formulation and temperature,[52,105,106] because these factors determine the rheokinetic behaviour of the process. There are universal equations for the dependence η(t), but well-known results from investigations of the viscous properties of linear polymers (melts and solutions) can be used to discuss the rheokinetics of reactive processing. If we consider a reactive mass, which can be treated as a homogeneous solution of a newly formed polymer in its monomer or in a solvent, we can write the following expression for viscosity of such a solution:

$$\eta = K_\eta M_w^a \varphi^b \qquad [2.66]$$

where K is an empirical constant; M_w is the weight-average molecular weight; φ is the concentration of the polymer in the solution; a and b are constants that are generally known for many polymer-solvent pairs; in many cases, a = 3.5 is an universal constant for polymer melts and concentrated solutions.

Different kinetic processes lead to different dependences of the values in Eq. (2.66) on the degree of conversion. In Ref.[105] formulas for the $M_w(\beta)$ and $\varphi(\beta)$ dependences were obtained for the principal reaction kinetics in the formation of linear polymers. Introducing these dependences into Eq. (2.66), yields the unique dependence of viscosity on the degree of conversion, $\eta(\beta)$.

For curing compounds, the dependence $\eta(\beta)$ can be described by two types of equations. In the first type, it is assumed that, as the gel-point is approached, $t \to t^*$, the viscosity increases without limit. The second type is an exponential equation, which does not contain any singularities.[106] The dependence of the viscosity of polyurethane on molecular weight and temperature can be represented by the following equation:

$$\eta = AM_w^a e^{E/RT} \qquad [2.67]$$

where A, a, and E are empirical constants. The average molecular weight is unambiguously related to the degree of conversion; moreover, this relationship is formulated such that as $\beta \to \beta^*$ (β^* is the degree of conversion at the gel-point), $M_w \to \infty$, which means that near the gel-point, $\eta \to \infty$. Therefore, Eq. (2.67) clearly reflects the existence of the gel-point, and the form of the function $\eta(\beta,T)$ can be found. This last problem was solved elsewhere.[44] It was shown that the whole range of experimental data on the viscous properties of polyurethane-based compounds used for reactive processing can be described by the following equation:

$$\frac{\eta(\beta,T)}{\eta_0(T)} = \left(\frac{\beta^*}{\beta^* - \beta}\right)^{a+b\beta} \qquad [2.68]$$

where $\eta_0(T)$ is the viscosity of the reactive system in its initial state; this function represents the temperature dependence of viscosity during the whole process, regardless of the influence of temperature on the kinetics of curing. The exponential equation for the time dependence of viscosity of a material being cured can be written as:[107]

$$\eta = \eta_0 e^{kt} \qquad [2.69]$$

where η_0 is the initial viscosity, which dependis on temperature; k is a constant representing the influence of the polymerization reaction kinetics on the viscosity growth. The equation for the dependence of viscosity on the degree of conversion can be formulated in an analogous manner:

$$\eta = \eta_0 e^{k'\beta} \qquad [2.70]$$

where k′ is an empirical constant.

Polymer synthesis is usually accompanied by a strong exothermal effect and, as a general rule, real process proceeds in non-isothermal conditions. This problem was considered in Section 2.6 for polyester synthesis, and the results discussed above are of generally applicable to all non-isothermal processes.

Real examples illustrating different types of time dependences of viscosity, can be found elsewhere.[52] It is worth mentioning that the rheokinetics of polymerization, even for a specific type of polymer (for example, polyurethane) depends on the composition, which determines both the kinetics of the process and the structure of the newly formed polymer. Clearly, the important factor is whether a linear or three-dimensional polymer is formed. In the first case, the viscosity increases

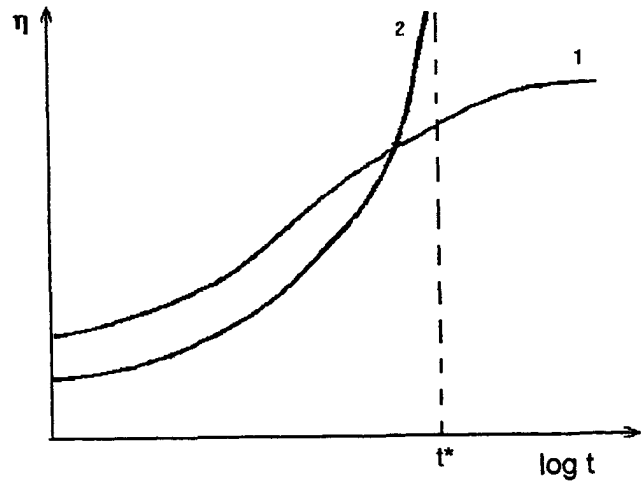

Figure 2.30. Increase in viscosity during synthesis of linear (curve 1) and cured (curve 2) polymers.

only to some finite level, but in the second case, the viscosity increases without limit as the gel-point is approached. This is shown schematically in Fig. 2.30.

Theoretical equations for describing time dependences of viscosity are known for linear polymerization only.[52] Difficulties arise when dealing with polymer curing, because there is no universal relationship between the structure of branched polymers (molecular weight, molecular weight distribution, branching characteristics) and their viscosity; therefore, it is impossible to construct a theoretical equation for dependence of viscosity on the degree of conversion of the functional groups. In the rheokinetics of branched polymers, particularly polyurethanes, the dependence $\eta(\beta,T)$ is always described by purely empirical formulas. The following equatiion is a typical illustration of this approach for three-dimensional addition polymerization leading to the formation of cured polyurethane:[44]

$$\eta = 4.747\times10^{-8}(M_w/M_{w,0})^{\frac{20.96\times10^2}{RT}-5.3176}\, e^{\frac{41.65\times10^3}{RT}} \qquad [2.71]$$

where $M_{w,0} = 796$ is the average molecular weight of the initial oligomer. The value of the weight-average molecular weight in this equation changes in the course of the reaction, and the dependence of M_w on the degree of conversion follows from Eq. (2.68). All numerical constants in this equation are derived from experimental data. According to this relationship the position of the gel-point is defined by an unlimited increase in molecular weight; consequently, $\eta\rightarrow\infty$.

The same authors who developed a rheokinetic model for polyurethane synthesis also proposed the following equation for the dependence $\eta(\beta,T)$:

$$\eta = A \exp\left[\frac{E}{RT}\right]\left(\frac{\beta^*}{\beta^* - \beta}\right)^{a+b\beta} \qquad [2.72]$$

where β^* is the degree of conversion at the gel-point; A, a, and b are empirical constants; for illustration, typical values of these constants for a test formulation (RIM 2200, produced by Union Carbide) are given:[3,47,108] $A = 10.3\times10^{-8}$ Pa s ; $E = 41.3$ kJ/mol; $\beta^* = 0.65$; $a = 1.5$; $b = 1.0$.

Filled polymeric systems are especially important in reactive processing. There are many publications devoted to the rheological properties of such systems.[109,110] The simplest model for filled polymeric liquids is a dilute suspension of inert particles, which means that the dynamic interactions between the suspended particles must be taken into account. These particles may be elastic, and their deformations influence the rheological properties of the liquid. Solid filler particles can interact with each other or with the liquid medium, and the various physical or chemical interactions affect the rheological properties of filled polymers. Liquid media used in reactive processing are always chemically active, and solid fillers can also influence polymerization kinetics in various ways, depending on the nature of the filler and the structure of the active groups in the oligomer.[111]

2.11.2 INFLUENCE OF SHEAR RATE ON THE INDUCTION PERIOD DURING OLIGOMER CURING

The role of shearing is especially important in the kinetics of oligomer curing.[112-114] It is related to the ability to maintain the reactive material in the fluid state for some finite time during the curing process. This time, t^*, called the induction period or "lifetime", is a very important material property, since the material can be processed only during this period. At $t > t^*$, viscosity increases sharply, and the material becomes solid.

The value t^* can be measured in two types of experiments. The induction period can be found by dynamic measurements that follow the changes in the viscoelastic properties of a material at low-amplitude deformations, i.e., the measurement of some critical point corresponding to t^*. This is a non-destructive method, and the value t_0^* obtained in this way reflects the "static" properties of a during material curing. The induction period can also be measured by a rotational viscometer, in which experiments are carried out at different shear rates and shear stresses. If the shear stress (or shear rate) is low, the "static" value of the induction period is obtained, because in this case, shearing does not influence the kinetics of curing. When the shear rate increases, experiments show that the induction period becomes shorter, until at very high shear rates the induction period completely disappears.[115] The dependence of the induction period on shear rate is illustrated in Fig. 2.31. Two points are of special interest here: (1) Shear stress is nearly constant during the induction period (since shear rate is also constant, to at least a first approximation, the viscosity of a reactive material can be treated as constant during the induction period), and the transition to the solid state is a critical phenomenon. (2) Non-Newtonian effects are weak at $t < t^*$, which is typical of low-molecular-weight oligomers. Shear stress remains constant during the whole induction period.

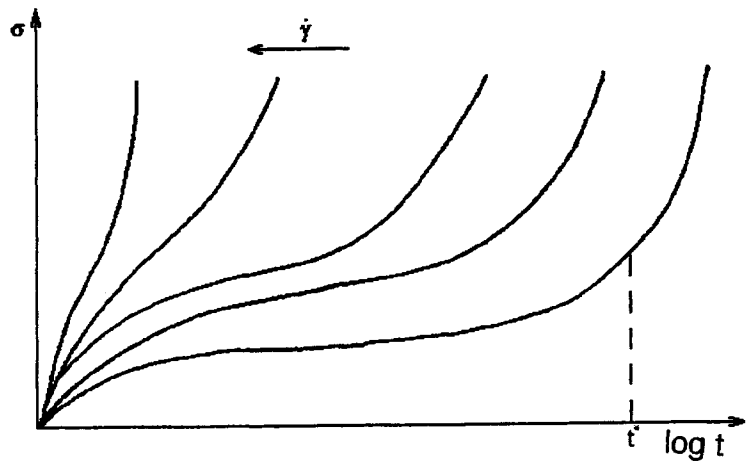

Figure 2.31. Influence of shear rate on decrease of an induction period in oligomer curing. An arrow shows the direction of increase in shear rate.

The dependence of the induction period on shear rate is essential for oligomer processing, because in real processes, shear rates on the order of hundreds of s^{-1} can be found. Loss of fluidity occurs much earlier than is predicted on the basis of the "standard" quality factor t_0^*, as measured under static or quasi-static conditions. Therefore, the nature of this effect and methods for describing it quantitatively must be considered. The intense heat dissipation during flow of a reactive liquid is one possible explanation. It leads to a temperature increase in the reactive medium and an increase in the reaction rate, which results in a shorter induction period in comparison with t_0^*. The deformations themselves can also play the role of a kinetic factor by influencing the rate of a chemical reaction under isothermal conditions.[116] In order to separate the two effects, let us examine the possible influence of heat dissipation on the shortening of the induction period. Comparison calculated results with experimental data should help to clarify the role of heat dissipation during the flow of oligomer reactive compounds.

The rate of heat generation in shear flow is determined by the power of the work done; this is the product of the shear rate and the shear stress. The resulting temperature change can be expressed as:

$$\frac{dT}{dt} = \frac{\sigma\dot{\gamma}}{C_p\rho} \qquad [2.73]$$

where σ is the shear stress; $\dot{\gamma}$ is the shear rate; C_p is the specific heat; ρ is the density. The heat output due to chemical reaction is neglected in this approximation. This assumption is valid for the

induction period, when the reaction is still very slow and curing is practically absent. Therefore "chemical" sources of heat are negligible. By considering a medium being defermed at a constant shear rate and allowing for the temperature dependence of viscosity (or shear stress), Eq. (2.73) can be rewritten for adiabatic conditions:

$$\frac{dT}{dt} = \frac{A\dot{\gamma}}{C_p\rho} e^{E/RT} \qquad [2.74]$$

where A is a pre-exponential factor; E is the activation energy of viscous flow. The focus of this problem is the criterion of curing (i.e., termination of the induction period) under non-isothermal conditions. This criterion, which summarizes inputs from the curing processes at various temperatures, can be formulated as:[117]

$$B\int_0^{t_n^*} e^{-U/RT(t)}dt = 1 \qquad [2.75]$$

where U is the apparent activation energy of the curing processes; t_n^* is the induction period for a non-isothermal process with an arbitrary pattern of temperature changes T(t); B is a normalizing constant, which can be expressed via the "static" induction period t_0^* at the initial temperature T_0 in the following way:

$$B = \frac{1}{t_0^*} e^{U/RT} \qquad [2.76]$$

Then we can rewrite Eq. (2.75) by replacing B with the expression from Eq. (2.76):

$$e^{U/RT_0}\int_0^{t_n^*} e^{-U/RT(t)}dt = t_0^* \qquad [2.77]$$

Eqs. (2.74) and (2.77) give us the principal solution of the problem being discussed, i.e., it is possible to calculate T(t) for different shear rates and then to find the upper limit of the integral in Eq. (2.77) for these rates. The solution becomes clearer if we choose dimensionless variables and transform Eqs. (2.74) and (2.77) into dimensionless form. Let us introduce a dimensionless temperature θ such that:

$$\theta = \frac{U}{RT_0^2}(T - T_0) \qquad [2.78]$$

The dimensionless shear rate δ is written as:

$$\delta = \frac{U}{RT_0^2} \frac{A\dot{\gamma}t_0^*}{C_p\rho} e^{E/RT_0} \qquad [2.79]$$

The dimensionless time τ and dimensionless non-isothermal induction period τ^* are written as follows:

$$\tau = \frac{t}{t_0^*}; \quad \tau^* = \frac{t_n^*}{t_0^*}$$

Two additional dimensionless values connected with the activation energies are also used:

$$\beta = \frac{RT_0}{U}; \quad \xi = \frac{E}{U}$$

Now we can rewrite the system of determining equations in dimensionless form:
evolution of temperature with time

$$\frac{d\theta}{d\tau} = \delta \exp\left[-\frac{\xi\theta}{1+\beta\theta}\right] \qquad [2.80]$$

criterion for a non-isothermal induction period

$$\int_0^{\tau^*} \frac{\theta}{e^{1+\beta\theta}} d\tau = 1 \qquad [2.81]$$

The solution of this set of equations gives the non-isothermal induction period $\tau^*(\delta)$ as a function of non-isothermal shear rate δ for different values of the parameters β and ξ. Fig. 2.32 shows the results of calculations for a wide range of dimensionless shear rates from 0.01 up to 100. The parameter β is equal to 0.03 and ξ varies from 0 to 1. At high shear rates, the decrease in the induction period is proportional to δ^{-1}. This means that a 100-fold increase in shear rate results in an almost 100-fold reduction in the induction period, which could well be catastrophic for material processing if the process rate is increased. The influence of the parameter ξ on $\tau^*(\delta)$ is signifcant only for high shear rates.

The results of the calculations shown in Fig. 2.32 represent a complete quantitative solution of the problem, because they show the decrease in the induction period in non-isothermal curing when there is a temperature increase due to heat dissipation in the flow of the reactive mass. The case where $\xi = 0$ is of particular interest. It is related to the experimental observation that shear stress is almost constant in the range $t < t^*$. In this situation the temperature dependence of the viscosity of the reactive mass can be neglected because of low values of the apparent activation energy of viscous flow E, and Eq. (2.73) leads to a linear time dependence of temperature:

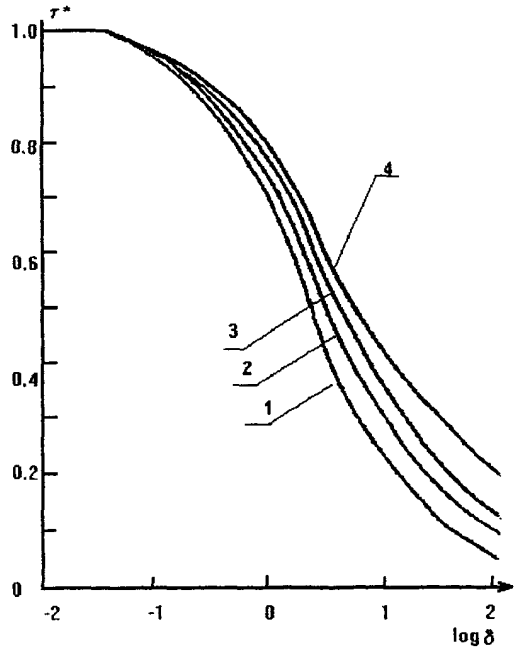

Figure 2.32. Predicted dependences of a dimensionless induction period in a non-isothermal process on dimensionless shear rate at different values of the parameter ξ: 0 (curve 1); 0.6 (curve 2); 1.2 (curve 3); 1.8 (curve 4).

$$T(t) = T_0 + \frac{\sigma_0 \gamma}{C_p \rho} t \qquad [2.82]$$

where $\sigma_0 = A\exp(E/RT_0)$ is the shear stress at $T = T_0$, which is assumed to be constant on the plateau corresponding to the induction period.

An approximate analytical solution of Eq. (2.77) can be found, and, in fact, experimental data correspond to the condition:

$$\frac{\sigma_0 \gamma t}{T_0 C_p \rho} << 0$$

Then we can use the following approximation:

$$e^{-U/RT(t)} \approx e^{-U/RT_0}\left(1 - \frac{\sigma_0 \gamma}{T_0 C_p \rho}\right) \approx e^{-U/RT_0}\, e^{\delta\tau} \qquad [2.83]$$

so the final equation is written as:

$$\int_0^{\tau^*} e^{\delta\tau} d\tau = 1 \qquad [2.84]$$

This is an equation for the dependence $\tau^*(\delta)$. An analytical solution of this equation is found by integration and some rearrangement:

$$\tau^* = \frac{1}{\delta}\ln(1 + \delta) \qquad [2.85]$$

where the dimensionless shear rate is written as follows:

$$\delta = \frac{U}{RT_0^2}\frac{\sigma_0 \dot{\gamma} t_0^*}{C_p \rho}$$

It should be emphasized that in this case the dependence $\tau^*(\delta)$ is general, since it is insensitive to changes in the parameter β, and the role of the activation energy U is completely reflected in the value of δ. The dependence $\tau^*(\delta)$ derived from Eq. (2.85) is very close to the dependence $\tau^*(\delta)$ shown in Fig. 2.32 for $\xi = 0$. This graph is especially convenient for comparing experimental data with theoretical predictions.

Let us discuss the experimental data on the curing of phenolic resins,[118] which are shown in Fig. 2.33. In order to make theoretical calculations, the following characteristics of the resin derived from the experimental data were used:[114,118] at $T_0 = 393K$, the "static" value of t_0^* corresponding to the limit of very low shear rates, equals 240 s; $\sigma_0 = 0.2$ MPa; $C_p = 2$ kJ/(kg K); $\rho = 1\times10^3$ kg/m^3; U = 41.8 kJ/mol. Using these values, the dimensionless shear rate can be expressed as

$$\delta = 0.72\dot{\gamma}$$

At a low shear rates equal to 0.015 s^{-1}, which is usually used to measure the induction period, δ=0.01. Fig. 2.32 shows that $\tau^* = 1$; i.e., we have measured the "static" limit of the induction period. The maximum shear rate used in the experimental investigations[118] was equal to 15 s^{-1}. The value δ corresponding to this shear rate was 10.8 and (according to Fig. 2.32) in this case, τ^*=0.2; i.e., we can expect a 5-fold decrease in the induction period to only 0.8 min. Although it is only an approximation, rather than an exact calculation, this 5-fold decrease in the induction period in comparison with the static limit, corresponds to the experimental data shown in Fig. 2.33.

The correspondence between the calculated results based on the model of heat dissipation due to viscous flow and the experimental data in the decrease of the induction period at high shear rates proves that the observed effect is adequately explained by this mechanism. The effects of shearing itself on the kinetics of curing are either absent or of secondary importance. If the experimentally observed decrease in the induction period is more pronounced than predicted by the dissipative model, then it is reasonable to consider additional heat sources, for example, the exothermal effects of a reaction. Heat flux from the surroundings can also influence the kinetics of

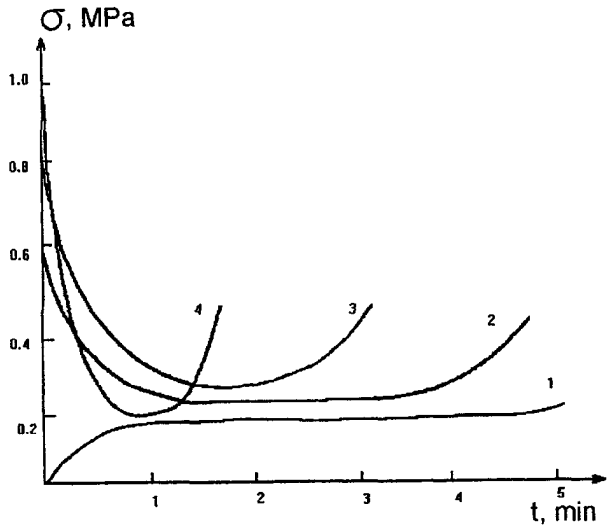

Figure 2.33. Experimental data illustrating the effect of a decrease in the induction period during curing of a phenolic-based compound at different shear rates: 0.015 s^{-1} (curve 1); 0.95 s^{-1} (curve 2); 3.75 s^{-1} (curve 3); 15 s^{-1} (curve 4).

curing. Non-isothermal curing may be caused by a linear temperature change in the surroundings, according to the expression

$$T(t) = T_0 + a_T t$$

where T_0 is the initial temperature and a_T is the rate of increase in temperature.

Eq. (2.85) is also applicable in this case, but the dimensionless shear rate must be replaced with another dimensionless parameter δ^*, which characterizes the non-isothermal effect. This is expressed as

$$\delta^* = \frac{E}{RT_0^2} a_T t_0^* \qquad [2.86]$$

Fig. 2.34 can be used to compare theoretical predictions for non-isothermal curing due to viscous heat dissipation with experimental data for two different curing materials.[119] For these two very different oligomeric systems, the theory gives adequate results, although the chemical curing mechanism is different in both cases. This is direct evidence that the effect is not caused by the influence of shearing itself on the chemical reaction kinetics. Rather, in both cases, the shearing of the induction period is due to the temperature increase resulting from heat dissipation.

Although the role of shearing has so far been restricted to dissipative heat generation, in some cases, which are also important in reactive processing, shear deformations can directly influence

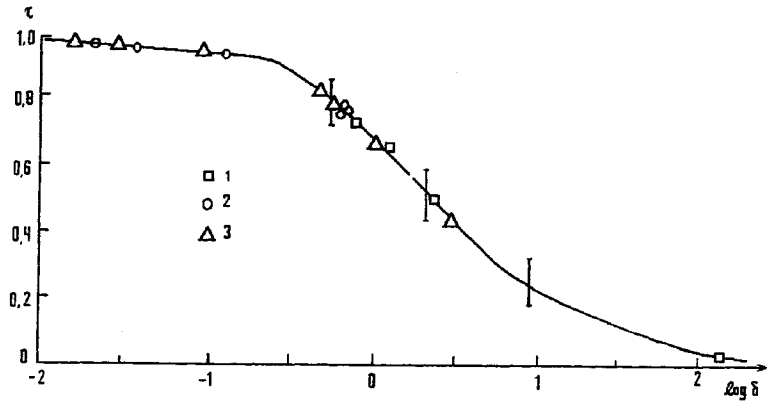

Figure 2.34. Comparison of theoretical predictions (curve, calculated from Eq. (2.85) according to the dissipative model of non-isothermal curing) with experimental data on the decrease of the induction period at high shear rates for phenolic-based compounds (vertical bars) and silicon-based composites at different initial temperatures: 150°C (1); 170°C (2) and 190°C (3).

the isothermal kinetics of a reaction. This depends primarily on the phase state of the polymerizing system,[120] because shearing influences the conditions under which phase transitions occur, and it is also important if the newly formed polymer is insoluble in the reactive medium. In such cases reactive processing occurs in a heterogeneous system and the reaction rate changes, depending on the phase state of the reactive medium.[111,120]

2.11.3 FLOW OF REACTIVE LIQUIDS

A flow of liquids with changing rheological properties is a necessary feature of reactive processing technology. The general theoretical treatment of the flow of reactive liquids is formulated using a cylindrical channel as a model of a tubular reactor. This is different than the model of a batch-process reactor discussed in Section 2.3, because it must include additional elements that reflect heat flux and the movement of the reaction products due to flow. It is reasonable to regard the process as quasi-stationary; this means that transient effects are determined by heat exchange processes, and the velocity profile follows temperature changes very rapidly.[121] In this case, the flow of a polymerizing liquid in a cylindrical tube is described by the following system of equations:

momentum balance equation

$$\frac{\partial P}{\partial z} = \frac{1}{r}\frac{\partial}{\partial r}\left[\eta(\beta,T) r \frac{\partial v_z}{\partial r}\right] \qquad [2.87]$$

continuity equation

$$\frac{1}{r}\frac{\partial}{\partial r}(rv_r) + \frac{\partial v_z}{\partial z} = 0 \qquad [2.88]$$

energy balance equation

$$\frac{\partial T}{\partial t} + v_r\frac{\partial T}{\partial r} + v_z\frac{\partial T}{\partial z} = \frac{\lambda}{C_p\rho}\left[\frac{\partial^2 T}{\partial r^2} + \frac{1}{r}\frac{\partial T}{\partial r} + \frac{\partial^2 T}{\partial z^2}\right] + \frac{Q_p k_0}{C_p\rho} f(\beta)e^{-E/RT} +$$

$$+ \frac{1}{C_p\rho}\eta(\beta,T)\left(\frac{\partial^2 V_z}{\partial z^2}\right)^2 \qquad [2.89]$$

where P is the pressure, z and r are the axial and radial coordinates, respectively, v_z and v_r are the axial and radial components of velocity, respectively, T is the temperature, C_p is the specific heat, Q_p is the enthalpy of a chemical reaction (polymerization), ρ is the density, and η is the viscosity, which (for a "rheokinetic" liquid) is a function of the degree of conversion β and temperature.

These equations must be supplemented by a kinetic equation for the time dependence of the degree of conversion $\beta(t)$, and the dependence of the viscosity of a reactive mass on β, temperature, and (perhaps) shear rate, if the reactive mass is a non-Newtonian liquid. The last two terms in the right-hand side of Eq. (2.89) are specific to a rheokinetic liquid. The first reflects the input of the enthalpy of polymerization into the energy balance, and the second represents heat dissipation due to shear deformation of a highly viscous liquid (reactive mass).

The influence of rheokinetics on flow can be summarized as follows:[122]

- there are marked changes in velocity profiles;
- the pressure-versus-output pattern is quite different than might be expected for a Newtonian liquid;
- the characteristics of the end-product are sensitive to the flow behaviour of a reactive liquid.

When a curing (solidifying) reactive medium fills a mold a rapid increase in viscosity can halt the flow, resulting in incomplete filling. A medium with a jump-like increase in its viscosity is a suitable model for theoretical analysis of flow of a solidifying liquid. It flows with relatively low viscosity up to a definite time limit, which can be treated as the "life-time" t^* of the material, and then the medium becomes solid-like and cannot flow. The life-time is a strongly temperature-dependent characteristic of a material, and decreases as the shear rate increases due to intensive heat dissipation during the flow of a viscous liquid. This phenomenon shows that it is very important to calculate the temperature fields in a flowing liquid, taking into account all sources of heat release, including hydrodynamic heat dissipation. Theoretical analysis has demonstrated and experiments have confirmed that highly viscous materials flowing near the walls of a channel can adhere as solid layers. This leads to a decrease in the cross-section of the channel and results in the deformation of the velocity profile.[46] Untimely solidification of the material can cause a sharp increase in pressure, leading to equipment shutdown and incomplete filling of the mold. In addition exothermal

effect during a reaction causes a rapid increase in the temperature of a reactive mass, and as a result, thermal decomposition of the material may occur.

The construction of a mold-filling model has been considered in the theory of thermoplastics processing. A rapid increase in viscosity also occurs in the flow of these materials, but the effect is different than in flow during reactive processing. The increase in viscosity of thermoplastic polymer materials is due to physical phenomena (crystallization or vitrification), while the increase in viscosity of reactive liquids occurs due to chemical polymerization reactions and/or curing. This comparison shows that the mathematical formulation of the problem is different in the two cases, although some of the velocity distributions may have similar features.

The most characteristic feature in models of two mold-filling stage is the existence of a stream with a moving free boundary.Therefore, in modeling a flow with the free boundary, it is reasonable to separate the stream into three parts: (1) the inlet into the channel; (2) the main region of stable flow; (3) the area close to the front of the stream. If we assume that the flow is smooth and neglect the inlet zone, then the most important factor is the flow near the free boundary. The interesting feature of the flow near the front of the stream is the so-called "fountain effect".[123] This phenomenon causes liquid particles around the axis of the channel to move with a higher velocity, resulting in shorter residence times. They are ejected through the front from the center to the walls, so that the flow lines are streams of a fountain. This transfer of the part of the reactive mass with the lowest degree of conversion to the near-wall layers has a major affect on the temperature field, degree of conversion, and viscosity.

Correct modeling of the flow near the front of a stream requires a rigorous solution of the hydrodynamic problem with rather complicated boundary conditions at the free surface. In computer modeling of the flow, the method of markers or cells can be used;[124] however this method leads to considerable complication the model and a great expenditure of computer time. The model corresponds to the experimental data with acceptable accuracy if the front of the streamis assumed to be flat and the velocity distribution corresponds to fountain flow.[125,126] The fountain effect greatly influences the distribution of residence times in a channel and consequently the properties of the reactive medium entering the mold.

2.12 RESIDUAL STRESSES AND STRAINS

2.12.1 PHYSICS OF RESIDUAL STRESSES IN UNIFORM MATERIALS

There are two possibilities: first, nonuniform or multicomponent polymer materials. Internal stresses may appear due to differences in the properties of various parts of an article and the existence of phase boundaries. Second, uniform materials, which seem quite homogeneous, can be amorphous or polycrystalline.The physics of the development of residual stresses in such materials will be discussed in this section.

Residual (or inherent) stresses are self-balancing stresses that exist throughout the volume of a body in the absence of external forces. The appearance and growth of residual stresses in non-loaded articles are typical of materials prepared by the reactive processing. A general source

of residual stresses is nonuniform polymerization throughout the material volume. The degree of conversion is therefore different in various parts of the material, and this results in different stages of evolution of mechanical properties and shrinkage. Inherent stresses can be so large that they significantly influence the mechanical behavior and dimensional stability of an article. Effects such as rupture of semi-finished products during machining are also known in practice. This is due to the superposition of residual stresses and stresses caused by an applied force.

The important role of residual stresses is typical of large-size articles made by reactive processing. The general cause of the phenomenon is that the material is prepared at temperatures higher than its temperature range of use. On cooling (or quenching), the non-uniform temperature field leads to a non-uniform temperature distribution inside the material. The mechanical properties of polymer materials depend on temperature; therefore, the properties in a medium are with non-uniform temperature distribution different at various points,and this difference results in stresses and strains. During cooling and transition of a material to a solid (elastic) state these stresses and strains are frozen and stored inside the material, because of the loss of molecular mobility and a large increase in relaxation times in the process of vitrification or crystallization.

The viscosity of an initial reactive mixture used for reactive processing is low, and shaping of the articles usually takes place in stationary molds; i.e., external loading does not play a significant role. The poor temperature conductivity of all polymer materials nevertheless contributes to non-uniform cooling. Inhomogeneous crystallization increases the differences in material properties. In addition the increase in molecular weight during polymerization, structural changes during crystallization, and the liquid-to-solid transition during cooling lead to a decrease in the specific volume of the material, i.e., to shrinkage. Since shrinkage also occurs in inhomogeneous conditions, this is a major source of inherent stresses.

One further reason for the development of residual stresses should be mentioned. This is the heterogeneity of the final state of a material which may occur even if the initial reactive mixture was homogeneous. This phenomenon is related to the differing diffusion rates of the various components of the reactive mass during a chemical reaction. This localized distribution of concentrations can be frozen upon solidification of the material.

2.12.2 MODELLING RESIDUAL STRESSES IN REACTIVE PROCESSING

The primary reason for the appearance of inherent stresses is inhomogeneity of the temperature and conversion fields within an article. Therefore calculations of the $T(z,t)$ and $\alpha(z,t)$ functions, which were discussed in Section 2.3, are the basis for estimating residual stresses. It is generally necessary to consider functions of all three coordinate directions. In many cases, it is important to know the final stress distribution and its change in time; this is why time t enters the functions $T(z,t)$ and $\alpha(z,t)$ as an independent argument.

In the majority of practical important situations, it is reasonable to neglect heat output due to deformations and its possible influence temperature and reaction rate. This simplifies the problem and splits it into two independent parts: first, calculation of the temperature and conversion fields, and second, estimation of the stresses from previously determined temperature and conversion

fields. The second part of the general problem will be discussed in this section. In this part of the problem the relationship between stresses and deformations must be established. This entails determining the rheological equation of state for a medium whose properties depend on temperature and degree of conversion; this is a very general problem in continuum mechanics.

Extensive theoretical investigations devoted to calculation of residual stresses have been carried out for metals. The principal theme of this work is assumption that residual stresses and strains are the result of differences between pure elastic and elastic-plastic deformations under fixed loading.[127, 128] The same mechanism, i.e., the appearance of plastic deformed zones, is responsible for the residual stresses arising during crystallization of metals, which occurs on quenching from the melt or cooling after welding.

The main difference between metals and polymers is related to the fact that transitions from one state to another in polymers occur (as a result of changing of environmental conditions, primarily temperature) not as jumps but continuously. This leads to the absence of a clearly defined line or transition front. Additionally, because of the low heat and temperature conductivity of polymeric materials, a change in material properties may take place over a large volume,or even simultaneously throughout the whole mass of an article, although the local transition rates and degrees of conversion may be different. Thus it is necessary to develop a macrokinetic model of the transition. This model must describe the combined effects of non-stationary heat transfer and reaction kinetics and is used to determine the temperature and conversion fields.

Every point of a body travels along a trajectory in the temperature-conversion field that is different from that of any neighbouring point. Residual stresses in polymers are a result of deformational inhomogeneities which arise in a material during solidification (crystallization or vitrification) through evolution of the temperature-conversion fields. They provide a "memory" of the stress state, which has been frozen into a material by solidification. Modeling the appearance and evolution of inherent stresses involves solving the system of interrelated equations for energy balance and the rheological equation of state (stress versus deformation), taking into account loading prehistory, temperature and conversion changes, and the dependence of material properties on these factors. The formulation of the problem is shown schematically in Fig. 2.35.

2.12.3 RESIDUAL STRESSES IN AMORPHOUS MATERIALS

Real polymeric materials are viscoelastic bodies. In a purely elastic material stresses $\sigma(t)$ are proportional to deformations $\varepsilon(t)$, and the coefficient of proportionality is Young's modulus E, i.e., at any time t

$$\sigma = E\varepsilon$$

Stresses in viscoelastic materials "remember" deformation prehistory and so are not an unambiguous function of instantaneous deformations; however, they may be expressed by a functional. For a linear viscoelastic material, the relationship between stresses and deformations can be defined by a pair of integral equations:[128, 129]

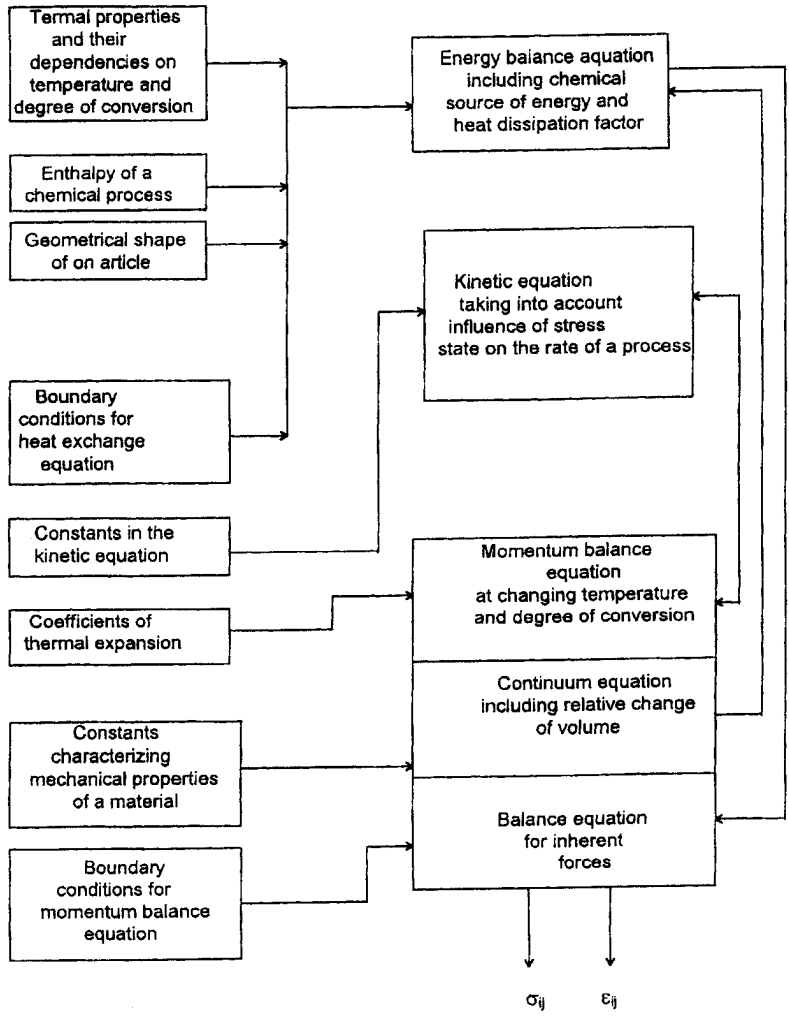

Figure 2.35. Functional relationships among systems of equations used to describe stress, temperature, and conversion fields in an article during processing.

$$2G_0 e_{ij} = s_{ij} + \int_0^t \Gamma(t - \tau) s_{ij} d\tau \qquad [2.90]$$

$$K_0 \theta = \sigma + \int_0^t U(t - \tau)\sigma(\tau) d\tau \qquad [2.91]$$

where $s_{ij} = \sigma_{ij} - \sigma\delta_{ij}$ is the deviator of the stress tensor; $e_{ij} = \varepsilon_{ij} - \varepsilon\delta_{ij}$ is the deviator of the deformation tensor; θ is the relative volume change; σ is an average (equal to negative pressure) stress; G_0 is the instantaneous shear modulus; K_0 is the instantaneous modulus of volume deformations (bulk modulus); Γ and U are kernels characterizing viscoelastic properties of a material, which represent its spectrum of relaxation times; both are functions of the difference between current and former times $(t - \tau)$.

This approach involves a limited number of material constants and functions, that characterize material properties. There are standard experimental techniques for measuring these viscoelastic properties in a material and well-developed mathematical methods for solving mechanical problems concerned with these properties. Therefore, this approach is often used to solve many applied problems. However, for calculating residual stresses, this general approach is too complicated because the material properties are changing during the whole formation cycle making it necessary to know the material constants and relaxational kernels as functions of temperature and degree of conversion. The relaxation properties of a material also change radically at the gel-point (critical point); in the vicinity of the gel-point, the relaxation spectrum not only shifts along the time scale but changes its shape.[130] This means that it is incorrect to use difference arguments in relaxation kernels, as in Eqs. (2.90) and (2.91); instead, it is necessary to use more complicated models that take into account changes in the shape of the relaxation functions. All this creates difficulties in solving mechanical problems, so that it is questionable whether the complex of material constants and functions which must be known to solve specific problems can be determined.

One method for overcoming this difficulty is to introduce the modified (or reduced) time t', which allows the use of integral relationships with different arguments. The definition of modified time is based on the principle of time-temperature superposition. This is the usual way to generalize temperature-dependent functions using the argument

$$t' = \frac{t}{a_T(T)} \qquad [2.92]$$

where $a_T(T)$ is the shift-factor or the function representing the temperature dependence of the relaxation properties of the material.

The most popular and widely used formula for the function $a_T(T)$ is the Williams-Landel-Ferry equation, which is quite adequate for amorphous polymers above the glass transition temperature:

$$\ln a_T(T) = -c_1 \frac{T - T_g}{c_2 + T - T_g} \qquad [2.93]$$

where c_1 and c_2 are constants; T_g is the glass transition temperature. If the temperature is a function of time T(t) then the modified time is calculated as

$$t' = \int_0^t a_T(T)dt \qquad [2.94]$$

The temperature dependence of the relaxation times introduced into mechanical equations by means of Eq. (2.93) was used to calculate the residual stresses in cooling amorphous polymers.[131-133] This is a very useful approach, which can be recommended for practical applications. A simplified version of this general treatment may also be useful. It is possible to consider vitrification of a material as a jump-like transition from a liquid to a solid state. This idea was advanced elsewhere,[134] where residual stresses in inorganic glasses were calculated by treating vitrification as a sequential solidification of layers of a viscous liquid on the rigid surface of a previously solidified material. In a liquid layer (not yet solidified) at $T > T_g$, only flow deformations can occur. In the transition through T_g, this deformation is frozen in and cannot change later on.

The calculation of residual stresses in the polymerization process during the formation of an amorphous material was formulated earlier.[128] The theory was based on a model of a linear viscoelastic material with properties dependent on temperature T and the degree of conversion β. In this model the effect of the degree of conversion was treated by a new "polymerization-time" superposition method, which is analogous to the temperature-time superposition discussed earlier.

A general method of applying viscoelasticity theory to unstable (changing) materials in varying temperature fields was proposed in a number of publications (see, for example Ref.[135]). In this approach, the state of a material is represented by the factor ψ, which is a function of a set of "structural" parameters

$$\psi = \psi(\psi_1, \psi_2, .., \psi_n) \qquad [2.95]$$

The general equation for the kinetics of the structural transformation is as follows

$$\frac{d\psi}{dt} = F(\psi,T) + G(\psi,T)\frac{dT}{dt} \qquad [2.96]$$

where the first term F represents the kinetics of the structural transformations due to chemical reactions, and the second reflects the quasi-equilibrium influence of temperature on material properties. In this model, the rheological equation of state connects the stress tensor, the deformation tensor, and the tensor of structural transformations. This model seems realistic and physically sound but is rather difficult to apply for solving problems, because it is not clear how to relate the material parameters of a medium to continuously changing structural factors.

By considering the polymerization process to be solidification of a reactive liquid, it is possible to model the process as a liquid-to-solid transformation with a moving front.[136-138] Chemical shrinkage resulting from changes in specific volume during polymerization was chosen as the determining factor. It was assumed that the width of the reaction zone was rather narrow, so that it was possible to treat it as a front. It was proposed that only elastic deformations could occur in the solid layer and that shrinkage deformations were superimposed on the elastic deformations inside a narrow transitional zone. This model was used to analyze non-isothermal polymerization in a hollow sphere in a reaction spreading from the center to the surface, from the surface to the center, and from both sites in double-sided front solidification.[139] It was found that the theoretical predictions adequately corresponded to some important practical observations, such as breaks in continuity, a decrease in strength of the materials, etc.

It is also quite reasonable to treat a reactive medium as a two-component material.[140,141] The initial state of the reactive mixture is a low-viscosity liquid, which passes into a uniform solid material as a result of chemical reactions. The ratio of solid-to-liquid components is determined by the degree of chemical conversion. This ratio is an important property of a reactive mixture, and can range from 0 to 1. The fundamental characteristic of such a two-component material is its specific free energy. This thermodynamic function is assumed to be the sum of the free energies of both components calculated from the degree of conversion:

$$\Phi(\beta) = \int_0^{\beta} \Phi_0[\varepsilon_i(\beta')d\beta' + (1 - \beta)\Phi_1(\varepsilon) \qquad [2.97]$$

where Φ is the total free energy; Φ_0 and Φ_1 are the free energies corresponding to the initial and final states of the material, respectively; ε_i is the elastic deformation tensor; β is the degree of conversion.

2.12.4 RESIDUAL STRESSES IN CRYSTALLIZABLE MATERIALS

The phase transition rate in the crystallization of polymeric materials is of the same order as the rates of the heat exchange processes accompanying crystallization. Consequently, the boundary between phases becomes spatially dispersed. This excludes the possibility of using methods based on the front transition model proposed for metals to calculate residual stresses in plastics.[148] It is possible to split the general problem and to find the temperature-conversion field independently. Then, assuming that the evolution of temperature $T(x,t)$ and degree of crystallinity $\alpha(x,t)$ in time t and in space (x is the radius vector of an arbitrary point in a body) is known, we can analyze the mechanical problem.[143]

Calculation of residual stresses in crystallizable materials is primarily based on the assumption that these materials can be treated as a two-component mixtures of initial and final products, as indicated in Eq. (2.97). In this case, the share of both components is determined by the degree of crystallinity α, which is changing in time. The initial product is a melt, for which $\alpha = 0$; the final

product is a solid material with an equilibrium degree of crystallinity equal to α_0. A polymer melt is a liquid, and in static conditions it can be loaded only by hydrostatic pressure. Thus, we can assume that the relaxation time of the initial material with respect to shear stresses is equal to zero. The stress-deformation state of the final product, i.e., the crystallized material, can be represented by an ideal elastic body, with a corresponding infinitely long relaxation time. The share of the final (crystallized) product is found as a solution of the energy balance and kinetic equations.

In order to derive the determining physical equation for the stress-deformation state of a two-component mixture, let us consider the expression for the change in the elastic potential energy during a continious transition from a liquid to a solid phase. Let this transition occur at time $t = t_0$ and let the quantity of material that undergoes the transition be equal to the increase in the degree of crystallinity $\Delta\alpha$. The specific elastic potential characterizing the new state of the material up to the time of a new transition can be written as

$$F(\varepsilon_0) = F_s(\varepsilon_0)\Delta\alpha_0 + F_l(\varepsilon_0)(1 - \Delta\alpha_0) \qquad [2.98]$$

where F_s and F_l are elastic potential functions for the solid and liquid phases, respectively. The detailed expressions for both components of the total elastic potential are as follows:

$$F_s(\varepsilon_0) = \frac{1}{2}(K_s - \frac{2}{3}G_s)I_1^2[\varepsilon_0(\Delta\alpha_0)] + G_sI_1[\varepsilon_0^2(\Delta\alpha_0)] -$$

$$- 3K_s\chi_sI_1[\varepsilon_0(\Delta\alpha_0)][T(t) - T(t_0)] + K_skI_1[\varepsilon_0(\Delta\alpha_0)] \qquad [2.99]$$

and

$$F_l(\varepsilon_0) = \frac{1}{2}K_lI_1^2[\varepsilon_0(\Delta\alpha_0)] - 3K_lI_1[\varepsilon_0(\Delta\alpha_0)]\chi_l[T(t) - T_0] \qquad [2.100]$$

where F is the total elastic potential function of the mixture (two-component material); ε_0 is the linear deformation tensor; K_s and G_s are volume and shear moduli, respectively, of a solidified material, depending on the current temperature T(t); $I_1[\varepsilon_0(\Delta\alpha_0)]$ is the first invariant of the deformation tensor ε_0, which depends on the degree of transformation $\Delta\alpha_0$; $I_1[\varepsilon_0^2(\Delta\alpha_0)]$ is the first invariant of the squared deformation tensor; χ_s and χ_l are coefficients of thermal expansion for the solid and the liquid phases, respectively, which may depend on temperature; T_0 is the initial temperature; k is the coefficient of volume shrinkage, which depends on the difference in density between the solid and liquid phases.

Let the next transformation occur at time $t = t_1$, and let its value be $\Delta\alpha_1$. Then the net degree of transformation at time t_1 equals $\Delta\alpha_0 + \Delta\alpha_1$. This change in the degree of transformation corresponds to the passage of a volume share of non-solidified material proportional to $\Delta\alpha_1$ into the solid state. Then, starting from time t_1, this volume share undergoes deformation together with the portion of previously solidified material whose share is $\Delta\alpha_0$. The specific elastic potential of such a two-component composite up to the next step in the transformation can be written as

$$F(\varepsilon_1) = F_s(\varepsilon_1)\Delta\alpha_0 + F_s(\varepsilon_1 - \varepsilon_0) + F_l(\varepsilon_1)(1 - \Delta\alpha_0 - \Delta\alpha_1) \qquad [2.101]$$

where ε_1 is the linear tensor of full deformation up to the next step of transformation, it depends on the sum $\Delta\alpha_0 + \Delta\alpha_1$; $F_s(\varepsilon_1 - \varepsilon_0)\Delta\alpha_1$ is the share of the specific elastic potential of the solidified part of a material which is proportional to $\Delta\alpha_1$; its deformation tensor equals $(\varepsilon_1 - \varepsilon_0)$, because at the moment t_1 its deformation state is regarded as zero (reference state).

Let us consider the n^{th} step of the transformation $\Delta\alpha_n$ at time t_n. Now, it is possible to write down the equation for the elastic potential of the material up to time t_{n+1}, when the next transformation $\Delta\alpha_{n+1}$ occurs:

$$F(\varepsilon_n) = F_s(\varepsilon_n)\Delta\alpha_0 + F_s(\varepsilon_n - \varepsilon_0)\Delta\alpha_1 + \ldots + F_s(\varepsilon_n - \varepsilon_{i-1})\Delta\alpha_i + \ldots$$

$$\ldots + F_s(\varepsilon_n - \varepsilon_{n-1})\Delta\alpha_n + F_l(\varepsilon_n)(1 - \sum_{i=0}^{n} \Delta\alpha_i) \qquad [2.102]$$

where ε_i is a function of the sum $(\Delta\alpha_0 + \Delta\alpha_1 + \ldots + \Delta\alpha_i)$, i.e., of the degree of transformation at time t_i. It is evident that the right-hand side of Eq. (2.102) is an integral sum and in the transition to the limit we have:

$$F[\varepsilon(t)] = \int_0^{\alpha(t)} F_s(\varepsilon[\alpha(t)] - \varepsilon[\alpha(\tau)])d\alpha(\tau) + F_l(\varepsilon[\alpha(t)])[1 - \alpha(t)] \qquad [2.103]$$

Using the expression for the specific free energy, it is possible to formulate the determining physical (rheological) relationship:

$$\sigma_{ij} = \frac{\partial F}{\partial \varepsilon_{ij}} = \int_0^{\alpha(t)} ((K_s - \frac{2}{3}G_s)I_1[\varepsilon(t) - \varepsilon(\tau)]\delta_{ij} + 2G_s[\varepsilon_{ij}(t) - \varepsilon_{ij}(\tau)] - 3K_s\chi_s[T(t) -$$

$$- T(\tau)]\delta_{ij} + K_s k\delta_{ij})d\alpha(\tau) - 3K_l\chi_l[T(t) - T_0]\delta_{ij} \qquad [2.104]$$

where δ_{ij} is the Kronecker symbol (tensor unit).

According to the model under discussion residual stresses are the result of deformational inhomogeneities in a material, which arise from the heterogeneity of the temperature-conversion fields in the course of crystallization and are stored during solidification. The important advantage of this approach is the evident introduction of the fundamental determining equation, Eq. (2.98), and the direct experimental methods for finding the material constants and functions used in the model. It is sufficient to measure the temperature dependence of the material constants of the initial material (melt) and the final product (crystallized solid). After establishing the main rheological equation (2.104) the boundary problem can be formulated in the usual way:

equilibrium equation

$$\nabla\sigma + f = 0, \quad x \in V \qquad [2.105]$$

boundary conditions

$$u = 0; \quad s \in S_u; \quad v\sigma = g; \quad x \in S_\sigma \qquad [2.106]$$

geometrical Cauchy condition

$$\varepsilon = \frac{1}{2}[(\nabla u)' + (\nabla u)] \qquad [2.107]$$

where σ is the stress tensor; u, f, and g are vectors of displacement, mass and surface forces, respectively; V is the volume including the solidified material; x is the radius-vector of an arbitrary point inside the volume V; S_u and S_σ are parts of the surface surrounding the volume V, where different boundary conditions are present; v is the radius vector of the unit normal to the surface S_σ; the point in Eq. (2.106) determines the scalar product of a vector by a tensor.

The generalized solution of this problem is found by the variational method of virtual displacements.[140] According to this principle, the sum of the virtual work done in traversing possible displacement path is equal to zero:

$$\delta A_0 + \delta A_Q = 0 \qquad [2.108]$$

where

$$\delta A_0 = \int_V \sigma_{ij}\delta\varepsilon_{ij}dV \qquad [2.109]$$

Eq. (2.109) describes the virtual work done by the inherent stresses inside the volume V. In this case, the virtual work done by the applied forces δA_Q equals zero.

If we consider a cylindrical body as a typical example of an article produced by reactive processing, we can write the variational equation as follows:

$$\delta A_\sigma = \int_V [\delta\varepsilon]\tau[\sigma]dV = 0 \qquad [2.110]$$

where $[\delta\varepsilon] = [\delta\varepsilon_r, \delta\varepsilon_\theta]$ is the matrix row and $[\delta\sigma]$ is the matrix-column. The problem formulated above was solved numerically by the finite element method. The displacements, temperatures, and degrees of crystallinity α, entering Eq. (2.104) were approximated by linear functions along the coordinate r inside all elements of the cylinder. The stress fields are calculated by integrating over the parameter α by means of step-by-step calculation of the deformation fields at each time interval.

Let us compare the calculated temperature fields to the experimental values for cylindrical articles made of polycaproamide (PA-6), since these fields are the starting point for further calculations. Cylinders of diameter 67 mm and length 300 mm were prepared by anionic activated polymerization,[144] which is commonly used in reactive processing. The sample is sufficiently long to be treated as homogeneous along the z-axis. The initial temperature was 228°C; i.e., it was a supercooled melt below the equilibrium melting temperature. The temperature of the surroundings

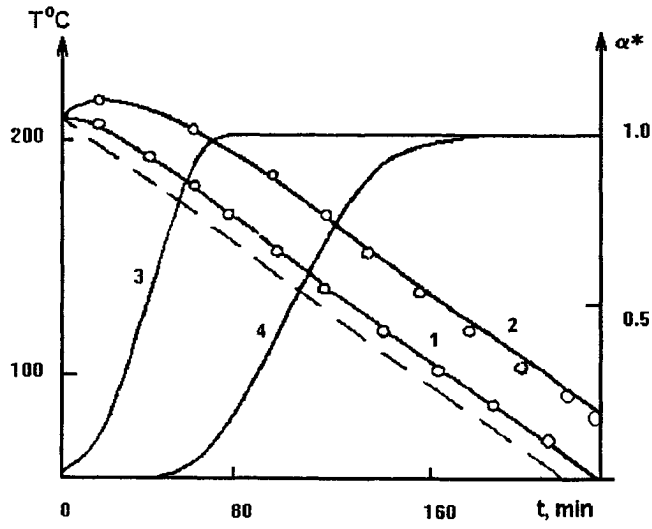

Figure 2.36. Evolution of the temperature (curves 1 and 2) and the degree of transformation (curves 3 and 4) at the surface (curves 1 and 3) and at the center (curves 2 and 4) of a cylinder of radius 34 mm. The dashed line shows changes in temperature of the surroundings. Solid lines are calculated. Points are from measurements.

changed linearly at a rate of 1 K min^{-1}. The constants of the equations were found by solving the inverse problem.

The results of the calculations and a comparison with experimental data are shown in Fig. 2.36. For convenience in comparison, the degree of crystallinity is normalized to its equilibrium value, so that the calculated function of the reduced crystallinity α^* changes from 0 to 1. Fig. 2.36 shows that a solution with the appropriate values of the constants fits the experimental data with high degree of accuracy. Both calculations and experiment show a pronounced inhomogeneity in temperature T and degree of transformation α^*, even for a cylinder with a relatively small diameter the difference in temperature can reach some tens of K.

It is also possible to investigate the development of residual stresses in cylindrical articles. The main parameters influencing the level of residual stresses, namely, the cooling rate and article size, were varied. The following values of the material parameters were used:

Coefficients of thermal expansion: $\alpha_s = 9\ 10^{-5}\ K^{-1}$; $\alpha_l = 2.8\ 10^{-4}\ K^{-1}$;

Poisson's ratios: $\mu_s = 0.34$; $\mu_l = 0.492$;

Volume modulus of elasticity for the liquid phase: $K_l = 3\ 10^3$ MPa.

Temperature dependencies of the volume and shear moduli for the solid phase were found experimentally[145] for polycaproamide (PA-6). The results of the calculations are shown in Figs. 2.37-2.41. These results demonstrate the evolution of the stresses σ_{ij} during crystallization and the

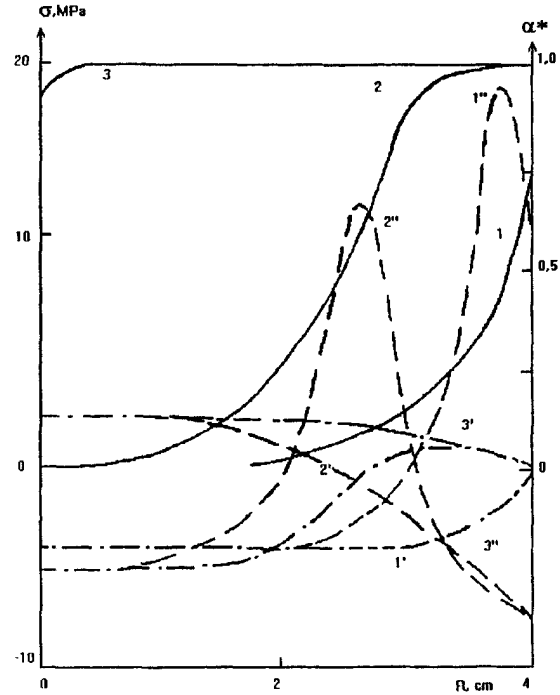

Figure 2.37. Distributions of the degree of conversion α^* (curves 1-3), radial σ_R (curves 1'-3') and circumferential σ_θ (curves 1''- 3'') stresses in a cylinder of radius 40 mm after 40 min (curves 1, 1'), 70 min (curves 2, 2') and 140 min (curves 3, 3') after the start of the process.

level of residual stresses expected after complete cooling of the article. First, let us discuss changes in σ_{ij} and α^* for a cylinder of radius 40 mm at a cooling rate of 1 K min^{-1}. The evolution of radial σ_r and circumferential σ_θ stresses is given in Fig. 2.37 for various times, including the final stage of cooling. The results show that the mechanical processes in reactive processing and formation of crystallizable polymeric articles can be successfully analyzed. In particular, it becomes possible to establish the interrelation between the stress-strain state of a material and values of the crustallinity α^*. Within 40 min from the beginning of solidification, α^* in the outer surface layers of the article reaches 75%, and is accompanied by large tensile circumferential stresses, while the central part of the article is under compressive stress. With increasing process time up to 70 min, α^* continues to increase but the surface circumferential stresses change sign to become compressive and the

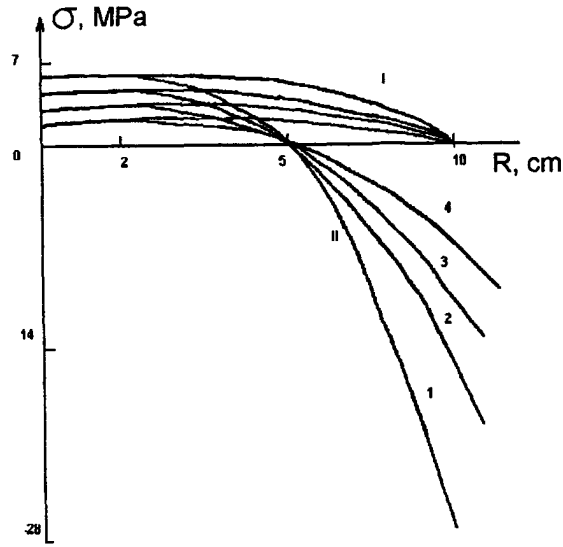

Figure 2.38. Distribution of residual stresses σ_R (curves I) and σ_θ (curves II) in a cylinder of radius 100 mm at a cooling rate of 2 K min^{-1} (curve 1), 1 K min^{-1} (curve 2), 0.75 K min^{-1} (curve 3), 0.5 K min^{-1} (curve 4).

volume under compression decreases. Growth of the zone of crystallized material leads to a further reduction of hydrostatic compression at the center and a decrease in tensile circumferential stresses. The residual stresses near the surface of the material change very little during the ensuing cooling process. The material reaches equilibrium crystallinity throughout its full volume at ≈140 min after the start of the process, and residual stresses are also fully developed at this time. These results confirm the approximations used to calculate residual stresses in crystallizable polymeric materials.

The influence of the cooling rate v_T on the level of residual stresses was investigated by a numerical method for a solid cylinder of radius 100 mm at cooling rates varying from 0.25 to 2.0 K min^{-1}. The results are shown in Fig. 2.38. It is clear that an increase in the cooling rate contributes to residual stress formation (Fig. 2.39). The influence of the size of an article on the maximum stresses is shown as a function of the cylinder radius at a constant cooling rate (Fig. 2.40). The size of an article significantly influences the level of residual stresses, and even in relatively small slabs, the residual stress can reach high values. Considering that the stresses σ_{ij} may be much higher than in the final state, as was shown in Fig. 2.37, and that the strength of a material at elevated temperatures is lower than at room temperature, mechanical damage of articles during processing (especially during cooling) is a definite possibility.

Residual stresses can be reduced by thermal treatment of polymeric articles after processing. The majority of investigations devoted to this technological method are based on an empirical approach which yields the optimal conditions, such as temperature, pressure, duration of treatment,

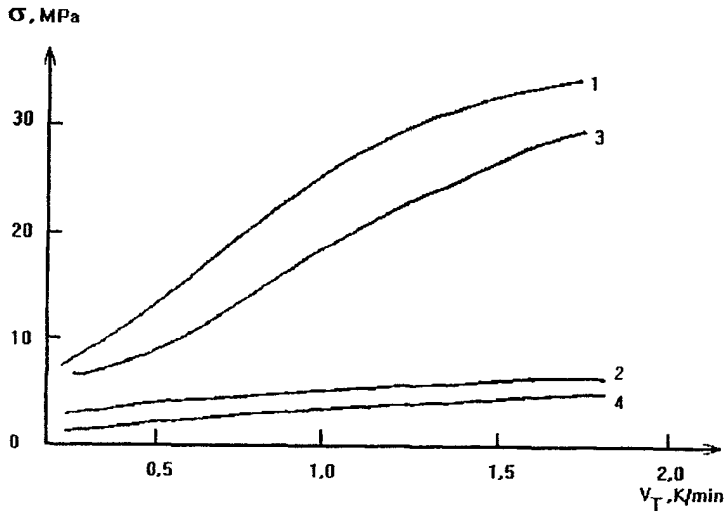

Figure 2.39. Dependences of maximum residual stresses σ_θ (curves 1 and 3) and σ_R (curves 2 and 4) on the cooling rate inside cylinders of radii 150 mm (curves 1 and 2) and 100 mm (curves 3 and 4).

environmental conditions, and so on. Thermal treatment of finished polymeric articles is a very energy-intensive and lengthy process. Thus, it is preferable to search for ways to reduce inherent stress formation during processing (process optimization) to minimize energy consumption and production time.

The experimental methods used to measure residual stresses are essentially the same for metals and polymers. The most widespread are mechanical methods, which can be destructive, non-destructive, and semi-destructive[146]. Destructive methods involve cutting off part of a sample; the residual part reacts to this procedure by deformations or displacements proportional to the inherent stresses. This approach is based on the Saint-Venant principle: the response in the residual part does not depend on the stress distribution in the cut part of a sample. After measuring the distribution of deformations, residual stresses in the initial sample can be calculated.

The choice of experimental method for measuring residual stresses depends on the geometrical shape of the sample. For example, to measure the inherent stresses in bars and plates, it is convenient to use the bending method, in which the outer layers of a sample are cut off one by one and the circular and axial deformations along the outer radius are measured. The accuracy of the results can be checked by cutting rings and following the deformation of the cut pieces.[146] Using this method, residual stresses were estimated for one typical case, a cylinder of radius 34 mm. The calculated data are presented in Fig. 2.40. A comparison of the experimental and calculated values of residual stresses is shown in Fig. 2.41. There is a good correlation of results; however, it was

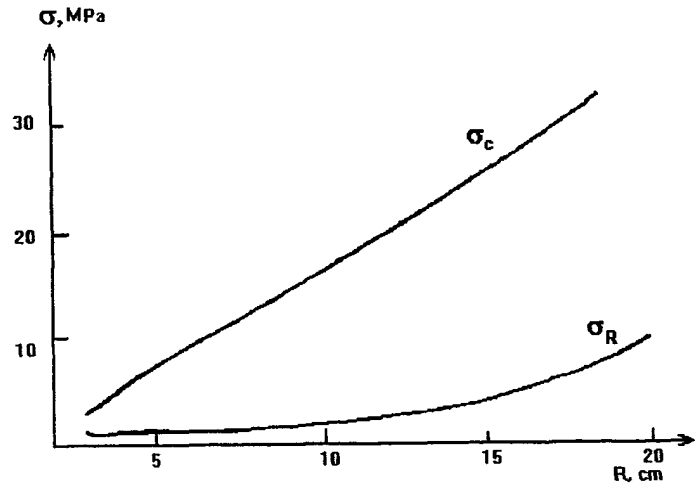

Figure 2.40. Distribution of residual stresses σ_R and σ_θ (marked on the curves) inside a cylinder of radius 34 mm at a cooling rate of 1 K min^{-1}

very difficult to measure the stresses in the vicinity of the center of the article (at R < 8 mm) with sufficient accuracy.This is explained by difficulties in preparing rings of small radius. The main disadvantage of the above method is its destructive character.

Semi-destructive methods are used primarily for samples with a complicated shape. The method consists of drilling small holes at selected locations in the article.

Non-destructive methods include holographic interferometry, resistance transducers, stress-sensitive covers, and other similar techniques. In practice, the following physical methods of non-destructive monitoring of residual stresses are commonly used: X-ray diffraction, measurement of dielectric properties, and ultrasonic control. The main purpose of these methods is to monitor the structural transformations or distortions taking place as a result of residual stresses and local deformations. However, the application of methods such as X-ray diffraction to measure distortions in unit cel dimensions, ultrasonics to measure elastic wave propagation velocities, etc., all encounter numerous experimental problems. Therefore, in ordinary laboratory conditions only quantitative estimations of residual stresses can be obtained.

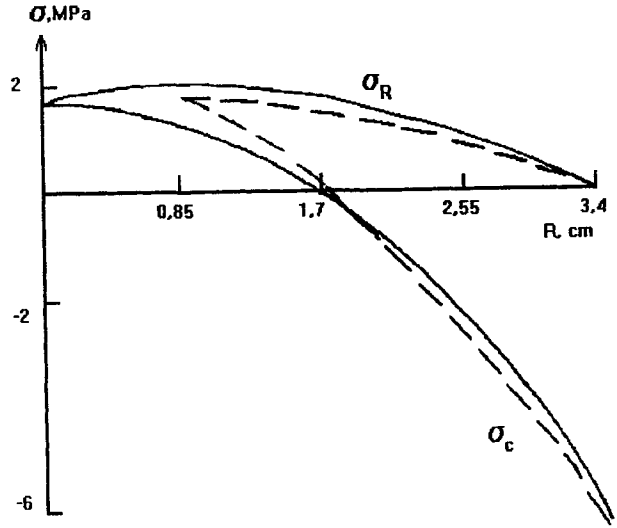

Figure 2.41. Comparison of calculated (solid lines) and experimental (dashed lines) dependencies of the maximum residual stresses σ_R and σ_θ (marked on the curves) inside a cylinder of radius 34 mm at a cooling rate of 1 K min^{-1}

3

RESEARCH AND CONTROL METHODS

3.1 GENERAL

The manufacture of products by reactive molding results in the superposition of interrelated chemical and physical phenomena. These include polymerization, crystallization, vitrification, heat transfer, rheokinetic effects, changes in the physical properties and volume of a material injected into a mold. It is quite natural that special experimental methods are required to study and control the complex processes which take place in molds.

The study and control of a chemical process may be accomplished by measuring the concentrations of the reactants and the properties of the end-products. Another way is to measure certain quantities that characterize the conversion process, such as the quantity of heat output in a reaction vessel, the mass of a reactant sample, etc. Taking into consideration the special features of the chemical molding process (transition from liquid to solid and sometimes to an insoluble state), the calorimetric method has obvious advantages both for controlling the process variables and for obtaining quantitative data. Calorimetric measurements give a direct correlation between the transformation rates and heat release. This allows to monitor the reaction rate by observation of the heat release rate. For these purposes, both isothermal and non-isothermal calorimetry may be used. In the first case, the heat output is effectively removed, and isothermal conditions are maintained for the reaction. This method is especially successful when applied to a sample in the form of a thin film of the reactant. The temperature increase under these conditions does not exceed 1K, and treatment of the experimental results obtained is simple: the experimental data are compared with solutions of the differential kinetic equation.

The situation becomes more complicated if experiments are carried out in non-isothermal conditions. First of all,many non-isothermal measurement procedures are possible. The selection of a particular method depends on the process characteristics and methods of interpretation. Scanning calorimeters, which measure the quantity of heat released as the ambient temperature is varied linearly. The rate of temperature change can be varied by the experimenter.

Another method for investigating non-isothermal polymerization is adiabatic calorimetry, because it is a convenient method for treating experimental data. A system is adiabatic if the temperature changes along the coordinates $\partial t/\partial x = 0$ and the Biot Number, Bi, is equal to zero. The $\partial t/\partial x$ value may be considered equal to zero at $Bi < 0.1$. These conditions are achieved by reliable thermal insulation of the reactive volume or by continuous measurement of the temperature of the reactant mass and regulation of the containment temperature in order to exclude temperature gradients and heat flux from the reactive volume to the surroundings. The simplest method of making measurements in adiabatic conditions is to monitor the temperature in the center of the polymer volume where near-adiabatic conditions are achieved because of the low thermal conductivity of the reactant mixture; in this case, the reactive volume must be sufficiently large.

The engineering requirements for reactive molding of large articles depend to a large extent on the changes in viscosity of the medium during polymerization. This is why it is important to measure the rheokinetics of the process, bearing in mind that these measurements are accompanied by increase in sample temperature due to heat output. Standard rotational viscometers[147] can be used, although their application is limited to the range in which deformations do not influence the material structure being formed by chemical reactions.

Dynamic mechanical analysis methods are frequently used to investigate polymerization and curing processes in reactive systems. These methods allow us to obtain both relative and absolute rheological characteristics of a material. Measurements can be made in both the fluid and solid states without affecting the inherent structure of the polymerizing system.

One of most popular techniques for dynamic mechanical analysis is the torsion pendulum method. In a modification of this method designed to follow curing processes, a torsion bar is manufactured from a braid of fibers impregnated with the composition to be studied; this is the so-called "torsional braid analysis" (TBA) method.[61,62,148] The forced harmonic oscillation method has been also used and has proven to be valuable. This method employs various types of rheogoniometers and vibroreometers,[149,150] which measure the absolute values of the viscoelastic properties of the system under study; these properties can be measured at any stage of the process. The use of computers further contributes to improvements in dynamic mechanical analysis methods for rheokinetic measurements. As will be seen below, new possibilities are opened up by applying computer methods to results of dynamic measurements.

Changes in the volume of the reactive mass during polymer synthesis permit the use dilatometric and gravimetric methods in laboratory research. In full-scale industrial applications, instruments that can measure the temperature changes due to reaction heat output, viscosity change, shrinkage, etc. are simultaneously used. Physical parameters such as electrical resistance and dielectric loss tangent have also been used. For high-rate processes, a laboratory installation for reaction injection molding might incorporate a calorimeter, a viscometer, and equipment for machining specimens for mechanical tests.

This chapter is devoted to a discussion of some new methods (particularly those based on computerized techniques) for research and control of the physical and chemical processes that occur dur-

ing reactive molding and that need to be quantitatively described to model real technological processes.

3.2 CONTROL OF RELAXATION PROPERTIES IN OLIGOMER CURING

Some new methods for measuring the relaxational modes of a material during the curing process have been proposed.[150-153] A new experimental technique for investigating the viscoelastic properties of polymeric materials is called Fourier-Transform Mechanical Spectroscopy (FTMS). The main advantage of the FTMS method is that the value of dynamic modulus components at different frequencies can be obtained in a single experiment without changing the sample. An inharmonic mechanical input is fed in, and then this input and the corresponding output signals are expanded as a Fourier series. The terms of both series are compared for the same frequency and give the values of the components of the dynamic modulus (or elastic modulus and loss factor) at this frequency. The FTMS method can measure rapidly changing values of viscoelastic properties of polymer materials undergoing polymerization, solidification, crystallization, etc.

Theoretical investigations show that there is only one signal that satisfies the condition of equal amplitudes in a Fourier expansion; this input signal is written as

$$x(t) = \frac{\sin 2\pi\omega_0 t}{\pi t} \qquad [3.1]$$

where x(t) is the input signal; ω_0 is the circular frequency of the main (senior) harmonic. The amplitudes of all terms in the Fourier series of this function are equal to one.

The FTMS method can be carried out by means of any mechanical forced oscillations generator. A computer synthesizes a signal of preset shape (for example, the signal described by Eq. (3.1) or simply a sum of harmonics) and transmits it through a digital-to-analog converter to the input of the generator. The output signal from the specimen is measured by forced transducers and directed through an analog-to-digital converter to the computer. Then the Fourier transformation algorithm, which separates the amplitude and phase of the main and junior harmonics of the same frequency is performed. These data serve as a basis for calculating the dynamic mechanical properties of the polymer system, i.e., the components of the shear modulus of elasticity, G^*, and the mechanical loss tangent $\tan\delta$ in the polymerization process and/or curing.

The FTMS method allows us to follow changes in several parameters that carry information on the role of different mechanisms during formation of an end-product by reactive molding. Specifically, the development of fluctuating entanglements of long-chain macromolecules can be distinguished from the appearance of rubber-like three-dimensional networks of chemical bonds.

Let us consider the application of the FTMS method for analysis of the evolution of relaxation properties during synthesis of a polyurethane based on macro(diisocyanate) and diamine. The instrument used was vibrorheometer with a cone-and-plane type measuring cell.[154] The experimental data were obtained for the main frequency of periodic oscillations $f_0 = 0.06$ Hz. In processing the experimental data, three frequencies were distinguished: f_0, $4f_0$, and $16f_0$; i.e., the frequency range was somewhat greater than one order of magnitude. One measurement gives the values of six quantities

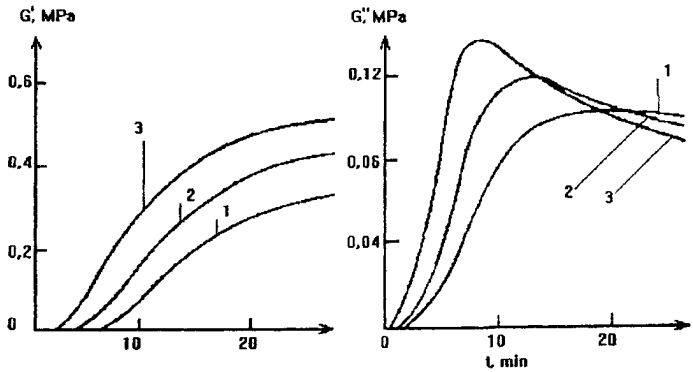

Figure 3.1. Time dependencies of the real G' (a) and imaginary G" (b) components of the complex dynamic modulus at the frequencies 0.0625 Hz (1), 0.25 Hz (2) and 1.00 Hz (3).

– the real G' and imaginary G" components of the complex dynamic shear modulus of elasticity G^* (or G' and the mechanical loss tangent tanδ) for three frequencies. Although the theory predicts equal amplitudes at all frequencies, including those which are $>>16f_0$; it is virtually impossible to use the higher terms of a series, because of increasing experimental errors due to the non-ideal form of the input signal (i.e., divergence from that given by Eq.(3.1)) and unavoidable performance errors in the transducers, transmitting systems, and so on.

The results of measurements of the dependencies $G^*(w,t)$ for three circular frequencies $w_0 = 2\pi f_0$, $w_1 = 4\pi w_0$, and $w_2 = 16\pi w_0$ are shown in Fig. 3.1. The lack of coincidence in the shapes of the time dependencies of the dynamic modulus components for different frequencies is obvious. This phenomenon is especially true for G", because the position of the maximum differs substantially along the time axis. In the most general sense, this reflects the contributions of the main relaxation mechanisms of the material to its measured viscoelastic properties.

The relaxation spectrum H(θ) completely characterizes the viscoelastic properties of a material. H(θ) can be found from the measured frequency dependence of the dynamic modulus of elasticity $G^*(\omega)$ by means of the following integral equation:

$$G^*(\omega) = G_0 + \Delta G \int_0^\infty \frac{i\omega\theta}{1 + i\omega\theta} H(\theta) d\ln\theta \qquad [3.2]$$

where G_0 is the equilibrium modulus of elasticity; ΔG is relaxation part of the elastic modulus, θ is the relaxation time. The calculation of H(θ) from the measured dependence $G^*(\omega)$ is valid when the frequency range covered by an experiment is sufficiently wide (several orders of magnitude). This is not the case with the results shown in Fig. 3.1; therefore, H(θ) cannot be determined from a single

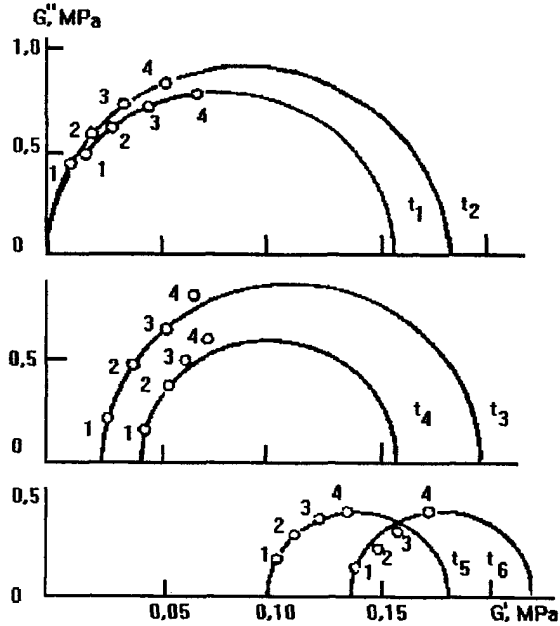

Figure 3.2. Evolution of the Cole-Cole diagrams during a curing process at $t_1 < t_2 < t_3 < t_4 < t_5 < t_6$. Frequencies: 0.0625 Hz (1), 0.25 Hz (2), 1.0 Hz (3) and 4.0 Hz (4).

experiment. Thus, the study of relaxation characteristics should be conducted for a model viscoelastic body with a limited set of constants. Cole-Cole diagrams, which show the interrelations between the dynamic properties of a material in a G"-vs- G' coordinate system, can also be used. This method excludes frequency from consideration as a parameter.

A Cole-Cole diagram is shown in Fig. 3.2. The experimental points in the G"- vs - G' coordinate system fall lie closely on a half-circle, with the exception of a narrow time interval very close to the transition (gelation) time, t^*. This curve corresponds to simplest model of a linear viscoelastic body with one relaxation time. In this case, $G^*(\omega)$ is expressed as follows:

$$G^*(\omega) = G_0 + \Delta G \frac{i\omega\theta_p}{1 + i\omega\theta_p} \qquad [3.3]$$

or

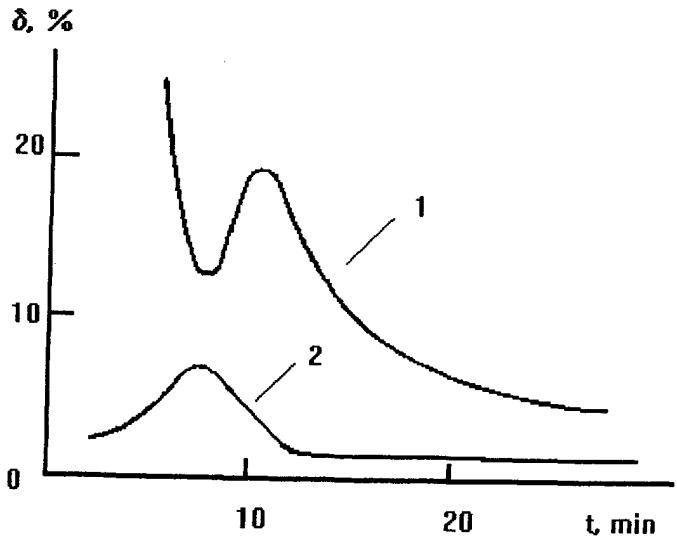

Figure 3.3. Root-mean-square error in fitting experimental data with three (1) and four-parametric (2) models.

$$G'(\omega) = G_0 + \Delta G \frac{\omega^2\theta_p^2}{1+\omega^2\theta_p^2}$$

and

$$G''(\omega) = \Delta G \frac{\omega\theta_p}{1+\omega^2\theta_p^2}$$

Here three constants appear: G_0 is the equilibrium modulus of elasticity; θ_p is the characteristic relaxation time, and ΔG is the relaxation part of elastic modulus. There are six measured quantities (components of the dynamic modulus for three frequencies) for any curing time. It is essential that the relaxation characteristics are related to actual physical mechanisms: the G_0 value reflects the existence of a three-dimensional network of permanent (chemical) bonds; θ_p and ΔG are related to the relaxation process due to the segmental flexibility of the polymer chains. According to the model, intermolecular interactions are modelled by assuming the existence of a network of temporary bonds, which are sometimes interpreted as physical (or geometrical) long-chain entanglements.

The determination of the three quantities G_0, θ_p, ΔG from six measured characteristics, i.e., the components of G^* at frequencies f_0, $4f_0$, $16f_0$ is carried out by minimizing root-mean-square error for each time t of during curing. Fig. 3.3 shows how the root-mean-square error δ for this calcu-

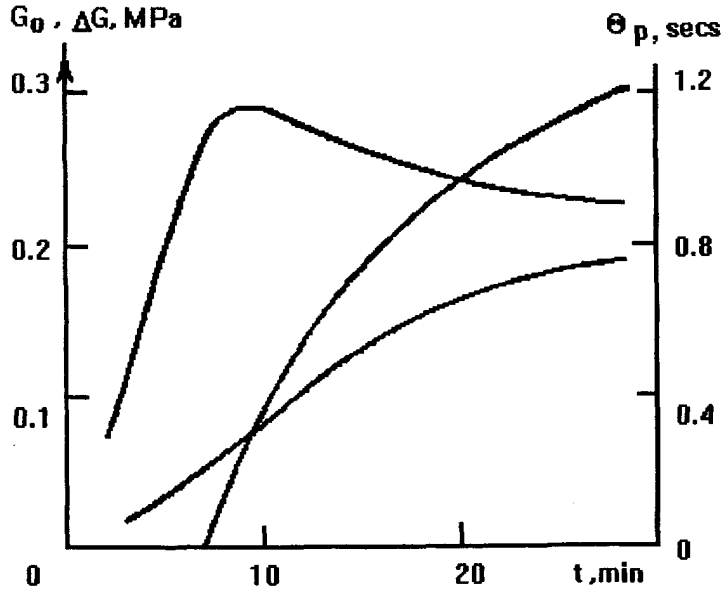

Figure 3.4. Dependencies of parameters G_0 (1), ΔG (2), and θ (3) of a three-constant model on time in polyurethane curing.

lation depends on time t. The error is always small, but during a certain narrow time interval close to a characteristic time, it rapidly increases. This means that a three-constant model of a viscoelastic body with one characteristic time near t^* inadequately reflects the relaxation properties of a material during curing. This is probably not accidental, but caused by an intrinsic feature of material behavior near t^*. As it will be shown later, a three-dimensional network of chemical bonds is formed at t^*; i.e., t^* is the gel-point of the system.

Fig. 3.4 shows the results of calculations of G_0, ΔG, and θ_p carried out according to Eq. (3.3). The parameter G_0 which is related to the density of the network of chemical bonds formed during curing, is zero at the start of the reaction but increases in value some time later. This time is obviously correlated with the beginning of gel formation, i.e., with the gel point t^*. Before this time, the viscoelastic properties of a system in the process of curing are determined by the fluctuating network of entanglements.

The model of a viscoelastic body with one relaxation time used above has one principal disadvantage: it does not describe the viscous flow of the reactants before the gel-point at $t < t^*$. Thus it is important to use a more general model of a viscoelastic medium to interpret the results obtained. The model must allow for flow and may be constructed by combining viscous and viscoelastic elements; the former has viscosity η_0 and the latter has a relaxation modulus of elasticity G_p and viscosity η_p,

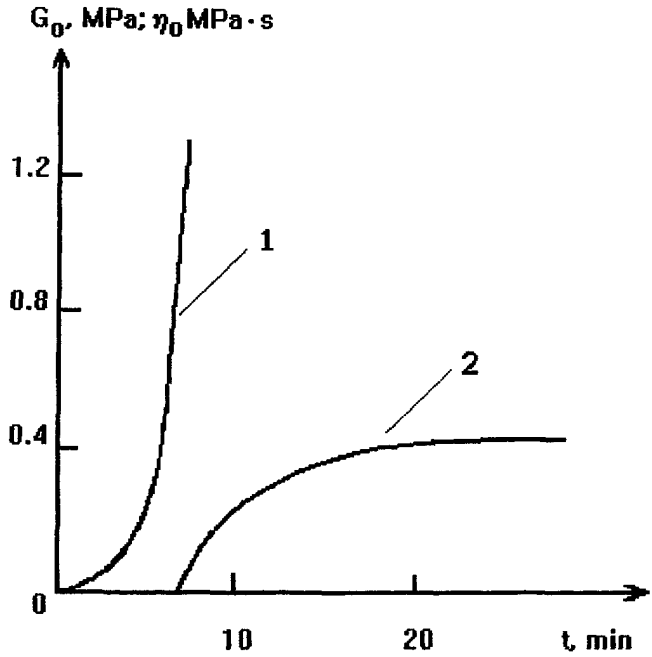

Figure 3.5. Dependencies of the parameters η_0 (1) and G_0 (2) of the four-constant model on time in the process of curing (parameters G_p and θ_p are the same as shown in Figure 3.4).

i.e., its relaxation time $\theta_p' = \eta_p/\Delta G_p$. This is the well-known Burgers model.[155] Let us now suppose that an equilibrium modulus of elasticity G_0 exists, although it should be understood that in the time interval during which the material is solidifying it retains its fluidity and $G_0 = 0$. Now let us process the same experimental data with the help of the four-constant (η_0, ΔG_p, $\theta_{p'}$ and G_0) model. The constants are calculated by to the same method as before. The error δ of this approximation is shown in Fig. 3.3 (the bottom curve 2). It is worth noting that in practice, the four constants were calculated from a model constructed from two Maxwell elements joined in parallel. This construction is formally equivalent to the Burgers model, because there is a direct and unambiguous correspondence between the two sets of constants;[155] however, the model chosen for calculation was determined mainly by the convenience and accuracy of the approximation. The constants of the double Maxwell model were then compared with the Burgers model.

The results of calculations of the time dependencies of the constants are presented in Fig. 3.5. In this case the root-mean-square error of approximation also has a maximum at a specific time, although its magnitude is substantially lower than for the three-constant model. This is to be expected with the four-contant model, because it is known that at t^* the relaxation spectrum of a curing polymeric material changes radically: it widens abruptly, and new relaxation modes appear.[130] The four-constant model is insufficient to describe a rapid change in relaxation properties; furthermore, the behavior of a real material near the gel-point (at the transition of the system to the heterophase state) is a new phenomenon that is not described by a simple model.

The following results are important consequences of the model evaluation. First, the existence of the gel point t^* is clearly simulated, because as a material approaches this point, $\eta_0 \to \infty$; i.e., the material loses fluidity at $t \to t^*$. Second, in the time interval, $t < t^*$, $G_0 = 0$; i.e., the model shows that there is no equilibrium modulus, because the network of chemical bonds is not formed yet. Therefore, the material behavior is described by a single value of viscosity η_0 and a single relaxation time θ_p. The existence of viscoelasticity in this interval is a result of a fluctuating network of intermolecular interactions (entanglements). Third, in the time interval $t > t^*$, we have $\eta_0 \to \infty$ and G_0 is not equal to zero; i.e., there are two types of interpenetrating networks, with chemical and physical bonds, respectively.Then, from the ensuing changes in G_0 and ΔG_p (together with θ_p), we may speculate that both networks are formed independently.

These results clearly indicate that the multi-frequency dynamic analysis method allows us to estimate the contribution of different relaxation mechanisms during curing of elastomers, and the changes in chemical and physical networks densities can be studied separately.

3.3 VISCOMETRIC STUDIES

Rapidly solidifying compositions used for reactive injection molding place some restrictions on measurement. In the time required to prepare the reaction mixture, place a sample in the measuring cell of an instrument, and achieve a steady state in the sample and the measuring system at a preset temperature, chemical conversion of the material may advance considerably, making viscosity measurements meaningless. The volume of lost information depends on the ratio of the transient time necessary to achieve a steady state in the sample and the characteristic time of the chemical reaction. The sensitivity of the reaction rate to temperature is also important. In order to avoid the necessity to maintain isothermal conditions for the measurements, a non-isothermal scanning method for viscosity measurements was proposed.[156]

In this method, the components of a reactive mixture are thermally conditioned and mixed at a low temperature, which retards the reaction during the preparatory stages. The working cell of a viscometer is thermally conditioned at the same temperature. When the sample is placed in the measuring device, a programmed heater controls the temperature changes. In the simplest case, the temperature changes linearly as:

$$T = T_0 + a_T t \qquad [3.4]$$

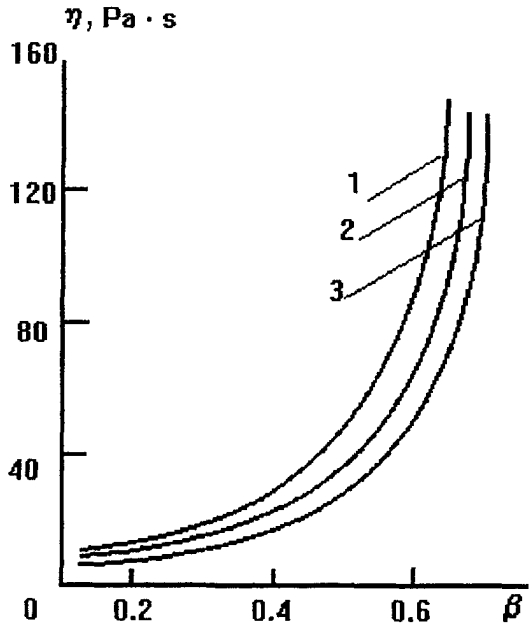

Figure 3.6. Changes in viscosity of polyurethane during non-isothermal curing at different scanning rates: 2 K/min (1), 8 K/min (2), 16 K/min (3).

where T_0 is initial temperature, t is time, and a_T is the rate of temperature increase. A series of experiments is carried out in different non-isothermal regimes (for example at different values of the rate a_T). The quantity of the reaction mass used in the experiments must be small in order to exclude the formation of temperature gradients throughout the sample volume. The exothermal effect of a chemical reaction can then be neglected, and the change in sample temperature can proceed according to the preset regime of the external heater. When a programmed heater is used, an appropriate initial temperature is determined experimentally for a particular composition prior to the measurements. In some cases, this procedure may be limited by crystallization of the components or other secondary effects.

Fig. 3.6 shows the results of viscosity determination for a linear temperature increase in a polyurethane based on poly(butadiene diol), diphenylmethane diisocyanate, and diamine.

In order to describe changes in the rheological properties of polyurethanes during curing, the following equation was proposed and proved to be correct:

$$\eta = k_\eta e^{E_\eta / RT} \left(\frac{\beta}{1-\beta} \right)^b \qquad [3.5]$$

where k_η is a pre-exponential factor; E_η is the apparent activation energy for viscous flow; β is the degree of conversion; b is an empirical constant; and T is the temperature. The temperature in this equation may be time-dependent, and can be described by various functions T(t). Values of the constants in this equation are determined from a non-isothermal experiment by computer methods. With these constants, Eq. (3.5) can be used to predict viscosity changes in a process with an arbitrary temperature regime.

3.4 CALORIMETRIC METHODS

Calorimetry is a basic technique for establishing reaction parameters and comparing theoretical predictions with experimental results. However, studies of rapid reactions pose considerable difficulties, because even the most sensitive calorimeters have a noticeable lag time. In many cases, this time lag distorts the experimental results on a quantitative and even on a qualitative level. The difficulty of separating the actual experimental signals caused by the effects being measured and the time-lagged signals is of general importance for inertial measuring circuits. Multiple numerical or graphical differentiation methods have been proposed as means of retrieving the true initial signals.[157]

If the measuring (transmitting) circuit of an instrument has linear characteristics (which requires separate experimental validation), the output signal of a linear instrument y(t) is expressed in terms of the input signal x(t) using the integral equation:

$$y(t) = \int_0^t x(\tau) h(t-\tau) d\tau \qquad [3.6]$$

where t is time; h(t) is the transfer (transmitting) function of the response of a linear instrument to an input pulse at t = 0, which transforms the initial signal x(t) into the measured one, y(t).

To determine the function x(t), it is necessary to find the solution of the integral of Eq. (3.6) for a known h(t) and measured y(t) functions. One proposed method of calculating x(t) assumes that the shape of the function x(t) is known beforehand and that the transfer function h(t) can be experimentally determined.[158] A more general solution uses Fourier transforms. If Eq. (3.6) is rewritten with the Fourier transforms of the functions x(t), y(t), and h(t - τ), which are denoted by Y, X, and H, then, using the convolution theorem:

$$Y(f) = X(f)H(f) \qquad [3.7]$$

where f is the cyclic frequency. If H(f) is nowhere zero, the solution of Eq. (3.6) can be written in the form:

$$x(t) = \int_{-\infty}^{\infty} Y(f)H(f)e^{i2\pi ft} df \qquad [3.8]$$

In real cases, the possibility of qualitative retrieval of the form of the function x(t) from y(t) is limited only by the requirement for accurate measurement of y(t), which may be very strict.

There are many known methods for solving of integral Eq. (3.8), but preference should be given to those which do not require a lot of calculations and which can be adapted to automated collection and processing of the experimental information in real time. For this purpose, the following conclusion is important:[159] the most accurate retrieval of the true signal shape is achieved when Eq. (3.8) is applied to results that have been preliminarily smoothed with a filter designed to provide the minimum mean-square error of smoothing.[160]

This method is basically simple: the measuring circuit of a linear thermal measuring instrument includes a low-frequency filter, i.e., a filter which passes only low-frequency signals and weakens high-frequency signals. If a true signal processed by the measuring circuit of a thermal instrument is delivered to a high-frequency filter, i.e., to a filter which weakens low frequencies and amplifies high ones, the resulting signal will be closer to the true form. In this case the closer the transmitting characteristic of the high-frequency filter is to the inverse of the transfer characteristic of the measuring instrument, the closer the output signal is to the true measured signal.

The requirements for the transfer characteristic H(f) of a thermal measuring device are as follows:

$$H^*(f) = \frac{1}{H^{-1}(f)} \quad \text{at } f < f_0 \qquad [3.9]$$

$H^*(f) = 0$ at high frequencies ($f \geq f_0$), where f_0 is the limiting cut-off frequency of the high-frequency filter, which is chosen according to the noise performance of the measuring instrument and the resolving time of the retrieved signal.

The transfer characteristics of the high-frequency filter defined by expression (3.9) are ideal. In practice, it is impossible to achieve the ideal filter, so various approximations of the ideal filter must be used. The design of filters approximating the ideal form have been discussed by numerous authors. One simple design uses a filter described by expression (3.9) with the addition of a second-order filter.[161]

Let us consider the application of this technique to a Calvet differential calorimeter. According to the standard procedure an ampoule with the reactant mix is placed in the measuring chamber. If the wall thicknesses of the measuring chamber and the ampoule are sufficiently small, the heat flux q passing through a unit wall area with a stepwise change in temperature is described by the expression:

$$q \propto 1 - e^{-t/\tau} \qquad [3.10]$$

where τ is the time constant characterizing the signal delay; its value is proportional to λ/C_p, where λ is the thermal conductivity and C_p is the specific heat. When the heat flux passes consecutively through the walls of the chamber and the adjacent ampoule, the heat flux through the unit area is proportional to:

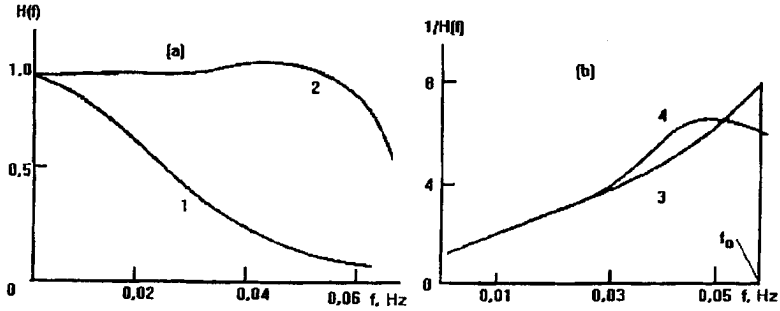

Figure 3.7. Unit-step responses of an instrument (a) and of a high-frequency filter (b) in the same frequency range 1 - no filter; 2 - with a filter; 3 - ideal filter characteristic; 4 - approximation by a second order Butterworth filter.

$$q \propto (1 - e^{-t/\tau_1})(1 - e^{-t/\tau_2}) \qquad [3.11]$$

where τ_1 and τ_2 are the time constants of the measuring chamber and the ampoule, respectively.

Using Eq. (3.11), we can formulate the response of the calorimeter n(t) as a stepwise pulse:

$$n(t_i) = \eta_0(1 - e^{-t_i/\tau_1})(1 - e^{-t_i/\tau_2}) \qquad [3.12]$$

where t_i is the time equal to $i\Delta t$; Δt is the time increment; n_0 is the steady-state value of the heat flux, measured in the units of the instrument.

The constants τ_1 and τ_2 in Eq. (3.12) can be determined experimentally by a standard algorithm of nonlinear programming by writing the desired (efficiency) function ε for this algorithm as follows:

$$\varepsilon = \sum_{i=0}^{N} [n_\theta(t_i) - n(t_i)]^2 \qquad [3.13]$$

where $n_\theta(t_i)$ is the experimental value of n at time t_i. After determining τ_1 and τ_2, we can find the unit-step response of the measuring circuit:

$$h(t_i) = \frac{1}{n_0}\frac{dn(t_i)}{dt_i} \qquad [3.14]$$

The modulus (absolute value) of the transient function in the frequency range H(f) is shown in Fig. 3.7. The structure of the filter is determined by the following expression:

$$x(t_i) = b_0y(i) + a_1x(t_{i-1}) + a_2x(t_{i-2}) \qquad [3.15]$$

where b_0, a_1, and a_2 are coefficients.

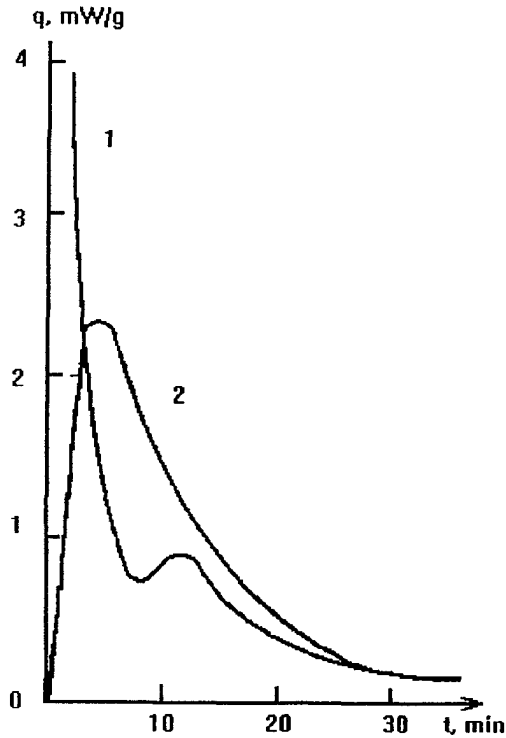

Figure 3.8. Experimental curves of heat output during polyurethane curing. 1 - true curve (as a result of filtration); 2 - no filtering (2).

The modulus of the gain factor of such a filter (Butterworth) is shown in Fig. 3.7 b (curve 4). The total unit-step response of a measuring instrument equipped with a filter determined by the second-order expression (3.12) is presented in Fig. 3.7a (curve 2). Verification tests of the method have given good agreement between theory and experiment.

Let us illustrate the action of the filter by an example of the restoration of the signal, beginning with the instrumental signal obtained during curing of a polyurethane sample directly in the working cell of a calorimeter. The type of polyurethane used in the experiments is characterized by considerable intermolecular interaction; thus we may expect two peaks in the heat output intensity curve. The first peak is related to the heat of chemical reaction, and the second is connected with the heat release which accompanies the formation of a network of intermolecular physical bonds. The magnitude of the second peak is considerably lower than the first. From an analytical point of view, it is of particular interest to separate the second peak from the background of the heat output caused by the chemical reaction. The curing temperature was 80°C. Curve 2 in Fig. 3.8 was obtained

with an instrument without filtering; and has only an insignificant inflection (if any) in the range $10 < t < 20$ min. This is explained by the thermal lag of the instrument and by the existence of two processes with characteristic times of the same order.

The use of a filter determined by Eq. (3.15) allows the true form of the signal to be restored (Fig. 3.8, curve 1). In this case, both the magnitudes of the quantities measured and the qualitative shape of the experimental curve change. The use of this filtration method has enabled us to broaden the frequency range of the instrument by about an order of magnitude and to reduce the effective time constant of the calorimeter from 4 min to 30 sec.

3.5 THERMAL PROBE METHOD

As a rule, reactive molding processes are accompanied by significant changes in the molecular mobility of various elements in the molecular structure of the reactive components. Thus, thermal method is among the most informative control techniques for these processes. In general, it would be preferable to use non-stationary methods operating in real time with small samples that do not need to be placed in a special constant-temperature enclosure. In this respect a new method using a pulsed thermal probe[162] is attractive and can be used to analyze some characteristics of reactive systems.[163,164]

The basis of the thermal probe method is the following. A test thermal pulse is sent to a wire probe located in the medium to be studied, and the system response to the local heat pulse is registered and analyzed. The length of a single pulse is about 10^{-5} - 10^{-4} s, and the frequency of successive pulses is up to 10 Hz; the volume subjected to the thermal pulses is approximately 10^{-3} mm^3. Two independent types of response relative to that of the surroundings are registered, depending on the choice of pulse parameters. The first response records changes in thermal activity of the material during the chosen time period. The thermal activity characterizes the reaction of the material to the thermal pulse in a non-stationary process. This value b is defined by the ratio

$$b = \left(\frac{\lambda}{\rho C_p} \right)^{1/2}$$

where λ is the coefficient of heat conductivity; ρ is the density, and C_p - is the specific heat of the sample.

The second response records the characteristic temperature T*. This temperature is a reflection of abrupt changes in the conditions of the contact between the probe and sample. For example, such changes can occur due to a break in the continuity of contact after the thermal shock. Analysis of the time and temperature effects is made by comparison with temperature changes during uniform heating. The temperature response depends on the sample composition, the properties of the surrounding medium, and on the rate of temperature increase.[163-165] The value of T* lies above the traditional temperature range of experiments on polymeric substances. The response to the temperature pulse is similar to that observed in spontaneous vaporization of overheated liquids.[166,167] Measurements of the characteristic temperature T* give the absolute value

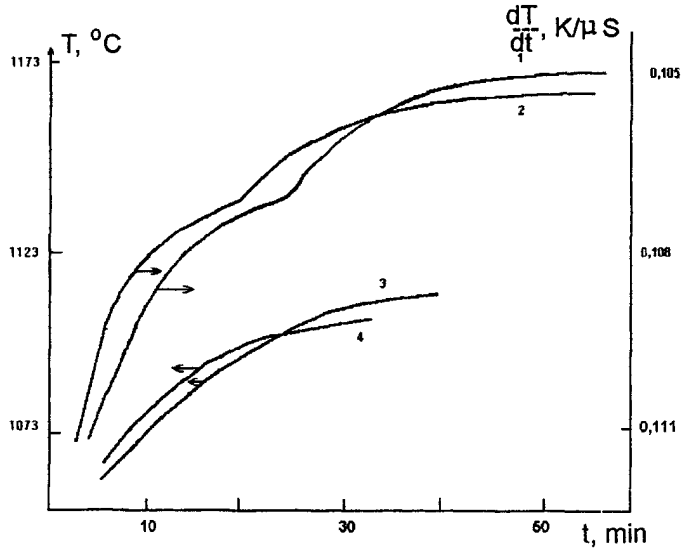

Fig 3.9. Dependences of the parameters T* and dT/dt(t_f) on time during curing of macro(diisocyanate) by diamine. T_0 = 90°C (curves 1 and 3) and T_0 = 70°C (curves 2 and 4).

of the effect, while the parameter b is a material parameter. Combining the two methods in a single experiment allows the nature of the thermal processes to be understood.

The main advantages of the method are: its rapidity, the minute quantity of sample material required, the independence of the quantity T* from the environmental temperature, and the compactness and stability of the instrumentation. Another advantage of the method for controlling solidification and component preparation is its sensitivity to the presence of low-molecular-weight compounds in a system.[163,168] It is also sensitive to changes in the molecular weight of the sample[164] and in the relaxation state, especially the glass transition. Analysis of the data shows that the T* level and the magnitude of its changes in a solidified system are determined mainly by the nature and quantity of the relatively low-molecular-weight components. The changes Δb reflects changes in the packing density and degree of order of the structural elements.

A platinum probe of diameter 200 ηcm and length 1 cm is the main element of the measuring system, serving both as a heater and as a resistance thermometer. The probe is included in a bridge circuit into which the current pulses are fed. The probe temperature (according to its resistance) vs time dependence is recorded. The out-of-balance voltage from the bridge provides a measure of the equivalent temperature change. The method is based on the high sensitivity of the probe to changes in heat exchange conditions, attributable to its surface-to-volume ratio.

Let us examine both measurement procedures. The rate of temperature increase dT/dt for a given volume heat output from the probe q(t) is determined by the heat flow dq/dt. A solution of

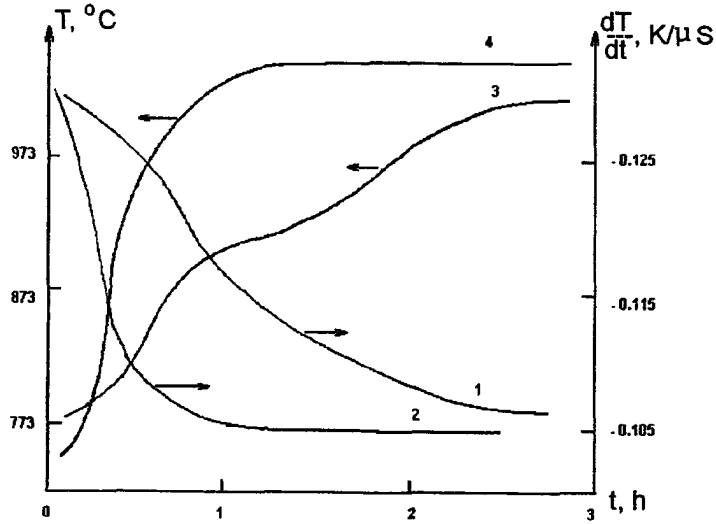

Figure 3.10. Dependences of the parameters T* and dT/dt(t_f) on time during curing of epoxy resin by triethanol aminotitanate. T_0 = 120°C. Content of curing agent 40 wt% (curves 1 and 4) or 15 wt% (curves 2 and 3).

the energy balance equation for experimental conditions (pulse time on the order of 100 - 400 μs) using the approximation dT/dt = const and l→∞ shows that the quantities dq/dt and b are proportional to each other. This result was confirmed by experiments.[164] An increase in thermal activity of a system during the solidification process or volatile additive removal leads to decreasing dT/dt at t = t_f, where t_f is a fixed time. Determining the temperature response requires separation of the characteristic high-frequency signal from the T(t) dependence and finding the T value at the instant of appearance. This response signal fixes the time of rapid change in contact conditions (for example, due to spontaneous vaporization) and is concerned with instantaneous changes in dT/dt. By applying correction factors for radial and end effects, it is possible to find probe surface temperature at its center part. This value is assumed to be the sample surface temperature T* at a specific time. The optimum pulse duration is 50 - 500 μs. The frequency is determined by the relaxation time in the sample surface layers, t_r, and can be varied within the limits of 0.01 - 1 Hz, depending on a reaction stage. The value of t_r is determined by measuring dT/dt at t = t_f before and after the heating pulse.

The results of dT/dt and T* measurements made during curing of two systems - macro(diisocyanate) based on poly(tetraethylene glycol) and 2,4-toluylene diisocyanate cured by diamine (MDA) and epoxy diene oligomer cured by triethanol(amine titanate) are shown in Figs. 3.9 and 3.10, respectively. The monotonic increase in the parameters, monitored in the experiment,

provides reliable results for process control. The most important results have been obtained from experiments carried out at different process temperatures T_0 and reagent ratios. It was found that both dT/dt and T*(t) changed and the magnitudes of their changes correlated with the rate of conversion $d\beta/dt(t)$ and the limiting value of the conversion degree for the given reaction conditions. For example, for epoxy oligomer curing at $T_0 = 90^{\circ}C$, which results in incomplete conversion (see Fig. 2.12), the limiting value of T* is close to $600^{\circ}C$. This is much lower than the T* values shown in Fig. 3.10. The initial T* value of the system is determined by the molecular weights M_n and properties of the reactant components. For the materials already studied,[163-165] this value changes from $220^{\circ}C$ for poly(methyl methacrylate) to $770^{\circ}C$ for MDI. The T*(t) curve for MDI is similar to the dependence $T^*(M_n)$ of polymer homologues. It is interesting to note that in poly(methyl methacrylate) polymerization this curve is convex with respect to the t axis. This effect is associated with a presence of monomer in a system until the end of the reaction.

The steepest part of the T*(t) curve, shown in Fig. 3.10, corresponds to the transition of epoxy resin into the rubbery state. In MDI curing and methyl methacrylate polymerization the amplitude of the response signal (T*) decreases monotononically and then becomes constant when the rigidity of the system reaches a certain level. The completeness of the reaction can be determined by saturation of the $dT/dt(t_f)$ curve. The product ρC_p is relatively insensitive to the transition of an oligomer to a polymer. The shape of the $dT/dt(t_f)$ curve is determined primarily by changes in the value of λ, which are directly related to the value of M_n and the structural characteristics of the polymeric material.[169]

4

PRINCIPLES OF REACTIVE MOLDING TECHNOLOGY

4.1. PREPARING COMPONENTS (PRELIMINARY OPERATIONS)

Reactive (chemical) molding technology and the equipment used depend on the geometrical shape of the article produced. In all cases, initial liquid products are delivered into a mold where the processes of polymerization (solidification), structure formation, and shaping proceed simultaneously.

The preliminary operations of preparation of the initial components can be carried out in special centralized chemical production plants or directly in the work bays where the articles are manufactured. When the initial components are obtained in the form of semi-finished products, the manufacturing process is simplified. Semi-finished products are single- or, more often, two-component mixtures, especially the prepolymers used in polyurethane production. Mixtures include chemical reactants and mixtures of polymers or oligomers with different additives required for final items.

The batch process equipment used for preparing the components is essentially a set of reactors equipped with heaters and agitators. They operate under vacuum or in an inert gas atmosphere. One of the main requirements of the chemical molding process is the production of pore- and defect-free articles. The volatile products and moisture must be thoroughly removed from the reactant mixture. Moisture imparts porosity to the final articles due to evaporation and the chemical interaction of water with the components of the reactant system, for example, with isocyanates in case of polyurethane formulations. In some cases, moisture can also inhibit the polymerization process, for example, anionic-activated polymerization of lactams. Many monomers, particularly acrylic compounds, require removal of the inhibitors to increase their shelf-life.

If a monomer or an oligomer is delivered in heated tanks, it is immediately pumped into a heated vessel for storage in controlled conditions. Other products, which are liquid during transportation, are treated in the same way. Components with melting points higher than room

temperature are melted. For this purpose storage containers are put into a thermostated cabinet or chamber where the materials are maintained at the temperature 10 to 20°C higher than their melting point to ensure complete melting of the reactants. Then the reactants are pumped into a heated vessel for storage. Preparation of solid components for mixing usually includes drying followed by screening and fractionation. The latter may not be necessary if a powder is highly soluble in the mixture. The conformity of all raw materials to the required standards is of particular importance for high-quality process operations. Molecular weight distributions (MWD) and the proportions and mixing of the initial reagents are especially important as these factors influence the kinetics of the polymerization process[170] and the quality of the end-products.

An important step in the production process is the preparation of a standard specimen. This specimen is used to qualify principle production parameters such as the long-term stability of the reactive mixture, polymerization cycle, and the performance characteristics of the material obtained. Simultaneous determination of the reaction parameters allows us to use mathematical modelling to optimize the reactive processing regime.

4.2. ENGINEERING FOR OPEN MOLD CASTING PROCESSES

4.2.1 GENERAL LAYOUT OF A PRODUCTION UNIT

Free injection of a reactant mixture to an open mold followed by polymerization and solidification (curing, crystallization, and so on) in thermostated sets is the most widely used method of manufacturing large-sized moldings, such as plates, slabs, and other items of a simple or complicated shape.

The process usually takes place in a batch reactor, which serves simultaneously as a vessel for preparing prepolymers and as a mixer. The design requirements of such a reactor are determined by the viscosity of the initial raw materials, the temperature at which preparation and mixing of the components are carried out as well as by lifetime of the reactant mixture. If the components of a mixture do not require special preparation, they are loaded into the reactor manually. If it is necessary to prepare a melt of a hardener or curing agent or to add a catalyst to the reactant mixture, another small reactor is added. Components prepared in this auxiliary reactor are quickly transported to a mixer by gravity or by means of a pump, either under vacuum or under pressure. The mass of the item produced is limited by the volume of the main reactor. Hence to increase output, the number and volume of the reactors must be increased. A variety of articles can be produced by free molding or casting in a stationary mold. For example, polyurethane can be manufactured in molding equipment suitable for stamping out sheets (e.g., diaphragms) or into massive blocks weighing up to several tones. Similarly, one can also obtain a vast assortment of large-sized moldings of epoxy resins, poly(methyl methacrylate), polyamide-6 and many other polymers and polymeric compositions can be produced.

High volume production requires continuous lines for preparing the components for mixing. These lines feed into continuous mixers and then through filling devices into the mold, all in a rational layout designed to allow continuous processing.

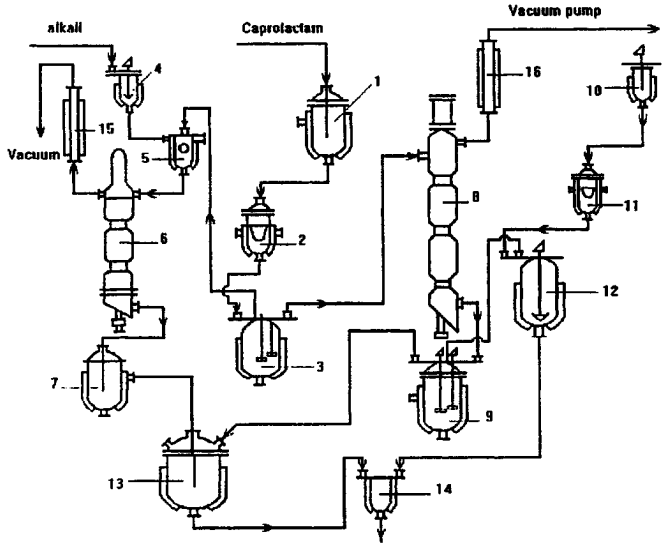

Figure 4.1. Flowsheet of production of a reactive mixture by activated anionic ε-caprolactam polymerization (explanations of numbers are in the text).

A basic two-reactor flow sheet for continuous component preparation is considered here for activated anionic polymerization of ε-caprolactam. According to this flow sheet, the whole ε-caprolactam melt delivered from storage is divided into two equal parts. One part is used to prepare the catalytic system and the other is mixed with activating additives. Upstream of mixing; the ε-caprolactam melt should be thoroughly dried. A rotary thin-film apparatus is usually used as a drier. This allows continuous processing, in contrast to lactam drying in batch processing, which is carried out periodically in a vessel, either under vacuum or with inert gas bubbling. Owing to the short residence time in the heated zone and the depression of the boiling point of water under vacuum, the monomer does not decompose or deteriorate. The availability of evaporators combinated with specially designed traps assures condensation of the lactam and its return to the apparatus.

When a 30% solution of NaOH is used as a catalyst, the caprolactam is dried and its sodium salt is formed at the same time (Fig. 4.1).The ε-caprolactam melt goes to a receiving vessel *1* and through a filter *2* before delivery to a collector *3*. Then melt is pumped to prepare the sodium salt of caprolactam and the activating system. An alkali solution is prepared in vessel *4* and then mixed with the necessary quantity of a monomer in reactor *5*. The mixture is dried in a rotary thin-film drier *6* (Na-caprolactam is formed at the same time) and gathered in a collector *7*. The other part of the monomer melt is pumped for drying from a vessel *3* to a second rotary thin-film drier *8* whence it goes into a vessel *9*. If the highly concentrated Na salt of caprolactam is prepared

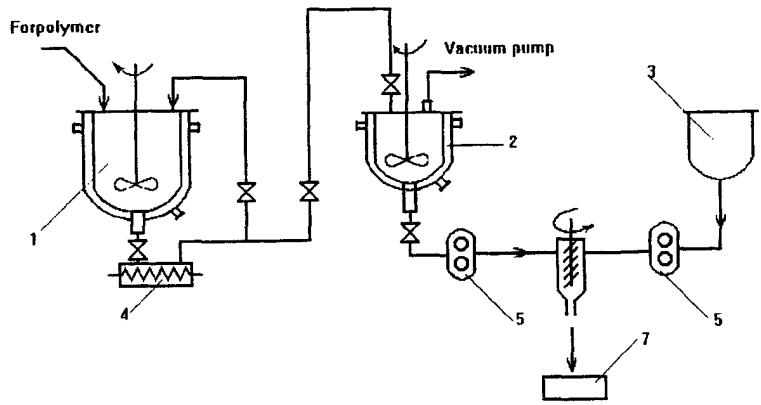

Figure 4.2. Flowsheet of production of cast polyurethane elastomer articles from a prepolymer by the continuous method: *1* - vessel to store prepolymer; *2* - vessel to prepare prepolymer; *3* - reactor for curing agent; *4* - transfer pump; *5* - metering pump; *6* - mixing device; *7* - mold.

beforehand followed by dilution to the necessary concentration, only part of the monomer is pumped from vessel *9* to prepare the activating system: the rest flows into reactor *13* to dilute the concentrated salt of caprolactam into the reactor *13*. An activator is delivered into a batcher *10* and then is passed through a filter *11* to mix with the monomer. An activating mixture is prepared in reactor *12*. The melt streams of the catalytic and activating systems are mixed in a 1:1 ratio in a mixing device *14*. To facilitate continuous production, multiple vessels are installed in the plant section where the catalytic and activating melt streams are prepared. The number and size of these vessels are determined by the unit capacity.

As a general rule, the reactors are vertical cylindrical vessels, either enameled or lined with glass. They can also be manufactured of stainless steel with jackets for delivering hot fluids. Water or steam may be used as heat transfer agents for ε-caprolactam. However, if temperatures up to 150°C are necessary, or in order to process other lactams, diphenyl mixture, silicon liquids, etc. are used as heat-transfer agent. Electric heating is also extensively used. It is necessary to bubble an inert gas through each vessel containing monomer melt to protect it against oxidation; this method can also replace mechanical mixing devices.

Flow sheets for preparing the components of various monomer and oligomer reactant mixtures do not differ significantly from each other, although they may have different sets of reactors. The choice depends mainly on the physical and chemical properties of the initial components. Fig. 4.2 shows a flow sheet for obtaining continuously molded polyurethane elastomers. Fig. 4.3 illustrates an elementary flow sheet for a batch process unit for manufacturing moldings of epoxy resin or epoxy-based composites filled with quartz sand.

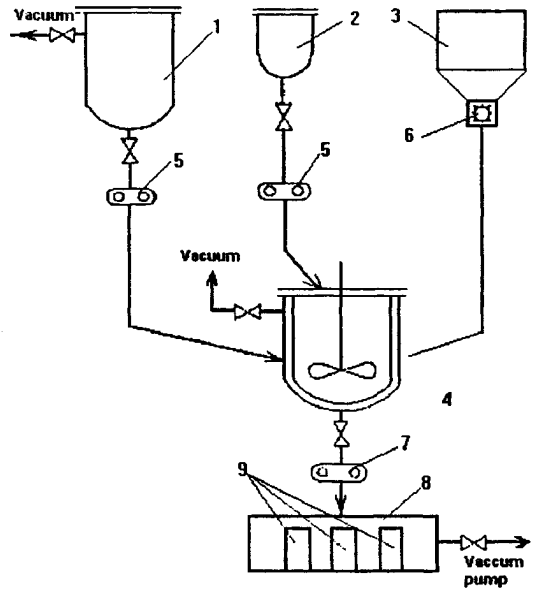

Figure 4.3. Flowsheet of a unit for producing moldings of epoxy resin-based compounds: *1* - vessel for preparing epoxy resin; *2* - vessel for preparing a curing agent; *3* - vessel for a filler; *4* - reactor-mixer; *5* - metering pump; *6* - metering device (batcher); *7* - valve; *8* - evacuated vessel; *9* - molds.

A special feature of the free molding (casting) process is the widespread use of small-size mobile units for various applications. In civil engineering, such units are extensively used for producing floor coatings, for hermetic sealing of joints, for thermal insulation of building elements with foamed materials, for applying protective surface coatings on concrete, etc.

4.2.2 COMPONENT METERING

Accurate metering of the components used to prepare prepolymers and their delivery into a mixing device is one of the most important conditions for successful production by the reactive molding method. The usual method for metering components in batch processes is weighing. In continuous processes, a volumetric method is used to meter two or more streams entering a mixing device. This method is sometimes used in batch reactors as well, particularly in production processes employing anionic activated ε-caprolactam polymerization. In this case, two streams of catalyzing and activating mixtures each with a viscosity of about 1 mPa s are delivered through pipelines with the same cross-section. Plunger, gear or screw pumps are used for volumetric metering. The first two types of pumps have proved to be very satisfactory in practice and are widely used in industry.

A working diagram of the most commonly used gear pump is shown in Fig. 4.4. The gears and body of the pump are assembled with the minimum possible gaps both at the circumference

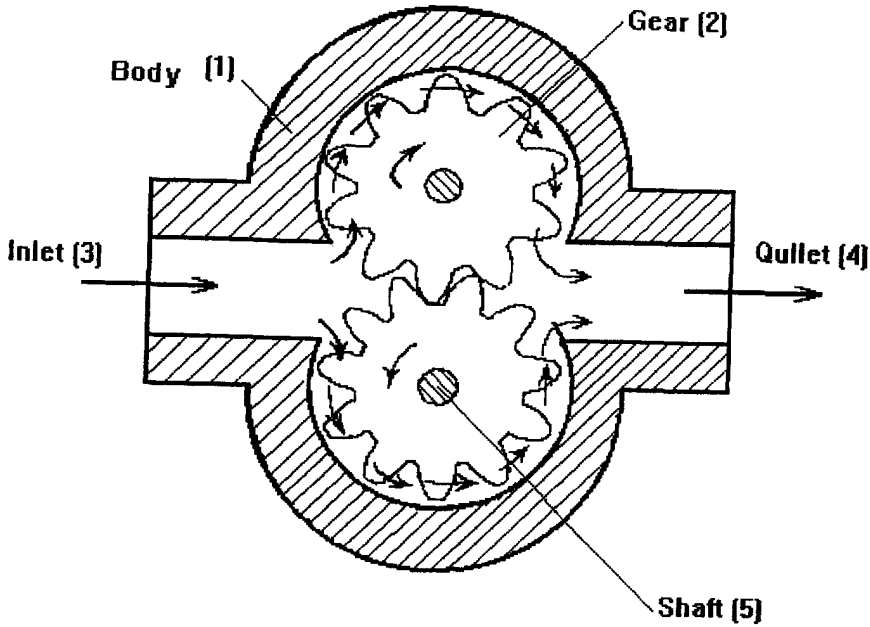

Figure 4.4. Gear metering pump: *1* - body; *2* - gear; *3* - inlet; *4* - outlet; *5* - shaft.

and in the plane of the gears. This is why the mixture can only pass through the tooth spaces as shown in Fig. 4.4. Fig. 4.5 shows a longitudinal section through a screw pump. The main elements of a screw pump are: driven screw flight *1*, driving screw flight *2*, suction chamber *3*, driving screw thrust bearing *4*, driven screw thrust bearing *5*, driving screw bottom *6*, driven screw bottom *7*, and delivery chamber *8*. The suction and delivery chambers are connected to each other by three parallel cylindrical holes in the pump body in which the three working screws rotate. The middle screw; it has right-hand thread and rotates clockwise as seen from the drive motor end. The two side screws with a left-hand thread are the driven screws; they rotate counter clockwise. The screw threads have a special shape, which creates seals at the contact. This design divides the pump along its length into a number of closed cavities formed by flight *2* of the driving screw, which enters bottoms *1* and *7* of the driven screws. When the screws rotate, the liquid delivered from suction chamber *3* fills bottoms *1*, *6* and *7* and then moves along the screws from the closed cavities into the delivery chamber. Thus a screw pump continuously transfers the liquid forward along the screw axis similar in principle to a continuously acting plunger pump. In this case, the movement of the liquid inside the pump may be linked to a hydraulic nut shifting continuously along the screws.

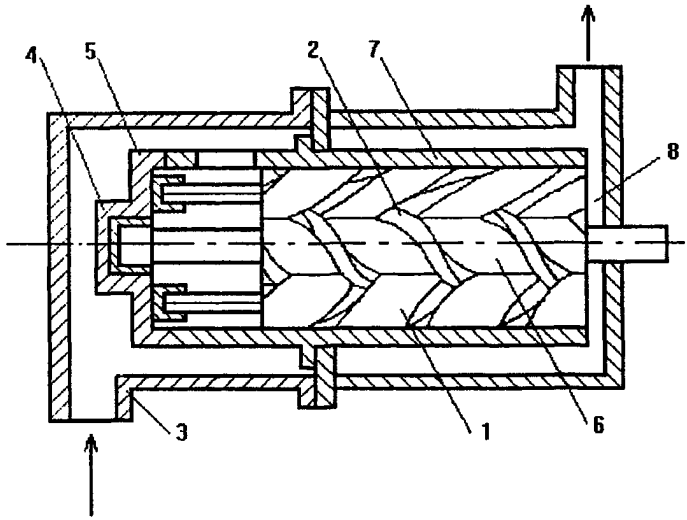

Figure 4.5. Screw metering pump (explanations are in the text).

The efficiency of screw pumps is about 70-80%. They work at high rotational speeds driven by a high-speed electric motor, and they can work continuously with no outages. Screw pumps are non-inertial, because there is no torque from the driving screw to the driven screws.

4.2.3 COMPONENT MIXING

The metering pumps continuously deliver the components into mixing devices. There are many designs for mixing devices, and the choice depends on the properties of the system being processed, e.g., viscosity, gel formation time, temperature, etc.

The simplest example of a device to for mixing two liquid streams to produce articles from low-viscosity monomers is the usual three-way cock. In most cases of batch processing of polyurethanes, epoxy resins, and polyesters with viscosities on the order of 100 Pa s and more, a reactor equipped with a set of agitators and working under vacuum serves as a mixer (Fig. 4.6.). One version of a mechanical mixer designed to mix liquid streams of different is shown in Fig. 4.7. It consists of a mixer drive *1* equipped with a cooling system for removing excessive heat transferred through the shaft from the working chamber and an agitator *2* with blades or a system of pins for better mixing of the components. The agitator is contained within shell *3* with heating system *4* to maintain the necessary temperature conditions in the mixing zone. Catalytic and activating streams enter the mixing zone through pipelines *5* and *6*. The mixer outlet is closed with controlled gate valve *7*, which may be operated by a general regulating system or by hand depending

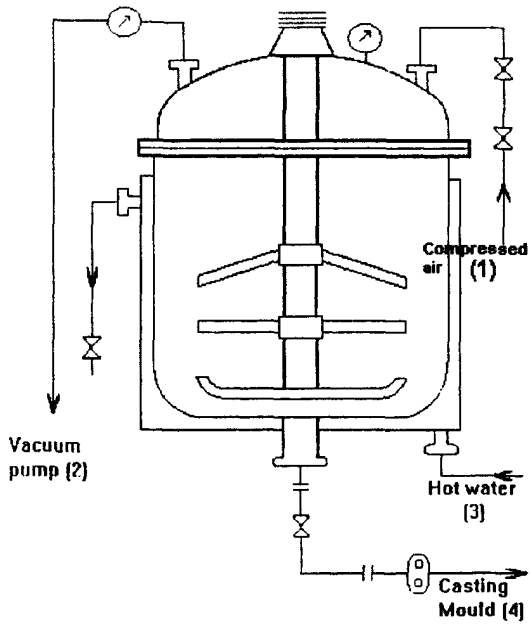

Figure 4.6. Reactor-mixer for viscous media: *1* - compressed air; *2* - to vacuum pump; *3* - hot water; *4* - to mold.

on the process selected. The mixing device outlet is a flexible hose *8*, which may be submerged in the mold being filled. Pipelines *9* and *10* assure solvent circulation.

The solvent circulation system is arranged in such a way that during the working cycle the solvent circulates through the working chamber; at the end of the working cycle the circulation system is closed off from the working chamber by means of a special device that blocks the system with a discharge valve so that a solvent can enter the chamber only if the valve is closed. A solvent washes the chamber thoroughly and passes the dissolved residues into a purifying system. The rotation speed of the agitators in mixing devices for oligomers may reach 30,000 rpm, with a pressure at the mixing head outlet of no more than 0.2 to 0.3 MPa. The dwell period of the components being mixed in the mixing chamber is several tenths of a second.

These dynamic mixing devices are usually installed in low-pressure processing lines, and one of their main advantages is that they achieve adequate mixing, even of oligomer materials, which are often difficult to mix. Washing a mixer with a solvent or blowing with air causes loss of part of the material and requires additional measures for solvent recuperation. If it is possible to decrease the viscosity of the components used in continuous molding of monomers and to improve compatibility, then the mixer design can be simplified.

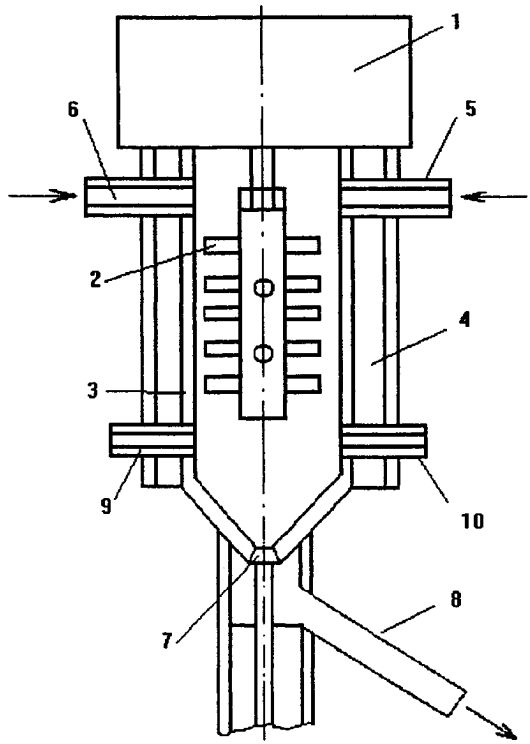

Figure 4.7. Mechanical mixing device (explanations are in the text).

Besides a three-way cock, other devices can also be used for mixing, for example a cone feeder with tangential reaction stream feed, a vessel equipped with disks rotating on their axes, a cylinder into which the initial components are fed turbulently, and various tubes for producing turbulent streams, etc.

4.2.4 POLYMERIZATION OR SOLIDIFICATION STAGE

After mixing of several streams, the reactive mixture goes into a mold where polymerization or solidification takes place. The behavior of materials in a mold depends substantially on the chemical nature of the initial raw materials, on mixture viscosity, on shrinkage during polymerization and solidification, on adhesion to the mold walls, and on temperature. The main feature of free casting is that the mold is either unpressurized or the pressure is no higher than 0.5 MPa if a mold is

replenished to compensate for shrinkage. These conditions permit the use of cheaper and simpler molds than the standard mold used for injection molding.

Open molds destined to produce work pieces with large machining allowances are extensively used. Aluminum and light alloys, polymeric materials, gypsum, sheet glass, plywood, tarpaulin, and board are commonly used for molds. When molding monomers, the very low viscosity (about 1 mPa s) of the initial mixture entering the mold should be taken into account, and its ability to interact chemically with the mold wall material should be taken into account. For molding oligomer mixtures, it is important to ensure that there are no dead zones, so that the air displaced from the mold can be removed freely; simple removal the article from the mold after polymerization or solidification must also be ensured. This is achieved by the design of the mold (for example, creation of tapers, lack of gaps in joints, simplicity of the joints in an open-type mold) and by cleanliness of the mold surface. The quality of the mold surface also determines that of the article surface. Thus, to obtain acrylic plastic with good optical properties, specially glasses must generally be used for the casting surface.

To obtain high-quality article surfaces, chromium plated and polished working surfaces are also used. In order to eliminate adhesion of items to the mold, the surface of the mold is coated with anti-adhesives, which are chosen according to the material being processed and the design of the mold. Organo-silicon, fluoroplastic, and other polymeric coatings are commonly used as anti-adhesives. Such coatings may be used repeatedly (up to 5 to 10 times). Another method relies on lubricating the mold surface with solutions of a polymer in a volatile solvent.

To increase the production rate, the casting devices and the molds are grouped into one unit. Linear, vertical rotary, and multi-layer units are the most common.[171]

A large exothermal effect resulting from chemical reactions is typical of these processes. When using oligomeric initial components, for example, formulations based on urethane prepolymers, epoxy resins, and lactams, self-heating may cause thermal decomposition. For this reason the correct choice of the initial solidification temperature is very important.

In radical polymerization, particularly in the large-scale production of poly(methyl methacrylate), the monomer may boil; hence the process should be carried out with continuous removal of reaction heat to eliminate overheating in the reactive volume. In this case, the choice of cooling method needs careful consideration.[172]

Different devices are used to maintain the preset temperature in a mold: cabinets, boilers, chambers, baths, infrared heaters, electromagnetic radiation, and so on. In a number of cases, solidification takes place owing to the heat output during the chemical reactions.

In commercial production, the molds are either filled with the initial reactive mixture and then transported for solidification, or they are located and filled in separate devices where polymerization proceeds. The last method is most often used in chemical molding (reactive processing) of articles from monomers, such as lactams; monomer polymerization proceeds at high temperatures accompanied by the release of monomer vapor into the atmosphere. The process itself is very sensitive to atmospheric oxygen and water and requires the use of an inert gas. For very high production rates where controlled atmospheres are used, throughput is increased by the use

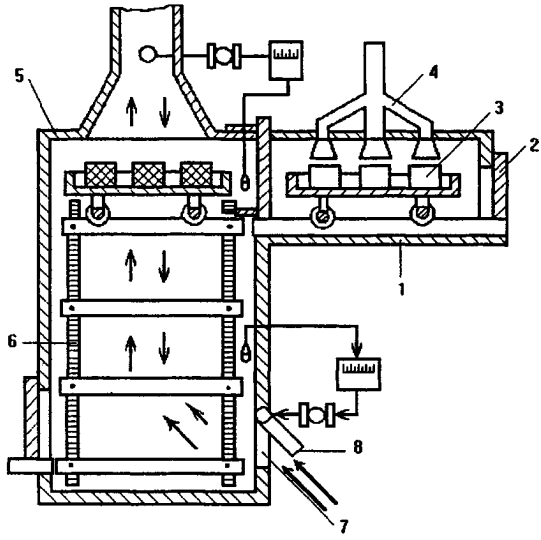

Figure 4.8. Closed sectional-type unit for continuous polymerization (explanations are in the text).

of multi-sectional units. Fig. 4.8 shows a closed sectional unit in which the molds gradually move through the various temperature zones required by the process.[173]

Such a unit is used in the production of slabs by the anionic activated ε-caprolactam polymerization. It has a chamber for filling molds *1* whose an entrance is closed by a lifting gate *2*. There are several molds *3* in the a chamber. The initial reactive mixture is injected through branch pipes *4*. After the molds are filled, polymerization takes place in the same chamber. The chamber *1* is connected to the top of the heat treatment chamber *5*, where there is a conveyer *6* with molds on it. The required speed of the conveyer may be found experimentally or by calculations. There is a port for unloading articles and another *7* with regulator valves *8* for feeding in cooling air at the bottom of the heat treatment chamber. The top of the unit is equipped with similar ports for air outlet. An advantage of this unit is a decrease in energy consumption due to the use of convective cooling.

Fig. 4.9 shows a diagram of an automatic line for chemical molding (reactive processing) of articles, which conveys the molds to a chamber for polymerization.[174] In this case, the mass and geometric shape of the items can be taken into account more accurately and the reaction rate in the mold can be chosen individually for each particular type and size of article by regulating the temperature regime. The automatic line has the usual apparatus for preparing, metering, and mixing the components (positions *1-5* as in the previous figures). A filling branch pipe is located above the inlet port of the mold *6* installed in a conveyer cradle *7*. The line also has a feeding unit *8*, and

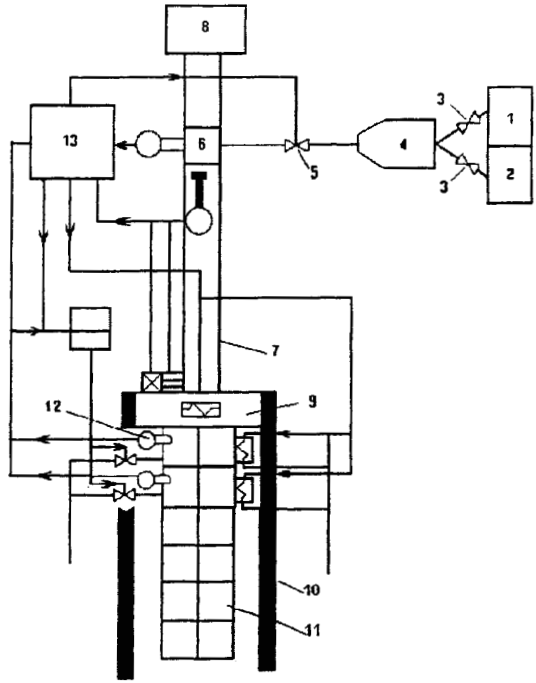

Figure 4.9. Automatic line for chemical molding (reactive processing) of articles with individual temperature regimes (explanations are in the text).

a mobile recharger *9* standing on rail tracks *10*, which are laid along both sides of the rows of polymerization cells *11*. The line has automatic control and monitoring instruments with transmitters *12*, data processing units *13*, and systems for maintaining the required temperature conditions.

The loading mechanism first places a mold preheated to the polymerization temperature onto the transporter; then the mold is positioned under a filling branch pipe of the mixing device which fills the mold with the reactive mixture, which is prepared from initial products fed by metering pumps from storage vessels. The filled mold goes to the unloading position and is taken away by a transporter controlled by an automatic goods addressing circuit. Data on the reaction mixture, its initial temperature, and the other characteristics of the process are delivered to the data processing unit simultaneously with a signal for operating the transporter. Based on the data obtained, the data processing unit selects a program for maintaining the proper temperature conditions in the polymerization cell. The transporter installs the mold in the cell; subsequently, the temperature

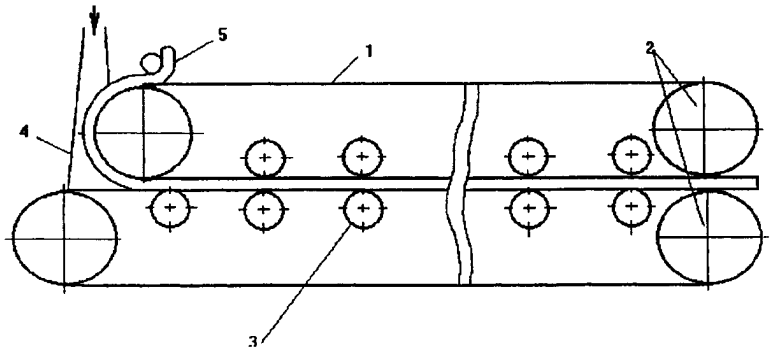

Figure 4.10. Diagram illustrating production of poly(methyl methacrylate) sheets by the continuous method: *1* - conveyer belts; *2* - drums; *3* - rollers; *4* - feeder; 5 - limiting strips.

conditions in the cell are maintained by the control unit by the preset program corrected according to the signal received from a temperature sensor. The end of the process is the signal for opening the cover of the polymerization cell, for calling up the transporter, and for unloading the finished article.

In the production of poly(methyl methacrylate) sheets or roll material, the polymerization mold is fabricated as two closed-loop stainless steel conveyer belts, which are stretched in parallel between two rollers. The belts move continuously; a gasket is inserted automatically on both edges, forming a chamber into which prepolymers are continuously fed (Fig. 4.10). The polymerization zone has gas or electric heaters.

Units for producing slabs of expanded (foamed) polyurethane are also equipped with a conveyer belt with side walls. The initial mixture is continuously fed onto the line, then foamed, and finally passed into a solidification chamber, where it is heated under IR lamps. Commercial lines for making slabs of elastic foamed polyurethane are up to 125 m long. The items produced can be up to 2 m wide and 1.5 m high.

When the mixture of monomers is cast in an open mold, the air bubbles formed at the jet nozzle in the mold usually have enough time to leave the material due to the low viscosity of the reactive liquid. When more viscous oligomers and prepolymers are used, particularly in the case of low-lifetime reactive mixtures, it may be necessary to use some simple procedures, for example, filling through a pipe immersed into the mold, to prevent the formation of air bubbles in the product.

The quality of the items produced by free casting may be improved by evacuating the mold. To do this it is necessary either to ensure that the mold is airtight and to connect it through a special valve to a vacuum line, or to put the mold into an airtight vessel.

Covering metallic shafts, rolls and rollers with rubber is required for many applications; such designs are used in the textile, printing, and many other industries. For producing coatings, molds with a vertical axis are often filled through inlet holes located along the diameters of the mold

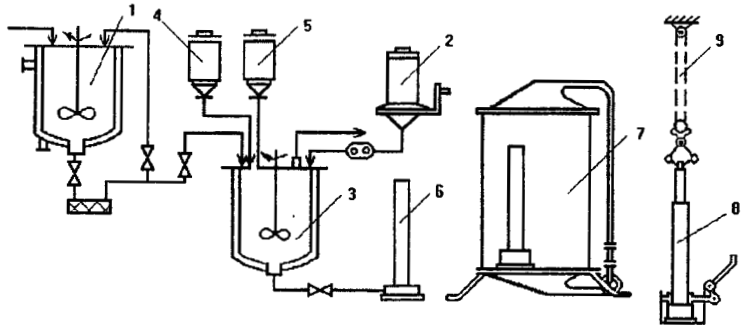

Figure 4.11. Section for manufacturing coated polyurethane rollers: *1* - reactor for polyester; *2* - batcher for modifying agent; *3* - reactor-mixer; *4* - batcher for diisocyanate; *5* - batcher for curing agents; *6* - mold for casting rollers; *7* - heat chamber for solidification; *8* - unloading device; *9* - transporting device.

bottom. A reactive mixture is fed from a mixer under pressure created by a compressor. Mold filling is terminated by shutting off the mold from the filling device by a gate valve after a certain quantity of a reactive mixture has entered. After solidification, the coated shafts are removed from the molds using a pressing-out device. A similar procedure is used to produce other tubular items coated with polyurethane, polyurethane-coated rollers for printing plants (Fig. 4.11).

The spraying of protective enamels without the use of solvents has became popular in coating industry. These enamels are mixtures of oligomeric products with different pigments; i.e., it is a typical example of reactive processing. A device for spraying these protective coatings is shown in Fig. 4.12.

Utilization of liquid casting compounds in manufacturing protective coatings allows the quantity of materials used for this purpose to be substantially increased. Rubbers have been widely replaced by polyurethane elastomers as coatings for rolls used in the paper, printing and metallurgical industries. In some cases, paper-making machines are fitted with pressing sections consisting of a pair of rollers: one is faced with granite and the other is coated with an elastic facing. Wet paper-making stock is fed on a cloth backing between the rolls, where it is dewetted. The more efficient the process the less the heat is required to dry the semi-finished product in a drying chamber with superheated steam. The metal core of the pressing roll is 0.5 to 1.5 m in diameter and up to 10 m long; 500 to 1500 kg of casting compound are required to coat it.

The use of cast polyurethane compounds instead of rubber is economical for several reasons, mainly owing to the higher wear resistance of the cover. Rolls with rubber facings need to be reground every 2 to 3 months while a polyurethane elastomer facing may operate effectively for more than two years without regrinding. The regrinding procedure itself is required to retain the necessary surface profile of the roll and to make grooves on the coating for better moisture removal.

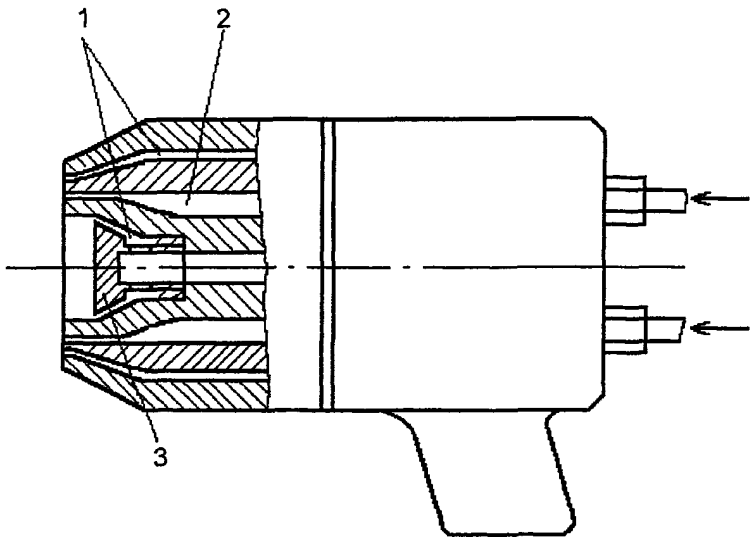

Figure 4.12. Device for spraying reactive compounds with a round stream: *1* - ring channels for hot air feeding; 2 - ring channel for reactive compound feeding; *3* - valve for regulating hot air supply.

If polyurethane, is used the wetness of a paper sheet at the roll exit decreases on average by 1.0 to 1.5%, and as a result, steam consumption decreases in the drying section. The improvement in rolling allows the working speed of the machine to be increased by 5 to 8%, and so paper production can be increased without additional investment. The life of the press cloths also increases by 15 to 20% when polyurethane is used instead of rubber.

When manufacturing coatings by reactive (chemical) molding, it is necessary to create a strong adhesive bond between the substrate and the coating. This is achieved by proper preparation of the substrate surface, which depends on the material and on the type of polymer used. As a rule, the surface is treated by chemical washing, electrochemical pickling, and various mechanical methods. The best results are achieved with shot-blasting followed by application of one or more intermediate layers. The layers are applied from solutions of oligomers in volatile organic solvents or from aero-dispersions followed by curing or drying.

The most efficient intermediate layers are polyurethane adhesives or glues.[175] In this case, the correct choice of molecular weight of the polyester and its ratio to diisocyanate is very important. The dependence of the adhesive strength on the molecular weight and the isocyanate-to-diol ratio is shown in Fig. 4.13. The best adhesion to metal is achieved when an intermediate layer based on low-molecular-weight polyester and at a ratio of NCO:OH = 2.5 is used.

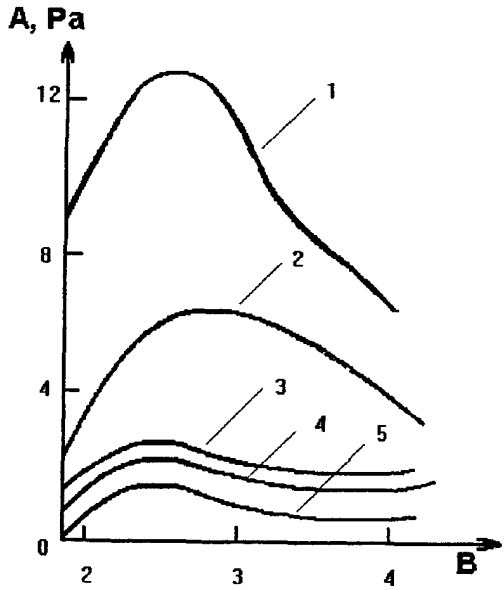

Figure 4.13. Dependence of adhesive strength A of the glue-metal joint on the isocyanate/diol ratio B (B is the mole ratio of 2,4-toluylene isocyanate to polyester) of a glue. Molecular weights of polyester are 500 (*1*); 1000 (*2*); 1700 (*3*); 2000 (*4*) and 2500 (*5*).

The overall dimensions and mass of pressing rolls and other similar coated cylinders do not allow coating to be carried out when they are vertically positioned. Therefore, the rolls are positioned horizontally, and the casting compound (reactive mix) is supplied through a distribution device simultaneously along its entire length.

4.3 MODELLING PROCESSES IN A MOLD DURING SOLIDIFICATION

Solidification of a preshaped article is the longest stage in a process cycle and in many cases this stage determines the duration of the process. After filling the mold, chemical reactions and physical processes take place, which lead to the formation of polymeric macromolecules, the formation of bonds between these macromolecules, and the growth of supermolecular structures. As a result, the material becomes solid when it is cooled below its melting point, and the article preserves its shape after removal from the mold. The mold cannot be opened until the polymer has gained sufficient rigidity and strength to retain its shape.

The stability of the shape of an article is partly determined by the value of its modulus of elasticity, but the required value of this parameter is not reached instantaneously and homogeneously throughout the volume of an article. Therefore, estimates of material stability must be made from the distribution of the elastic modulus throughout the volume of an article and its evolution in time. In this approach, the modulus must reach the necessary minimum value at any point in the material before the mold can be opened.

The reactive mix is injected or poured into a preheated mold, since a high temperature is necessary to accelerate the chemical reactions leading to formation of the polymeric product. Although an increase in temperature shortens the process cycle, it is important to remember that superposition of heat from an external source and the exothermal effect of the chemical reactions can result in undesirable temperature increase in an article, leading to thermal runaway and decomposition of the polymer.

Determination of the process parameters that ensure a permissible temperature profile and optimal solidification path is based on the general principles of the theory of batch reactors formulated in Section 2.7. Let us illustrate this approach with the example of solidification of a urethane-based compound for use as a coating.[176]

After filling a mold in the form of a thin rectangular parallel pipe, a reactive mass can be represented by a layer of width H and length L ($H << L$). This layer is positioned between the mold wall at temperature T_m, and the surface of the item is at temperature T_i (Fig. 4.14).

A quantitative description of the solidification process of a reactive mixture is based on the kinetic equations for that define the reaction parameters. One of these parameters is the "calorimetric" degree of conversion, which describes the linear propagation of polymeric chains:

$$\beta(t) = \frac{q(t)}{Q} \qquad [4.1]$$

where β is the relative degree of conversion; $q(t)$ is the heat flux at time t and Q is the enthalpy of a reaction. The kinetic equation for the parameter β can be written as

$$\frac{d\beta}{dt} = k_0 f_\beta(\beta) \exp\left(\frac{-U}{RT}\right) \qquad [4.2]$$

where t is the current time; k_0 is a pre-exponential factor; U is the apparent activation energy of the chemical reaction; and $f(\beta)$ is a kinetic function.

Experimental investigation of the chemical reaction kinetics for a polyurethane compound gives the following expression for the function $f(\beta)$:

$$f_\beta(\beta) = (1 - \beta)(1 + c_0\beta) \qquad [4.3]$$

The values of the constants in Eqs (4.2) and (4.3) are: $U = 49$ kJ/mol; $k_0 = 3.8 \times 10^6$ s^{-1}; $c_0 = 1.1$. The second kinetic parameter is the "rheological" degree of conversion (or transformation). The increase in the dynamic elastic modulus G(t) for various temperatures is shown in Fig.

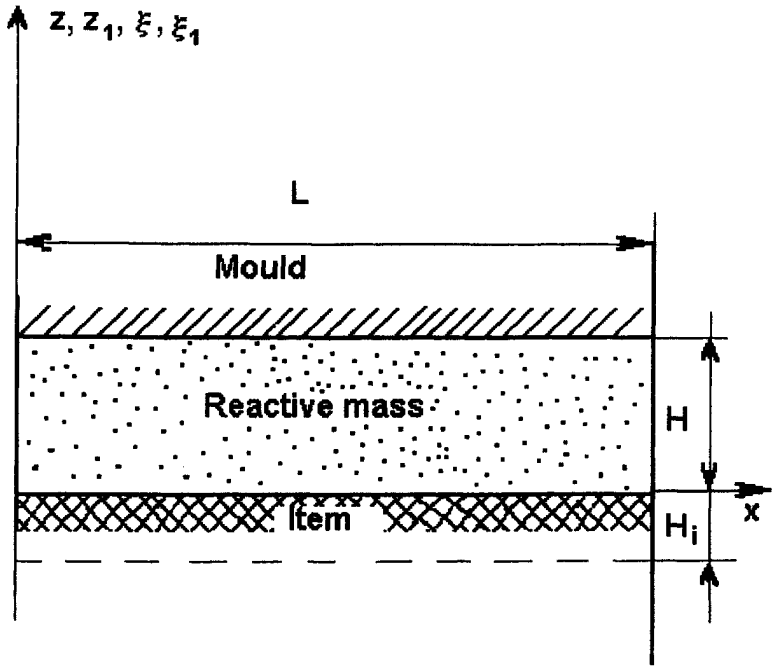

Figure 4.14. A model of a thin rectangular mold.

4.15. The values of the modulus of the end product depend on temperature; therefore it is necessary to introduce the equilibrium degree of conversion as a reference point:

$$\eta_{eq} = \frac{G_{\infty,T}}{G_{\infty,20}} \qquad [4.4]$$

where η_{eq} is the equilibrium (limiting) "rheological" degree of conversion; $G_{\infty,T}$ is the elastic modulus of the end product, which is reached at temperature T after the end of a chemical reaction in isothermal conditions; $G_{\infty,20}$ is the same for the temperature of 20°C.

The experimental data shown in Fig. 4.16 can be approximated by an empirical equation:

$$\eta_{eq}(T) = \frac{A_G}{T^{b_G}} \qquad [4.5]$$

where (for the case under discussion) $A_G = 1.92$; $b_G = 3.44$. The kinetic equation for the "rheological" degree of conversion is written as:

$$\frac{d\eta}{dt} = k_\eta f_\eta(\eta) \exp\left(\frac{-E_\eta}{RT}\right) \qquad [4.6]$$

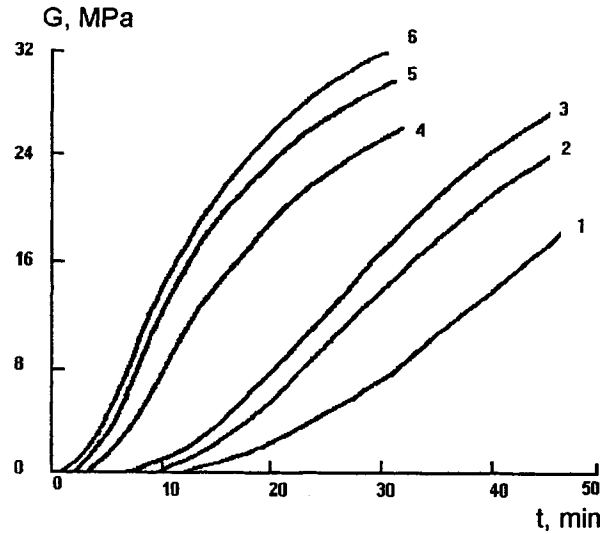

Figure 4.15. Time evolution of the shear dynamic modulus during curing at two temperatures: 23°C (curves *1* - *3*) and 61°C (curves 4 to 6) and different frequencies: 3 s^{-1} (curves *1* and 4); 12 s^{-1} (curves *2* and *5*) and 25 s^{-1} (curves *3* and *6*).

The meaning of the symbols in Eq. (4.6) is the same as in Eq. (4.2); the difference is that symbols in Eq. (4.6) relate to the "rheological" instead of the "calorimetric" degree of conversion. The "rheokinetic" function $f_\eta(\eta)$ is expressed as follows:

$$f_\eta(\eta) = [\eta_{eq}(T) - \eta](1 + c_\eta\eta)^{a_G} \qquad [4.7]$$

The values of the constants are: E_η = 28 kJ/mol; k_η = 513 min^{-1}; a_G = 1.92. Experiments have shown that values of $G > 0$ appear in the course of a chemical reaction at a "calorimetric" degree of conversion $\beta = 0.8$; this clearly demonstrates that "rheological" and "calorimetric" degrees of conversion are not equivalent.

For a complete description of the temperature and degree conversion fields throughout the volume of an article it is necessary to add a term for the heat of chemical reaction to the energy balance equation:

$$\frac{\partial T}{\partial t} = \frac{\lambda}{C_p\rho}\left(\frac{\partial^2 T}{\partial x^2} + \frac{\partial^2 T}{\partial z^2}\right) + \frac{Qk_\beta}{C_p\rho} f_\beta(\beta)\exp\left(\frac{-E_\beta}{RT}\right) \qquad [4.8]$$

where λ is the thermal conductivity; C_p is the specific heat ; ρ is the density; Q is the enthalpy of the chemical reaction; x and z are coordinates along and across the polymeric layer, respectively.

It is also necessary to write down the energy equation for an substrate of width H_i on of which the polymeric layer is positioned:

$$\frac{\partial T}{\partial t} = a_i\left(\frac{\partial^2 T}{\partial x^2} + \frac{\partial^T}{\partial z_i^2}\right) \qquad [4.9]$$

where a_i is the thermal conductivity of the substrate material and z_i is a coordinate directed normal to the surface. It is convenient to search for a final solution in terms of dimensionless variables. If we recall that $H_i << L$ and $H << L$ we come to the following system of equations:

$$\frac{\partial \theta}{\partial \tau} = \frac{1}{\Omega}\frac{\partial^2 \theta}{\partial \xi^2} + \chi \exp\frac{\sigma_\eta \theta}{1 + \nu_\eta \theta} \qquad [4.10]$$

$$\frac{\partial \eta}{\partial \tau} = \exp\frac{\theta}{1 + \nu_\eta \theta} \qquad [4.11]$$

$$\frac{\partial \beta}{\partial \tau} = \kappa_\beta \exp\frac{\sigma_\eta \theta}{1 + \nu_\eta \theta} \qquad [4.12]$$

$$\frac{\partial \theta}{\partial \tau} = \delta_i \frac{\partial^2 \theta}{\partial \xi_1^2} \qquad [4.13]$$

The boundary conditions are:

$$\text{at } \theta = 0,\ \theta_1 = 1, \quad \text{at } \xi = 1,\ \theta(x,\xi) = \theta_m \quad \theta(x,\xi) = \theta(x,\xi_1); \quad \frac{\partial \theta(x,\xi)}{\partial \xi} = \frac{\partial \theta(x,\xi_1)}{\partial \xi_1}$$

The initial conditions (at $\tau = 0$) are:

$$\beta(x,\xi) = \beta_f(x,\xi); \quad \eta(x,\xi) = 0$$

In all these equations we have used the following of notation for the dimensionless variables: $\tau = tk_\eta$ is dimensionless time; $\xi = z/H$, $\xi_1 = z_1/H$ are dimensionless coordinates; θ_f and β_f are the spatial distributions of the temperature and calorimetric degree of conversion. As a first approximation it is reasonable to accept that

$$\theta_f(x,\xi) = \theta_0 = \text{const}; \quad \beta_f(x,\xi) = 0$$

In a more sophisticated analysis these functions can be found as the solutions of the dynamic and energy balance equations for filling a mold. θ_m is the dimensionless temperature of the mold; T_0 is the initial temperature of the reactive mixture; $\omega = (H^2 k_{\eta T})/a$ is the dimensionless factor characterizing the ratio of time scales for heat transfer and the chemical reaction. Other dimensionless variables are as follows:

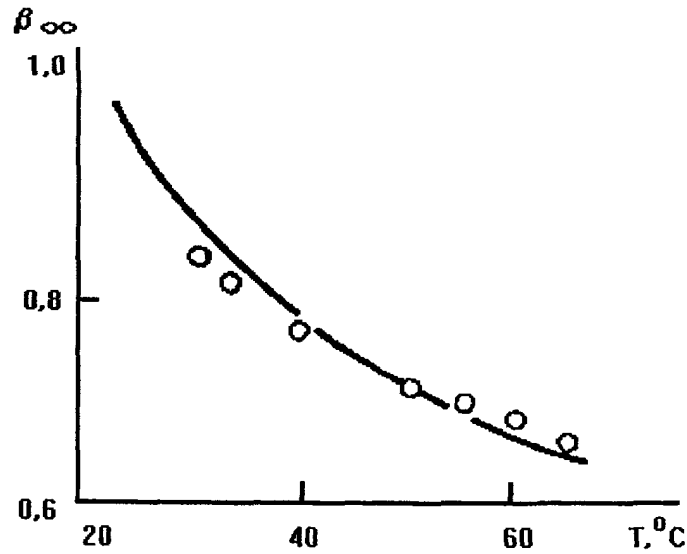

Figure 4.16. Temperature dependence of the equilibrium value of the "rheological" degree of conversion. Points - experimental; solid line - calculated.

$$\chi = \frac{\Delta H}{C_p \rho}\frac{k_{\beta T}}{k_{\eta T}}\frac{E_\eta}{RT_0^2}; \quad \kappa_\beta = \frac{k_{\beta T}}{k_{\eta T}}; \quad \delta_i = \frac{a_i}{H_i^2 k_{\eta T}}; \quad k_{\beta T} = k_\beta e^{\frac{-E_\beta}{RT_0}};$$

$$k_{\eta T} = k_\eta e^{\frac{-E_\eta}{RT_0}}; \quad \alpha' = \frac{\lambda_i}{\lambda}\frac{H}{H_i}; \quad \theta = \frac{E_\eta}{RT_0^2}(T - T_0)$$

The system of Eqs (4.10) - (4.13) was solved numerically by the method of finite differences, starting with Eq. (4.11) at the nodes of the network with $\beta = 0.8$. The process was assumed to be over when the minimum value of the "rheological" degree of conversion throughout the volume of the article had reached a preset level of conversion, η^*; the calculations were ended at this time.

The results of calculations for two values of the initial temperature of the reactive mass T_0 are shown in Fig. 4.17. For $T_0 = 70^\circ C$, the curves are practically insensitive to the value of ω. This is explained by the fact that the mold temperature is lower than the initial temperature of the reactive mass (polyurethane composition) and therefore the layers of polymeric material close to the surface of the mold cool rapidly down to the temperature T_s, because this temperature is strictly constant.

At mold temperature higher than $40^\circ C$ (Fig. 4.17), the total cooling time is determined by the thickness of the layers contacting the surface of the article. The approach to η^* in these layers is dependent on the heat flux from the hot mold and this is why there is some increase in solidification

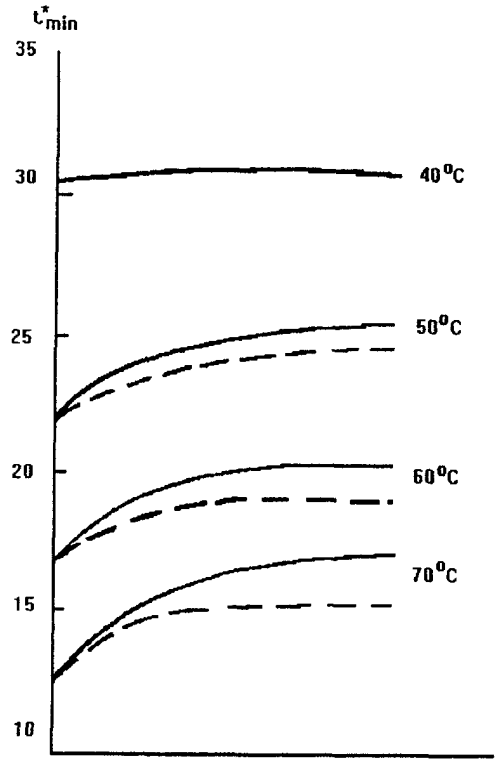

Figure 4.17. Dependences of the solidification time on the parameter ω at different mold temperatures. Solid lines - for the initial temperature $T_0 = 40^\circ C$; dotted lines - for $T_0 = 70^\circ C$.

time with an increase in ω. In general, $\omega < 1$ and the characteristic time for heat exchange is much less than the characteristic time for the chemical reaction monitored by measuring η. The calculations show that the solidification time is determined primarily by the mold temperature and is only weakly dependent on other factors related to the parameter ω.

For the polyurethane composition considered here the maximum (adiabatic) temperature jump is equal to 25 K. This means that at ordinary working temperatures of the mold, i.e., 40 - 80°C, the maximum increase in the material temperature does not reach an unacceptable level of close to 200°C, where thermal degradation of the polymer can begin. We can restrict the maximum temperature growth T_{max} by using the mathematical model based on Eqs. (4.10) - (4.13) and then constructing T_{max} - vs - ω curves for various mold temperatures. These provides a means of choosing the optimum process parameters when the temperature must not exceed T_{max}.

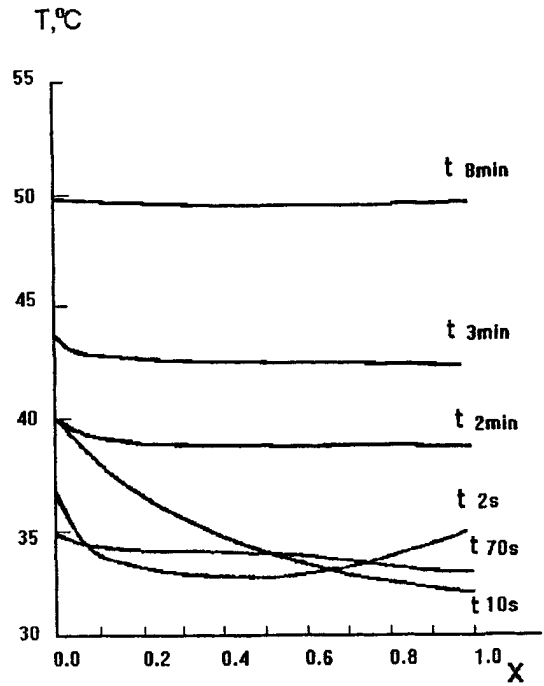

Figure 4.18. Temperature distribution along the contact boundary between reactive mass and a solid wall at different times (marked on the curves).

To analyze the temperature distribution in any real situation, it is necessary to consider mold filling and solidification simultaneously. An example illustrating temperature distributions at various times along the length of a polymeric layer at the surface of a solid wall is shown in Fig. 4.18. The initial temperature and conversion distributions are not constant but reflect mathematical simulations of various conditions at the mold filling stage.

4.4 CASTING INTO ROTARY MOLDS

4.4.1 TECHNOLOGICAL BASIS

One of the methods of obtaining products from reactive mixtures is centrifugal and rotational molding which are widely used in manufacturing articles from melts and powders. Sleeve-type (hollow cylindrical articles) are obtained by centrifugal molding (casting), and thin-wall three-dimensional seamless tanks are produced by rotational molding. Centrifugal molding may be treated

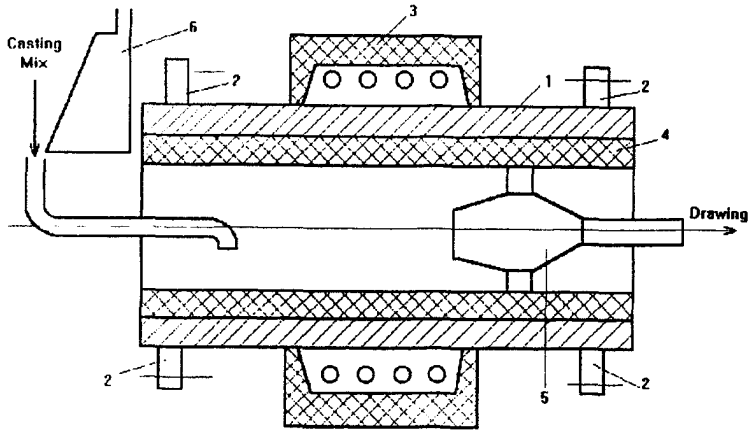

Figure 4.19. Layout of a unit for centrifugal casting (molding) of tubular blanks: 1 - rotary mold; 2 - mold rotation rollers; 3 - heating chamber; 4 - blank; 5 - rotary gripper of finished pipe extender; 6 - exhaust ventilation.

as a particular case of rotational molding because in the latter, the mold rotates relative to two axes and in the former, relative to one axis. The same reactive mixtures that are prepared for stationary molding are also used for rotary processing. The mixture filling the mold is pressed against the mold walls by centrifugal forces and is polymerized. Compared with casting in a stationary mold, molding in a rotary mold allows more effective removal of air inclusions (occluded air), the mechanical properties of the material are improved, and the amount of waste is reduced because there is less need for further mechanical processing of the final products. Centrifugal molding of tubular polycaproamide products by anionic activated ε-caprolactam polymerization has become common practice. Fig. 4.19 shows the layout of a unit for centrifugal molding of tubular polycaproamide products in a mold with a horizontal axis of rotation.[177] This unit is intended for making articles with unlimited axial dimensions. Products with axial dimension not exceeding their diameter can be molded in cylindrical units with vertical axis of rotation.

Casting of tubular polycaproamide items by centrifugal molding is carried out at lower rates of rotation than those used for processing conventional thermoplastic materials because the viscosity of the polycaproamide melt is lower than that of the majority of other thermoplastic polymers. The rotation speed depends on the size and shape of the item as well as on the mixture reactivity and may vary from of 100 to 200 rpm. The mixture is poured through the open end of a rotating mold heated to 140 to 160°C, and then the mold is blown through with nitrogen. After a short induction period, the temperature of the mix increases by 50 to 60°C due to the heat of polymerization. Mold rotation is stopped after 15 to 20 min. The item is removed from the mold at the temperature of 120 to 140°C and then put into a heating cabinet for programmed cooling. As in molding in stationary molds, it is necessary to coat the mold surface with anti-adhesive or to maintain a high polish.

Opening the mold and removing items is considerably easier with polymers showing a high shrinkage (5 to 15%).

In rotational molding of anionically polymerized ε-caprolactam one can produce vessels up to 10 m^3, fuel tanks of various shapes, and other seamless large-sized items. As a rule, the mold rotates with different speeds about the two axes in such a way that the reactive mixture flows to the mold walls with minimal net centrifugal force. When molding long items, a greater difference in rotation speeds is required than when molding round items.

Although the polymerization of ε-caprolactam was described above, there is no difference in principle from the process flow sheets for centrifugal molding of items from other polymers and oligomers. Nevertheless, in most cases, the high temperatures used in lactam polymerization are not required, and the flow sheet as a whole is simplified. In industrial practice, poly(methyl methacrylate) pipes,[172] and sheets of polyurethanes and unsaturated polyesters are obtained by centrifugal casting.

It is of interest to consider the process for applying protective coating to rotating cylindrical surfaces, such as gumming rollers, or for applying of internal and external anti-adhesive coatings to pipes, etc. This technology is considerably more economical than coating by casting into the gap between the mold and the working surface, because the laborious manufacture of molds is unnecessary. Fig. 4.20 illustrates various techniques for applying protective internal and external polyurethane coatings. In this case, an experimental or theoretical investigation of the required rotational parameters is necessary and must take into account the rheokinetics of curing mixture to be applied.

The selection of optimum conditions for rotary molding requires extensive experimental investigations of the various processing regimes. Recently, another way has been developed, i.e., simulation of the flow of a liquid system polymerized in a rotary (rotating) mold.[178]

4.4.2 HYDRODYNAMIC PHENOMENA DURING MOLDING IN A ROTARY MOLD

A complete analysis of the hydrodynamic phenomena occurring during molding into rotating molds is rather complicated. The main problem here is the need for accurate determination of the shape of the free surface of a rotating liquid. Hence, most approaches are based on the movement of thin liquid films on a solid surface. In this analysis boundary layer theory is used to examine the flow of thin films because the thickness of a film is small compared to its longitudinal dimensions. For the particular case of a Newtonian liquid flowing down a vertical (or inclined) wall by gravity, we can experimentally observe three different thin film flow regimes: purely laminar (Reynolds Number, Re <20), wave, and turbulent modes. In practice, particularly in the application of enamels by spraying, it is important to evaluate the hydrodynamic behavior of materials with more complicated dependences of apparent viscosity on shear stress. In this context, the influence of the yield stress on the layer thickness of the material flowing down the solid surface is especially important.

The geometrical characteristics of the flow field for free movement of a Newtonian liquid on the surface of the rotating cylinder with a horizontal axis is shown in Fig. 4.21 (after[179]). In

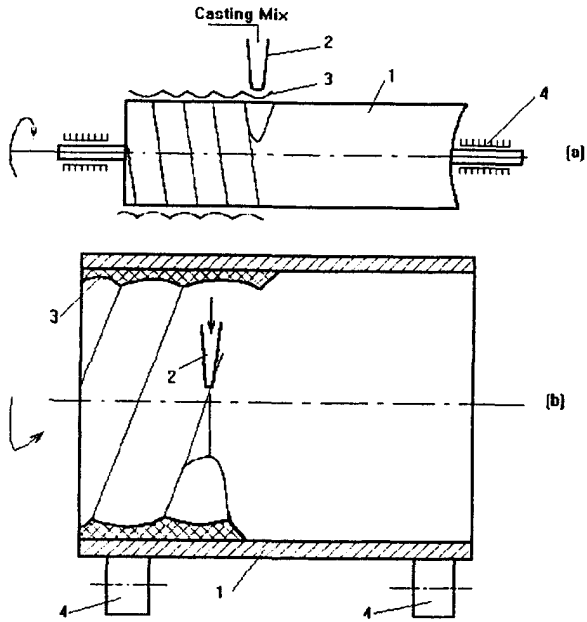

Figure 4.20. Elementary process flow sheets for molding an internal (a) and an external (b) anticorrosive coatings by the continuous/subsequent filling method: 1 - cylinder (shell) being coated, rotating on supports; 2 - movable filling device; 3 - coating being molded; 4 - bearings.

this case, we need to examine only a thin layer of liquid if $R/b >> 1$ (b is the mean thickness of the liquid layer, R is the cylinder radius, and the ratio $R/b = N$, where N is a dimensionless geometric criterion). The other dimensionless variables which characterize the flow are:

dimensionless radial velocity $v^*_r = v_r/\omega R$,
dimensionless circumferential velocity $v^*_0 = v_0/\omega R$,
dimensionless radius $x = r/R$,
Froude Number $Fr = \omega^2 x/g = \omega^2 r/gR$,
Reynolds Number $Re = \omega R/v$.

Here v_r is the radial speed of the liquid, v_0 is circumferential velocity of the liquid, ω is the velocity of rotation of the cylinder.

The solution of the hydrodynamic problem of boundary layer flow, excluding the effects of surface tension, requires simplification of the formulation; this is achieved by introducing the flow function ψ. Then the transition to a system of differential equations written for a new coordinate system (turn angle and flow function) can be made, and we can find the form of the free surface

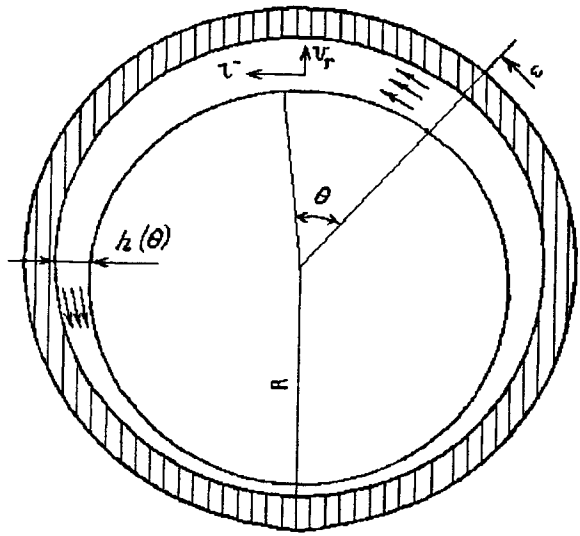

Figure 4.21. Geometrical scheme of a flow field pattern for a rotating liquid film with a variable thickness h(θ). [Adapted, by permission, from J. A. Deiber, R.L. Cerro, *Ind. Eng. Chem. Fund.*, **15** (1976), 103.]

of a rotating liquid which is the boundary flow line. The reduction of the proper system of differential equations to dimensionless form shows that the ratio between the Froude and Reynolds numbers determines the zones of qualitatively different behavior of a liquid on a rotating surface. These zones with their calculated boundaries are shown in Fig. 4.22. Four different modes are possible:

A is solid-like rotation,
B is the zone of a falling film,
C is an oscillating boundary layer,
E corresponds to unstable solutions.

Two additional parameters are the angular position of the point at which the film thickness is maximum, 0_{rot}, and the ratio of the maximum thickness of the film to its mean thickness ε. The zone of large Re and small Fr is shaded in Fig. 4.22 in the right bottom. The existence of circular closed flow lines proves to be impossible; hence, a stable solution of the hydrodynamic problem is also impossible. The zone of quasi-solid rotation A is marked in the top left corner; film flow is absent here and $1 \leq \varepsilon < 1.01$. This zone is reached either at Fr = const by decreasing Re (due to an increase in viscosity) or at Re = const by increasing Fr (through an increase in ω). Two transient zones are marked with the numbers 1 and 2 in the lower unstable zone of Fig. 4.22. In zone 1, the

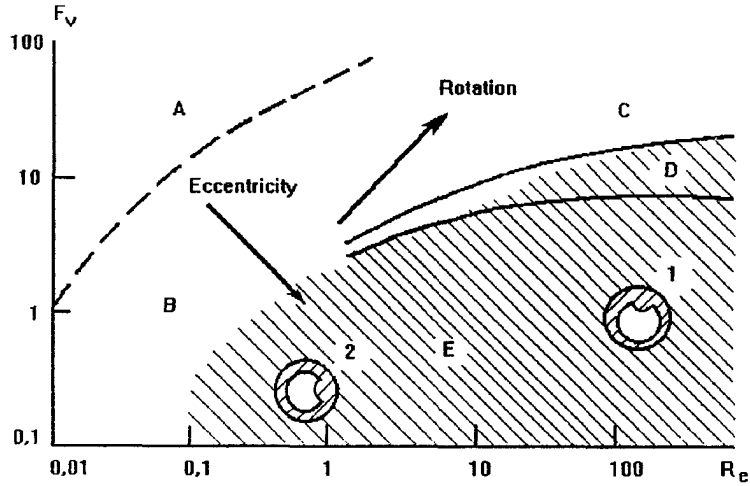

Figure 4.22. Results of calculations showing different flow modes as a function of the Reynolds and Froude Numbers (explanations are in the text). [Adapted, by permission, from J. A. Deiber, R. L. Cerro, *Ind. Eng. Chem. Fund.*, **15** (1976), 103.]

film thickness becomes large and drops of liquid are torn off and fall to the bottom. If tearing-off occurs below the uppermost point, a new flow mode characterized by formation of a cascade becomes possible. For practical processing, the mode corresponding to the top left corner of the diagram with $\varepsilon \approx 1$ is the most favorable. It follows from the figure that the inequality $Fr/Re > 100$ is the condition for quasi-solid rotation.

In reacting mixtures, the viscosity depends not only on the temperature, but also on the conversion. The viscosity decrease that occurs for a short period at the beginning of the process is due to the increase in temperature, whereas later on, there is a viscosity increase due to the chemical reaction. Hence, a rather complicated picture of flow behavior is observed in rotary molding. Based on an experimental study the flow of polyester resins,[180] four main modes of flow of reactive liquids during rotation were established: film flowing-down (cascading), ring-shaped flow, hydrocyst, and quasi-solid rotation. In principle, hydrocyst is a new mode characterized by flow of a stable laminar secondary stream with local accumulation of material. Hydrocyst is an instability which is determined by centrifugal (viscous and gravitational) forces. This phenomenon is observed at higher angular velocities than in ring-shaped flow. The different flow modes for a reacting liquid can be identified by its location on the dimensionless Fr-Re diagram (Fig. 4.23).

In reaction molding, the reactive mixture is initially poured or injected into the mold bottom as a pool. As the mold rotates, the mixture moves along the mold surface and becomes uniformly distributed on the wall in the ideal case. For example, let us suppose that the process begins from point M in Fig. 4.23 at a fixed value of ω and mean film thickness b. As the viscosity increases as

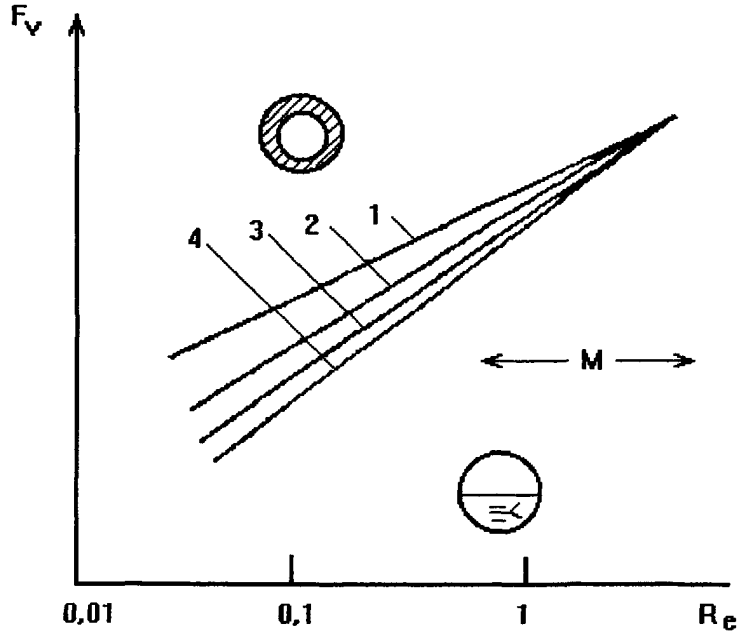

Figure 4.23. Different possible flow modes in rotary processing of polyester resin: 1 - quasi-solid rotation; 2 - stable hydrocyst; 3 - rotation in an annular (ring-shaped) layer, 4 - cascade flow. [Adapted, by permission, from I. L. Throne, I. Gianchandani, *Polym. Eng. Sci.*, **20** (1980), 913.]

a polymerization proceeds, the polymer film movement changes from cascade to ring-shaped flow, then to hydrocyst, and, finally, to rotation as a quasi-solid body. If gelation occurs during the hydrocyst-type flow, the end product will be rejected as defective. Hence, it is necessary to pass to the quasi-solid rotation mode well before the moment of gel formation. This can be achieved by changing the rotation speed and the kinetics of the viscosity increase. If, for example the wall thickness is increased 4 times, the initial point will move to the right from M. This will cause premature gel formation and will lead to the appearance of a wavy surface. An increase in the cylinder radius substantially relaxes the rigidity of the hydrodynamic conditions. This means that it is simpler to manufacture large items with uniform walls than small articles, which is one more reason why rotary reactive processing is especially favorable for producing large-scale articles. The time necessary to achieve the optimal flow mode is also of practical interest. This factor depends on viscosity, rotational speed, and film thickness.

4.5 POLYMERIZATION IN A TUBE REACTOR

Tube reactors or engineering apparatus involving flow in tubes are frequently encountered in polymer synthesis and reactive processing. The production of long ("infinite") articles with arbitrary cross-section from thermoplastic polymers is an example of plug-type polymerization and processing in a tube reactor. It is a mass production operation in which a melt of a newly synthesized polymer is immediately transformed into a long "one-dimensional" end product (tube, bar, and so on) during the same process operation.[181] This method permits the economical production of high-quality polymers in a simple process without any additional finishing operations. The practical realization of this approach as an integrated process requires several different parts,[182] but the tube reactor is at the center of the operation.

A typical example of a tubular reactor for one-step processing of a newly synthesized polymer is described in a number of patents.[183,184] This device consists of a high-pressure tube with the temperature profile regulated along its length. An extrusion die is mounted at the outlet end of the reactor. Continuous feeding is provided by a piston pump.

Many processes involving the flow of a reactive liquid along a tube are known, which makes theoretical analysis of the flow of polymerizing liquids, i.e., fluids with time-dependent rheological properties, relevant to the tubular polymerization reactors and similar plant equipment used in reactive processing.

One new factor that must be considered that is absent in classical hydrodynamics is the change of viscosity with time as a consequence of the chemical reactions proceeding during flow. It is therefore necessary to know the kinetics of these reactions and the dependence of the rheological properties of the liquid on the degree of conversion. The physical movement of a reactive liquid along a tube is quantitatively dependent on whether the reactive mass remains fluid during the whole polymerization process or loses its fluidity due to formation of a three-dimensional polymer network. Finally, we must remember that the phenomena occurring during reactive processing are generally non-isothermal.[185,186]

There are three main sources of non-isothermal effects which can play different roles in real processes:

- heat exchange with the environment as the channel walls are heated or cooled;
- heat output due to the heat of the polymerization reaction;
- dissipative release of deformation energy during flow inside a channel, as we are dealing with highly viscous liquids.

The relative influence of these factors is different at the beginning and near the end of the process. The heat output resulting from chemical reactions is usually greatest at the beginning, when most of the individual chemical transformations take place and the reaction rate highest. However, other situations in which the reactions are self-accelerating are also encountered. Dissipative heat output becomes greater at the end of the process when high-molecular-weight products with very high viscosity appear in the reactive medium. It is clear that there is a very complicated nonlinear interrelationship between the heat effects, the kinetics of the chemical

reactions, and the hydrodynamic situation inside a reactor. Relations connecting all these phenomena can be found by mathematical modelling of the process.

4.5.1 FLOW WITHOUT TRANSITION TO THE SOLID STATE

There are some fundamental investigations devoted to analysis of the flow in tubular polymerization reactors where the viscosity of the final product has a limit (viscosity $\eta < \infty$); i.e., the reactive mass is fluid up to the end of the process. As a zero approximation, flow can be considered to be one-dimensional, for which it is assumed that the velocity is constant across the tube cross-section. This is a model of an ideal plug reactor, and it is very far from reality. A model with a Poiseuille velocity profile (parabolic for a Newtonian liquid) at each cross-section is a first approximation, but again this is a very rough model, which does not reflect the inherent interactions between the kinetics of the chemical reaction, the changes in viscosity of the reactive liquid, and the changes in temperature and velocity profiles along the reactor.

Thus we need to develop a more realistic "rheokinetic" model and assume that a severe inhomogeneity in the rheological properties of reactant mix over the reaction volume is a necessary feature of the real situation in any tube reactor; this is of fundamental importance in any analysis of the problem. The volume distributions of temperature, reactant concentrations, degree of conversion, and residence time directly influence the viscosity distribution, the hydrodynamic flow pattern and the polymerization process. In all real situations involving the flow of polymerizing liquids through a tube reactor, the dependence of viscosity on time and on the degree of conversion is of primary importance. Therefore, we need to solve a system of rigorous equations for the volume distributions of all these parameters simultaneously. The equations for the simple degenerate models cannot reflect the characteristics of flow of "rheokinetic" liquids and should not be used. Both the simplest models of a stirred tank reactor or a plug-flow reactor and their modifications and combinations (dispersion model, cell model, cascade model, etc.) are very restricted in their ability to describe the polymerization process in a real tubular reactor, because they all digress from an accurate description of liquid flow; i.e., they deliberately ignore the rheokinetics of the process. This is also true for models such as a stirred tank reactor combined with back flow,[187] the two-dimensional cell model,[188] etc., which would be quite adequate to model chemical reactors for processes involving low-molecular-weight products.

It is commonplace to use averaged models: zero-dimensional, where the averaging of temperature T, degree of conversion β, and other factors is over the volume; or one-dimensional where averaging is over the section. In some cases, the models give basic information on the processes occurring in a tubular polymerization reactor. For example, such an analysis proved that the dependence of the pressure drop P on the flow rate Q (pressure drop - flow rate characteristic) in a flow of a polymerizing liquid, i.e., liquid with time dependent viscosity, is nonlinear and may be nonmonotonic, even in the isothermal case[189] shown in Fig. 4.24. However, none of these models is sufficient for engineering design.

If a liquid with constant viscosity η flows through a tube, the P(Q) function is described by the well known Poiseuille equation, which can be written as

$$P = K\eta Q$$

where K is a geometrical factor, calculated from the tube dimensions.

If the viscosity varies during flow for some reason (decreases with rising temperature or increases as a result of a chemical reaction such as polymerization), the linear Poiseuille P-vs-Q relation is violated and the pressure drop - flow rate curve may become nonmonotonic. This effect in polymerizing reactors can be explained by the fact that the most viscous products of a reaction are swept out of the reactor with increasing flow rate and are replaced. Instead, a reactor is refilled with a fresh reactive mixture of low viscosity. This leads to a decrease of the volume-averaged integral viscosity and therefore the pressure drop decreases. This can be illustrated by the following relationship:

$$P = KQ \int_0^L \eta(z)dz$$

where z is the coordinate measured along the reactor and L is the full length of the reactor. It is evident that with a decrease in the integral in this equation, the pressure drop becomes smaller. The potential for a nonmonotonic pressure - output relation in a tubular reactor must be examined to ensure safe operation and control, etc.

Let us analyze the possible operational situations shown in Fig. 4.24. If we gradually increase the pressure at the inlet section of the reactor we reach the peak of the P(Q) curve. Then, there is an abrupt transition from the steady state on the left-hand branch (low flow rate and high conversion) to the state on the right-hand branch (high output and low conversion). With a pressure changes in the opposite direction, the jump from the right-hand to the left-hand branch will occur in some other place, as shown by the arrows in the figure; this indicates that hysteresis will be operative. All points on the declining part of the curve (negative slope) correspond to unstable states, which cannot be reached if the pressure drop is preset. If the output rather than the pressure is fixed we can work at any point on the P-vs-Q, since all the conditions at these points are stable.

Unstable branches on the P(Q) curve and the appearance of hysteresis loops can occur for various reasons usually connected with an increase in viscosity. Thus, a non-monotonic P(Q) curve was first encountered in an analysis of the flow of a hot inert (non-reactive) liquid in a cold tube when the viscosity of the liquid was strongly dependent on temperature.[190] The intense dissipative heat output may have been the reason for the instability in the flow of an inert liquid.[191] In both cases, the reason for the nonmonotonic in P(Q) dependence was the strong dependence of viscosity on temperature, which is equivalent here to time dependence for viscosity. Detailed investigations of the hysteresis transitions shown in Fig. 4.24 proved that they have a wave character;[192] in this case, the transition occurs at a constant flow rate.

An analogy can be seen between these phenomena and the decrease in volume-averaged viscosity in the flow of a polymerizing liquid through a tubular reactor as described in Eq. (4.14). In real situations, the flow of a polymerizing liquid is always non-isothermal, which leads to a very

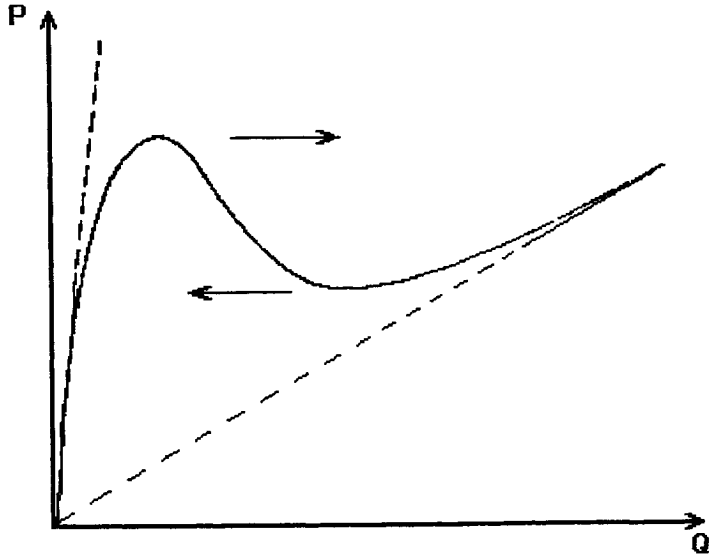

Figure 4.24. Nonmonotonic dependence of a pressure drop on flow rate, showing possible instability in flow through a tubular reactor.

complicated superposition of hysteresis phenomena of different origins. To further analyze a one-dimensional model of a tubular reactor we need to introduce variable viscosity as a new dominating factor. In this case, the degree of conversion influences viscosity more strongly than the changing temperature. To a first approximation, it will not influence P(Q) dependence but not the temperature and conversion distributions. However, changing to a two-dimensional model, i.e., calculating radial distributions of all parameters, radically changes the whole picture and leads to fundamentally new results.

4.5.2 THE ROLE OF RADIAL DISTRIBUTIONS

A complete analysis of the role of the radial distributions of all the parameters that determine the flow through a tubular reactor during polymerization is a very complicated, and it is doubtful whether general solutions can be found. However, solutions can be obtained for various situations for a system with known kinetic and rheological properties, because we will be searching for specific details rather than for a general physical picture of the process. It is also possible to carry out a general analysis at certain simplified models, which nevertheless include the principal rheokinetic effects.

As a first approximation, the several authors assumed a fixed constant parabolic velocity profile.[193,194] However, this approach is generally inadequate for a rheokinetic liquid because, first, real velocity profiles have a very different shape (as will be demonstrated below), and second,

they transform along the stream. These effects lead to a different thermal and kinetic situation than would be expected from a model with a parabolic velocity profile and as a result, the predictions of this model may be wrong. This was clearly demonstrated when a proposal for styrene polymerization in a tubular reactor was examined.[195] In a previous publication,[194] where a parabolic velocity profile was assumed, this idea was considered to be feasible, but a more realistic rheokinetic model which allowed for transformations in the velocity profile, subsequently showed that the proposal was unacceptable, because it required an excessively long polymerization reactor.[195] A comparison of the predictions of these two investigations proved that only rheokinetic models should to be used to obtain useful and unambiguous theoretical predictions.

Another approach[196, 197] described a solution obtained by assuming a predetermined velocity profile derived from experiments.The governing factor was the heat exchange conditions, which were characterized by the Biot Number. A model based on estimating temperature effects on velocity profiles is quite permissible for traditional reactions involving low-molecular-weight compounds,[198] but cannot be applied directly to flows for which the viscosity changes due to a chemical polymerization reaction.

Non-isothermal phenomena lead to a number of interesting results obtained from analyses of two-dimensional flows of liquids with viscosities that are strongly temperature-dependent. For example, an attempt was made to determine how a heat pulse propagates during the flow of an inert liquid. The result was rather obvious: the initial perturbation ("wave") became attenuated as it propagated. The primary aim of this investigation was to expand the analogy between combustion processes and non-isothermal flows, where the source of heat output in the latter case is energy dissipation in a viscous medium. The mutual interaction between hydrodynamic dissipative heat output and the thermal effect of a chemical reaction can lead to the phenomenon of "hydrodynamic ignition".[199]

The intense heat dissipated by viscous flow near the walls of a tubular reactor leads to an increase in local temperature and acceleration of the chemical reaction, which also promotes an increase in temperature; the local situation then propagates to the axis of the tubular reactor. This effect, which was discovered theoretically, may occur in practice in the flow of a highly viscous liquid with relatively weak dependence of viscosity on degree of conversion. However, it is questionable whether this approach could be applied to the flow of ethylene in a tubular reactor as was proposed in the original publication.[199] In turbulent flow of a monomer, the near-wall zone is not physically distinct in a hydrodynamic sense, while for a laminar flow the growth of viscosity leads to a directly opposite tendency - a slowing-down of the flow near the walls. In addition, the nature of the viscosity-versus-conversion dependence $\eta(\beta)$ also influences the results of theoretical calculations. For example, although this factor was included in the calculations in Ref.,[200] it did not affect the flow patterns; because of the rather weak $\eta(\beta)$ dependence for the system that was analyzed.

The investigation by Lynn and Huff[201] was the first one in which the true velocity profiles during polymerization in a tubular reactor were determined. The idea of the dependence of the hydrodynamic field on the varying rheokinetics during a chemical reaction is quite fruitful and has

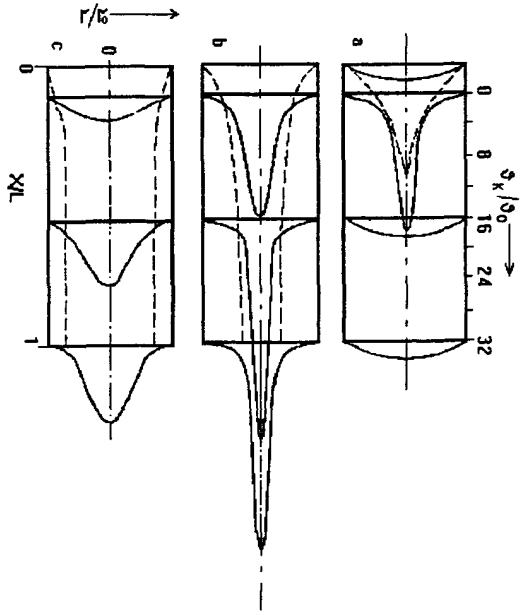

Figure 4.25. Profiles of axial velocities in the flow of a rheokinetic liquid through a tubular reactor. Flow rate increases from (a) to (c). The dashed lines denote the boundary between the high-viscosity product (high degree of conversion) and the low-viscosity reactant (breaking through stream).

been exploited by many authors. A complete formulation of the problem and the results of numerical calculations can be found in several publications.[195,201-204] The main assumptions made were the following: the flow remains laminar; the condition for adhesion to the wall is fulfilled; there is a large jump in viscosity (by at least two orders of magnitude) due to polymerization. The most important result of all these investigations is that a strong transformation of the velocity profile occurs in the reactor, and concave flow velocity profiles appear, which are completely anomalous from the point of view of traditional hydrodynamics. The general cause of this phenomenon is the action of a positive feedback mechanism.

This phenomenon can be understood on the basis of the following qualitative arguments. A small flow velocity near the walls leads to longer residence times for the liquid elements in a reactor that are closer to the walls. This results in higher degrees of conversion and progressive increases in viscosity. Thus, the flow in this zone continues to slow down. In the axial zone, the same positive feedback has the opposite effect. At first, the liquid on the axis moves faster and has a smaller residence time, so both the degree of conversion and the viscosity are lower in comparison with the fluid layers near the walls. In the end, two sharply demarcated zones of flow are superimposed on the usual flow velocities profiles (Fig. 4.25): a zone of slowly moving, highly viscous high-molecular-weight product near the walls of the reactor and an axial zone consisting of a fast

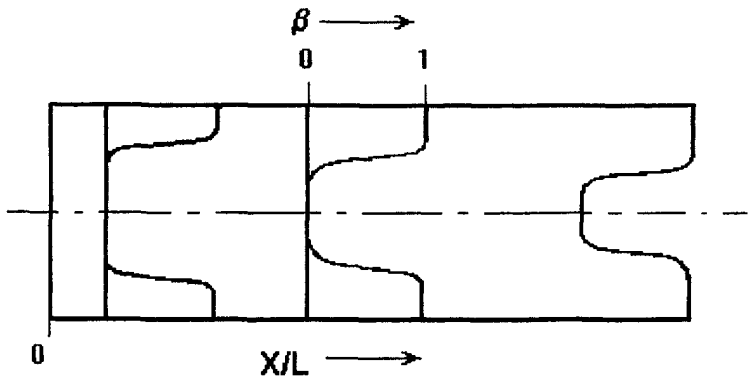

Figure 4.26. Profiles of monomer conversion along a reactor.

stream of reactants with a low degree of conversion (Fig. 4.26). The relationship between these two zones and the manner of their mutual transformation along the channel depend on net the volume output, the characteristics of the viscosity dependence on conversion, and the reactor length. Clearly, thermal effects can also influence the hydrodynamic picture, but this is generally a second-order effect, because the dependence of viscosity on the degree of conversion is much stronger than its temperature dependence.

The three situations shown in Fig. 4.25 need some comment. First, if flow rates are small, the stream of reactants remains entirely within the reactor, and we have a parabolic profile at the inlet section. Going downstream we see a strong change in the velocity profile, namely, the formation of sharply protruding curves as the chemical reaction proceeds. As this is a very slow flow, and there is enough time to complete the reaction over the full cross-section of the reactor, the velocity profile becomes parabolic again when we approach the outlet section as shown in the upper part of Fig. 4.25. However the viscosity of the final product near the exit is much higher than that of the initial reactants at the beginning of the reactor.

Second, if the flow rate is very high, we have breakthrough of the initial reactants that had insufficient time to react to reach any significant degree of conversion. Then we have a thin almost motionless near-wall layer of material with a high degree of conversion and a central fast stream of low viscosity material, which is close in chemical nature to the initial reactants, because the reaction time was too short. This situation is shown in the lower part of Fig. 4.25.

Finally, we have a third intermediate case where the velocity profile changes along the whole length of the reactor and we have a highly protruding profile at the outlet section of the tube as shown in the middle part of Fig. 4.25. The increase in viscosity due the polymerization reaction, the changes in the velocity profile, and the formation of protruding curves result in a large difference between the maximum and average velocities. For a Poiseuille parabolic profile, this ratio is equal

to 2 but in rheokinetic liquid flow, the ratio of the axial viscosity to the flow-averaged velocity can exceed 10 or 20. The key question is, what is the reactor length and residence time required to achieve full conversion of the initial reactants to a polymer? Let this time be T and the flow-averaged velocity be V. Then for a zero-order approximation, we may assume that the flow in the reactor is plug-type (velocity is constant over the cross-section); then the reactor length L_0 is calculated by a self-evident formula:

$$L_0 = VT$$

For a first approximation, when we assume a Poiseuille parabolic profile, the necessary length L_p is two times larger:

$$L_p = 2L_0$$

because the axial velocity (for the portion of material with minimum dwell time) is twice as high as the average velocity. Finally, for a real rheokinetic model with highly protruding velocity profiles, the necessary reactor length for full chemical conversion L_{RK} is much higher than L_0 and we can write

$$L_{RK} = NL_0$$

where the constant $N >> 1$.

These arguments explain why it is unacceptable to use a tubular reactor for synthesis of polystyrene: the required tubes would be too long, as is clear from the last formula were $N >> 1$. This result reflects the main disadvantage of tubular polymerization reactors if no additional devices are used to mix the reactants in different sections. Moreover it shows that such devices, averaging portions of a material with different degrees of conversion are necessary for successful operation of tubular reactors. Unfortunately, changes in operation (changes in the wall temperature, organization of recycling, separate reactant feeds, etc.) will not help to get rid of the phenomena described above, i.e., non-uniform conversion, protruding velocity profiles, and reactant break-through.

Quantitative analysis has shown that when there are major increases in viscosity from the initial reactants to the final products, the main characteristics of the flow pattern are determined by the ratio of these viscosities,[205] and this effect dominates when there are large changes in viscosity at relatively low degrees of conversion.

There are many more theoretical and modelling calculations involving the flow of rheokinetic liquids, than there are experimental data which could be correlated with theoretical predictions. No measured velocity profiles have been published for the flow of reactive liquids, although some overall properties were measured in a tubular reactor used for lactam polymerization.[206,207] In this case, the viscosity of the reactants increased by a factor of 400 due to the formation of high-molecular weight products. This led to a sufficiently strong distortion of the velocity profile that the quantities calculated for a real rheokinetic liquid and for the zero-approximation case of plug flow or the first-approximation of a parabolic profile were distinctly different. The experimental data and

calculated values of average conversion β_{av} and minimal residence time t_{min} were compared. The value of β_{av} was calculated as

$$\beta_{av} = \frac{1}{Q}\int_0^R \beta(r)v(r)2\pi r dr$$

where v(r) is the radial distribution of axial velocity, r is the current radius (radial coordinate), R is the radius of the tube reactor.

It was found that the maximum deviation between the experimental and calculated values of β_{av} for different experimental conditions (various flow rates, initial temperatures and concentrations) did not exceed 1%.

The value of t_{min} corresponds to the maximum velocity at the tube axis (at r = 0). Experimental values of t_{min} were found by radioactive tracers; the deviation between the measured and calculated values of t_{min} was less than 10%.

It is worth noting that when the Poiseuille flow model was used, the divergence in the average conversion amounted to 50%, whereas the divergence in the minimum residence time exceeded 100%. This shows that the use of the plug and parabolic flow models is incorrect in principle. The inadequacy of both simplified models was confirmed by direct comparison of their predictions of changes in the concentration of a radioactive tracer with time. Meanwhile, the rheokinetic model gave reasonably accurate predictions[205] in all cases.

4.5.3 "HYDRODYNAMIC" MOLECULAR WEIGHT DISTRIBUTION

The technological and practical properties of a polymeric material are determined by its average molecular weight and molecular weight distribution (MWD). If a polymer is synthesized in an ideally stirred reactor,so that it is perfectly homogeneous, the MWD of the end product is a function of the polymerization reaction mechanism and can be easily calculated if we know the content of a reactive mix, the kinetics of the reaction, and its duration. This is not true for a tubular reactor because the end product is a result of mixing species with different polymerization histories. Layers moving at different distances from the tube axis have been in the reactor for different amounts of time due to the existence of a radial distribution of velocities. Therefore, the MWD of the end product is a function of the mechanism and kinetics of the polymerization reaction (as in the case of a stirred reactor) and also of the specific hydrodynamic conditions during material flow through the reactor. The last factor is important only if we have incomplete conversion over part of the cross-section. If the tubular reactor is long enough for complete conversion over the whole cross-section, the resulting MWD will be determined by kinetic factors only. However, the length of the reactor is more important in most practical situations; therefore calculation of the "hydrodynamic" MWD, or MWD-H (i.e., an MWD depending on the hydrodynamics of the flow of the reactive liquid), is of general importance for reactive processing.

Let us analyze isothermal polymerization in a tubular reactor of finite length.[208] The formulation of the hydrodynamic problem is based on some obvious assumptions:

$$\frac{\partial v_z}{\partial r_0} >> \frac{\partial V_z}{\partial z}; \quad v_z >> v_r$$

Then we can use the following system of equations (reduced to dimensionless variables) to describe the flow in a tubular reactor:

$$v = \int_r^1 \frac{rdr}{\eta(\beta)} \Big/ \int_0^1 \frac{r^3 dr}{\eta(\beta)} \qquad [4.14]$$

$$\frac{\partial \beta}{\partial \tau} + v\frac{\partial \beta}{\partial x} = Daf_1(\beta) \qquad [4.15]$$

$$\Delta p = \int_0^1 \left[\int_0^1 \frac{r^3 dr}{\eta(\beta)} \right]^{-1} dx \qquad [4.16]$$

where $x = z/L$ and $r = r_0/R$ are the dimensionless axial and radial coordinates, respectively; $v = v_z/v_0$ is the axial component of the dimensionless velocity; $\tau = tv_0/L$ is dimensionless time; Da is the Damköhler number, which is the dimensionless ratio of the characteristic flow time to the characteristic reaction time; $v_0 = Q/\pi R^2$ is average output velocity; $p = P\pi R^4/[2QL\eta(\beta)]$ is the dimensionless pressure; $f_1 = f_\beta(\beta)/k_{\beta T}$ is the dimensionless kinetic function; R is the radius of the tubular reactor; L is its length; Q is the volume output (flow rate), which is assumed to be constant in time; β is the degree of conversion calculated from the change in monomer concentration in the reactive mix; $k_{\beta T}$ is the initial reaction rate at constant temperature; $\eta(\beta)$ is the viscosity depending on the degree of conversion. The boundary conditions are the usual ones: at the initial degree of conversion β_0 the viscosity is $\eta(\beta_0)$; at the initial time $\tau = 0$:

$$\beta = \beta_0; \quad v(r_0) = 2(1 - r_0^2)$$

at the wall $(r_0) = 1$:

$$v = 0$$

at $x = 1$:

$$\frac{\partial \beta}{\partial x} = 0; \quad \frac{\partial v}{\partial x} = 0$$

at the axis of the reactor ($r_0 = 0$):

$$\frac{\partial v}{\partial r_0} = 0; \quad \frac{\partial \beta}{\partial r_0} = 0$$

Solving the system of Eqs (4.15) - (4.16) allows us to find the velocity and degree of conversion distributions for the stationary state.

Now we shall discuss the method used to calculate the "cup"-averaged MWD-H, in which all portions of a polymerized liquid are mixed and averaged in a "cup" (vessel) positioned after the reactor. In this analysis, recourse was made to the so-called "suspension" model of a tubular reactor. According to this model, the reaction mass is regarded as an assemblage of immiscible microvolume batch reactors. Each of these microreactors moves along its own flow line. The most important point is that the duration of the reaction is different in each microreactor, as the residence time of each microvolume depends on its position at any given time, i.e., on its distance from the reactor axis.

The radial distributions of velocity and degree of conversion in each section of the reactor, including the outlet section, are time-independent, as we are considering a steady state working apparatus. Therefore we can find the volume dW, which flows out of the reactor through a layer of the width dr (the subscript showing that r is a dimensionless value is omitted) at a distance r from the axis:

$$dW = 2\pi r v(r) dr$$

The influence of the rheokinetic factor v(r) is quite evident in this relationship.

The degree of conversion inside this volume is constant, but the MWD function $q_w(n, r)$, where n is the degree of polymerization, depends on r. This is a reflection of different reaction time in the various layers of the polymer. The residence time distribution function f(r) for the reactive mass in a reactor is determined from rheokinetic considerations, while the MWD for each microvolume $q_w(n,t)$ is found for various times t from purely kinetic arguments. The values t and r in the expressions for q_w are related to each other via the radial distribution of axial velocity.

MWD of a polymer at any reactor cross-section is given by:

$$p_w = \int_{t_{min}}^{\infty} f(t) q_w(n,t) dt$$

where t_{min} is the minimum residence time of the reactive mass in the cross-section under consideration (at the axis of the reactor); f(t) is the distribution of residence times. In order to calculate f(t), it is necessary to solve the rheokinetic problem, i.e., to derive the velocity distribution and change along the reactor. Then we can find the cup-average MWD, i.e., MWD-H, and $\rho_w(n)$. The latter is defined as

$$\rho_w(n) = \int_0^1 rv(r)q_w(n,r)dr \qquad [4.17]$$

This equation clearly demonstrates the difference between instantaneous MWD $q_w(n)$ and MWD-H $\rho_w(n)$: we see that the definition of $\rho_w(n)$ includes hydrodynamics of flow of a reactive liquid through a reactor.

It is worth noting that averaging in Eq. (4.18) is possible for the MWD only. Therefore, if the molecular number distribution $q_n(n)$ is known, it is necessary to derive the MWD by the usual formula:

$$q_w(n) = \frac{nq_n}{M_n} \qquad [4.18]$$

where M_n is the number-averaged molecular weight. Eq. (4.18) has meaning only if the reactor is of limited length and polymerization is not completed over at least some part of the cross-section; i.e., t_{min} at the axis of the reactor is not sufficient for complete polymerization. In the opposite case, the MWD is the same for any value of r and MWD-H is equal to the instantaneous MWD.

As an example of the application of the general relationships and definitions let us analyze a specific polymerization. We shall discuss anionic activated polymerization of ω-dodecalactam, which has been thoroughly investigated.[209] It is important that polymerization of this monomer can be treated as approximately isothermal, because the heat of polymer formation from ω-dodecalactam is very low and, so the increase in temperature caused by this source can be neglected.[210]

Assuming that we are dealing with so-called "living" polymerization (in the absence of chain termination in the course of polymerization), the kinetic mechanism of ω-dodecalactam polymerization with instantaneous initiation can be written as

$$P_{(n)} + M \rightarrow P_{(n+1)}$$

The initial conditions are as follows:

at t = 0 (initial time)

$$[P_{(1)}] = [P]_0; \quad [P_{(n)}] = 0 \quad \text{for } n > 1; \quad [M] = [M]_0$$

where $[P]_0$ is the concentration of active centers, at which polymerization proceeds; $[P_{(n)}]$ is the concentration of macromolecules having the degree of polymerization n; [M] is the monomer concentration. The MWD for "living" polymerization is well known:[211] it is the Poisson distribution described by the function:

$$q_n(n) = \frac{\tau^{n-1}}{(n-1)!}e^{-\tau} \qquad [4.19]$$

Here τ is the "generalized" time, which is

$$\tau = \delta\beta(t)$$

where β is the current degree of conversion, depending on the current time t; δ is the limiting (maximum possible) degree of conversion. For the case under discussion the generalized time can be calculated as

$$\tau = \int_0^1 k[M(t)]dt = \frac{[M]_0}{[P]_0}[1 - e^{k[P]_0 t}] = \delta\beta(t) \qquad [4.20]$$

and

$$\delta = \frac{[M]_0}{[P]_0}$$

For the Poisson distribution

$$M_n = 1 + \tau = 1 + \delta\beta$$

Now we can write the equation for MWD-H according to its definition, Eq. (4.18):

$$\rho_w(n) = \frac{n}{(n-1)!}\int_0^1 rv(r)\frac{[\delta\beta(r)]^{n-1}}{[1+\delta\beta(r)](n-1)!}e^{-\delta\beta(r)}dr \qquad [4.21]$$

By using some known expressions for the moments of MWD [211] and changing the order of integration by t and n, we can obtain formulas for the moment Λ (upper case) of MWD-H, in terms of the moment λ (lower case) of "chemical" MWD $q_w(n)$. The resulting equation is as follows:

$$\Lambda_i = \int_0^1 rv(r)\lambda_i(r)dr \qquad [4.22]$$

As expected the moments of MWD-H depends on the velocity distribution v(r). The first three moments of MWD-H calculated for the Poisson MWD are the most representative features of MWD-H. They are calculated as:

$$\lambda_0 = \frac{1}{1+\tau} \qquad [4.23a]$$

$$\lambda_1 = 1 \qquad [4.23b]$$

$$\lambda_2 = \frac{1+\tau^2+3\tau}{1+\tau} \qquad [4.23c]$$

The averaged molecular weights are the ratios of the moments:

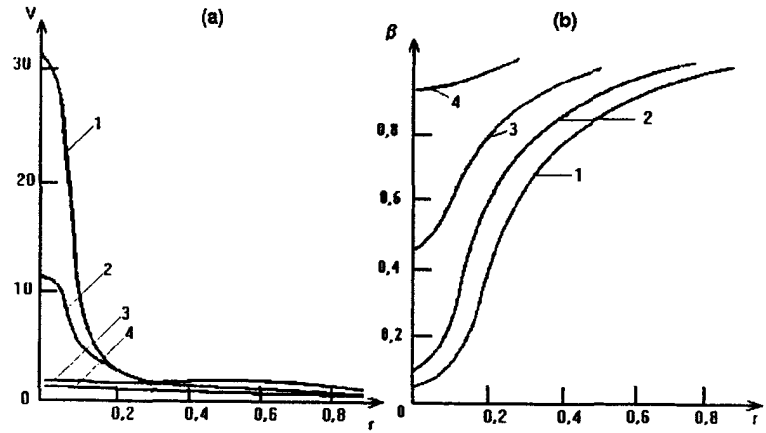

Figure 4.27. Velocity profiles (a) and distributions of the degree of conversion (b) along the radius of a tubular reactor at [A] = 0.7 mol%. The Da/Da* values are: 0.2 (*1*); 0.3 (*2*); 0.5 (*3*) and 1 (*4*).

$$M_n = \frac{\Lambda_1}{\Lambda_0}; \quad M_w = \frac{\Lambda_2}{\Lambda_1}; \quad \frac{M_w}{M_n} = \frac{\Lambda_0\Lambda_2}{\Lambda_1^2}$$

Now we can find all the parameters of MWD-H by solving the hydrodynamic, Eqs. (4.14) - (4.16), because the solution is a function of v(r) and β(r). The theoretical relationships discussed above can be illustrated by the results of calculations of MWD-H for anionic polymerization of ω-dodecalactam.[210] The viscosity η(β) during isothermal polymerization, when the degree of conversion has reached β, is described by the equation:

$$\eta(\beta) = k_{\eta T}\beta^a\left(\frac{\beta}{[A]}\right)^b + \eta_0 \qquad [4.24]$$

where $k_{\eta T}$, a and b are empirical constants; η_0 is the viscosity of the monomer; [A] is the initial concentration of the activator. For the case under discussion, at T = 180°C, the parameters in Eq. (4.24) are:

$$a \approx 1; \quad b = 2.3; \quad k_{\eta T} = 0.025; \quad \eta_0 = 0.01 \text{ Pa s}$$

and the kinetic function for the initial part of the polymerization, at least up to β ≈ 0.7, is:

$$f_1(\beta) = 1 - \beta$$

Calculations were carried out for different values of the Damköhler Number (i.e., for various reactor lengths) and various concentrations of the activator [A], which determines the number of active centers and therefore the final degree of polymerization. The ratio Da/Da* was used, as a

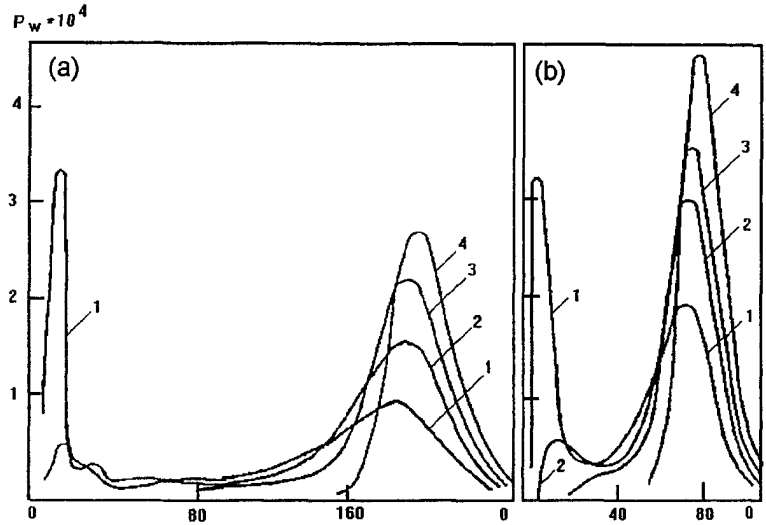

Figure 4.28. MWD-H of a polymer at different [A] = 0.5 mol% (a) and 1.2 mol%(b). The Da/Da* values are: 0.2 (*1*); 0.3 (*2*); 0.5 (*3*) and 1 (*4*).

measure of the length of a reactor, where Da* is the value of Da which gives a degree of conversion $\beta=0.9$ (close to complete conversion) at the axis of the reactor.

Fig. 4.27 represents the velocity profiles v(r) and degrees of conversion $\beta(r)$ at the exit of a reactor for different values of Da/Da* and constant [A] = 0.7 mol%. At Da = 0.5 (a rather low degree of conversion at the axis of the reactor), a low-viscosity stream flows out (breaks through) into the central zone (Fig. 4.27 b, curves 1 and 2). This means that the end-product leaving the *reactor is a mixture consisting of two species (fractions) with very different molecular weights*, leading to the appearance of a pronounced bimodal MWD-H, which is not due to the chemical process but is a direct consequence of the hydrodynamic situation in the reactor.

The results of calculations of MWD-H from Eq. (4.17) are shown in Fig. 4.28, where the influence of both factors, Da and [A], is shown. It can be seen that for increasing Da (i.e., increasing reactor length) the height of the low-molecular-weight peak decreases, the high-molecular-weight peak height increases, and MWD-H approaches a unimodal MWD, which in the limit, becomes a very sharp Poisson distribution. When [A] decreases, a polymer with higher molecular weight is obtained; the value of the average molecular weight is a function of the parameter δ. At low degrees of conversion, the distance between the low- and high-molecular-weight peaks in MWD-H is large. Increasing the concentration of active centers results in a decrease in the average molecular weight and a decrease in this distance. When the value of Da is increased beyond 0.5, MWD-H becomes essentially unimodal. There is no point in calculating "average" values of MWD M_n, M_w or their

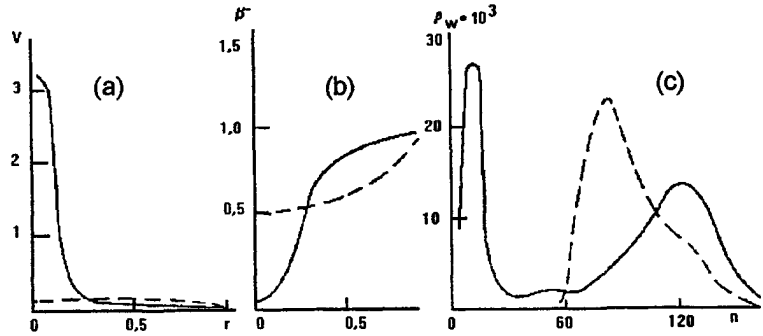

Figure 4.29. Comparison of velocity profiles (a), degrees of conversion (b) and MWD-H (c) for calculations carried out for a rheokinetic model with changes in of the velocity profile along the reactor (solid lines) and for an unchanging Poiseuille velocity profile (dashed lines). Values of the parameters in calculations: $Da/Da^* = 0.2$; [A] = 0.7 mol%.

ratio (as a measure of the width of the MWD) while the MWD-H of the final product is still bimodal. Calculations indicate that in the transition to a unimodal MWD-H with increasing β, the ratio M_w/M_n quickly approaches 1; i.e., the distribution becomes Poisson-like.

It is also instructive to compare the results of calculations of MWD-H for a real rheokinetic model with a hypothetical situation in which there is a the Poiseuille profile along the full length of the reactor (Fig. 4.29). In all instances, the MWD-H corresponding to the Poisseuille velocity profile remains nearly unimodal (from the very beginning of the reactor when $\beta << 1$ at the reactor axis). It follows from these results that the assumption of a Poiseuille profile that remains unchanged along the length of the reactor leads to completely unrealistic predictions for the MWD-H pattern of the end product. The same is true for any other constant velocity distribution, for example, those based on power-type rheological equations for the flow curve of a polymer. Only those rheokinetic models, that take into account the transformations in the velocity profile along the reactor due to a chemical reaction can present a correct picture of the real properties of an end product polymerized in a tubular flow reactor.

4.6 POLYMER COATING BY SPRAYING

Polymer coatings are one of the main protection methods against corrosion and are also widely used to decorate articles, equipment, and structures for industrial and domestic use. These coatings are films made of high-molecular-weight compounds formed on a solid surface.

The coating process consists of the following stages:

- preliminary operation of preparing a polymeric material or reactant composition for application;

- cleaning and preparation of the substrate surface before spraying the polymer material
- coating application and formation;
- physical and chemical treatment and mechanical machining of the applied coating and quality control.

The preparation of polymer materials for coating requires the choice of a suitable composition, depending on the expected use, followed by composition preparation and processing. The choice of polymer depends on the physical, chemical, and mechanical properties of the materials themselves and on the intended purpose of the coating being applied.

Individual polymers as materials for film formation have the following disadvantages: high melt viscosity, a narrow interval between the flow and decomposition temperatures, insufficient adhesion to coated surfaces (for example to steel), low mechanical strength, etc. Therefore, compositions consisting of polymer mixtures with different additives are widespread at present. Solvents, plasticizers, pigments, fillers, curing agents, surfactants, and other functional materials are commonly employed as additives in coating compositions.[212-214]

Depending on article geometry and size, its engineering and technological complexity, conditions of use and the type of polymer material, different methods for applying coatings are used. In general, they differ from each other, in the state of aggregation of the material being applied. The main methods of coating application are the following: manual (hand-brushing, roller-coat, tampon methods), dipping, sponging, spraying (pneumatic, hydrodynamic, electrostatic), electrical sedimentation, injection molding, fluidized bed coating, cladding, and lining (gluing of sealant and film materials).[212-216]

Spraying of polymer solutions and melts is the most widespread method in industry.[217] The high productivity and efficiency of the process and the possibility of continuous regulation of quality and coating thickness to produce coatings with the specified quality are the main advantages of this method. The essence of the spraying method is that the liquid is initially ejected as thin jets, which break up into droplets of different sizes. Jet fragmentation occurs as a result of a sharp pressure drop in the stream of compressed air inside the spray nozzle for pneumatic spraying or by the action of electric forces in electrostatic spraying.

To achieve the main process requirements (ability to be applied by different methods: by hand, spray, electropaint), and to provide the necessary decorative, physical, and mechanical properties, organic solvents are used in concentrations up to of about 50% to modify the viscosity and other rheological characteristics of the some polymer compositions. During the application and formation of the coating, the solvents evaporate into the atmosphere as pollutants. This serious disadvantage of formulations based on the use of solvents as "intermediate" carriers has provided the incentive to develop polymer compositions and application technologies which yield the required rheological characteristics either without solvents, or at least with low concentrations of them.

Materials with a higher content of non-volatile components are the most attractive for use in industry. This group of polymer compositions contains binders of lower molecular weight, but higher reactivity. These provide coating materials with the necessary high fluidity and high concentration of film-forming components. As a result, the traditional methods of applying coatings

(roller, brush, spray) can be used under normal curing conditions without the addition of large amounts of solvents to reduce viscosity.

The formation of network structures in polymers is of great importance in forming coatings from oligomers by reactive processing. This type of coating is usually formed by polymerization and polycondensation of reactive oligomeric products such as oils, unsaturated polyesters, oligo(ester acrylates), and alkyd and epoxy resins.[216,218] Polyurethanes, polyesters, and silicon organic oligomers are also used as coatings in reactive processing.

A typical example of a new formulation used for producing coatings by reactive processing for coating is an alkyd-based air-drying composition containing up to 80% nonvolatile components. This material has superior decorative and protective properties compared to traditional polymer compositions. Great progress has also been made in the development of thermal curing materials based on epoxy, polyester, acryl and acryl urethane binders.[218-221] In order to improve the processing properties of these compositions, liquid rubbers are extensively used as a polymer base and simultaneously act as low-viscosity solvents.[219] Thus, the admixture of epoxy oligomers with liquid rubbers allows a number of important technical problems to be solved: they improve both the mechanical and the protective and adhesion properties of the final coatings.

When preparing coatings from reactive compositions, a thin layer of material is first applied to the item. The coating material adheres to the item by gravitational, magnetic, centrifugal or adhesion forces. The prepared article with its reactive layer is then placed in a chamber where the final polymeric coating is formed.

This method is used for producing cable insulation from film-forming material without the use of solvents.[220,221] The key element of this technology is passage of the wire or cable through a molten oligomer bath with a viscosity close to that of the lacquers used in wire enameling. The chosen coating material should not be reactive at the bath temperature used in the coating process. The coated wire then passes to high-temperature oven, where, in a short period of time, the resin is transformed into a hard elastic film by a polymerization reaction.

Reactive processing has also been proposed for use in the continuous production of insulated cables.[222] In this case, the reagents are first mixed and then injected into a tubular reactor. Previously heated cable moves along the axis of the reactor and the insulating coating is formed. The principal advantage of this method is that the chemical reaction occurs, during the process rather than before coating. As a result the process cycle is reduced and economies are achieved through lower energy consumption and increased productivity.

The pneumatic spraying method is one of the best for protective coating of large-sized items. Some versions of this method are described in Ref.[223] for spraying of high-viscosity materials. A method employing an external gas flow to atomize liquid jets or films is one of the most effective.[224,225] In traditional gas or liquid spraying technologies, liquid jets are carried by coaxial or transverse gas flows, whose mass flow rate often exceeds those of the liquid. Another scheme was proposed,[226] in which it is suggested that the gas should be added to the liquid before injection of the stream into the exit nozzle. In this case, a gas-liquid mixture flows out the sprayer and, as a result, the size of the liquid droplets being sprayed. However in this technique, the sprayer design

becomes more complicated, its size increases, and stratification of the two-phase mixture a long exit channels may appears. This can lead to instability of the exit flow and inhomogeneity of the drop sizes during spraying. Nevertheless, the advantages of the method proposed[226] have led to a search for ways to improve it and adapt it to current requirements.

It was also suggested[227] that the spray streams can be improved by blowing a gas into the liquid stream just before it exits from the sprayer channel into the open space. Investigations of liquid spraying in an experimental setup allowed the authors[227] to determine the main features of the process. Water at room temperature was used as the spray liquid, and argon and helium were tried as the blowing gases.

The equipment described in Refs [223-227] is mainly used for spraying materials with stable rheological properties. For processing rheokinetic liquids, special equipment has to be designed. This equipment must work with the low-viscosity material present at the initial stages of the process. It is also necessary to allow for possible inadequate life times of the reactive mixtures, the need for through mixing of the components, and methods for equipment washing. These are the main problems in processing of reactive materials. The studies in this field are insufficient because of numerous technological uncertainties in coating processes and lack of understanding of the fundamental aspects of the process.

The process of creating a protective coating from a reactive liquid by spraying consists of preparation of the required composition of low viscosity reagents and solid fillers, transporting the mixture through a spraying device, to the item surface. Temperature conditions are monitored inside the channel of the spraying device and on the product surface. In order to make a high-quality coating and to improve the stability of its properties, it is necessary to solve the following problems:

- provision of a high-quality finely dispersed spray of the coating material during the whole cycle;
- production of a coating with minimum porosity and admissible surface waviness;
- solidification of the coating on the item while maintaining its geometric size and shape to exclude leaks.

Successful solution of these technical problems depends on the initial viscosity of the material in the sprayer, the surface tension of the material, changes in the rheokinetic properties during the process, sprayer design, and jet configuration.

The reactive mixture is heated to the necessary temperature in the spraying device (above the temperature at which the reaction starts), dispersed, and then applied to a surface in a uniform layer. The efficiency of the device depends on preserving the fluidity of the reactive mixture as it moves along the channel, preservation of the necessary degree of conversion of the reactive mixture at the exit from the nozzle for an adequate time, and sufficient dispersion of the jet leaving the nozzle of the sprayer.

Creating or maintaining uniform distributions of temperature, flow rate, and conversion degree appear to be most important during the flow of chemically reactive liquids, especially since the reaction leads to changes in material viscosity of several orders of magnitude. Even in the

simplest streams (flow in a pipe or through a rectangular cross-section) changes in flow kinematics when the liquid sticks to the channel walls leads to the appearance of inhomogeneities across the channel. Loss of material fluidity at high degrees of conversion leads to gradual overgrowth of the channel by solidified material, a phenomenon that is intensified by heat supply.

Plug-like flow and uniform volume heating (or cooling) leading to a flat chemical reaction front (uniform conversion at each section of the channel) may be regarded as an ideal flow systems. Maintenance of complete (or close to it) sliding conditions at the walls is one of the ways to achieve this goal.

4.6.1 DEVICES FOR SPRAYING LIQUIDS

Various types of sprayers and pneumatic nozzles which allow us to produce finely dispersed gas-liquid jets and aerosols with drops 500-10 μm in diameter are used to create coatings. Two ways of producing finely dispersed jets are known:

- spraying under the influence of centrifugal forces;
- spraying due to the action of streams of a compressed gas.

In the first case, the liquid being sprayed is poured onto a plane rotating disk from the center to the circumference.[228] Breakup of the liquid film on the disk surface leads to the production of polydisperse drops, even at low rates of liquid supply. It is possible to obtain a narrower, almost monodisperse distribution of drop sizes with total weight of satellite drops of not more than 3-5% of the main fraction by a cut-off baffle in the disk center.[229] The surface of the disk is radially grooved, and on rotation produces a number of streams equal to the number of grooves. These streams disintegrate into drops of almost monodisperse composition at the disk edge. The disk surface and its parts are made of materials that are not wetted by the liquid being sprayed, so that there are equal flow conditions for all streams.[228]

In the second case, disintegration of a liquid jet into drops is achieve by high-velocity streams of compressed air flowing out of holes positioned at the stream perimeter.[230, 231] Porous permeable bushings with a ring cavity around the bushing for uniform mixing of a liquid and a gas are used to inject the liquid into the air stream.[232,233] This design provides a uniformly mixed two-phase stream with a droplet size of about 10-20 μm.

Aerosols and mists are formed when liquids are sprayed using compressed gas; However this increases the proportion of waste liquid. In order to eliminate waste, a porous diaphragm resembling a cut-off cone is used. Its smaller base borders the face between the nozzle for the liquid and holes for the gas; the larger base is connected to the spraying head and forms chambers connected via holes to create a peripheral enclosing air stream.[234]

One suggested technique for spraying chemically reactive liquids is to force air through porous ring sections of the tube into the flowing liquid to act as a lubricant. Use of this technique in sprayer devices break up the liquid stream even before it exits from the nozzle, and hence reduces dispersion of the drops in the jet. When a chemically reactive liquid flows through a channel, functional heating occurs at the walls and spreads to the center of the stream. Thus to achieve a uniform conversion degree through the cross-section of the channel, it is desirable to create

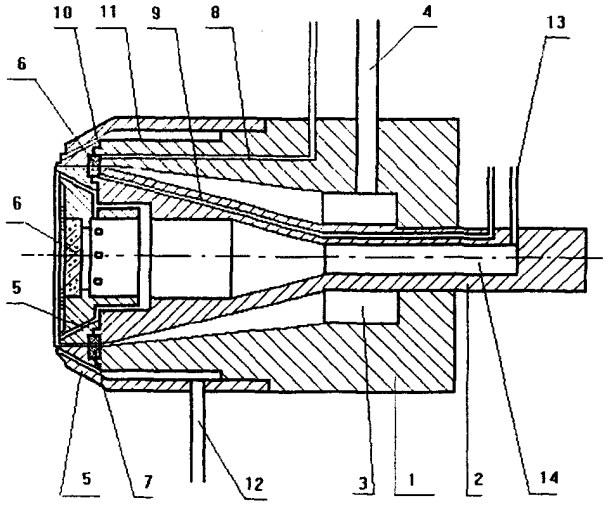

Figure 4.30. Device for spraying high-viscosity liquids (for an explanation of the positions, see in the text).

conditions such that the material slides easily along the walls of the spraying device by means of a gas lubricant supply. This allows us to decrease the pressure at the exit, which is also important.

A typical device for spraying chemically reactive materials, designed with the proceeding remarks in mind, is shown in Fig. 4.30. It consists of: a body 1, a core 2, between which there is a channel 3 for supplying the spray liquid by a pipe line 4. Channel 3 tapers towards the exit and forms an exit ring nozzle 5 on which internal and external walls of which porous rings 6 and 7 are placed. The rings are connected by channels and tubes 8 and 9 to a pressurized system. A housing 10, forming channel 11, which provides ring clearance, is placed on body 1 on the external boundary of this gap. Gas for blowing the liquid jet is supplied to channel 11 by means of a pipeline 12. To blow the liquid on the inner surface, gas from pipeline 13 moves to the internal cavity 14 of the core 2. Then, one part of the gas stream goes through the ring clearance through passages to the blower and the other part goes to a porous spacer 16. The surfaces of the nozzle 5 and the channel 3 are covered with a fluoroplastic, heat-resistant anti-adhesive material. Core 2 is connected to a power drive providing circular rotation.

The spraying device works in the following way. The prepared liquid mixture of reactive components flows to channel 3 through pipeline 4, and is distributed in a circular direction by the rotation of core 2. This movement simultaneously reduces the apparent viscosity of the liquid. Then the liquid goes to the ring nozzle 5. Porous rings 6 and 7 are placed on the external and internal surfaces of nozzle 5 at a distance of (1 - 20)h from the exit (where h is the distance between the

external and internal surfaces of nozzle 5). The blower gas at the necessary pressure enters to channel 5 through the porous rings by pipelines and channels 8 and 9. A lubricating film, formed on the walls by the gas permeating through the porous rings 6 and 7, sharply decreases friction between the wall and the moving liquid stream.

A sharp decrease in wall friction in the flow of visco-elastic liquids (including chemically reactive liquids) leads to the formation of low pressure zones. The gas flows into these zones, which leads to disruption of the liquid stream in nozzle 5. Additional gas blown into the disrupted liquid stream through the ring gaps by pipelines 11 and 15 causes separation of the liquid into smaller droplets, thus improving spray dispersion.

The porous rings are positioned at a distance of (1 - 20)h from any exit, because if they are positioned any closer, stream rupture inside the channel cannot be guaranteed. If they were placed at a further distance, the disrupted stream reforms into a compact stream further along the channel, which would prevent proper dispersion of the spray jet.

Coating of the channel 3 and nozzle 5 surfaces with fluoroplastic prevents the stream of hot gas from heating the liquid channel walls due to the good heat insulations properties of this covering material. This makes it possible to shift the zone where the chemical reaction starts towards the exit from the sprayer. The use of fluoroplastic makes it possible to prevent sticking of the reactive liquid to the channel walls because of its anti-adhesive properties. Using this device for spraying high-viscosity liquids ensures the following advantages:

- improved coating quality due to increased spray dispersion at the local gas supply to the nozzle;
- increased process output due to a reduction in shut downs, which are usually necessary for channel cleaning when processing reactive materials.

4.7 REACTIVE EXTRUSION OF PROFILE PARTS

Reactive processing by extrusion is primarily used for manufacturing profile parts from polycaproamide (Nylon 6), synthesized by anionic activated polymerization of ε-caprolactam. Another application of reactive extrusion is processing of thermoplastic materials modified by reactive additives, which can be introduced as co-monomers or separate components of a mixture.[235] Continuous polymerization or reactive modification in extrusion can be successfully realized if stationary processing conditions are achieved, in particular, a constant ratio between the initial reactive system (low-viscosity liquid) and the high-viscosity newly formed product need to be maintained. Perhaps the most important consideration in continuous extrusion of reactive systems is controlling the temperature polymerization regime by removing the excessive heat of polymerization, which eliminates thermal runaway and stabilizes the temperature profile throughout reactive mass.

The main problem (or disadvantage) in reactive processing by extrusion is the choice of the reaction rate. If it is too fast (due to unexpected temperature rise during processing) the extruder-reactor may become plugged. If it is too slow the process is lengthy; i.e., a long residence time is required to complete the reaction. Thus the extruder has to be very long and/or the velocity

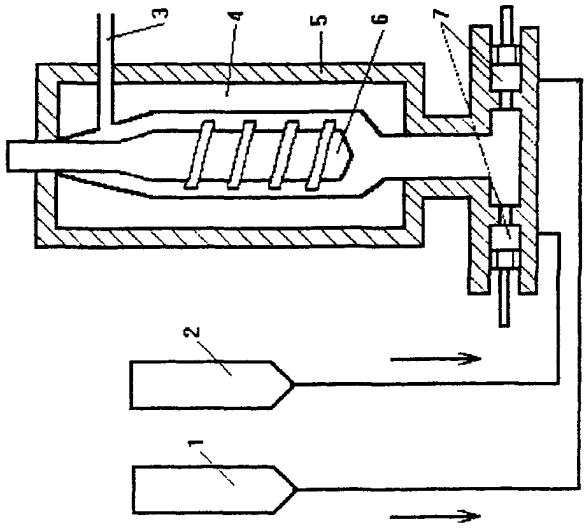

Figure 4.31. One-section single screw extruder used in reactive processing (for an explanation of the numbers see text).

of movement along it must be very low. The main method of adjusting the process rate is to vary the activity of the catalyst and/or the activator used in polymerization. The temperature sensitivity of the reaction rate must be taken into account in designing an extrusion-reactor unit.

The first attempts to create an extrusion process for reactive processing were based on the use of a one-section single screw extruder.[236] The principal parts of this unit are shown in Fig. 4.31. The head part of the unit is typical for reactive processing. It consists of two separate tanks, one containing a mixture of a monomer and a catalyst and the other containing a mixture of a monomer and an activator (*1* and *2* in Fig. 4.31). Metering pumps *7* inject both components into the inlet of the extruder, which consists of a screw *6* placed in a barrel *4*, which is fitted with heaters *5*. Mixing of the components of the reactive system takes place due to rotation of the screw. Polymerization proceeds during the movement of the reactive mass along the extruder, and the newly formed product is ejected through a profiling die *3*. In anionic activated ε-caprolactam polymerization in an extruder-reactor, the process takes approximately 25 min at 225 - 240°C. The final product (polycaproamide) contains 11 - 12% of monomer residues, which limits the applications of articles made from this material. The process in the extruder can be shortened by using an intermediate storage tank.[237] In this case, necessary the residence time for a reaction in the extruder need be no more than 10 - 12 min.

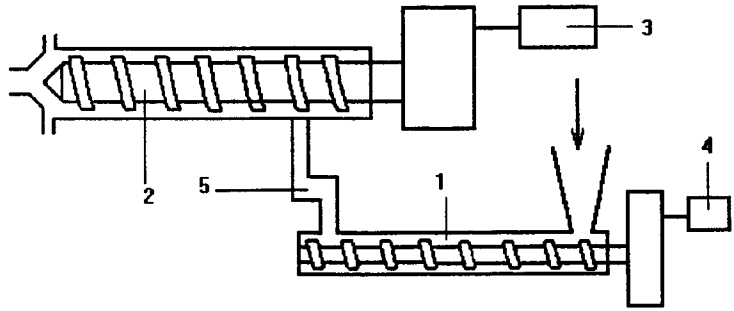

Figure 4.32. Two-section single screw extrusion unit for reactive processing.

The main difficulty in encountered in using one-section single screw extruders is separating and coordinating the different stages of the polymerization process, because the reaction rate is not constant, but is changing from start to finish of the process. This is the reason why such simple devices are not used in industry. This difficulty can be overcome by using a set of single screw machines arranged in series, which makes it possible to separate the various stages of a polymerization process. Changes in residence time can be easily controlled by regulating the screw rotation speed in the separate extruders. A typical layout of a two-section extrusion unit is shown in Fig. 4.32.[238] There are two independently operated extruders (*1* and *2* in Fig. 4.32), each with its own regulated drive (*3* and *4*). The reactive mass flows from the first to the second section through a transfer tube *3*. The first section is used for melting and homogenization of the initial reactive mixture, and the screw rotation speed in this extruder is high. Most of the polymerization process and extrusion of the product through a die occur in the second section where the screw rotation speed is low. Correlation of the operation of both sections is achieved by adjusting the rotation speed of both screws. The governing parameter is pressure which is measured in the transfer tube *5*. This transfer tube is a passive element of the production line.

Twin screw extruders have also been proposed for use in reactive processing of ε-caprolactam. Intermeshing corotating screws with a minimal gap between the threads are self-cleaning, thus eliminating the growth of newly formed polymer on the screw surfaces.[239] An example of a twin screw extruder is shown in Fig. 4.33. This machine, built by the *Werner und Pfleiderer Company*, has two intermeshing screws rotating in the same direction. The screws have interchangeable sections, which have transportation and mixing functions. This design eliminates undesirable shifts of the polymerization zones, but has the same disadvantage as one-section single screw extruders: the constant rotation speed is incompatible with the varying rate of polymerization along the length of the extruder.

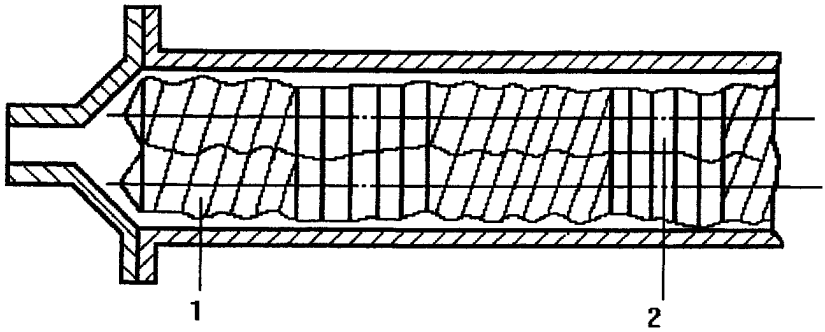

Figure 4.33. Twin-screw extruder for reactive processing. Each screw consists of meshing (1) and compressive (2) inter changeable sections.

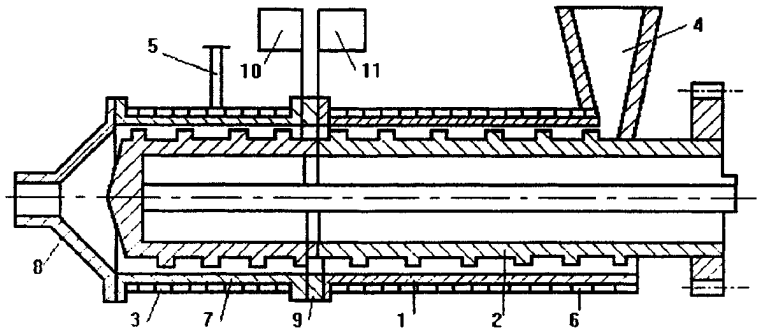

Figure 4.34. Double screw extruder with two separated screws placed in series inside a common barrel (explanation of the numbers see text).

A possible design of an extruder for reactive processing is shown in Fig. 4.34.[240] Two screws are installed on the same axis inside a common barrel *1* but they have independent drives. This design eliminates stagnation zones, where the extruder is obstructed by the polymeric product. Independent drives for both screws permits the choice of optimal rotation speeds, i.e., to synchronize the polymerization rate with the residence times of the reactive mass in both stages of the process.

The extruder shown in Fig. 4.34 can be used for anionic activated ε-caprolactam polymerization. In this case, the operation of the extruder proceeds as follows. An initial reactive mixture (prepared earlier by mixing a two-component system) is passed through a feeding (loading) arrangement *4* to the inlet section of the transporting screw *2*. During movement along this screw,

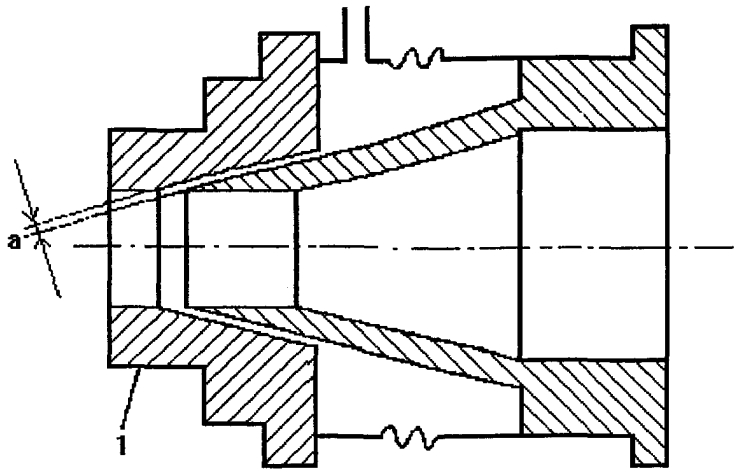

Figure 4.35. Extrusion die for reactive processing with a gap (of the width *a*) for injecting a lubricant.

polymerization takes place only to a very limited extent. Metering screw *3* creates the necessary pressure to extrude the a final product through a profiling die. The geometry of the thread, the rotation velocity, and the temperature regime inside the channel are chosen so that the end of the polymerization zone corresponds to the outlet section of the extruder and the entrance to the profiling die allows the *8*. The two parts of the extruder are separated by a stiff perforated membrane, or diaphragm *9*, with installation of two screws in the same barrel. The shape and size of the holes in the diaphragm are found experimentally and depend on the type of polymer being synthesized. This diaphragm also smoothes out pressure fluctuations, which arise at the inlet section of the metering screw as a result of the operation of the transfer screw. Speeds of rotation of both screws are adjusted by the regulating unit in response to signals fed from the pressure transducers mounted on both sides of the diaphragm.

The transducer *11*, mounted before the diaphragm measures the pressure created by the transfer screw. This pressure depends on the output of the screw and the hydrodynamic resistance of the diaphragm. The transducer *10* mounted beyond a diaphragm measures pressure, depending on output of the metering screw i.e., the pressure created by the transfer screw and pressure drop through the diaphragm. Then both values of pressure can be varied by varying the rotation speed of the screws, because their speed determines the throughput.

The operating temperature is controlled by the regulated heaters *6* and *7*. Volatile products, which can appear as a result of chemical reactions or evaporation of low-molecular-weight components (water residues and others) are removed through the outlet tube *5*.

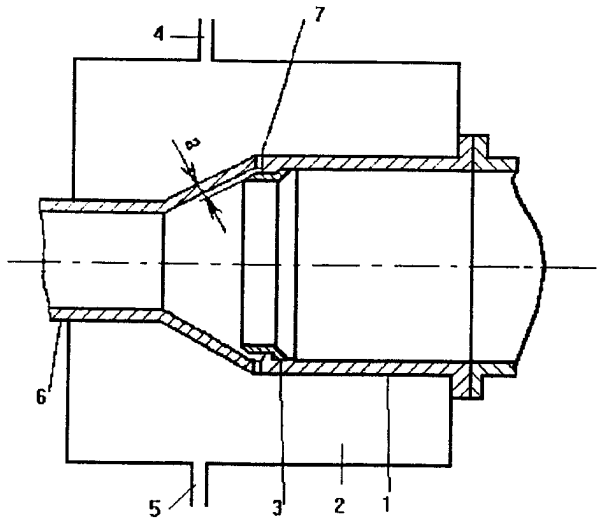

Figure 4.36. Extrusion die for reactive processing with an interchangeable sleeve (for an explanations of the numbers see text).

The viscosity of the reactive mass increases significantly at the end of the polymerization zone and results in a pressure increase. In addition, undesirable excessive polymerization and even incipient crystallization can occur near the walls of the extrusion die, because the material velocity in the near-wall zone is very low (theoretically zero at the wall). Thus it is necessary to design special dies, some of which have been proposed and used in practice.[183,241,242] The goal of all these designs is to exclude direct contact between the polymeric material and the wall. Fig. 4.35 illustrates how this can be achieved by injecting a liquid or a gas between the melt and the wall, to provide a low-viscosity lubricating layer. The thickness of the lubricating layer (a in Fig. 4.35) can be regulated by shifting the outer conical part of the die (*1* in Fig. 4.35).

Another design for introducing a lubricating layer is shown in Fig. 4.36.[243] In this design the extrusion die consists of a body *1* with a jacket *2* and a sleeve *3*. Feeding and removal of the lubricating liquid (or gas) occur through inlet *4* and outlet *5* tubes. The body of the die is connected to a crystallization furnace, where the polymerized material crystallizes. The die operates in the following manner. As the polymeric mass moves along the die, the lubricating gas or liquid is pumped from a jacket through holes *7* into the ring cavity of width a. The pressure in the cavity a is controlled by changing the gas (or liquid) feed rate through the inlet tube *4*. The necessary pressure in the lubricating layer is regulated by the rheological and adhesion properties of the reactive mass being processed. Using a die of this design allows us to decrease the pressure necessary for extrusion

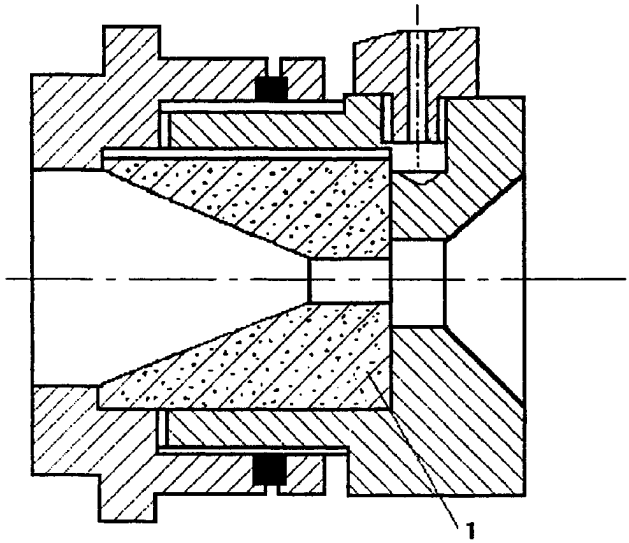

Figure 4.37. Extrusion die for reactive processing with walls (1) made of porous material.

and to facilitate plastic deformation of the reactive mass by making it more homogeneous. In general, the quality of the end product is improved and the production rate increases.

An original design of an extrusion die is shown in Fig. 4.37.[244] The walls of the die are porous, changing along the length of the die. Lubricating liquid is pumped through the porous walls and creates a thin low-viscosity layer between the wall and the moving polymeric material. The operation of the die is controlled automatically. The layout of the control system and its main elements are shown in Fig. 4.38.[245]

Reactive extruders and extrusion dies of different designs can be easily included in standard technological scheme of polymer production plants, such as those for polycaproamide synthesis, as shown in Fig. 4.39. In this case, a reactive material premixed in a tank *1* is fed into a static device *2* for prepolymerization, where part of the polymerization process takes place. Then the reactive mixture enters the extruder-reactor *3*. The necessary temperature distribution is maintained along the extruder. Transfer of the reactive mass proceeds by a system of two coaxial screws mounted in series in a common barrel. Controlling the relative rotation speed of both screws provides the necessary residence time for the reactive mass in the extruder, so that the material reaching the outlet section of the die is a finished polymer.

This lubrication principle is also used in this plant: a lubricant gas or liquid pumped through a ring sleeve leads to a decrease in the required pressure and improved quality of the end product. Clearly the lubricant gas or liquid must be inert in relation to the reactive mass and must not interact with the die material. Crystallization of the newly formed polymer takes place inside a calibrating

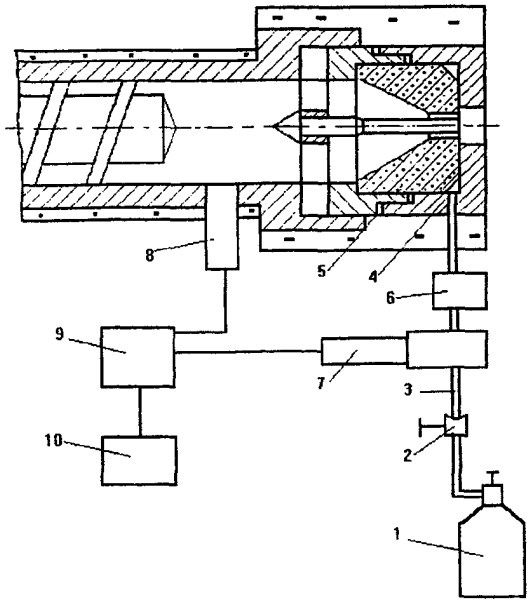

Figure 4.38. Extrusion die with automatic pumping of a lubricant. Layout of regulating system: 1 - high pressure cylinder; 2 - air pressure regulator; 3 - joining tubes; 4 - lubricating chamber; 5 - porous element; 6 - room for the liquid lubricant; 7 - transducer for lubricant pressure; 8 - transducer for polymer material pressure; 9 - electronic governing unit; 10 - recording unit.

device *5*, where the temperature continuously decreases along the path of material movement. After leaving the calibrating device, the final extrusion is cut off by a knife *6*. Some finishing operations (for example thermal treatment in a special oven) can be done on the cut extrudate, if necessary.

Plant processes using reactive extrusion look promising from the point of view of productivity, labor costs, and the possibility of making various polymer extrusions for different applications. However practical design of such equipment is difficult due to the complexity of the various physical and chemical processes involved in the overall process. Therefore, it is important to turn to mathematical models, based on separate laboratory investigations of the main process paramaters. In some cases known methods of designing screw extruders for processing thermoplastic polymer materials can be used and applied to the functional zones of two-screw extruders.[246,247] provided we account for changes in the rheological properties of the material in the different zones.[248] This

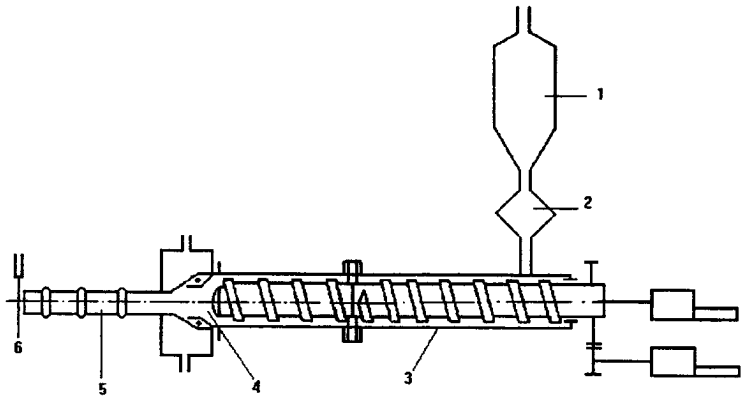

Figure 4.39. Technological scheme for producing extruded parts from polycaproamide (for an explanation of the numbers see text).

approach, although rather complicated, allows the qualitative distributions of velocity, temperature, degree of conversion in an apparatus to be assessed. Quantitative results can also be obtained, although they require much more information about the properties of the material and especially of the rheokinetics of the process at different temperatures. Nowadays, the reactive extrusion process is the subject of numerous investigations because of its engineering and economical advantages.

4.8 FRONTAL PROCESSES

4.8.1 PRINCIPLES

Front polymerization processes are of interest primarily for formation of massive articles from materials which undergo severe shrinkage during reactive processing. This method holds the promise of reducing the level of residual stresses and to form massive monolithic items. There are several versions of frontal processes used in engineering practice at present, such as zone polymerization and polymerization with continuous build-up of polymeric layers.

A typical example of frontal polymerization is the polymerization of methyl methacrylate (or an oligomer), placed inside a long aluminum tube;[249] these tubes continuously dip into a bath with a liquid heated up to temperature of 70 - 80°C. The part at the tubes above the bath are cooled so that the reactive material does not polymerize. Polymerization shrinkage is compensated by continuous injection of a monomer or oligomer into the reaction zone. The appropriate combination of injection rate, velocity of tube movement through the reaction zone, and tube diameter are chosen according to experimental studies of the process.

The possibility of feeding additional reactive material into the reaction zone is a determining factor in processing defect free articles. This is true not only for reactive processing but also for

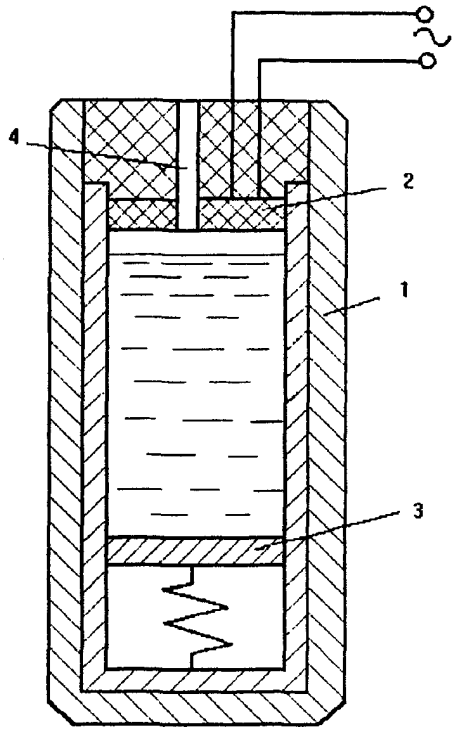

Figure 4.40. A model reactor for front polymerization in the synthesis of slabs from "anionic" polycaproamide. 1 - insulation cover; 2 - plane heater; 3 - bottom; 4 - safety-valve.

traditional injection molding of thermoplastic materials.[250] A similar frontal process, which uses a thin layer of reactive mixture, can be employed for anionically activated ε-caprolactam polymerization. In this case, the initial components, heated up to the reaction temperature, are injected into the reaction zone portion by portion. The polymer builds up layer by layer,and the newly formed material passes on to the end of the process at a temperature of 150 - 200°C.[251]

The most favorable conditions for reactive processing of monolithic articles are created when the frontal reaction occurs at a plane thermal front. For example, a frontal process can be used for methyl methacrylate polymerization at high pressure (up to 500 MPa) in the presence of free-radical initiators. The reaction is initiated by an initial or continuous local increase in temperature of the reactive mass in a stationary mold, or in a reactor if the monomer is moving through a reactor. The main method of controlling the reaction rate and maintaining stability is by varying the temperature of the reactive mass.[252]

One of the most interesting uses of frontal processes is in anionic activated lactam polymerization. The heat source for this process is the heat of polymerization but heat output due to crystallization of a newly formed polymer. Frontal polymerization of ε-caprolactam with the formation of polycaproamide slabs can be realized in the reactor shown in Fig. 4.40.[253] A cylindrical reactor is equipped with an insulating adiabatic cover *1*, plane heater *2*, bottom *3* and a control valve *4*. The upper and lower covers are insulating to minimize heat exchange with the surroundings. A reactor heated to 75 - 95°C is filled with an initial reactive mass at the same temperature. It is important to maintain close contact between the heater surface and the reactive mass. Then the heater is switched on and the temperature of the layer of reactive mix contacting the heater is rised to 150-200°C, which initiates the polymerization process inside this layer. Then heat input from the heats of polymerization and crystallization allows the process to continue in the neighboring layer and so on. The adiabatic temperature increase arising from these two energy sources equals 90°C. The characteristic time of the process is determined by the velocity of the temperature front, which depends on the composition of the reactive mass (governing the rate of chemical reaction) and the initial conditions. The approximate size of the layer, where the primary reaction is initiated, is about 5 mm.

The choice of the temperature of the initial reactive mass (75 - 90°C) is dictated by two requirements: firstly, the reactive mass must be liquid; secondly, the reaction rate in this temperature range must be negligible. It was established in preliminary experiments that the temperature of the heater surface needs to be 75 - 125°C higher than the initial temperature of the reactive mass. The necessary operation period for the heater depends on the initial temperature of the reactive mixture and its reactivity (i.e., on its composition). The temperature of the heater does not influence the properties of the final product or the stationary kinetics of the process. The local temperature increase inside the adjoining layer must be supplemented by a heater for 30 - 50 min. This is the time required to set up the reaction front; after that, the front exists by itself and propagates due to the exothermal heating effects of chemical reaction and crystallization.

The velocity of the polymerization front is 0.065 - 0.18 mm/s, and the temperature of the polymer at the end of the process is about 170 - 180°C. The degree of crystallinity reaches 40 - 50%. The newly formed polymeric slab has no cracks, blow holes or crazing. The mechanical properties of the material are homogeneous throughout the entire volume and are close to those of a material synthesized in a stationary mold.

Frontal polymerization carried out as described above can be turned into a continuous process. In order to do this, it is necessary: to move the newly formed polymer and the reactive mixture in the direction opposite to the direction of spreading of a thermal front at a velocity equal to the velocity of the front development; to feed the reactor with a fresh reactive mass.[254] Control of the process, choice of process parameters and proper design of the equipment require solving the system of equations modelling the main physical and chemical processes characteristic of frontal reactions.

4.8.2 FRONT DEVELOPMENT IN SUPERIMPOSED PROCESSES

The theoretical approach to modelling frontal polymerization is based on the well developed theory of the combustion of condensed materials.[255,256] The main assumptions made in this approach are the following: the temperature distribution is one-dimensional; the development of the reaction front is described by the energy balance equation, including inherent heat sources, with appropriate boundary and initial conditions. Wave processes in stationary and cyclical phenomena which can be treated by this method, have been investigated in great detail. These include flame spreading, diffusion processes, and other physical systems with various inherent sources.

As we know, several heat sources can exist. The most typical heat source in frontal reactions is the heat of reaction. Chemical reactions at the front can be sequential[257] or independent. In both cases, analysis of the kinetics the overall reaction allows us to solve the problem of heat wave propagation, and thus to understand how the reaction progresses. The reaction zone can be very narrow, as for example in combustion problems. Thus allows us to treat a reaction front as a surface. Such an approach allows us to determine the main features of the process, i.e., to distinguish between different wave propagation regimes, and the critical conditions for its realization, and also to find the propagation velocity of the polymerization front and the distance between neighboring reaction zones. The appearance of several reaction zones is explained by the low reaction rate at the initial temperature; thus the characteristic time for approaching a steady polymerization or combustion regime is less than the characteristic time of reaction, and so the secondary reaction wave can propagate through the products of the primary reaction.

In some cases, the heat source can include both the heat of polymerization and the heat output of crystallization of the newly formed products. This is the case in anionic activated ε-caprolactam polymerization. This dual heat source must be included in the energy balance equation. As was discussed above, the temperature dependence of the crystallization rate is somewhat complicated. Nevertheless, the propagation of the heat wave is analogous to other well-known cases of wave propagation from consecutive reactions.

Theoretical modelling and analysis of the results for the superimposed processes of polymerization and crystallization was carried out for wave propagation in anionic activated reaction of ε-caprolactam polymerization.[258] In the steady situation, the process is described by the system of differential equations:

$$u\frac{dT}{dx} = a\frac{d^2T}{dx^2} + \frac{Q_p}{C_p\rho}f_p(\beta,T) + \frac{Q_c}{C_p\rho}f_c(\beta,\alpha,T) \qquad [4.25]$$

and

$$u\frac{d\beta}{ax} = f_p(\beta,T); \quad u\frac{d\alpha}{dx} = f_c(\beta,\alpha,T) \qquad [4.26]$$

where u is the wave propagation velocity; Q_p and Q_c are the heats of polymerization and crystallization, respectively; C_p is the specific heat; ρ is density; a is the coefficient of temperature

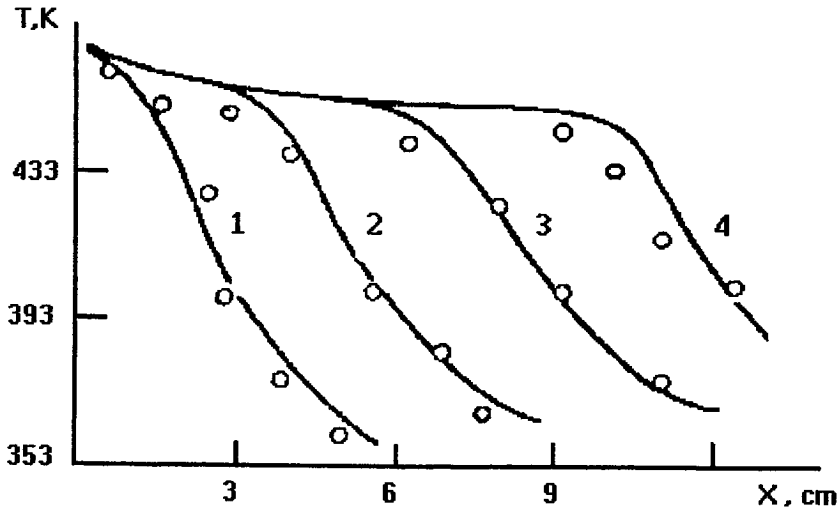

Figure 4.41. Comparison of experimental data (points) with the results of calculations (solid lines) for propagation of a polymerization wave in the synthesis of polycaproamide. 1 - distance from the plane of initial setup of the reaction. Curves correspond to different time from the start of a reaction: 1 - 30 min; 2 - 60 min; 3 - 90 min; 4 - 120 min.

diffusivity; α and β are the degrees of conversion in crystallization and polymerization, respectively; f_p and f_c are kinetic functions for polymerization and crystallization, respectively; according to the discussion of the problem (see Ch. 2) these functions can be written in the following form

$$f_p(\beta,T) = k_p e^{-E_p/RT}(\beta + c_p)(1 - \beta) \qquad [4.27]$$

and

$$f_c(\beta,\alpha,T) = k_c e^{\left[-\frac{E_c}{RT} - \frac{\psi T_m}{T(T_m - T)}\right]}(\alpha + c_c)[\beta\alpha_\infty(T) - \alpha] \qquad [4.28]$$

where k_p and k_c are pre-exponential constants in the kinetic equations for polymerization and crystallization, respectively; E_p and E_c are the apparent activation energies of both processes; c_p and c_c are the self-acceleration constants in the kinetic equations describing crystallization and polymerization; α_∞ is the temperature-dependent equilibrium degree of crystallinity; T_m is the melting temperature; x is the coordinate axis in the front propagation direction.

The boundary conditions for temperature are:

$$T(-\infty) = T_0; \quad T(\infty) = T_{lim} = T_0 + \Delta T_{max} \qquad [4.29]$$

and for the degree of conversion:

$$\beta(-\infty) = 0; \quad \beta(\infty) = 1; \quad \alpha(-\infty) = 0; \quad \alpha(\infty) = \alpha_\infty \qquad [4.30]$$

where T_0 and T_{lim} are the initial and final temperatures of the reactive mass and T_{lim} is determined by the net temperature rise ΔT_{max} due to the heats of polymerization and crystallization.

Solution of the system of Eqs (4.25) - (4.29) gives the velocity of wave propagation. Numerical values of the constants in the kinetic equations for polymerization and crystallization were found from a standard calorimetric experiment. Then we can find the solution and compare it with experimental data,as is done in Fig. 4.41. The results are quite satisfactory. This means that the theoretical model of front polymerization (with crystallization of the newly synthesized product) correctly represents main features of the process and can be used for plant design.

It can be shown that three different modes of front propagation during the formation of polycaproamide can be observed, depending on the relationship between the process parameters. In the first mode, which was found experimentally, the zones of polymerization and crystallization coincide. In the second mode these zones are separated in space. The third mode, which was predicted theoretically, is characterized by a non-monotonic distribution of the degree of crystallinity. However, it is not clear whether this situation can actually be observed in anionic ε-caprolactam polymerization because even slight variations in parameters transfers the system into another regime.

4.9 REACTIVE INJECTION MOLDING (RIM)

4.9.1 INTRODUCTION

If a mold is filled by free casting without additional pressure, no rigid connection between the injection pipe and the mold is necessary. This approach is not suitable for processing complicated articles which are to be used without machining or other finishing operations. This can only be achieved by continuous replenishment with fresh reactive material in order to compensate for polymerization shrinkage. This technique is especially important in high-temperature processes or in processing highly reactive compounds. Continuous replenishment is achieved by reactive injection molding under pressure. The difference between reactive injection molding and traditional technology for processing thermoplastic or thermosetting materials is the reduced heat and mechanical energy consumption required to melt the granules or powder and the use of much lower pressures than are needed to transport highly viscous polymer melts.

Several reactive injection molding techniques are used in practice; the most typical of these is shown in Fig. 4.42. In this method, the reactive mixture is prepared in vacuum mixers, as in reactive free casting then injected through a regulated valve into a mold at a pressure of 0.1 - 0.4 MPa. Airtight molds are used in this technique, and therefore the material can be transported under vacuum. After the mold is filled, a valve shuts off the main feed of material, but simultaneously a fresh supply of reactive mixture continues to replenish the mold through a gate valve. All the lines and the gate valve are cooled, but the mold is heated. Effective replenishment is guarantied by choosing a temperature that maintains a liquid outer layer of reactant mix when the rest of the mass

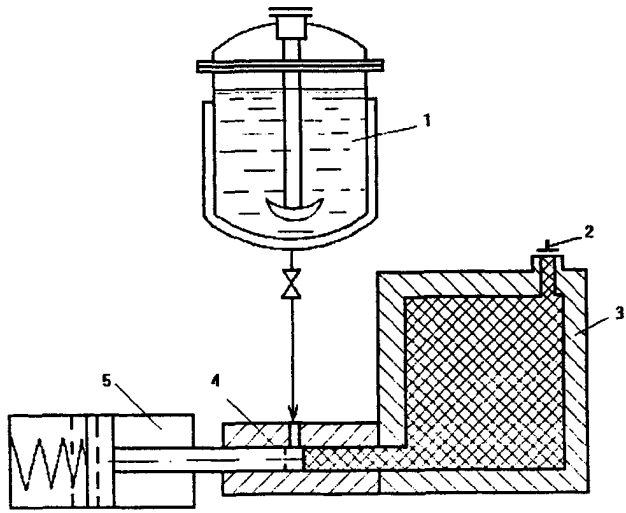

Figure 4.42. Scheme of the equipment used for reactive injection molding. 1 - reactor; 2 - safety-valve; 3 - mold; 4 - piston-rod; 5 - device for feeding a mold under pressure.

has become a gel. The reactive mixtures intended for reactive injection molding must meet a number of stringent quality criteria. They must remain liquid for a long time at low temperature (long lifetime), but must polymerize quickly at elevated temperatures. It must also be borne in mind that cleaning and washing reactive injection mold is virtually impossible unless they are dismantled.

The so-called RIM-process (reactive injection molding) is a current realization of the reactive molding process. The heart of the process is the shock mixing of the reactive ingredients, which is achieved by collision of two jets injected at a pressure of 10 - 20 MPa. The reactive mixture is injected into the mold in a laminar flow regime; the pressure at this stage does not exceed 0.1 - 0.4 MPa.[259] The practical development of this method relies on automatic control systems and modern high quality equipment.

The most successful application of the RIM-process is in the production of polyurethane-based materials. Other systems, such as composites based on polycaproamide, epoxy resins, and unsaturated polyesters can also be processed by reactive injection molding. New reactive systems have also been specially created for the RIM-process[260] because of the exceptional opportunities it offers for manufacture of finished articles from engineering plastics with a high modulus of elasticity and impact strength. The automotive industry, which is the main customer for RIM-articles, can utilize this technology to manufacture of massive parts such as body panels, covers, wings, bumpers and other made of newly developed plastics.

RIM-technology is used primarily for producing massive parts weighing from 1 to 25 kg. In some applications, the articles can weigh up to hundreds of kilograms. The RIM-method has important economic and technological advantages over traditional injection molding of thermoplastic materials processing these articles. The most effective application of RIM-technology is in the manufacture of large sheets and thick components; in traditional injection molding machines these applications require very high clamp pressures to process thermoplastic polymers. The RIM-process is especially effective for mass-produced parts, but also can be used to manufacture individual articles when the cost of a mold for traditional injection molding is much higher than that for RIM-technology; because of the low pressure used in the RIM process, there is no need for a mold with heavy strong walls.

4.9.2 GENERAL REQUIREMENTS FOR COMPOSITIONS USED IN THE RIM-PROCESS

The general requirements for compositions, that can be effectively used in the RIM process depend on the conditions of the main process operations, each of which imposes some requirements on the reagents in the reactive mix. The following list is an overview of these requirements:

Reagents	Materials stable at temperatures up to 100°C, or even 150°C, which can be transported by pumping
Metering	Two-component mixtures; deviations from the stoichiometric ratio must not exceed 1%
Mixing	The Reynolds number in mixing operations must be >200
Mold filling	The ratio of the mold filling and gelation time must not exceed 0.5
Curing (solidification)	No volatile products must appear; shrinkage must be compensated; chemical reactions and phase transitions (crystallization) must proceed quickly, regardless of the size of the article
Removal from a mold	Reaction must be 95%complete; no interaction with the anti-adhesive; minimal removal time.

It is clear that polymers that are synthesized in solutions, emulsions or suspensions are not appropriate for RIM technology. The use of monomers or oligomers that are polymerized above their melt temperature is also unlikely, because the a mold needs initial heating in order to initiate the reaction and then must be cooled to solidify the article. This is not convenient for industrial operations. There are some additional special requirements. For example, the formation of volatiles is generally undesirable but may be useful if the RIM-process is used for manufacturing porous articles.[23]

Some typical operating parameters for processing various polymers by the RIM method are listed in Table 4.1. Table 4.2 contains the main performance characteristics of polymers produced by the RIM process.

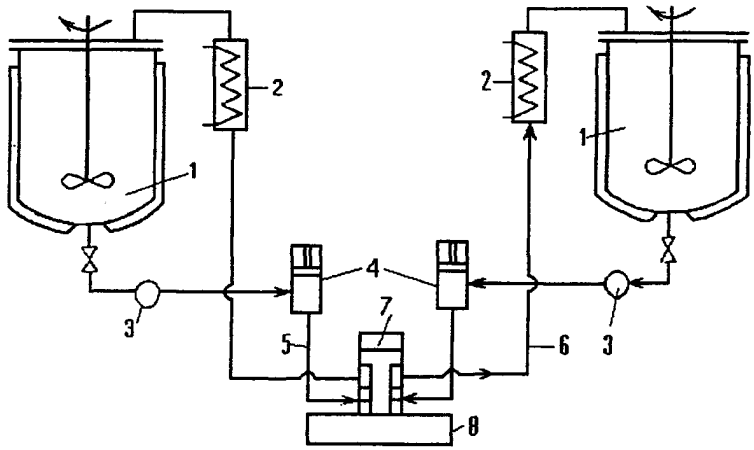

Figure 4.43. Plant layout for reactive processing. 1 - tanks for reagents; 2 - heat exchangers; 3 - low-pressure pumps; 4 - high pressure metering pumps; 5 - low-pressure recycling line; 6 - high-pressure recycling line; 7 - chamber for shock mixing; 8 - mold.

Table 4.1. Operating parameters for processing polymers by the RIM-method[261]

Polymer	Temperatures		t_s, s	Q_p, kJ/mol	U, kJ/mol	Sh, %
	T_0, °C	T_m, °C				
Polyurethanes	40	70	45	84	59	5
Polyureas	40	70	30	84	13	5
Polycaproamide	100	130	150	42	88	10
Unsaturated polyesters	25	150	60	67	126	20
Epoxy resins	60	130	150	126	67	5

Notation: T_0 is the initial temperature of the reactive composition; T_m is the mold temperature; t_s is solidification (curing) time; Q_p is the heat of polymerization; U is the apparent activation energy of the chemical reactions; Sh is shrinkage

Table 4.2. Main performance characteristics of unfilled materials produced by RIM-technology

Property	Polyurea	Epoxy	Poly(cyclo pentadiene)	Block copolyamide A-B-A
σ_b, MPa	30-35	65-75	32-35	40-50
E, GPa				
in extension	0.08-0.1	2.5-3.0	1.8-1.9	1.4
in bending	0.7-0.8	2.6-2.8	1.8-2.0	0.8-0.85
ε, %	300-400	5-6	7	200
A, kJ/m	-	5-10	45-55	40-50
$\alpha \times 10^5$, K^{-1}	14	4	5	12

Notation: σ_b is the strength limit in extension; E is the modulus of elasticity; ε is the elongation at break; A is the impact strength; α is the coefficient of linear thermal expansion

4.9.3 PLANT LAYOUT FOR THE PROCESS

The plant layout for the RIM-process and all the main parts are shown in Fig. 4.43: *1* -storage tanks for reagents; *2* - heat exchangers; *3* - low pressure pumps; *4* - high pressure metering pumps; *5* and *6* - of high and low pressure, recycling lines respectively; *7* - mixing chamber; *8* - mold. The process is monitored and controlled by a microprocessors system. This installation is used for processing polyurethane-based compositions and other reactive systems.

During operation, the initial reagents are transported by low pressure pumps through the heat exchangers to the high pressure pumps. These pumps create pressure on the order of 15 - 25 MPa and meter the two streams in the required ratio into a mixing chamber, where the reactive components are mixed by shock collision. Then the prepared reactive mixture passes through a transition zone where turbulent flow transforms into a laminar stream. This allows mold filling to proceed in a quiet frontal regime without the formation of flow disturbances and vortices. The transition from turbulent to laminar flow can be achieved by various engineering designs.

The metering systems can work in either of two operating regimes: recycling and feeding. The low pressure recycling regime provides a homogeneous stream with uniform temperature. This is especially important when a filler is added to the reactive mix for processing reinforced parts.

The mixing system must provide high-speed feeding of both components into the mixing chamber, synchronization of feeding, a well-mixed turbulent stream, and adequate facilities for cleaning the mixing chamber and ridding it of polymer residues. A special line, through which solvents can be circulated at high pressure, is used to clean the mixing chamber. For high-capacity units, mechanical cleaning by a plunger that enters the chamber after the end of mixing is used.[262] A typical design of such a unit is shown in Fig. 4.44. According to this method, the start and finish of mixing and, consequently, the time of feeding the mold are exactly determined by the location

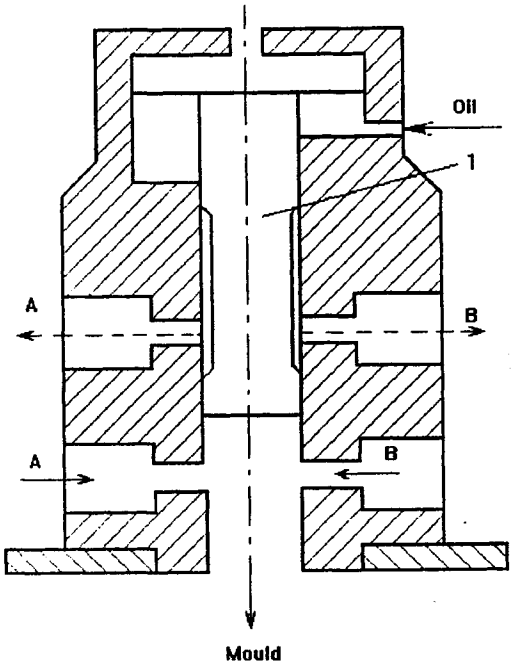

Figure 4.44. Functional design of a mixing chamber with mechanical cleaning. 1 - plunger for feeding reagents A and B and for cleaning the mixing chamber; 2 - mixing chamber.

of the plunger, which opens and closes the inlets. As a general rule, the main components of the reactive mix are injected into the mixing chamber to meet each other (as shown in the figure) and supplementary additives are fed in perpendicular to the main direction. There are other designs of mixing chambers in which reagent injection is controlled by special inlet valves, rather than by a plunger.

The molds in a RIM-process plant are located in a separate assembly, which has devices for opening and clamping a mold and, in some cases, for changing it. The pressure in the RIM-process is considerably lower than in traditional injection molding of thermoplastics; thus, the requirements for the mold material are less rigid. Molds may be made from aluminum or reinforced plastics, since high-strength steel is not necessary.

Removal of the article from the mold is lengthy process because anti-adhesive lubricants have to be sprayed on the on a mold surface before every injection, in an operation that takes up to 25 - 30% of the full cycle. In reactive molding of polyurethane-based compounds, internal lubricants are used in combination with surface coatings. This allows us to remove articles from a mold many times with a single coating treatment. One of the compounds used as an internal lubricant is silicon-organic liquids.

RIM is new the most popular technique for producing polyurethanes or polyureas. In polyurethanes synthesis two streams, containing polyols and isocyanates (i.e., a prepolymer and a curing agent), are mixed under pressure. These streams are metered and injected into the mixing chamber, and then the reactive mixture passes to the mold. Depending on the formulation used, a rigid plastic or an elastomer can be obtained as the final product. A feature of the compositions used in the RIM-process in comparison with free-cast polyurethane compounds is their short "life-time". Mechanical mixing is not required, and for this reason, stream collision under pressure is the preferred mixing technique. In some cases, the pressure can reach 150 MPa or more.[262]

Polymerization reactions are always exothermal; this is why mold heating is usually not necessary. However, in some cases the initial mold temperature must be high; for example, a mold used for reactive molding of polycaproamide (Nylon-6) must be heated to 130°C in order to melt the monomer. In reactive processing of polycaproamide, the reactive components are also injected into the mixing chamber as two separate streams. The ratio of catalyst to activator is less of a determining factor than the ratio of the components in polyurethane processing; in the case of polyamides, this ratio influences only the polymerization rate. Polymerization under pressure is an excellent way to compensate for shrinkage and to obtain articles of complex shape.

The length of the process cycle for polycaproamide and its copolymers depends on the formulation of the reactive mixture and the molding regime. On average the cycle time for processing block-(copolyamide esters) is about 2 min, and parts do not require further solidification after molding. Removal of polyamide articles from the mold is relatively easy, but the full cycle is much longer than in polyurethane processing. This is due to the crystallization process, because it is much more difficult to regulate the crystallization rate than the polymerization rate. The most popular method for accelerating crystallization uses nuclei of crystallization, which can be inorganic or organic finely dispersed materials.[263] Shortening the cycle can also be achieved by introducing small amounts of a foaming agent into the composition. For example, nitrogen can be injected under pressure into the reactive system. Slight foaming increases the reaction rate and the final product has a small cell structure providing a sufficient level of impact strength.

Molding plants are universal and can be used for processing a wide range of materials, including polyamides, polyurethanes, epoxy resins, and other RIM-formulations. To give some idea of the technical capabilities of RIM-machines main technological features of a Krauss-Maffei (Germany) unit, known as NBC-RIM-*star*-40 machine, are listed below.

Capacity (for both components), l/min	5 - 90
Volume mixing chamber, l	10
Volume of a shot (ratio of components 1:1), l	8
Accuracy of metering, %	0.5
Volume of mold, l	100 - 250
Maximum temperature, °C	150
Maximum pressure, MPa	10
Power consumption, kW	70
Overall dimensions, m	3x3

This installation is built on the modular principle. Component output is measured by a gear counter, and there are various possibilities for programming the operating cycle of the unit.

One interesting application of RIM-technology is the production of gum-coated parts. Liquid polymerizing mixtures flow easily around inserts and can adhere strongly to metal surfaces. Inserts can be made of practically any material, except those which interact with components of the RIM-mixture. There are few other technological processes that can produce gummed parts of any size and shape by a one-shot procedure.

4.9.4 PROCESSING OF REINFORCED COMPOSITES

Recent developments in industrial applications of RIM-technology are related to the processing of highly loaded composites, which can contain up to 90% of a filler.[262] A filler can be introduced into the reactive mix during its preparation stage or it can injected into the mold and impregnated with the mix in the mold filling stage. Only filler consisting of short cut fibers can be added to the reactive mix in the mixing stage, since the filler is injected through small orifices into the mixing chamber. Milled glass fibers and cut glass roving are commonly used as fillers in the RIM-process. In this case the length of the strands cannot exceed 1.5 mm. However, the longer the fibers the stronger is the reinforcing effect. Therefore, it is preferable to use long fibers in the form of a mat placed inside the mold. This allows the production of a composite material with valuable performance properties. Glass fibers are widely used in processing composites based on unsaturated polyesters and epoxy resins.

In processing polyurethanes by RIM-technology, short fibers can be introduced into both the polyol and isocyanate streams. Adding glass fibers to the polyol stream greatly increases the viscosity of this component, which results in complications in mixing and to a certain extent, lowers the quality of mixing during shock collision. Therefore the filler content (e.g., milled glass fibers) must not exceed 40% of the mass of the end product. The maximum content of cut glass roving of length 15 mm is 15%, and the efficiency of cut fibers is about three times higher than that of milled fibers. In all cases, the fiber surface is treated with a finishing agent to improve their adhesion to the polymer matrix.

Some other fillers have also been tried in the RIM-process, primarily carbon black, mica, wollastonite (calcium silicate), carbon and organic fibers, and so on.[262] The strength-to-weight ratios for mica and wollastonite exceed that of glass fiber, but mica is very abrasive and hygroscopic, and wollastonite has a low length-to-diameter ratio. The latter parameter is very important because it determines the efficiency of fibers in reinforcing a matrix. When fibers of constant diameter exceed a certain critical length, an increase in load results in rupture rather than plastic elongation of the polymer matrix. Typical examples of the changes in properties of polyurethane-based plastics reinforced by 1.5 mm cut glass fibers is shown below.

Content of filler, %	0	10	20	25
Limiting strength, MPa	42-44	49-51	68-70	71-73
Breaking elongation, %	100	40	28	28
Shrinkage, %	2.5	2.0	1.2	1.2

Two factors are especially important in processing filled composites: increased abrasive wear of equipment and the high viscosity of the reactive mixtures, which are suspensions of fillers in low-molecular-weight liquids. Therefore, these liquids are metered by means of high-pressure piston pumps, and special gasket materials are used.[260] In addition wear-resistant materials such as tungsten carbide are used for parts that come in contact with composite materials during processing.

Another problem encountered in processing of filled composites by the RIM-process is sedimentation of the filler in tanks, transport tubes, etc. In order to overcome this problem the tanks are fitted with stirrers, so that the filled liquid is forced to circulate in the intervals between shots. Finally, it is necessary to consider the possibility of breakdown of the filler structure; if this occurs, there is usually an adverse effect on the properties of a final product.

4.9.5 MODELLING MOLD FILLING

Reactive processing consists of three principal stages:[264]

- mixing,
- filling the mold,
- exposure of the material in the mold until it becomes rigid enough to be extracted from the mold without distortion.

The material necessary to form the article is not prepared before injection; instead component mixing and preparation of the reactive material take place during processing, starting in the mixing chamber of the molding machine. Thus, chemical reactions and changes in the rheological properties of the material occur during its passage through the plant. In addition, in order to increase the reaction rate the components of the reactive mixture and the feed lines are heated, so the process proceeds in non-isothermal conditions. Formation of the final product and the major part of the viscosity increases take place in the mold after filling. Therefore, the pressure drop in the feed lines is not high; this is the main reason why reactive processing does not require high pressures and power consumption. Nevertheless, chemical reactions are possible during material flow in the feed lines. This may result in premature gelation and incomplete filling of the mold. In some applications, the mold can be very long (for example when reactive processing is used to form a thin coating layer), and it is impossible to separate the flow in the feed lines and the mold.

Mold-filling processes in which flow and chemical reactions are superimposed with continuous changes in the rheological properties of the liquid are of particular interest in modelling. The importance of this theoretical analysis stems from the trend toward using reactive processing to produce articles of complex shape and large size.[265] In this case, the problems of incomplete curing and formation of molding lines due to contact of the streams in the mold with the inserts are the most important. Molding lines appear if the temperature the of stream contact locations is relatively low and/or the viscosity of the reactive material becomes too high for rapid diffusion. Increases in viscosity and decreases in concentration of the reactive groups prevent formation of a uniform material, and then molding lines appear inside and on the surface of the final product. This degrades the appearance of the article and results in interior product quality due to a decrease in strength.

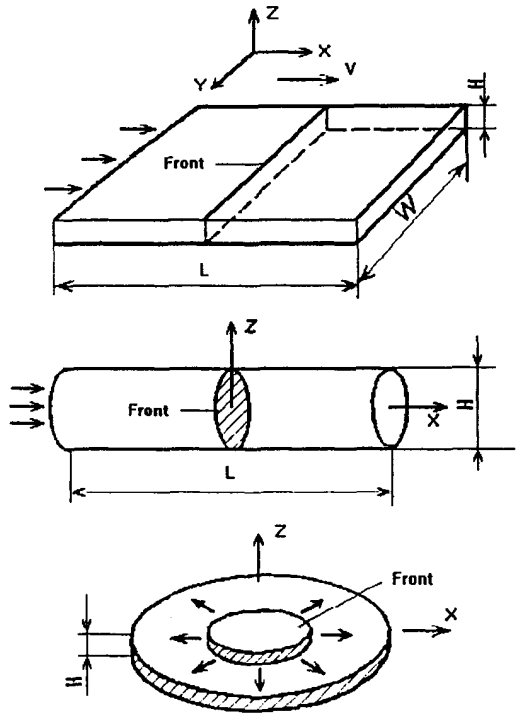

Figure 4.45. Three basic mold shapes.

If reactive processing is used for coating solids (metal or other materials), the surface changes in viscosity and concentration of reactive groups also influence adhesion to the substrate and thus the quality of coating. Generally speaking, an increase in viscosity and the decrease in concentration of the reactive groups in a macromolecule results in a reduction in the adhesive strength of the coating. Therefore, it is important to know the interrelation between the process parameters and the properties of the material at various stages of coating formation.[266] Among the effects observed in reactive processing, one is especially important in coating formation. In some cases, the stream front loses its stability and small air bubbles are trapped by the polymer,[267] reducing the quality of the coating surface. Filling a cavities of various shapes with liquids possessing different rheological properties (including "rheokinetic" liquids) has been discussed in many publications because of the importance of this stage in injection molding of polymers. The details of flow clearly depend on the geometry of the cavity (mold). In principle, it is possible to find a solution to the hydrodynamic problem for a cavity of arbitrary form by finite element analysis.[268]

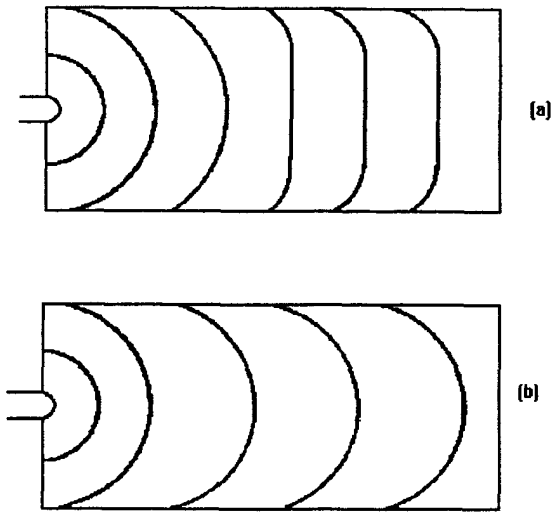

Figure 4.46. Evolution of the melt front in the mold filling process in isothermal (a) and non-isothermal (b) conditions.

However the search for solutions is time-consuming even with modern computers, and results have only limited value, because they do not provide an understanding of the influence of the main geometrical and technological factors on the qualitative pattern of the process. Therefore, models of the flow in channels of relatively simple shape have became very popular.[269-271]

It is usually assumed,[270] that any complicated mold shape can be regarded as a combination of simple geometrical elements. Three standard elements can be treated as the basic ones: a cylindrical cavity of constant diameter, a plane rectangular channel with a constant gap, and a plane disk of constant width (Fig. 4.45). It is also assumed that a characteristic dimension (diameter, gap, width) can vary along the direction of flow, shown by the arrows in Fig. 4.45. The majority of investigations have been devoted to flow and filling of long rectangular molds, and in fact many typical molded articles are formed of combinations of thin plates.[265] Experimental investigations of flow in cavities, including visualization of streams, are very important for checking the calculated results from the theoretical model.

The first systematic investigations of the movement of a front inside a cavity were made for a disk-shaped mold, and the results were documented by photographs.[272] Later papers[273,274] devoted to experimental observations of mold filling were published as this area of research became more popular. Investigations of radial flow in a transparent half-disk mold[275] and high-speed photographic documentation of flow in both a plane rectangular and the complicated mold for

isothermal and non-isothermal situations[276] were also published. It was established[276] that at moderate flow velocities, movement of the liquid is quite regular. Typical results for liquid flow for the case when the wall and melt are the same temperature are shown in Fig. 4.46 a (view from above). It is seen that at the early stages of filling, the flow is strictly radial and the stream front is rounded. However, the shape of the flow front changes along the length of the mold.

If the melt is hotter than the mold walls (200°C and 80°C, respectively) the pattern changes. Fig. 4.46 shows that the shape of the front remains unchanged to the end of the process. However, if the velocity becomes very high, another type of flow is observed, in which a melt injected into the mold forms a jet, which reaches the opposite wall of the mold. After the tip of the jet touches this back wall, regular straightforward filling occurs. Another type of jet filling is also possible, in which the stream turns back after reaching the back wall, and the liquid begins to move in the opposite direction. In this situation, regular mold filling becomes possible, as the returning stream fills the mold almost completely.[265]

It was established experimentally that a jet-type of flow appears when the characteristic size of the stream is less than the minimal gap between the walls of the mold.[277] This proves that the cause is related to the ratio between the size of the injection nozzle and the coefficient of swelling of the elastic liquid moving inside the mold rather than to the axial momentum of the moving liquid. This conclusion is also supported by evidence that highly filled polymers, which are less elastic than pure melts, form jet-like patterns at lower flow speeds.

Jet-like flow is undesirable for high quality processing; therefore, various methods of suppressing jet formation have been proposed.[278] One method relies on positioning the injection point close to the opposite wall, such that the melt reaches it at the beginning of mold filling, and after that, the regular process occurs. Another method uses a fan nozzle, which increases one of stream dimensions, and thus lowers the momentum of the liquid. Jet formation is undesirable in injection molding of thermoplastics because this type of flow leads to appearance of molding lines, which spoil the performance properties and surface quality of the article. Jet-type flow is also encountered in injection molding of thermoplastics; this mold-filling regime occurs when the nozzle size is much less than the mold size.

Experimental investigations of filling a thin rectangular mold with a reactive mixture showed that disturbances in stable flow are possible. Three filling patterns, depending on the injection rate, can occur: stable, unstable, and transient.

In addition to high-speed photography, which was used to obtain the results discussed above, other methods have been used to visualize flow, for example, the tracer method.[279-281] A typical experimental device consists of a capillary viscometer connected to a mold, which is a simple model of plunger-type injection molding unit.[279] A special device was used to introduce tracers of different colors in regular succession. After sample solidification, it is possible to examine the position of the various colors on the surface (Fig. 4.47 a) or through the volume by cutting sections (Fig. 4.47 b). It can be seen that the tracers are positioned symmetrically near the surfaces and that they have a V-type shape, with the tip oriented toward the stream.

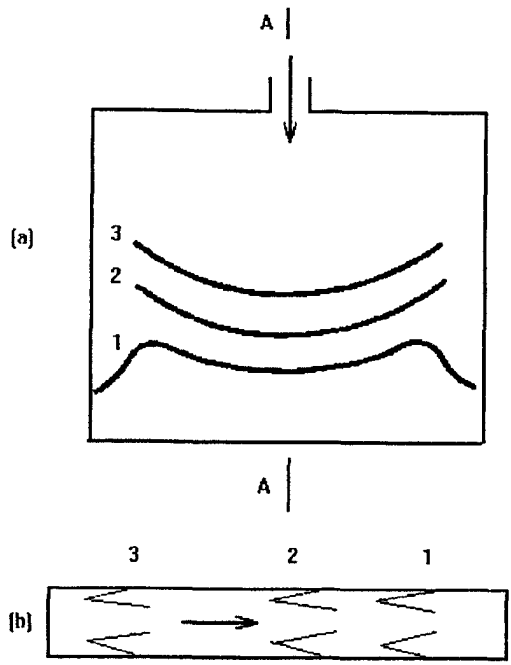

Figure 4.47. Scheme illustrating tracer distributions after mold filling. a - view from above; b - cut along A - A section (figures correspond to tracers of the same color). [Adapted, by permission, from L. R. Schmidt, *Polym. Eng. Sci.*, **14** (1974), 798.]

Another method of visualization[282] uses a rectangular mold which is not completely filled and has inserts located at different positions inside it. This method demonstrated the position and form of the stream front at different injection times (Fig. 4.48). The inserts split the stream and changed the direction of front development. Molding lines formed beyond the insert, where the different parts of the stream joined. Changes in flow direction influence the molecular orientation of the polymer in the mold; therefore, it is reasonable to expect that the orientation and properties of the end product will be inhomogeneous. It is also important to visualize the flow in the mold so that any surface defects and weak points at molding lines can be detected. It is evident that molding lines appear where two fronts meet, i.e., where the normals to the fronts are oriented in opposite directions or meet at an angle.[282]

The method of incomplete mold filling is effective for investigating injection molding of fiber glass-loaded polypropylene and polystyrene melts.[283] After solidification, samples were prepared for microscopic investigation . The authors determined the distribution and orientation of the fibers in different sections of the article and thus were able to clarify the pattern of flow in different parts of the mold as a function of the process parameters. They concluded that the width of the (cavity)

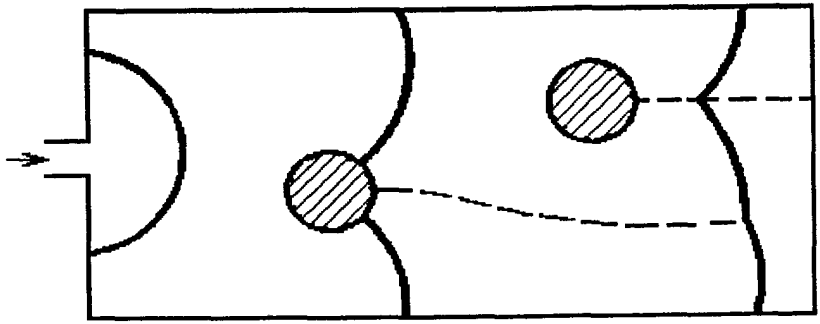

Figure 4.48. Diagram illustrating propagation of the front line and appearance of welding lines (dotted lines) at filling a plane mold with inserts.

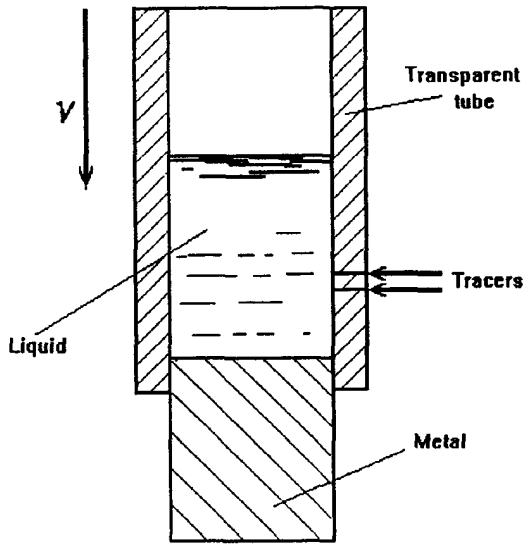

Figure 4.49. A device used for visualization of a stream. [Adapted, by permission, from D. J. Coyle, J. W. Black, C. W. Macosko, *AIChE J.*, **33** (1987), 1171.]

mold was the determining factor in fiber orientation rather than such parameters as volume output, melt temperature, and glass fibers content.

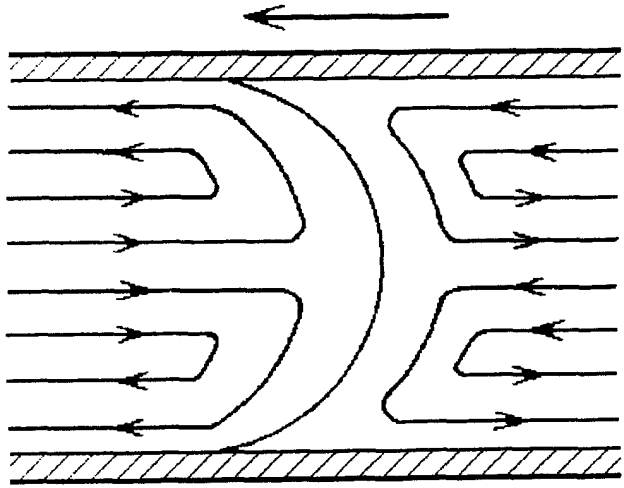

Figure 4.50. "Fountain" and "reverse fountain" effects.

Detailed kinematic investigations of flow near the front of a stream were undertaken.[284] A diagram of the experimental device is shown in Fig. 4.49. In the experimental procedure, a liquid was placed in a chamber with transparent walls above an aluminum piston, which was driven downwards by connection to a suitable drive. This resulted in the appearance of streams inside the liquid,and three different flow zones could be distinguished. The so-called "fountain" effect discussed in Section 2.11 appeared near the free surface, while a reverse fountain flow was observed below the moving surface. It is interesting to note the movement of two liquids with different densities, when one liquid is used as a piston to push the other (analyzed experimentally and theoretically).[285] If the boundary between the two liquids is stationary and the walls of the chamber move at constant velocity, then the pattern of flow is as shown in Fig. 4.50, where flow trajectories corresponding to front and reverse fountain effects are clearly shown. Two other flow patterns - developed flow inside the main part of the chamber and circulation near the surface of the aluminum piston - were also observed.

The volume of liquid in these experiments must be large enough so that circulation flow near the piston does not influence the flow pattern in other parts of the liquid. These experiments were performed with different liquids, both Newtonian and non-Newtonian (shear-thinning). The introduction of tracers allowed the authors to obtain pictures showing the movement and deformation of the tracers when they appeared near the front of the stream. In the beginning, a Poiseuille-like velocity profile is present (Fig. 4.51 a). Then the material reaches the region of fountain flow,

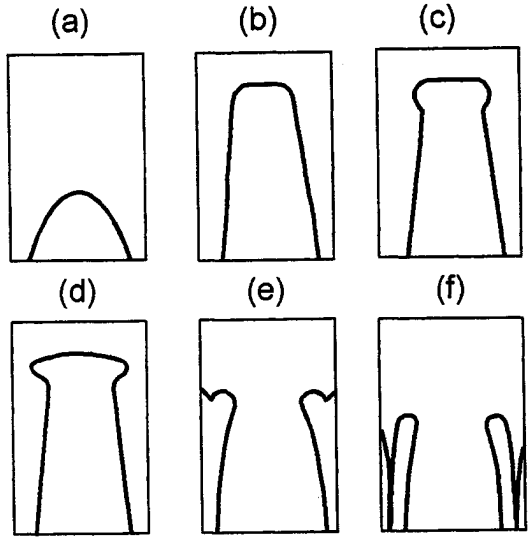

Figure 4.51. Consecutive stages of tracer deformation in the region of fountain flow.

where it undergoes extensional deformations (Fig. 4.51 b), and a transverse component of velocity appears. As a result, a rather peculiar velocity profile with a "hat" is documented (Fig. 4.51 c and d). Subsequently the material moves primarily in the direction of the walls, extends along the walls, and comes back to the region of the main stream (Fig. 4.51 e and f). Part of the tracer always stays near the free liquid-air boundary and forms a thread-like track. When the tracer reaches a boundary surface, its mirror reflection appears. This reflection is distorted when it occurs at the curvilinear surface of the liquid-air boundary.

Analysis of numerous experimental data obtained by various methods of flow visualization led the investigators to the conclusion that in all cases it is possible to separate three main regions with essentially different flow patterns. Fig. 4.52 shows these regions for a rectangular channel.

The first region is in the volume close to the inlet pipe. A liquid initially entering the mold flows in the radial direction until it reaches the walls of the mold. In other words, this type of flow is important only at the start of the filling process. As filling proceeds, the flow stream lines near the inlet are still complex, but the inlet volume is small in comparison with the whole volume of the mold. There is not enough time for significant changes in the properties of thermoplastic materials or reactive components during flow in this region. This region is therefore excluded from consideration in mathematical simulations of mold filling.

The second region is the volume where fully developed flow occurs. If we consider a thin mold, which is the most common model, it is reasonable to assume that there is one-dimensional

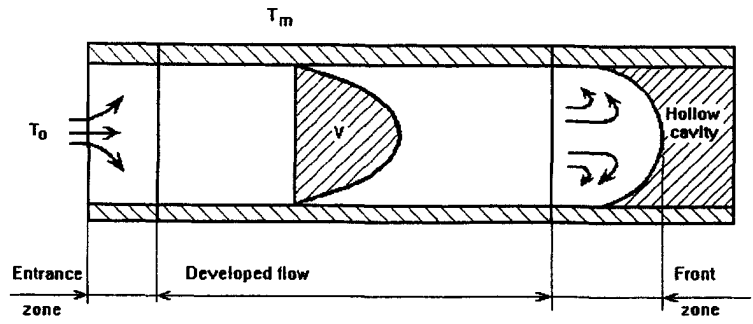

Figure 4.52. Structure of the flow stream in injection molding during filling of a plane cavity.

flow in the axial direction (for rectangular or cylindrical molds) or in the radial direction (for a disk mold). The flow is nonsteady and non-isothermal. The flow is also accompanied by cooling and solidification in the molding of thermoplastics or polymerization and exothermal temperature increase in injection molding of reactive liquids.

The third region of flow near the front is of special interest. The important feature of this region is the fountain effect, which must be considered in modelling all types of mold filling. It is important not only for estimating the hydrodynamic flow pattern, but also because the deformation of the macromolecules near the front influences their orientation and the properties of the end product.

One of the key parameters in reactive processing is the distribution of residence times and temperatures for all particles in the liquid, because their reactivity depends on temperature, and the degree of conversion is determined by the dwell time inside the mold. Since the fountain effect changes residence time distribution from that in the hypothetical case of steady unidimensional flow, this factor becomes especially important in chemical (reactive) processing, more so than in standard injection molding of thermoplastic materials.[284]

An artificial method of incorporating the fountain effect into the general description of flow was proposed.[49] In this publication numerous combinations of process parameters were analyzed, and velocity profiles and distributions of temperature and degree of conversion were calculated. Variation of the process parameters over a wide range of values established the principal qualitative situations encountered in filling a mold. As an obvious example, it is interesting to compare Figs. 4.53 a and b. In the second figure, the rate constant of the chemical reaction is four times higher than in the first, the filling time is also longer. It is clear that the velocity profiles (positions of isovels) for the two cases shown are quite different. In the second case, the degree of conversion reaches 90%, resulting in the appearance of a thick viscous liquid layer and a strongly protruding velocity profile with a very large gradient (Fig. 4.53 b).

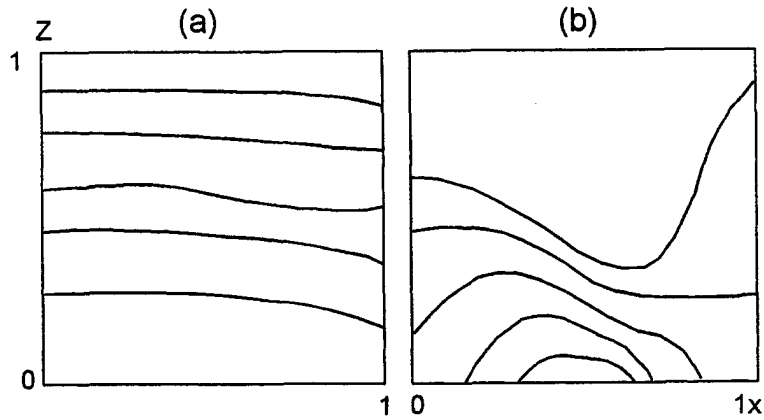

Figure 4.53. Locations of the lines of constant velocity at the finish of mold filling for a rate constant equal to k_0 (a) and $4k_0$ (b).

The possibility of predicting the molding time cycle, maximum temperature increase and processibility of a material was investigated[286] by modelling the combined processes of mold filling and solidification; the problem was solved by a simplified system of markers and cells.[287] Analysis of the calculated results showed that development of local regions of high conversion near the walls did not result in channel blocking and that relatively fresh material continued to move in the central part of the channel. The flow stopped only when gelation occurred at the front of the stream. The velocity profile distributions show that flow does not cease in regions of high conversion, but the appearance of a gelled layer near the walls results in jet-like flow of the liquid in the mold. This particular type of instability leads to the production of defective articles articles.

Calculations indicate[286] that, in order to shorten processing time, it is much more effective to increase the initial temperature of the reactive mixture than to increase the temperature of the mold walls. This is a consequence of the high activation energy and low thermal diffusivity of the reactive mix. Then, by solving the system of energy balance and kinetic equations, we can optimize the process by choosing the temperature thereby minimizing the molding time. However, in general, the higher conversion reached during the mold filling stage does not result in a short overall cycle time, because conversion is not homogeneous through out the entire mold, and a long delay in conversion of some parts of the reactive mix is quite possible.

A complete description of model of filling a rectangular mold and the subsequent solidification of an article was developed,[47] and in this case a fountain effect near the stream front was included. The authors used the model to predict pressure increase during mold filling, and the distribution of the degree of conversion and temperature at both stages (filling and solidification). The results

corresponded closely with experimental data on temperature and pressure patterns for reactive processing of a polyurethane-based composition.

Analysis of the various stages in mold filling is based on two dimensionless criteria: the Graetz Number, Gz, which is a measure of the ratio of convective to conductive heat exchange:

$$Gz = \frac{v_{av} c \rho H^2}{\lambda L}$$

and the gelation criterion, G, which is equal to the ratio of the time of flow to the time of a gelation reaction. Here, v_{av} is average flow velocity inside the mold; c is the specific heat; ρ is the density; H and L are transverse and longitudinal characteristic dimensions; λ is a coefficient of thermal conductivity.

Numerous calculations and measurements showed that in normal situations, the pressure increases during mold filling in reactive processing is low, and that an appreciable pressure increases is possible only if gelation occurs before complete filling and blocks the flow. A small value of the gelation criterion G and a large value of the Graetz Number are indicative of a slight degree of reaction and negligible heat exchange during mold filling. As a result, the viscosity of the reactive liquid stays almost constant. It is therefore reasonable to explore the simplest model with constant viscosity equal to the initial viscosity of the reactive mass. This constant-viscosity model predicts a linear increase of pressures with time which corresponds to experimental data. However if the assumed values of G and Gz are incorrect, then a model of a linear pressure increase is inadequate to explain the experimental observations.

If mold temperature is higher than the initial temperature of the reactive liquid, the critical value of the gelation criterion[47] G_{cr}, which depends on the Graetz Number,[322] can be found. When $G > G_{cr}$, deviations from a linear pressure increases with time are observed. The role of the Greatz number is explained by the temperature dependence of the reaction rate coupled with the mold wall acting as a heat source. If the Graetz Number is lower, a greater quantity of heat is transferred to the moving liquid. It was established by experiments,[47] that the critical value G_{cr} is related to the criterion of premature gelation and is approximately equal to 0.8 of the latter value.

A typical estimate of the critical value G_{cr} is discussed in Ref.;[47] it was shown that if $Gz > 10$, then gelation happens at $G > 0.17$; if the Graetz number lies between 2 and 10, $G_{cr} = 0.06$. These results apply only to the specific system investigated[47] but since the viscosity changes in a similar manner for other reactive mixes the authors of the cited publication believe that analogous conclusions are valid for other systems.

An analysis of the temperature distribution in a mold (Fig. 4.54) at the final moment of filling for two reactive systems with different values of G shows that the temperature along the central line increases monotonically downstream (at distance x) from the inlet nozzle. At high values of the gelation criterion, the temperature at locations close to the injection nozzle is maximum near the mold wall. Moving down stream, the position of the temperature maximum shifts to the center, except at the frontal zone. Here the temperature is nearly constant, because the major part of the

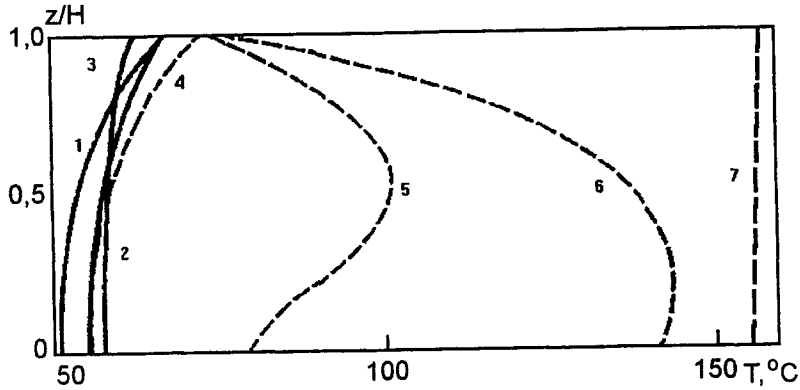

Figure 4.54. Patterns of temperature evolution at the end of mold filling for high (solid lines) and low (dotted lines) values of G. Figures on the curves approximately correspond to x/L values equal to: 0.15 (1); 0.7 (2); 1 (3); 0.05 (4); 0.6 (5); 0.9 (6).

material circulates to the front from the center of the stream. If G is small, the maximum temperature is near the wall along the whole length of the mold, because the heat output from the chemical reaction is low; nevertheless the temperature near the front of the stream is again almost constant. A comparison of the calculated pressure drop with and without the fountain effect in the frontal zone showed that when G is small, the difference in results is negligible, but at high values of G the discrepancy becomes large.[47] This result confirms the importance of correctly modeling the flow in the frontal zone.

A detailed analysis of the distributions of conversion, temperature and velocities was carried out[126] using a model, which included the fountain effect at the front of the stream. A comparison of the results was made for molds of different geometrical form (plane cavity, cylindrical and disk-like shapes) for the same temperature, average output and cross-sectional width of the mold. It was established that the distribution of the degree of conversion is qualitatively the same in all these cases (Fig. 4.55).

An interesting feature of the conversion profile is the existence of a maximum located between the wall and the axis of the mold. This effect is explained by the superposition of the influence of temperature and residence time on the kinetics of the reaction: a liquid moves faster in the central zone than at the wall, therefore the residence time is longer near the walls, but temperature is higher in the center; therefore the reaction rate of the material near the walls is lower than in the center. As a result, there is a point between the center and a wall where the degree of conversion is maximum. The results in Fig. 4.55, also answer the question about the role of the fountain effect:

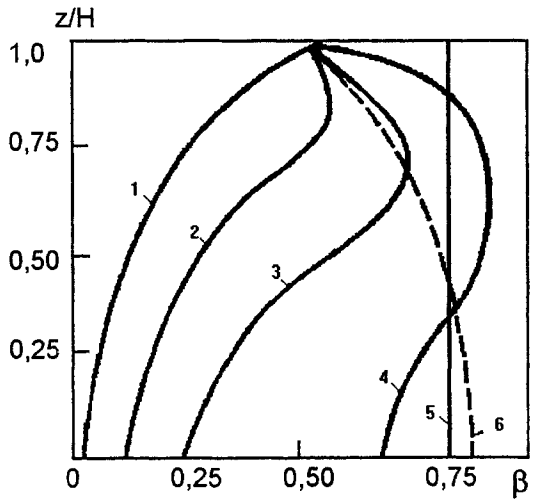

Figure 4.55. Conversion distribution at the finish of mold filling. Figures on the curves show the relative values of x: $<x_1 <x_2 <x_3 <x_4 <x_5 = x_6 = L$. Curve 6 is calculated for the case when the fountain effect was not taken into account in the calculations. [Adapted, by permission, from C. N. Lekakou, S. M. Richardson, *Polym. Eng. Sci.*, **25** (1986), 1272.]

the dotted line corresponds to the results of calculations using the model without the fountain effect at the front, i.e., without transverse convection. It can be seen that the degree of conversion appears too low at the wall and is overestimated in the center than in a more realistic model.

A disk-like mold is a separate case. The average flow velocity for a constant-volume injection rate does not depend on the axial position of the front in plane and cylindrical molds, but in a disk-like mold with an inlet nozzle located at the center. The front slows down as the stream moves from the inject to the periphery of the mold. This results in higher conversion at the final stage of mold filling. If a polyfunctional oligomer is used for reactive processing this effect can lead to gelation and incomplete filling. The magnitude of the shift in the flow in a disk-like mold is only one half of the possible shift in a rectangular plane mold at the equivalent process conditions.

The reactive processing at polyurethane - unsaturated polyester mixtures, which is of special interest this problem has also been investigated.[288] Making compounds of these polymers after polymerization is impossible because neither can be melted or disolved. However, the reactive processing technique makes it possible to prepare materials based on these polymers by injecting of the components of the reactive mix into a mixing chamber. This approach allows us to obtain materials with new performance characteristics and enlarged areas of applications.

In these polyurethane/unsaturated polyester mixtures chemical reactions and physical entanglements proceed simultaneously during processing and in the mold. The final goal of this process is the formation of a polymer composite with interpenetrating networks. These networks provide

good cohesion between regions with partly separated phases without the formation of chemical bonds. By controlling such factors as temperature and pressure during injection, it is possible to vary the formation of physical bonds and thus the properties of the end product according to customer requirements

Optimization of the reactive processing of mixtures of interpenetrating polymers can be achieved by varying the initial temperatures of the reactive components and the mold and the concentration of the catalyst.[288] The authors of the cited publication assume that the time the material spends in the mold and the maximum temperature increase during polymerization are the two most important parameters of reactive processing. Shortening the residence time of a material in the mold can be achieved by increasing the reaction rate. This may seem economically desirable, but the temperature increase may adversely affect the properties of the final product. Solving this contradiction provides the optimum processing conditions.

The mathematical model developed[288] included two stages of the process, i.e., mold filling and curing. However, the main focus was on to the second stage, because the filling time is short and does not effect the duration of the cycle as a whole or the maximum temperature increase. The latter two parameters were considered to be the most important ones. It was found that the initial temperature of the reactive mixture did not appreciably influence the residence time required to create the desired properties in the end product. Changing the mold temperature or the concentration of an activator leads to analogous results if a thin mold is used. In fact the temperature of the material inside a thin mold is nearly constant. With increase of the mold width, heat transfer becomes more difficult and there is a maximum effect of the reaction rate on the temperature increase, because the process approaches adiabatic conditions. Moreover, in a high temperature mold, the level of the temperature maximum is reduced. This occurs because the initial temperature increase for highly reactive compositions is explained primarily by the exothermal effect of the chemical reaction, since the heat input by conductive heat transfer from the wall is small; in this situation most of the heat generated by reaction corresponds to the initial increase in temperature.

A simple calculation method, which takes into account the fountain effect, was proposed.[289] In this approach the flow is assumed to be laminar and unidimensional. The front of the stream is regarded as straight (plane), perpendicular to the walls of the mold and moving with a constant average velocity v_{av}. Then the following dimensionless variables are introduced:

$$x^* = \frac{x}{l_f}; \quad z^* = \frac{2z}{H}; \quad v^* = \frac{V(z^*)}{v_{av}}$$

where x and z are axial and transverse coordinates, respectively; l_{fr} is the length of the mold filled by the material, i.e., the coordinate of the front (distance from the inlet up to the line of the front); H is width of the mold.

A coordinate of a point, containing liquid moving with velocity v_{av} is designated z^*_{av}. As the front line is assumed to be straight, the fountain effect is described by the assumption that transverse flow occurs along this line from the part of the cross-section where the velocity is high

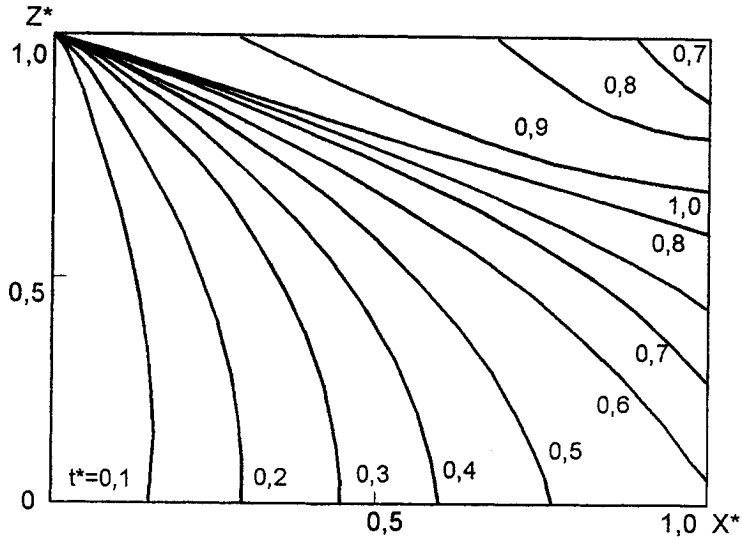

Figure 4.56. Pattern of time-space distribution of the residence time in filling of a mold by a Newtonian liquid. Figures on the curves are t^* values.

$(0 < z^* < z^*_{av})$, to the zone, where the velocity is low $(z^*_{av} < z^* < 1)$. Liquid particles reaching the front line at z^* (calculated from the axes) leave this point and return to the main stream at the point with a coordinate z^*_*. Then according to the mass balance the following equality is holds:

$$\int_0^{z^*_*} (v^* - 1)dz^* = \int_{z^*_*}^{1} (1 - v^*)dz^*$$

This equality represents the net effect of fountain flow. For a Newtonian liquid we have:

$$v^* = \frac{3}{2}[1 - (z^*)^2]; \quad z^*_{av} = \frac{1}{\sqrt{2}}$$

These two relationships yield the following differential equation:

$$(z^*_*)^3 - z^*_* + z^* - (z^*)^3 = 0$$

This equation has an analytical solution, which allows us to check the correctness of the proposed approach. To do this, the authors calculated lines of movement of tracers and compared the results with other published data,[47,284] where the same effect was studied using more complicated models

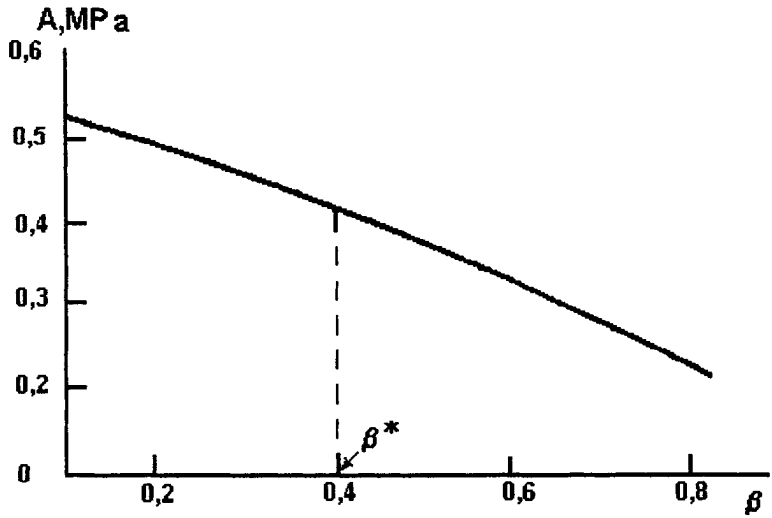

Figure 4.57. Dependence of the adhesive strength on the degree of conversion on a boundary surface.

and computer methods. The comparison demonstrated that the simplified approach did not provide the details although the net effect of fountain flow was represented adequately.

In the investigation,[288] all liquid particles were divided into three groups. The first group consisted of particles which entered the mold first; i.e., at $t = 0$ they form the front line. These particles had the maximum residence time. The second group consisted of particles which did not reach the front at all. The third was an intermediate group, and included particles which entered the mold later than the particles of the first group but still reached the front of the stream. A diagram in the $x^* - z^*$ plane was constructed,[288] which showed positions of the particles of these three groups (Fig. 4.56). Calculations were carried out to determine the distributions of residence times for liquid particles of these three groups for a Newtonian and a non-Newtonian power-type liquid. If the kinetics of the chemical reaction is known, it is possible to find the distribution of the degrees of conversion.

The following equations were proposed[289] for the energy and mass balances when the reactive liquid occupies a mold (after flow is completed):

$$\frac{dT^*}{dt^*} = \frac{1}{Pe}\frac{2l_f}{H}\frac{\partial^2 T^*}{\partial (z^*)^2} + \frac{Da}{Pe}\frac{2l_f}{H}k^*(1 - c^*)^n$$

and

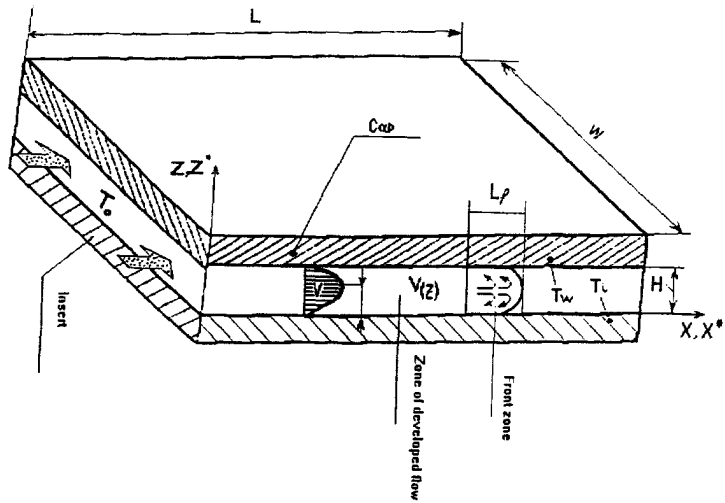

Figure 4.58. A scheme illustrating filling a plane cavity (see also Figure 4.52).

$$\frac{dc^*}{dt^*} = \frac{Da}{Pe}\frac{2l_f}{H}k^*(1-c^*)^n$$

where Da and Pe are the Damköhler and Peclet Numbers, respectively; a star * indicates dimensionless (reduced) variables. The reaction rate in this model is described by an nth order kinetic equation.

For the range of variables encountered in reactive processing, the Peclet Number values are rather large, which makes it is possible to neglect conductive heat transfer. We can then assume that the temperature and the degree of conversion for any liquid particle depend on residence time inside the mold only, and the curves of constant residence time in $x^* - z^*$ coordinates are also curves of constant temperature and constant degree of conversion.[289] Clearly, this approach is applicable for processes with short mold filling times and negligible conductive heat transfer.

Let us illustrate the main theoretical results by discussing a mold-filling model when the mold contains a metal insert to be coated with a polyurethane compound.[266] Two principal conditions must be met in this case. First, the total pressure drop must not exceed the limiting power of the molding machine. Second, the degree of conversion of the reactive mass at the moment of contact with the surface of the insert must not be higher than some critical level β_{lim}, which is determined by the requirement for sufficient adhesion between the polymer and the metal, because the adhesive

strength depends on the degree of conversion (Fig. 4.57, see also experimental data in Fig. 4.13). It is assumed that ideal mixing of components of a reactive mass proceeds before entering the mold, so that the liquid filling the mold is homogeneous and its properties at the inlet do not change with time.

Recall that we are discussing the process of covering the cylindrical metal surface of an insert with a polyurethane coating. The thickness of the coating is much less than the diameter of the insert and thus the mold, which is the gap between the metal insert (lower part of the diagram in Fig. 4.58) and the cap (upper part of the scheme in Fig. 4.58) can be considered as flat and rectangular (as was shown in Fig. 4.52 and with some additional details in Fig. 4.58). Its dimensions are: length L, width H, transverse dimension W, equal to $2\pi R$, where R is the radius of the insert. We have $W/H >> 1$ and $L/H >> 1$, so the stream is assumed to be two-dimensional.

In accordance with the usual process conditions, the initial temperature of the reactive mixture T_0 and the upper cap temperature T_w are constant during filling, and the temperature of the insert T_i equals the ambient temperature (20^oC). The model takes into account that during filling the temperature of the insert increases due to heat transfer from the reactive mix. It is assumed that the thermal properties and density of both the reactive mass and the insert are constant. It is reasonable to neglect molecular diffusion, because the coefficient of diffusion is very small;[264] therefore, the diffusion term is negligible in comparison with the other terms in the mass balance equation.

Three zones coexist during mold filling:[290] the inlet region, the main (fully developed) stream and the front of the stream. The initial reactive mass can be assumed to enter the mold continuously and uniformly through the inlet cross-section, so that inlet effects can be neglected. Flow inside the mold is non-isothermal, and the viscosity depends on the temperature and the degree of conversion. Therefore, changes in the flow profile (changes in the axial component of velocity and the appearance of a transverse velocity component) along the mold are inevitable. However, as $L/H >> 1$, it is easy to prove that in the region of developed flow, the axial component of velocity v is much larger than the transverse velocity, and the latter can be ignored. Therefore the trajectories of the liquid particles in the mold can be considered to be straight and parallel to the axis of its long axis. This is not true for the frontal zone because the fountain effect results in obligatory two-dimensional flow[123] and "fresh" portions of mix are taken from the central part of a stream to the mold walls (as shown in Fig. 4.58). Clearly, this influences the temperature and degree of conversion. An exact description of flow in this zone requires the solution of a flow problem involving a free surface.[291] Marker techniques and finite element methods can be used for this purpose. However, even if we ignore the changes in the liquid properties and heat and mass transfer phenomena at the front, attempts to find an exact solution lead to considerable complications in the model. Meanwhile, simplified calculation methods involving analytical simulation of the flow in the front zone based on experimental data appear to be quite adequate for solving applied problems.

Flow patterns are different in the three main zones of the stream. Therefore, it is reasonable to search for separate solutions for each zone and then to join solutions at the zone boundaries. The three governing equations for the main stream zone can be written on the following form:

momentum balance equation:

$$\rho\frac{\partial v_x}{\partial t} = -\frac{\partial P}{\partial x} + \frac{\partial}{\partial z}[\eta(\beta,T)\frac{\partial v_x}{\partial z}] \qquad [4.30]$$

energy balance equation:

$$\frac{\partial T}{\partial t} + v_x\frac{\partial T}{\partial x} = \frac{\lambda}{C_p\rho}\frac{\partial^2 T}{\partial x^2} + \frac{Q_p k_0}{C_p\rho} f_\beta(\beta)e^{-U/RT} \qquad [4.31]$$

kinetic equation:

$$\frac{\partial \beta}{\partial t} + v_x\frac{\partial \beta}{\partial x} = k_0 f_\beta(\beta)e^{-U/RT} \qquad [4.32]$$

The condition that the feed rate G_0 = const must be included in the system of equations:

$$\int_0^H v_x dz = G_0 \qquad [4.33]$$

where U and k_0 are parameters of the kinetic equation; $f_\beta(\beta)$ is a phenomenological kinetic function; Q_p is the heat of polymerization; H is the height of the mold (the gap between the insert and the cap). All other symbols used in these equations are as usual. The momentum balance equation can be easily transformed into a dimensionless form:

$$\frac{H}{L}\,Re\,\frac{\partial v^*}{\partial t^*} = \frac{\partial p^*}{\partial x^*} + \frac{\partial}{\partial z^*}[\eta(\theta,\beta)\frac{\partial v^*}{\partial z^*}] \qquad [4.34]$$

where θ and β and all variables marked with a star are dimensionless, and $Re = \rho v_{av}H/\eta$ is the Reynolds Number.

It is reasonable to assume that in the vast majority of cases encountered in reactive processing $Re << 1$ and $(H/L)Re << 1$. Thus, we can consider the flow to be quasi-stationary and that temperature changes occur quickly after alterations in the temperature and degree of conversion distributions.[202] Now we can rewrite the system of balance equations in the following dimensionless form:

momentum balance equation:

$$\frac{dP^*}{dx^*} = \frac{\partial}{\partial z^*}[\eta^*(\theta,\beta)\frac{\partial v^*}{\partial z^*}] \qquad [4.35]$$

energy balance equation:

$$\frac{\partial\theta}{\partial t^*} + v^*\frac{\partial\theta}{\partial x^*} = \frac{1}{Gz}\frac{\partial^2\theta}{\partial z^{*2}} + \frac{Da}{\gamma} f\beta(\beta)e^{\theta/(1+v\theta)} \qquad [4.36]$$

kinetic equation:

$$\frac{\partial\beta}{\partial t^*} + v^*\frac{\partial\beta}{\partial x^*} = Daf\beta(\beta)e^{\theta/(1+v\theta)} \qquad [4.37]$$

constancy of output:

$$\int_0^1 v^* dz^* = 1 \qquad [4.38]$$

In addition, it is necessary to use the equation for the dependence of viscosity on the degree of conversion and temperature:

$$\eta(\theta,\beta) = \varphi(\beta)e^{-\sigma\theta/(1+v\theta)} \qquad [4.39]$$

Dimensionless variables and groups entering all these equations are defined in the following manner:

$$x^* = \frac{x}{L};\quad Z^* = \frac{z}{H};\quad t = \frac{tv_{av}}{L};\quad P^* = \frac{P}{P_0};\quad \theta = \frac{U}{RT_0^2}(T - T_0);\quad \eta^* = \frac{\eta}{\eta_0};\quad v^* = \frac{v_x}{v_{av}};$$

$$Da = \frac{k_{\beta,T}L}{v_{av}};\quad Gz = \frac{v_{av}H^2C_p\rho}{\lambda L};\quad \gamma = \frac{RT_0^2C_p\rho}{UQ_p};\quad v = \frac{RT_0}{U};\quad v_{av} = \frac{Q_0}{WH};\quad \eta_0 = \eta(T_0,\beta_0)$$

$$\varphi(\beta) = \left(\frac{\beta}{1-\beta}\right)^b;\quad k_{\beta,T} = k_0e^{-U/RT};\quad P_0 = \frac{GL\eta_0}{WH^3}$$

where T_0 and β_0 are the temperature and the degree of conversion at the inlet section. The temperature distribution in the surface layer of the insert (of width H_i) is described by the following balance equation:

$$\frac{\partial T}{\partial t} = a_i\left(\frac{\partial^2 T}{\partial z_i^2} + \frac{\partial^2 T}{\partial x^2}\right) \qquad [4.40]$$

where a_i is the coefficient of thermal conductivity of the insert material and z_i is a coordinate coinciding with the z-axis but with the origin at $z_i = -H_i$. By taking into account the condition $(H_i/L) << 1$, it is possible to neglect the conductive heat transfer along the x-axis, and to use the following dimensionless form of Eq. (4.40):

$$\frac{\partial\theta}{\partial t^*} = a^* \frac{\partial^2\theta}{\partial z_i^2} \qquad [4.41]$$

where $a^* = a_i L/v_{av}H^2$ is the reciprocal of the Graetz Number; z_i^* is a dimensionless coordinate for the insert. The initial conditions for the system of Eqs. (4.35) - (4.37) and (4.41) are:
at $t = 0$

$$\theta(x,z) = 0; \quad \beta(x,z) = \beta_0; \quad \theta(x,z_i) = 0$$

The boundary conditions are:
at $z^* = 0$ and at $z^* = 1$

$$v(x,z) = 0$$

at $x^* = 0$

$$\theta(x,z) = 0; \quad \beta(x,z) = \beta_0;$$

at $z^* = 0$

$$\frac{\partial\theta}{\partial z^*} = 0$$

If the temperature of the upper cap (Fig. 4.58) T_w is constant, then the heat exchange condition at the cap - polymer boundary (at $z^* = 1$) can be written as:

$$\theta(x,z) = \theta_w \qquad [4.42]$$

where θ_w is the dimensionless temperature of the cap. Heat exchange through the polymer - insert boundary (at $z^* = 0$ and $z_i^* = 1$) is determined by the following equalities:

$$\theta(x^*,z^*) = \theta(x^*,z_i^*); \quad \frac{\partial\theta(x^*,z^*)}{\partial z^*} = a_r \frac{\partial\theta(x^*,z^{*_i})}{\partial z_i^*} \qquad [4.43]$$

where $a_r = (\lambda_i/\lambda)(H/H_i)$ is the "reduced" coefficient of thermal conductivity and λ_i is the thermal conductivity of the insert material.

The system of equations with initial and boundary conditions formulated above allows us to find the velocity distributions and pressure drop for the filled part of the mold. In order to incorporate effects related to the movement of the stream front and the fountain effect, it is possible to use the velocity distribution obtained[285] for isothermal flow of a Newtonian liquid in a semi-infinite plane channel, when the flow is initiated by a piston moving along the channel with velocity u_0 (it is evident that u_0 equals the average velocity of the liquid in the channel). An approximate quasi-stationary solution can be found. Introduction of the function ψ, transforms the momentum balance equation into a biharmonic equation. Then, after some approximations, the following solution for the function ψ was obtained:[285]

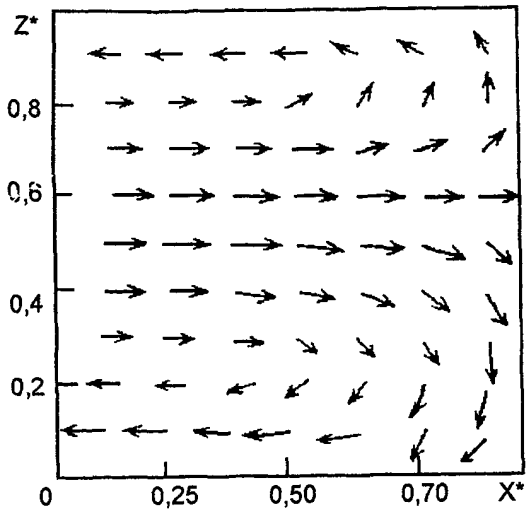

Figure 4.59. Distribution of the relative velocity vector in the front region during mold filling.

$$\psi = \frac{u_0 z^*}{2}\left[1 - \left(\frac{z^*}{H}\right)^2\right](1 - e^{-x5^{1/2}/H} \qquad [4.44]$$

The meaning of the symbols is the same as above.

This equation can be used as a basis for calculating the velocity components in the plane front zone. Analysis of this equation shows that, at a distance $x^* = H$ from the surface of the piston, the flow can be treated as unidimensional to within an error of less than 1%. Then, based on this result, we can assume that the length of the front zone l_f (Figs. 4.52 and 4.58) equals H and that the line dividing the stream into main and frontal zones is positioned at this distance from the front. The stream can be treated as unidimensional up to this line.

Now let us introduce dimensionless variables for the front zone:

dimensionless velocity components

$$u_x^* = \frac{u_x}{u_0}; \quad u_z^* = \frac{u_z}{u_0}$$

where u_x and u_z are the velocity components; x* is the dimensionless longitudinal coordinate:

$$x^* = \frac{x}{l_f}$$

The x^* axis coincides with the x-axis; its origin is located at the boundary between the two zones and is moving together with a flowing liquid (Fig. 4.58).The distribution of the axial velocity component in the front zone $u_x(z)$ at the line dividing the two zones is the same as the velocity distribution v(z) for the main stream. Below this boundary, the distribution of velocities will be designated as $v_f(z)$. Let the viscosity of a liquid through the front zone be constant. Then the component u_z^* is found from the following equation:

$$u_z^*(x^*,z) = [v_f(z) - 1][1 - e^{-(1-x^*)5^{1/2}}] + 1 \qquad [4.45]$$

This equation shows that $u_z^*(z) = v_f(z)$ at $x^* = 0$ and $u_z^*(z) = 1$ at $x^* = 1$; i.e., u_x is equal to the average velocity v_{av}. Now we need the balance equation:

$$l_f^* \frac{\partial u_x^*}{\partial x^*} + \frac{\partial u_z^*}{\partial z^*} = 0 \qquad [4.46]$$

where $l_f^* = l_f/H$ is the dimensionless length of the front. Finally, we can write the equation for the u_z distribution:

$$u_z(x^*,z) = \frac{5^{1/2}}{l_f^*} e^{-(1-x^*)5^{1/2}} \left[\int_0^z v_f(z)dz - z \right] \qquad [4.47]$$

Fig. 4.59 illustrates the flow pattern determined by Eqs (4.45) and (4.47). The distribution of the velocity vectors is shown for the case when the axial velocity component equals (u_x^*- 1). Eqs. (4.45) and (4.47) allow us to find temperature and degree of conversion distributions in the frontal zone based on the fundamental balance equations. These equations differ from Eqs. (4.36) and (4.47) because they take into account convective heat transfer along the z-direction. The dimensionless forms of the main determining equations are as follows:

energy balance

$$l_f^* \frac{H}{L} \frac{\partial \theta}{\partial t^*} + u_x^* \frac{\partial \theta}{\partial x^*} + u_z^* l_f^* \frac{\partial \theta}{\partial z^*} = l_f^* \frac{H}{L} \frac{1}{Gz} \left[\frac{\partial^2 \theta}{\partial z^{*2}} + \frac{1}{l_f^*} \frac{\partial^2 \theta}{\partial x^{*2}} \right] + Da \frac{l_f^* H}{\gamma L} f(\beta) e^{\theta/(1+v\theta)} \qquad [4.48]$$

kinetic equation

$$l_f^* \frac{H}{L} \frac{\partial \beta}{\partial t^*} + u_x^* \frac{\partial \beta}{\partial x^*} + u_z^* l_f^* \frac{\partial \beta}{\partial z^*} = Da\, l_f^* \frac{H}{L} f(\beta)\, e^{\theta/(1+v\theta)} \qquad [4.49]$$

where the meaning of all symbols is the same as before. The temperature and degree of conversion distributions at the boundary between the frontal and the main stream zones are determined from the solution for the main stream, i.e., at $x = x_f$ and at $x^* = 0$:

$$\theta(x,z) = \theta(x^*,z); \quad \beta(x,z) = \beta(x^*,z) \qquad [4.50]$$

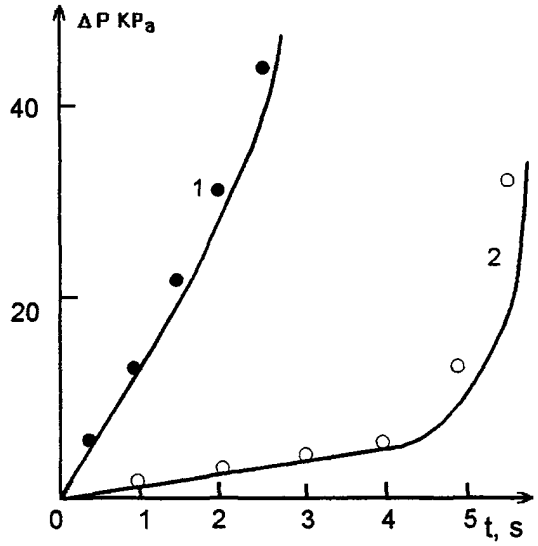

Figure 4.60. Changes in pressure drop during the process of filling a mold. Points - experimental. Curves are calculated for two different processing regimes.

This system of equations allows us to take account of the flow in the frontal zone and the influence of the fountain effect on the distributions of variables in the main stream zone. The equations for this rather complicated model can be solved numerically by computer. Comparison of the calculations with experimental data shows that the maximum deviations of the predicted values from the experimental points do not exceed 15% (Fig. 4.60).

For known values of the parameters in the kinetic equation for a specific reactive mix, it is easy to calculate the dimensionless factors γ and ν. Then the flow pattern in the mold filling process is completely determined by the dimensionless Da and Gz Numbers and the boundary conditions. The Damköhler Number characterizes the ratio of the rates of chemical reaction and convective heat transfer and the Graetz Number is a measure of the ratio of the convective heat flux due to a moving liquid to the heat flux due to the conductivity of the liquid.

We have discussed the use of reactive processing for coating a metal surface with a polymeric layer. In this case, the main quality criterion for the process is the provision of adequate adhesion between the polymer and the metal. To achieve this the process must provide the appropriate degree of conversion at the metal-polymer boundary at the moment of termination of mold filling. This must not exceed a certain critical level, which, according to Fig. 4.57, this level is $\beta^* = 0.4$. This, then, is the principal limitation in the choice of process parameters: the maximum degree of conversion at the metal surface during filling must not exceed 0.4.

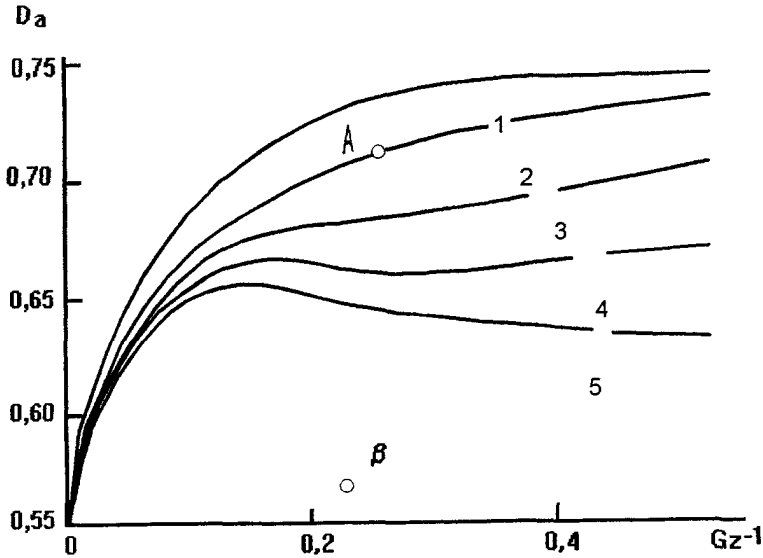

Figure 4.61. Dependence of the limiting values of the Damköhler Number on the reciprocal Graetz Number at $\beta^* = 0.4$. $T_0 = 40^\circ C$. Temperature of the mold: 20°C (1); 40°C (2); 50°C (3); 60°C (4) and 70°C (5).

As an example, let us analyze mold filling with a model polyurethane formulation. Let the kinetics of curing be described by an equation with the self-deceleration term (as was discussed above). The following values of the parameters were used: U = 49.1 kJ/mol; $k_0 = 3.8 \times 10^6$; $\xi = 1.1$; $\Delta T_{max} = 25.8^\circ C$ where ΔT_{max} is the maximum expected increase in temperature for adiabatic curing.

From the mathematical model of the process of filling a mold containing a metal insert formulated above, we can construct a diagram that shows the dependence of the Damköhler Number on the reciprocal Greatz Number for a constant initial temperature of the reactive mass $T_0 = 40^\circ C$ for a range of mold temperatures. The results of the calculations are shown in Fig. 4.61. Values of the Da and Gz Numbers corresponding to the points in this figure define the limits for the filling process. The area below any curve contains the set of Da and Gz Numbers corresponding to degrees of conversion at the metal-polymer boundary less than the limiting value $\beta^* = 0.4$; i.e., this area represents permissible filling regimes for a specified mold temperature. The area above any curve corresponds to $\beta > \beta^*$ and indicates that attempts to carry out molding under these flow and temperature conditions would lead to poor adhesion.

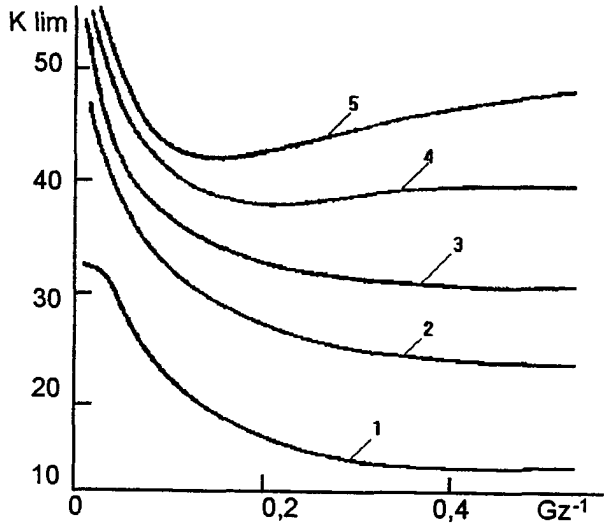

Figure 4.62. Dependence of the coefficient P_0 on Gz^{-1} at different mold temperatures: 20°C (1); 40°C (2); 50°C (3): 60°C (4); 70°C (5).

These results of theoretical calculations can be illustrated by the following example. Suppose we need to manufacture a cover 3 mm thick for an insert with the following dimensions: length L=1.5 m, diameter 0.25 m. The volume feed rate for mold filling is assumed to be $G_0 = 1\times10^{-4}$ m^3/s. Then for a reactive mixture with the kinetic parameters discussed above we obtain: Da=0.85 and $Gz^{-1} = 0.31$. As can be seen from Fig 4.61, the point with these coordinates lies above all the curves. This means that for any specified mold temperature T_m, the degree of conversion in the layer contacting the metal surface exceeds the critical level; therefore, the chosen volume feed rate is inadmissible, and we need to increase the output. At $G_0 = 1.2\times10^{-4}$ m^3/s we have Da = 0.71, and the corresponding point (point A in Fig. 4.61) lies on the limiting curve for $T_m = 40°C$. Consequently, the limiting value of the degree of conversion at the moment of complete filling reaches β^* at the contact layer. At $T_m = 20°C$, β is less than β^*, but at $T_m > 40°C$, β exceeds β^*. Increasing the feed rate up to $G_0 = 1.5\times10^{-3}$ m^3/s corresponds to a transition to the point with the coordinates Da = 0.56 and $Gz^{-1} = 0.21$ (point B in Fig. 4.61). The position of this point shows that reactive processing is possible for any mold temperature.

Industrial equipment use for reactive processing is limited by the permissible injection pressure. The model being discussed can also be used to estimate the pressure drop necessary to fill the mold. The pressure changes during the filling process, and the time dependence of the pressure is determined by the rheokinetic properties of the reactive mixture and the dimensions

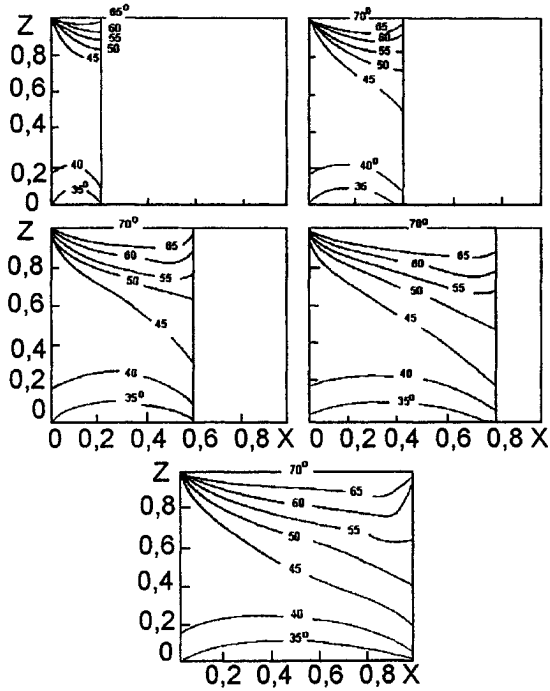

Figure 4.63. Isotherms for five positions of the stream front for a regime marked by point D in Figure 4.56.

sizes of the mold. At fixed values of the Da and Gz Numbers, the pressure drop may vary, depending on the value of the coefficient K, which characterizes the process parameters. The limiting values of this coefficient K_{lim} are shown in Fig. 4.62 as a function of Gz^{-1}, and K_{lim} is defined as:

$$K_{lim} = \frac{\Delta P_{lim}}{\Delta p}$$

where Δp is the predicted dimensionless pressure drop at termination of mold filling and ΔP_{lim} is the maximum permissible pressure drop in the processing equipment; as a general rule, ΔP_{lim} does not exceed 1 MPa.

If for any real situation $K < K_{lim}$, as determined from Fig. 4.62, then the pressure drop during processing will not exceed the permissible level. Fig. 4.62 also shows that decreasing Gz^{-1} and increasing the mold temperature results in a considerable increase in K_{lim}.

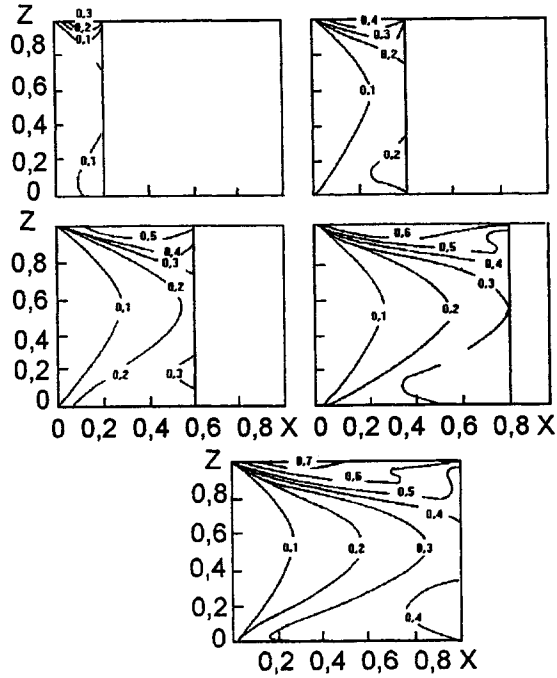

Figure 4.64. Lines of constant degrees of conversion for five positions of the stream front for a regime marked by point D in Figure 4.56.

Figs. 4.63 - 4.66 illustrate the location of lines of constant values of temperature, degree of conversion, velocity and viscosity for five consecutive positions of the front of a stream, which correspond to the following values of the axial coordinate x_f*: 0.2, 0.4, 0.6, 0.8, and 1.0. These lines of constant values of the process variables are calculated for the flow and property values designated by the point D in Fig. 4.61. In this case, the mold temperature T_m = 70°C, the initial temperature of the reactive mix T_0 = 40°C, and the initial temperature of the insert T_i = 20°C. An area above the horizontal line of symmetry of the mold cavity (i.e., the upper part of the cavity) contacts the "hot" surface of the mold and the lower part is in contact with the surface of the cooler metal insert. Thus, we can conclude that the distributions of temperature, degree of conversion, viscosity and velocity of movement of the reactive mix along the mold are related to the ratios between the transfer rate and the chemical reaction, which are characterized by the values of the Da and Gz Numbers.

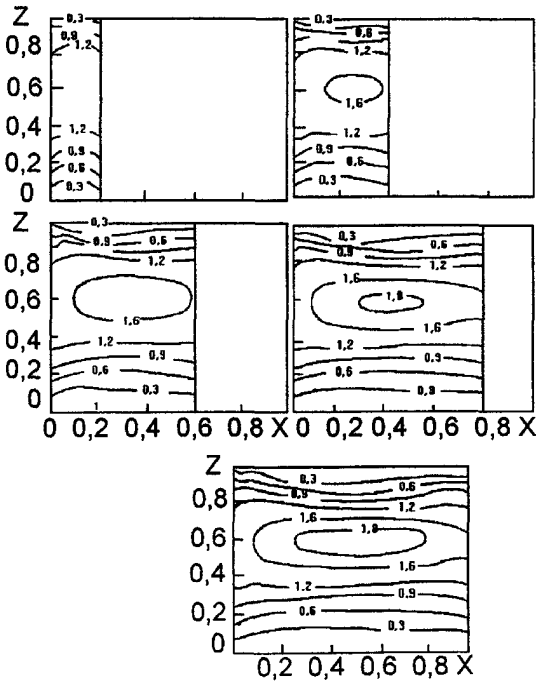

Figure 4.65. Lines of constant velocities for five positions of the stream front for a regime marked by point D in Figure 4.56.

4.9.6 PROCESSABILITY DIAGRAMS

The mathematical model discussed above allows us to find all the parameters of a technological process, such as changes in pressure and output, temperature distributions, and the degree of conversion. The determining factors are: the geometrical form and dimensions of the mold, the mold temperature, the initial temperature of the reactive mass, the rheokinetics of polymerization (curing), and the details of the processing equipment. This approach is very useful for detailed analysis of a technological process, but there are some difficulties in applying it to practical problems, because we need a lot of additional information before we can obtain the final quantitative results. Therefore, it would be convenient to generalize the results of experimental investigations and modelling in order to choose the main parameters in reactive processing and to establish their

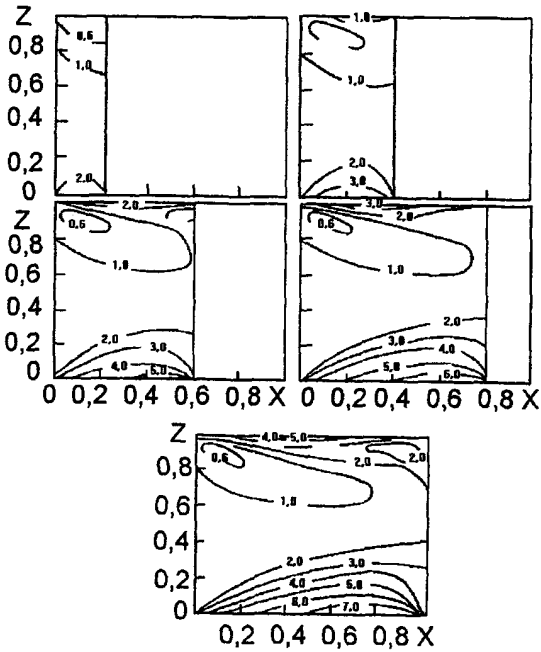

Figure 4.66. Lines of constant values of viscosity for five positions of the stream front for a regime marked by point D in Figure 4.56.

permissible limits. It would also be desirable to construct graphic diagrams which would clearly define the limits of variation of the process parameters for molding specific articles. These diagrams must exclude such undesirable effects as incomplete mold filling, thermal degradation of the polymer, unstable flow of the reactive mix in the mold, and so on. The final goal of the diagrams is to optimize the process for maximum output and quality of the end products.

These processibility diagrams have been devised for injection molding of thermoplastic materials[265] for correlating the temperature of the melt with the injection pressure (Fig. 4.67). The central area in this diagram characterizes the permissible processing regime for a specific polymer and mold. This area is bound by four curves. A polymer does not flow below the lower line (its temperature is too low). Thermal degradation takes place above the upper curve (the temperature is too high). To the right of the right-hand curve, the melt viscosity is too low, and the melt flows

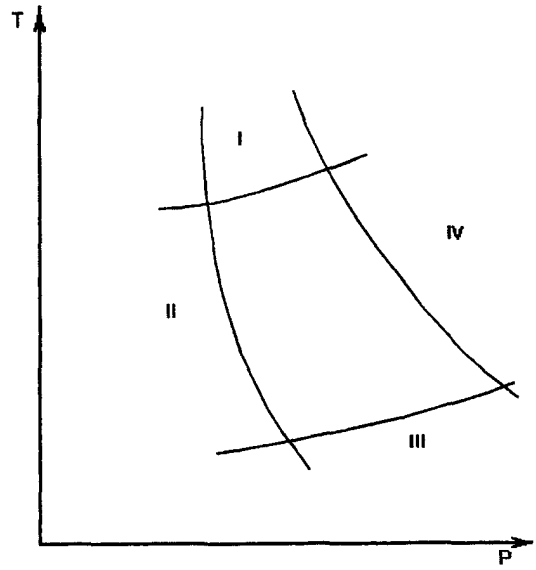

Figure 4.67. Processability diagrams (moldability) for injection molding of thermoplastic materials. I - thermal degradation zone; II - incomplete filling; III - melting; IV - burn. [Adapted, by permission, from Z. Tadmor, C. G. Gogos, *Princ. Polym. Process.*, (1979), 591.]

through all the gaps and clearances between the parts of the mold. To the left of the left-hand line, the fluidity of the melt is low or the pressure is insufficient to fill the mold. These diagrams are usually based on laboratory experiments using a "standard" spiral mold as a model.

Several methods for estimating processibility have also been proposed for reactive processing. For example, a processability diagram for the reactive processing of epoxy-based compounds derived experimental investigations is shown in Fig. 4.68.[292] Diagrams of this type are drawn for a specific reactive mix and for a "standard" plane rectangular mold of constant width. The determining factors are the initial temperature of the reactive mass and the mold temperature. There are some inadmissible regions shown in this figure. First (I), at temperatures below a certain limit, T_0, the quality of mixing of the reactive components is inadequate. Second (II), there is a region, where complete mold filling cannot be achieved. Third (III), the temperature of a reactive medium may exceed the permissible limit due to the exothermal effect of the reaction. Fourth (IV), the process may proceed too slowly, so that it becomes uneconomical.

These diagrams can be constructed for articles of different sizes. They show, areas corresponding to the recommended processing conditions and inadmissible values for the process parameters. As a general rule, an increase in article size results in a considerable contraction of the

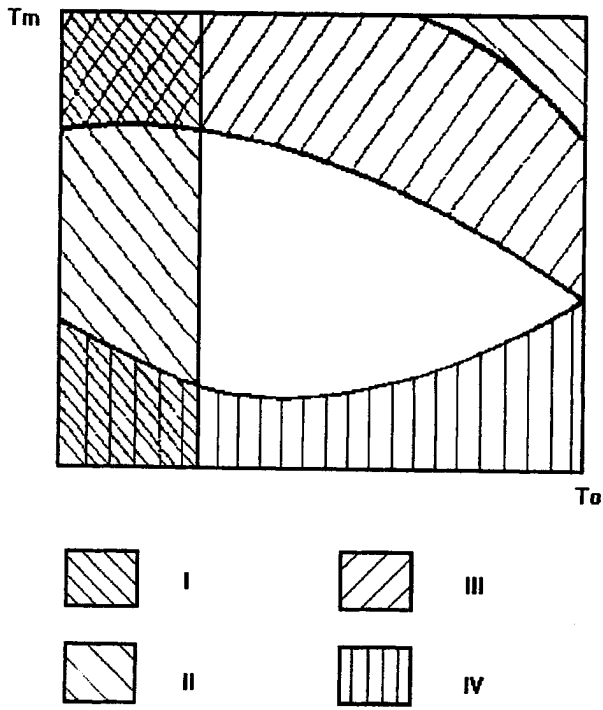

Figure 4.68. Diagrams for the choice of permissible values of mold temperature and initial temperature of a reactive mass. I - mixing; II - filling; III - T_{max} > temperature of degradation; IV - t > t_{max}. [Adapted, by permission from L. T. Manzione, J. S. Osinski, *Polym. Eng. Sci.*, **23** (1983), 583.]

recommended processing zone, whereas a decrease in articles size results in the opposite tendency. This effect is especially important at the curing stage; generally speaking, it is explained by the poor thermal conductivity of polymeric materials. Therefore, the curing process for thick articles takes place in near-adiabatic conditions with a significant temperature increase in the central part of the article. The temperature distribution is much more homogeneous in thin items due to the relatively intense heat exchange with the surroundings.

The prevention of premature gelation must be regarded as one of the most important criteria for choosing the technical parameters for mold filling.[293] The authors of the cited publication assume that predicting the maximum pressure increase is important primarily for injection molding of

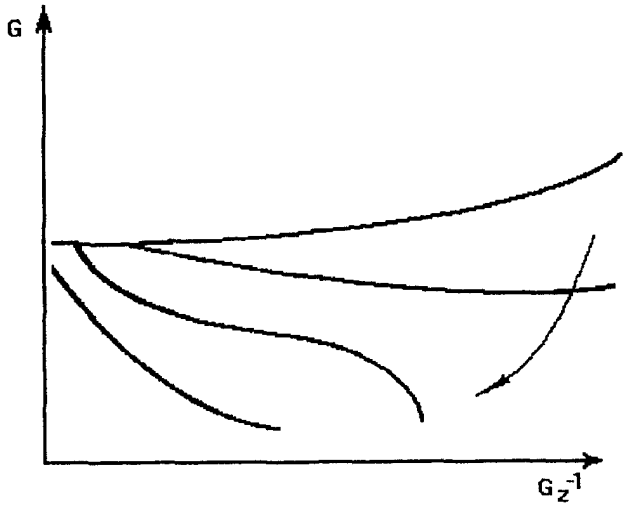

Figure 4.69. Nature of dependences of the gelation criterion G on the reciprocal Graetz Number at different mold temperatures. The arrow shows the direction of increasing wall temperature. T_0 = const. [Adapted, by permission from S. R. Esevez, J. M. Castro, *Polym. Eng. Sci.*, **24** (1984), 431.]

thermoplastic polymer materials. An intolerable increase in pressure during reactive processing can only occur due to premature gelation when the mold is partially filled. The set of determining factors for mold filling includes the following parameters: the Graetz Number, the gelation criterion[47] at the initial temperature T_0, and the mold temperature T_m. Based on the model of a thin rectangular cavity,[47] a processability diagram can be constructed like the one shown in Fig. 4.69.[293] The curves in this figure are the limiting values of the gelation criterion as a function of the reciprocal Graetz Number for different values of dimensionless mold temperatures and a constant initial temperature for the reactive mix. Each of these curves is the lower limit of a diagram of processability, corresponding to regimes excluding premature gelation due to incomplete filling.

This approach proved to be valid for modeling the mold filling process when thin coatings were prepared.[266] It was assumed that the main factor influencing the quality of the end product was the degree of conversion at the boundary surface, which provided the necessary adhesive strength. If this critical value of the degree of conversion is known, we can construct processability diagrams, which show the dependences of the Damköhler Number on the reciprocal Graetz Number

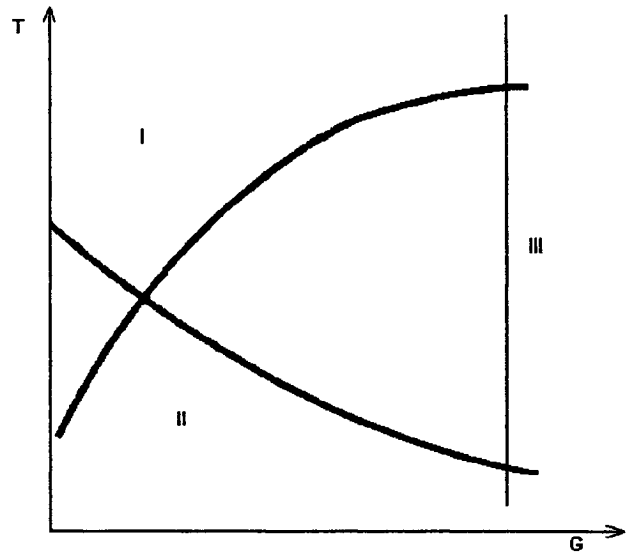

Figure 4.70. Processability diagram (moldability) for the stage of mold filling in reactive injection molding: dependence of material temperature (or average temperature on flow rate G). I - premature filling; II - poor impregnation mixing; III - flow instabilities.

(as in Fig. 4.61) at different mold temperatures and the chosen initial temperature of the reactive mix.

The curve $Da(Gz^{-1})$ is limiting, because it corresponds to process parameters, which provide the minimum necessary level of adhesive strength. The area below this curve (at a definite mold temperature T_m) corresponds to the Da and Gz^{-1} Numbers, for which the degree of conversion is less than the critical level; these parameters do not provide the maximum output. Points above this curve, represent inadmissible process parameters, which do not provide the required level of polymer-metal adhesive strength.

The dependence of the minimum time necessary to complete the molding process (when some limiting degree of gelation is reached), can be found as a function of the Damköhler number.[293] The latter also determines the maximum temperature of the material in the mold at different wall temperatures.

A different approach to constructing processability diagrams, shown schematically in Fig. 4.70, was proposed elsewhere[281] for reactive mixtures. Undesirable process parameters, which could lead to defects in processing during mold filling, are also shown. Relatively simple methods were proposed for constructing processability diagrams for reactive materials, and their predictions

fit the experimental data well.[47] The limiting curve, which characterizes the quality of mixing in preparing a reactive mixture, is represented via the Reynolds Number:[295]

$$Re = \frac{4G\rho}{\pi D\eta T_0} \qquad [4.51]$$

where G is the volume feed rate; η is the viscosity of the most viscous component in a mixture.

Curve II, representing the poor impregnation, is found from the gelation criterion. The limiting curve III for the regime of unstable flow depends on the average velocity v_{av}, which is calculated in a standard manner as

$$v_{av} = \frac{L}{t_f} \qquad [4.52]$$

where t_f is the time necessary to fill the mold, which, for polyurethanes depends on the polyol-to-isocyanate ratio in the reactive mixture. The limiting value of v_{av} was found experimentally.[296]

LIST OF SYMBOLS

Latin symbols

A, a	empirical constants in different equations
A	adhesive strength
A	impact strength
A_0	initial concentration of diamine
[A]	concentration of an activator
$[A]_0$	initial concentration of an activator
a	coefficient of temperature diffusivity
a_i	coefficient of thermal conductivity of an insert (in coating process)
a_r	reduced thermal conductivity
a_T	rate of increase (or decrease) in temperature
a_T	shift-factor (ratio of relaxation times at two temperatures)
B, b	empirical constants in different equations
B_0	coefficient of self-acceleration (in kinetics of crystallization)
[C]	concentration of a catalyst
C_p	specific heat
C, c	concentration of reagents (or functional groups)
C_0	initial concentration
c_0	constant of self-acceleration (in chemical kinetic equations)
c_1, c_1	empirical constants
D	geometrical size (depth)
E	modulus of elasticity in extension (Young's modulus)
E	apparent activation energy of viscous flow
E	empirical constant
F	different functions and empirical constants
F	total elastic potential function of a mixture (for a two-component material)
F_s, F_l	elastic potential functions for solid and liquid phases, respectively
f	front-factor
f	frequency
f	functionality of an activator
f	vector of body forces
f_0	main frequency
G	volume feed rate
G	modulus of elasticity (in shear)
G'	dynamic modulus
G_0	instantaneous shear modulus
G_∞	equilibrium modulus of elasticity
$G'_{\infty, 20}$	dynamic modulus at the end state at 20°C
g	vector of surface forces
H	geometrical size (height)
H	relaxation spectrum
H_S	Shore hardness
I_1	first invariant of the deformation tensor
K, k, k', k_1, k_2	empirical constants in different equations
k	coefficient of volume shrinkage
K_0	initial rate of a chemical reaction
K_0	instantaneous modulus of volume deformations

k_0	pre-exponential factor in a kinetic equation
$k_{0,T}$	initial rate of a reaction at temperature T_0
k_f, k_r	rate constants of direct (forward) and reverse reactions, respectively
L, l	geometrical sizes
l_f	length of the frontal zone
M_0	molecular weight of a monomer
[M]	concentration of a monomer
M_n	number-averaged molecular weight
M_w	weight-averaged molecular weight
$[M]_0$	initial concentration of a monomer
m	empirical constant
N, n	ordinal numbers
N_n	number-averaged degree of polymerization
n	empirical constant, exponent
P	pressure
P_0	initial pressure (at the inlet to a mold)
Q	heat (enthalpy) of a chemical reaction
Q_c	heat (enthalpy) of crystallization
Q_p	heat (enthalpy) of polymerization
q	heat flux
R	universal constant
[R]	concentration of reactive groups
$[R]_0$	initial concentration of reactive groups
$[R]_\infty$	final concentration of reactive groups
S	area of a surface
S_u, S_σ	parts of a surface in contact with surroundings with different boundary conditions
T	temperature
T_0	initial temperature
T_g	glass transition temperature
T_i	temperature of an insert (in coating process)
T_m	melting point
T_m	temperature of a mold
T_s	temperature at the surface
T_{sur}	temperature of surroundings
T_w	temperature at a wall
T^*	characteristic temperature
t	time
t^*	critical time (e.g. time of gelation)
t_0^*	"standard" (isothermal) induction period of curing, measured in static or quasi-static conditions
t_n^*	induction period for curing in nonisothermal conditions
t_g	time for glass transition (in curing)
U	apparent activation energy of a chemical reaction
u	velocity
u	displacement vector
u_0	velocity of a piston in a channel
u^*	dimensionless velocity
u_x, u_z	components of velocity
u_x^*, u_z^*	dimensionless components of velocity
V	volume

v	radius vector of the unit normal to the surface S_σ
v_{av}	average velocity
v_f	velocity of the front of a stream
v_x, v_r	axial and radial components of velocity
W	geometrical size (width of a mold)
w	maximum water absorption
x, y	arbitrary functions
x, y, z	Cartesian coordinates
Y	concentration of epoxy groups
z_0	size (half-width) of a plate

Dimensionless Numbers

a^*	reciprocal of the Graetz Number
Bi	Biot Number
Da	Damköhler Number
G	gelation criterion
Gz	Graetz Number
Pe	Pecklet Number
Re	Reynolds Number
δ	Frank-Kamenetzky criterion

Greek symbols

α	degree of crystallinity
α	thermal coefficient of linear expansion
α_s, α_1	thermal coefficients of linear expansion for solid and liquid phases, respectively
α_∞	equilibrium degree of crystallinity
α^*	reduced crystallinity (ratio of the current degree of crystallinity to its equilibrium value)
β	degree of conversion (in a chemical reaction)
β	dimensionless parameter (of different structure)
β^*	characteristic (critical) degree of conversion
β_c	"calorimetric" degree of conversion
β_{ch}	"chemical" degree of conversion
β_{th}	"thermal" degree of conversion
β_{rh}	"rheological" degree of conversion
β_∞	limiting degree of conversion
$\dot{\gamma}$	shear rate
$\Delta\alpha$	degree of transformation (in crystallization)
ΔG	relaxation part of modulus
ΔP	pressure drop
ΔP_{lim}	limiting pressure drop (process parameter)
ΔT_{max}	maximum (adiabatic) rise in temperature
δ	dimensionless shear rate
δ	loss angle (in periodic oscillations)
δ_{ij}	Kronecker symbol
ε	elongation at break
ε_0	linear deformation tensor
ε_i	elastic deformation tensor

ε_r	residual deformation
ε_∞	rebound elasticity
η	viscosity
η	initial viscosity of a reactive liquid
$[\eta]$	intrinsic viscosity
η_0	initial value of viscosity
η_0	viscosity of a monomer
θ	dimensionless temperature
θ	relative change in volume
θ	relaxation time
κ	heat transfer coefficient
λ	thermal conductivity
μ_s, μ_l	Poisson's ratio for solid and liquid phases, respectively
ν	dimensionless parameter
ξ	coefficient of self-deceleration (in chemical kinetic equations)
ξ	dimensionless parameter
ξ	empirical constant
ρ	density
Σ	electrical strength
σ	stress tensor
σ	components of stress tensor (with different number subscripts)
σ_b	strength limit in extension
τ	dimensionless or generalized time
τ^*	critical value of dimensionless time
τp	strength limit in bending
τ	dimensionless time of gelation in nonisothermal curing regime
Φ	total free energy
Φ_0, Φ_1	free energy corresponding to initial and final states of a material, respectively
ϕ	concentration
χ_s, χ_l	volume coefficients of thermal expansions of solid and liquid phases, respectively
ψ	function introduced for solving the balance equation for flow at the front of stream
ω	circular frequency
ω_0	main circular frequency

REFERENCES

1. Sekiguchi H., *Nippon Kagaky Zasshi*, **88**, 577 (1967).
2. Frunze T. M., *Uspekhi Khimii*, **48** (**10**), 1856 (1979).
3. Macosco C.W., *RIM Fundamentals of Reaction Injection Molding,* Oxford Univ. Press. (1989).
4. Gladyshev G.P., Popov V.A., *Radical Polymerization at High Degrees of conversions*, Nauka, Moscow (1974) - in Russian.
5. Boenig H.V., *Unsaturated polyesters*,
6. Sedov L.N., Mikhailova E.V., *Unsaturated polyesters*, Khimiya, Moscow (1977) - in Russian.
7. Updegraff I.H., *Handbook of Composites.* Ch. 2, *Unsaturated Polyester Resins.*
8. Yung S.E., *Progr. Org. Coat.*, **4** (**4**), 225 (1976).
9. *Polim. Tworz. Wielkoczastecak*, **29** (**10-12**), 424 (1984).
10. Rezenberg V.A., Oleinik E.F., Irzhak V.I., *Zh. Vsesoyuznogo Khim. Obshch. im. Mendeleeva*, **23**(**3**), 272 (1978).
11. Paquin A.M., *Epoxydverbinungen und Epoxydharze*, Berlin, Springer Verlag (1958).
12. Lee H., Neville C., *Handbook of Epoxy Resins,* N.-Y., McGraw-Hill (1967).
13. *Developments in polyurethanes - 1* (Ed. J.M. Buist), Applied Science Publ. Ltd, London (1978).
14. Wright P., Cumming A.P.C., *Solid Polyurethane Elastomers,* MacLaren & Sons, London (1969).
15. Lipatov Yu., Kercha Yu.Yu., Sergeeva L.M., *Structure and Properties of Polyurethanes*, Naukova Dumka, Kiev (1970) - in Russian.
16. Lipatova T.E., *Catalytic Polymerization of Polymers and Formation of Polymeric Networks*, Naukova Dumka, Kiev (1974) - in Russian.
17. Saunders J.H., Frish K.C., *Polyurethanes*, Interscience Publ., John Wiley and Sons, N.- Y. - London (1964).
18. Beghishev V.P., Starkov V.M., *Mekhanika Elastomerov*, Krasnodar, **3**, 60 (1980).
19. English L.K., *Mater. Engng.* **103** (**10**), 39 (1986).
20. Averko-Antonovich L.A., Kirpichnikov P.A., Smyslova R.A., *Polysulphone Oligomers and Sealants*, Khimiya, Leningrad (1983) - in Russian.
21. Enikolopov N.S., Vol'fson S.A., *Plasticheskie massy*, (**1**), 39 (1978).
22. Rozenberg B.A., Enikolopov N.S., *Zh. Vsesoyuznogo Khim. Obshch.im. Mendeleeva*, (**5**), 524 (1980).
23. Berlin A.A., Shutov F.A., *Foams Based on Reactive Oligomers,* Khimiya, Moscow (1978) - in Russian.
24. Matjika L., Haitman C., Macosco C.W., *J. Appl. Polym. Sci.*, **30**, 2787 (1985).
25. Vespoly N.P. Alberino L.M., *Polym. Process Eng.*, **3** (**1-2**), 127 (1985).
26. Tret'yakov Yu.D., *Vestnik Akadem. Nauk SSSR*, (**2**), 98 (1987).
27. Ivanova S.L., Kulichikhin S.G., Alkaeva O.F., Akimushkina N.N., Vyrskii Yu.P., Malkin A.Ya., *Vysokomol. soedin.*, **20A** (**12**), 2813 (1978).
28. Korshak V.V., Frunze T. M., Davtyan S.P., e.a., *Vysokomol. soedin.*, **21A** (**9**), 1960 (1979).
29. Malkin A.Ya., Ivanova S.L., Frolov V.G., Ivanova A.N., Andrianova Z.S., *Polymer*, **23** (**11**), 1791 (1982).
30. Malkin A.Ya., Ivanova S.L., Frolov C.G., Andrianova Z.S. *Vysokomol. soedin.*, **21A** (**3**), 632 (1979).
31. Malkin A.Ya., Frolov C.G., Ivanova A.N., Andrianova Z.S., Alekseychenko L.A., *Vysoko mol. soedin.*, **22A** (**5**), 995 (1980).
32. Malkin A.Ya., Ivanova S.L., Frolov V.G., Kulichikhin S.G., Beghishev V.P., *Plasticheskie massy*, (**4**), 28 (1980).

33. Camargo R.E., Gonzales V.M., Macosko C.W., Tirrell M., *Rubb. Chem. Techn.*, **56**, 744 (1983).
34. Sibal P.W., Camarago R.E., Macosko C.W., *Polym. Process Eng.*, **1(2)**, 147 (1984).
35. Lobst S.A., *Polymer Eng. Sci.*, **25**, 425 (1985).
36. Lin D.I., Ottino J.M., Thomas E.L., *Ibid.*, **25**, 1155 (1985).
37. Malkin A.Ya., Ivanova S.L., Korchagina M.A., *Vysokomol. soedin*, **19A (10)**, 2224 (1977).
38. Ivanova S.L., Korchagina M.A., *Plasticheskie massy*, **(8)**, 48 (1980).
39. Kulichikhin S.G., Ivanova S.L., Korchagina M.A., Malkin A.Ya., *Vysokomol. soedin.*, **24A (2)**, 430 (1982).
40. Kulichikhin S.G., Demina M.I., Frolov V.G., Malkin A.Ya., *Ibid.*, **30A**, (1988).
41. Kotel'nikov V.A., Danilovskaya L.V., Kurashev V.V., Frunze T. M., *Ibid.*, **29A (5)**, 395 (1987).
42. Vasil'ev N.I., Kholodenko B.V., Andrianova G.P., *Ibid.*, **26B (19)**, 72 (1984).
43. Vasil'ev N.I., Kholodenko B.V., Lyubimov V.K., Irzhak V.I., *Ibid.*, **27A(9)**, 1940 (1985).
44. Lipshitz S.D., Macosko C.W., *Polymer Eng. Sci.*, **16(2)**, 803 (1976).
45. Lipshitz S.D., Macosko C.W., *J. Appl. Polym. Sci.*, **21**, 2029 (1977).
46. Castro J.M., Lipshitz S.D., Macosko C.W., *AIChE Journal*, **28**, 973 (1982).
47. Castro J.M., Macosko C.W., *Ibid.*, **28(2)** 250 (1982).
48. Beghishev V.P., Bolgov S.A., Lavochnik Yu.B., Malkin A.Ya., *Vysokomol. soed.*, **27A (9)**, 1852 (1985).
49. Domine J.D., Gogos C.G., *Polymer Eng. Sci.*, **20**, 847 (1980).
50. Yokono H., Tsuzuku S., Hira Y., Gotch M., *Ibid.*, **25**, 959 (1985).
51. Hsu T.J., Lee L.J., *Ibid.*, **25**, 951 (1985).
52. Malkin A.Ya., Kulichikhin S.G., *Rheokinetics*, Hüthig & Wept, in press.
53. Apicella A., Nicolais L., Iannone M., Passavini P., *J. Appl. Polym. Sci.*, **29**, 2083 (1984).
54. Kulichikhin S.G., *Vysokomol. soed.*, **27A**, 2150 (1985).
55. Arutyunyan Kh.A., Davtyan S.P., Rozenberg B.A., Enikolopyan N.S. *Ibid.*, **16A (9)**, 2115 (1974).
56. Arutyunyan Kh.A., Davtyan S.P., Enikolopyan N.S., Rozenberg B.A., *Ibid.*, **17A (2)**, 289 (1975).
57. Otsubo Y., Amari T., Wataraba K., *J. Appl. Polym. Sci.*, **29**, 4071 (1984).
58. Tung C.M., Dynes P.J., *Ibid.*, **27**, 569 (1982).
59. Winter H.H., *Polymer Eng. Sci.*, **27**, 1698 (1987).
60. Gannani E., Higgis B.G., Powell R.L., *Ibid.*, **26**, 1563 (1986).
61. Gillham J.K., *Ibid.*, **19**, 676 (1979).
62. Enns J.B., Gillham J.K., *J. Appl. Polym. Sci.*, **28**, 2567 (1983).
63. Harran D., Laudonard A., *J. Appl. Polym. Sci.*, **32**, 6043 (1986).
64. Khramova G.I., Bolotnikova L.S., Zaitzev B.A., Panov Yu.N., *Plasticheskie massy*, **(5)**, 56 (1982).
65. Malkin A.Ya., Stolin A.M., Kulichikhin S.G., Mayzelia V.V., Avdeeva G.M., Puhgachevskaya N.F., Chopornuak S.G., *Mekhanika kompozit. mater.*, **(2)**, 362 (1980).
66. Han C.D., Lem K.-W., *J. Appl. Polym. Sci.*, **28**, 743 (1983).
67. Han C.D., Lem K.-W., *Ibid.*, **28**, 763 (1983).
68. Lem K.-W., Han C.D., *Ibid.*, **28**, 779 (1983).
69. Kamal M.R., Sourour S., *Polymer Eng. Sci.*, **13**, 59 (1973).
70. Kamal M.R., Ryan M.E., *Ibid.*, **20**, 859 (1980).
71. Kamal M.R., Sourour S., Ryan M.E., *Soc. Plast. Eng. Techn. Paper.*, **19**, 187 (1973).
72. Pasatcioglu S.Y., Fricke A.L., Hassler J.C., *J. Appl. Polym. Sci.*, **24**, 937 (1979).
73. Horie K., Mita I., Kambe H., *J. Polym. Sci.*, **A-1**, **8**, 2839 (1971).
74 Han C.D., Lem K.-W., *J. Appl. Polym. Sci.*, **28**, 3155 (1983).

75. Han C.D., Lem K.-W., *Ibid.*, **29**, 1879 (1984).
76. Lem K.-W., Han C.D., *Ibid.*, **28**, 3185 (1983.
77. Lem K.-W., Han C.D., *Ibid.*, **28**, 3207 (1983).
78. Yap C.Y., Williams H.L., *Polymer Eng. Sci.*, **22**, 254 (1982).
79. Shirokova L.G., Al'shitz I.M., Tsubina Kh.V., Golubkov A.G., *Plasticheskie massy*, (**7**), 35 (1979).
80. Frank-Kamenetskii D.A., *Diffusion and heat exchange in chemical kinetics*, Nauka, Moscow (1967) - in Russian.
81. Barzykin V.V., Merzanov A.G., *Doklady AN SSSR*, **120** (**6**), 1271 (1958).
82. Semionov N.N., *Uspekhi fiz. nauk*, **23** (**3**), 251 (1940).
83. Merzhanov A.G., Zelikman E.G., Abramov V.G., *Doklady AN SSSR*, **120** (**3**), 639 (1968).
84. Zelikman E.G., *Zh. fiz. khim.*, **43** (**1**), 236 (1963).
85. Manelis G.B., Smirnov L.P., *Fizika goreniya i vzryva*, (**5**), 659 (1976).
86. Chechilo N.M., Khvilitskii R.Ya., Enikolopyan N.S., *Doklady AN SSSR*, **204**, 1180 (1972).
87. Aruryunyan Kh.A., Davtyan S.P., Rozenberg B.A., Enikolopyan N.S., *Ibid.*, **223**(**3**), 657 (1975).
88. Beghishev V.P., Vol'pert V.A., Davtyan S.P., Malkin A.Ya. *Ibid.*, **279** (**4**), 909 (1984).
89. Maksimov E.I., *Teor. osnovy khim. tekhnol.*, **7** (**3**), 380 (1973).
90. Malkin A.Ya., Beghishev V.P., Keapin I.A., *Polymer*, **24** (**1**), 8(1983).
91. Beghishev V.P., Keapin I.A. Malkin A.Ya., *Vysokomol. soedin.*, **24B** (**9**), 656 (1982).
92. Malkin A.Ya., Beghishev V.P., Keapin I.A., *Polymer Eng. Sci.*, **24**, 13 (1986).
93. Malkin A.Ya., Keapin I.A., Bolgov S.A., Beghishev V.P., *Ing. fiz. zh.*, **46** (**1**), 124 (1984).
94. Ziabicki A., *Appl. Polym. Symposia*, (**6**), 1 (1967).
95. Ziabicki A., *Polimery*, **12**(**9**), 405 (1967).
96. Mandelkern L., *Crystallization of Polymers*, McGraw-Hill, N. Y., 1964.
97. Beghishev V.P., Keapin I.A. Andrianova Z.S., Malkin A.Ya., *Vysokomol. soedin.*, **25A** (**11**), 2441 (1983).
98. Beghishev V.P., Keapin I.A. Andrianova Z.S., Malkin A.Ya., *Ibid.*, **25B** (**5**), 343 (1983).
99. Malkin A.Ya., Beghishev V.P., Keapin I.A. Andrianova Z.S., *Polymer Eng. Sci.*, **24**, 1402 (1984).
100. Frunze T. M., Kurashev V.V., Kotel'nikov V.A., e.a., *Vysokomol. soedin.*, **20 B**(**3**), 206 (1978).
101. Davtyan S.D., Zhirkov P.V., Vol'fson S.A., *Uspekhi Khim.*, **53**, 251 (1984).
102. Beghishev V.P., Bolgov S.A., Malkin A.Ya., Subbotina N.I., Frolov V.G., *Vysokomol. soedin.*, **22 B**(**2**), 124 (1980).
103. Malkin A.Ya., Beghishev V.P., Bolgov S.A., *Polymer*, **23** (**3**), 385 (1982).
104. Kulichikhin S.G., Reutov A.S., Miroshnikova I.I., Minakov V.T., Malkin A.Ya., *Vysokomol. Soedin.*, **33** (**5**), 57 (1992).
105. Malkin A.Ya., *Polymer Eng. Sci.*, **20**(**6**), 1035 (1980).
106. Malkin A.Ya., *Uspekhi Khim.*, **50** (**1**), 137 (1980).
107. Kamal M.R., *Polymer Eng. Sci.*, **14** (**3**), 231 (1974).
108. Castro J.M., Macosco C.W., *Soc. Plast. Eng. Tech. Papers*, **26**, 434 (1980).
109. Malkin A.Ya., *Adv. Polymer Sci.*, **96**, 69 (1990).
110. Utracki L.A., Khanh T.Vu, "Filled polymers", Ch.7 in *Multicomponent Polymer Systems*, I. Miles and S. Rostami, Eds, Longman Sci. & Tech., Harlow, UK, 1991.
111. Dutta A., Ryan M.E., *J. Appl. Polymer Sci.*, **24** (**3**), 635 (1979).
112. Malkin A.Ya., *Plasticheskie massy*, (**4**), 47 (1982).
113. Malkin A.Ya., Beghishev V.P., *Rheol. Acta*, **Bd.21**(**4/5**), 629 (1982).
114. Malkin A.Ya., Beghishev V.P., *Polym. Process Eng.*, **1** (**1**), 41 (1983).
115. Sokolov A.D., *Plasticheskie massy*, (**7**), 43 (1979).

116. Malkin A.Ya., Merzhanov A.G., Frunze T. M., e.a. *Doklady AN SSSR*, **258**(**2**), 402 (1981).
117. Leonov A.I., Shwartz A.I., *Vysokomol. Soedin.*, **14A**, 695 (1972).
118. Danilkin N.N., Kanavets I.R., *Plasticheskie massy*, (**1**), 29 (1970).
119. Malkin A.Ya., Shuvalova G.I., *Vysokomol. soedin.*, **27B (11)**, 865 (1985) .
120. Malkin A.Ya., Kulichikhin S.G., *Makromol. Chem., Macromol. Symp.*, **68**, 301 (1993).
121. Bostandzhiyan S.A., Merzhanov A.G., Pruchkina N.M., *Zh. prikl. mekhaniki i tekhn. fiz*, (**5**), 38 (1968).
122. Malkin A.Ya., Zhirkov P.V., *Teor. osnovy khim. tekhn.*, **20** (**6**), 784 (1986).
123. Rose W., *Nature*, **191**, 242 (1961).
124. Bigg D.M., *2-nd Annual Technical Conference SPE: Technical Papers*, San Francisco, 301 (1974).
125. Castro J.M., Macosco C.W., *AIChE Journal*, **29** (**3**), 373 (1983).
126. Lekakou C.N., *Polymer Eng. Sci.*, **26** (**18**), 1264 (1986).
127. Pozdeev A.A., Nyashin Yu.I., Trusov P.V., *Residual Stresses*, Nauka, Moscow (1982) - in Russian.
128. Moskvitin V.V., *Mechanics of Visco-ElasticMmaterials*, Nauka, Moscow (1972) - in Russian.
129. Day W.A., *The Thermodynamics of Simple Materials with Fading Memory*, Springer Tracks on Natural Philosophy, **22**, Berlin (1972).
130. Kastner S., *Polymer*, **20** (**11**), 1322 (1979).
131. Lee E.N., Rogers T.G., *J. Appl. Mech.*, **32** (**4**), 874 (1965).
132. Coxon L.D., White J.R., *J. Mat. Sci.*, **14**, 1114 (1979).
133. Lee S., Vega J., Bogue D.C., *J. Appl. Pol. Sci.*, **31**(**8**), 2791 (1986).
134. Indenbom V.L., in *Fizika tverdogo tela*, AN SSSR, Moscow- Leningrad, v.**1** (1959).
135. Bolotin V.V., Vorontsov A.N., *Mekhanika polimerov*, (**5**), 790 (1976).
136. Turusov R.A., Davtyan S.P., Shkadinski K.G., e.a., *Doklady AN SSSR*, **247** (**1**), 97 (1979).
137. Klychnikov L.V., Davtyan S.P., Khudyaev S.I., Enikolopyan N.S., *Mekhanika kompozit. mater.*, (**3**), 609 (1980).
138. Turusov R.A., Rozenberg B.A., Enikolopyan N.S., *Doklady AN SSSR*, **260**(**1**), 90 (1981).
139. Klychnikov L.V., Davtyan S.P., Khudyaev S.I., Enikolopyan N.S., *Mekhanika kompoz. mater.*, (**4**), 673 (1985).
140. Shaffer B.W., Levitsky M., *Trans. ASME*, Ser.E, **96**, 652 (1974).
141. Levitsky M., Shaffer B.W., *J. Appl. Mech.*, (**9**), 654 (1975).
142. Balandin G.F., Introduction to the theory of slab formation. Part 2: *Formation of Macrostructure*, Mashinostroenie, Moscow (1979) - in Russian.
143. Malkin A.Ya., Beghishev V.P., Shardakov I.N., Shadrin O.A., Bolgov S.A., *Vysokomol. soedin.*, **29A** (**9**), 1992 (1987).
144. Beghishev V.P., Bolgov S.A., Malkin A.Ya., *Vysokomol. soedin.*, **21B** (**9**), 714 (1979).
145. Lavochnik Yu.B., Beghishev V.P., Shadrin O.A., *Stress-Strain State and Strength of Designs*, Ural NTS, Sverdlovsk, 129 (1982) - in Russian.
146. Birger I.A., Residual stresses, Mashgiz, Moscow (1963) - in Russian.
147. Malkin A.Ya., e. a., *Experimental Methods of Polymer in Physics*, Prentice-Hall (1983).
148. Lewis A.F., Gillham I.K., *J. Appl. Polym. Sci.*, **7**(**2**), 685 (1963).
149. Isaev A.I., Konstantinov A.A., Kulakov A.K., *Mekhanika polimerov*, (**3**), 541 (1976).
150. Malkin A.Ya., Beghishev V.P., Mansurov V.A., *Vysokomol. soedin.*, **26B** (**4**), 869 (1984).
151. Malkin A.Ya., Beghishev V.P., Mansurov V.A., *Vysokomol. soedin.*, **27A** (**7**), 1551 (1985).
152. Malkin A.Ya., Bolgov S.A., Beghishev V.P., Mansurov V.A., *Rheol. Acta*, **31**, 345 (1992).
153. Holly E.E., Venhataraman K., Chambon F., Winter H.H., *J. Non-Newtonian Fluid Mech*, **27** (**17**), 7 (1988).

154. Malkin A.Ya., Mansurov V.A., Beghishev V.P., *Vysokomol. soedin.*, **29A** (3), 663 (1987).
155. Vinogradov G.V., Malkin A.Ya., *Rheology of Polymers*, Springer, Heidelberg (1980).
156. *USSR Inventor's Certificate* **1 242 756**.
157. Calvet E., Prat H., *Microcalorimetrie. Applications physico-chimiques et biologiques*, Masson, Paris (1956).
158. Muzovskaya N.Yu., Kuznetsov V.V., Tikhomirova N.S., Chalykh A.E., Malkin A.Ya., *Vysokomol. soedin.*, **26A** (5), 1110 (1984).
159. Arsenin V.Ya., Ivanov V.V., *Radiotekh. i elektronika*, (1), 167 (1969).
160. Malkin A.Ya., Beghishev V.P., Bolgov S.A., Mansurov V.A., *Vysokomol. soed.*, **31A** (1), 208 (1989).
161. Otnes R.K., Enochson L., *Applied time Series Analysis. Basic Techniques*, New York (1978).
162. Pavlov P.A., *Dynamics of Boiling of Highly Superheated Liquids*, Ural Branch AN SSSR, Sverdlovsk (1988).
163. Skripov P.V., Beghishev V.P., Puchinskis S.E., Bolgov S.A., *Polym. Sci. USSR*, **34**, 85 (1992).
164. Skripov P.V., Puchinskis S.E., Beghishev V.P., Lipchak A.I., Pavlov P.A., *J. Appl. Polym. Sci.*, in press.
165. Skripov P.V., Nikitin E.D., Beghishev V.P., e.a., *Polymers in Extreme Environments: Conference Preprints*, London, P.29 (1991).
166. Skripov V.P., *J. Non-Equilib. Thermodyn.*, **17**, 193 (1992).
167. Biesenberger J.A., Sebastian D.H., *Principles of Polymerization Engineering*, John Wiley & Sons, New York, Chap. 6 (1983).
168. Skripov P.V., Puchinskis S.E., Pavlov P.A., Babushkin V.P., *5-th International Symposium on Solubility Phenomena*: Abstracts, P.89 (1992).
169. Choy C.L., *Polymer*, **18**, 984 (1977).
170. Ehntelis S.G., Evreinov V.Yu., Kuzaev A.I., *Reactive oligomers*, Khimia, Moscow (1985) - in Russian.
171. Morozov Yu.L., Sembaeva R.A., *Kauchuk i rezina*, (11), 33 (1978).
172. Marek O., Tomka M. *Akrylové Polymery*, Stàtní Nakladatelství Technické Literatury, Praha (1966).
173. *USSR Inventor's Certificate* **634961**.
174. *USSR Inventor's Certificate* **852895**.
175. Labutin A.L., *Anticorrosion and Germetic Materials Based on Synthetic Rubbers*, Khimiya, Leningrad (1982) - in Russian.
176. Lavochnik Yu.B., Beghishev V.P., *Synthesis and Properties of Network Polymers and Compositions*, Ural Branch AN SSSR, Sverdlovsk (1990) - in Russian.
177. Kostenko Yu.N., Kayan V.M., Korsunski V.S., Rastegaev P.S., *Plasticheskie massy*, (5), 25 (1972).
178. Malkin A.Ya. e.a., *Plasticheskie massy*, (9), 26 (1984).
179. Deiber J.A., *Ind. Eng. Chem. Fundam*, **15(2)**, 102 (1976).
180. Throne I.L., Gianchandani I., *Polym. Eng. Sci.*, **20(13)**, 899 (1980).
181. Hemmel H., Kesler H., Zendath S., *Kunststoffe*, **Bd.59(7)**, 405 (1969).
182. Schung Reiner, *Kunststoffe*, **Bd.59(6)**, 339 (1969).
183. *DDR Patent* **204891**.
184. *DDR Patent* **135825**.
185. Stolin A.M., Malkin A.Ya., Merzhanov A.G., *Uspekhi khimii*, **48(8)**, 1492 (1979).
186. Stolin A.M., Malkin A.Ya., Merzhanov A.G., *Polym. Eng. Sci*, **19(15)**, 1065 (1979).
187. Budtov V.P., Konsetov V.V., *Heat exchange in polymerization processes*, Khimiya, Leningrad (1983) - in Russian.

224. Schmidt M.J., Castro J.M., *Polymer Eng. Sci.*, **25 (9)**, 541 (1985).
225. Leferbe A.H., *Atomization and Sprays*, N.Y., Hemisphere Publ. Corp, (1989).
226. Dityatin Yu.F. et al, *Spraying of Liquids*, Moscow, Mashinostroyenie, (1977) - in Russian.
227. Khasuy A., *Technique of Spraying*, Moscow, Mashinostroyenie, (1975) - in Russian.
228. Wang X.F., Leferbe A.H., Martin C.A., *J. Propul. & Power*, **4(4)**, 293 (1988).
229. Gel'gand B.E. et al, *Doklady AN SSSR*, **316**, 355 (1991).
230. *USSR Inventor's Certificates* **567504** and **927324**.
231. *USSR Inventor's Certificates* **732641** and **939110**.
232. *FRG Application for Patent* **2537953** (1976).
233. *USSR Inventor's Certificate* **975104**.
234. *USSR Inventor's Certificate* **1171106**.
235. Lambla M., *Polymer Process Engng*, **5(3&4)**, 297 (1987-88).
236. *Fr Patent* **1243632**.
237. *GB Patent* **923137**.
238. *US Patent* **3860220**.
239. Hling G. *Kunststofftechnik*, (**10**), 351 (1968).
240. *USSR Inventor's Certificate* **674929**.
241. *Fr Patent* **2271917**.
242. *Fr Patent* **2271918**.
243. *Jp Patent* **53-4546**.
244. *USSR Inventor's Certificate* **4550017**.
245. *USSR Inventor's Certificate* **1348206**.
246. Pervadchuk V.P., Yankov V.I., Boyarchenko V.I., *Inzh. fiz. zh.*, **41(1)**, 94 (1981).
247. Savenkova O.V., Skulskiy O.I., Slavnov E.V., *Fluid Mechanics - Soviet Research*, **16(3)**, 128 (1987).
248. Bostandzhiyan S.A., Boyarchenko V.I., Kargapolova G.N., *Inzh. fiz. zh.*, **18(6)**, 1069 (1970).
249. *US Patent* **2057674**.
250. *USSR Inventor's Certificate* **274344**.
251. *USSR Inventor's Certificate* **522204**.
252. *USSR Inventor's Certificate* **446516**.
253. *USSR Inventor's Certificate* **1155606**.
254. *USSR Inventor's Certificate* **1174445**.
255. Zel'dovich Ya.B., *Zh. fiz. khim.*, **22**, 27 (1966).
256. Khaikin B.I., Merzhanov A.G., *Fizika goreniya i vzryva*, (**3**), 36 (1966).
257. Merzhanov A.G., Rumanov E.N., Khaikin B.I., *Zh. prikl. mekhaniki i tekhn. fiz.*, (**6**), 99 (1972).
258. Beghishev V.P., Vol'pert V.A., Davtyan S.P., Malkin A.Ya., *Doklady AN SSSR*, **279 (4)**, 909 (1984).
259. Morton-Jones D.H., *Dev. Inject. Mold*, **3**, 1 (1985).
260. Alberino L.M., *Polym. News*, **11**, 135 (1985).
261. Macosko C.W., *Plastics Engineering*, **25(4)**, 21 (1983).
262. Taneja U., Sharma K.K., *Popular Plastics*, **30(6)**, 36 (1985).
263. *USSR Inventor's Certificate* **937475**.
264. Broyer E., Macosko C.W., *AIChE Journal*, **22(6)**, 268 (1976).
265. Tadmor Z., Gogos C.G., *Principles of Polymer Processing, John Wiley & Sons, New York - Brisbane - Chichester - Toronto (1979).*
266. Lavochnik Yu.B., Beghishev V.P., *Dynamics of viscous liquids*, Ural Branch AN SSSR, Sverdlovsk (1987).

188. Shrenk L., Kuester J.L., *J. Appl. Polym. Sci.*, **18(12)**, (1974).
189. Vaganov D.A., *Zh. prikl. mekhaniki i tekhn. fiz.* (**2**), 168 (1975).
190. Pearson J.R.A., Shsh I.T., Viera E.S.A., *Chem. Eng. Sci.*, **28(11)**, 2079 (1973).
191. Merzhanov A.G., Stolin A.M., *Zh. prikl. mekhaniki i tekhn. fiz.*, (**1**), 65 (1974).
192. Zhirkov P.V., Estrin Ya.I., *Polym. Proc. Eng.*, **2(2/3)**, 219 (1984).
193. Maximov Eh.I., Peregudov N.I., Butakov A.A., *Fiz. goreniya i vzryva*, (**4**), 568 (1975).
194. Wallis J.P.A., Ritter R.A., Andre H.A., *AIChE Journal*, **21(4)**, 686 (1975).
195. Lynn S., *AIChE Journal*, **23(2)**, 387 (1977).
196. Fahien R.W., Stankowich I., *Chem. Eng. Sci.*, **34(11)**, 1350 (1979).
197. Ahmed M., Fahien R.W., *Ibid.*, **35(4)**, 889 (1980).
198. Ahmed M., Fahien R.W., *Ibid.*, 897.
199. Grishin A.M., Nemirovskii V.B., Panin V.F., *Fizika goreniya i vzryva*, (**2**), 156 (1977).
200. Sala R., Valz-Gris F., Zanderighi L., *Chem. Eng. Sci.*, **29(11)**, 2205 (1974).
201. Lynn S., Huff J.E., *AIChE Journal*, **17(2)**, 475 (1971).
202. Bostandzhiyan S.A., Boyarchenko V.I., Zhirkov P.V., Zinenko Zh.A., *Zh. prikl. mekhaniki i tekhn. fiz.* (**1**), 130 (1979).
203. Malkin A.Ya., Sherysheva L.T., Kulichikhin S.G., Zhirkov P.V., *Polym. Eng. Sci.*, **23(15)**, 805 (1983).
204. Grishin A.M., Nemirovskii V.B., Panin V.F., *Zh. prikl. mekhaniki i tekhn. fiz.* (**1**), 72 (1985).
205. Vaganov D.A., *Ibid.*, (**1**), 96 (1984).
206. Malkin A.Ya., Zhirkov P.V., *Polym. Proc. Eng.*, **2(213)**, 207 (1984).
207. Malkin A.Ya., Ehnenshtein G.A., e.a., *Teor. osnovy khim. tekhn.*, **20(3)**, 344 (1986).
208. Malkin A.Ya., Lavochnik Yu.B., Beghishev V.P., *Polym. Proc. Eng.*, **1(1)**, 71 (1983); **2(1)**, 27 (1984).
209. Malkin A.Ya., Kulichikhin S.G., Ivanova S.L., Korchagina M.A., *Vysokomol. soed.*, **22A(1)**, 165 (1980).
210. Malkin A.Ya., Ivanova A.N., Ivanova S.L., Andrianova Z.S., *Inzh. fiz. zh.*, **34(4)**, 636 (1978).
211. Berlin A.A, Volfson S.A., Enikolopyan N.S., *Kinetics of Polymerization Processes*, Khimiya, Moscow (1978) - in Russian.
212. Polyakov K.K., Paima V.I., *Technology and Equipment for Producing Powder Polymeric Coatings*, Mashinostroyenie, Moscow (1972) - in Russian.
213. Kamenev E.I., Myasnikov G.D., Platonov M.P., *Applications of Plastic Materials: Reference book*, Khimiya, Leningrad (1985) - in Russian.
214. Belyi V.A., Dovgyalo V.A., Yurkevich O.R., *Polymeric Coatings,* Nauka i tekhnika, Minsk (1976) - in Russian.
215. Vandenburg A.K., Piliposyan P.M., *Electrochemical Spraying of Installation*, Energoatomizdat, Moscow (1984) - in Russian.
216. Karyakina M.I., Poptsov V.E., *Technology of Polymeric Coatings*, Khimiya, Moscow (1983) in Russian.
217. Yakovlev A.D., *Chemistry and Technology of Varnish Coatings,* Khimiya, Leningrad (1981) - in Russian.
218. Sorokin M.F., Kochnova Z.A., Shode L.G., *Chemistry and Technology of Film Forming Compounds,* Khimiya, Moscow (1989) - in Russian.
219. Alekseev A.G., Kornev A.E., *Magnetic Elastomers,* Khimiya, Moscow (1987) - in Russian.
220. Moiba O.V., Krainova O.N., *Varnishing Materials and Their Applications*, (1), 31 (1991).
221. Tartakovskaya A.M., Nikolaeva G.G., Levitan N.A., *Ibid.*, (**3**), 25 (1990).
222. Mayofis I.M., *Ibid,* (**1**), 18 (1989).
223. *USSR Inventor's Certificate*, **240796**, *GB Patent*, **1094907**, *Fr. Patent*, **1455649**.

267. Castro I.M., Macosko C.W., Gritchfield F.E., Steinly E.S., Takett L.P., *J. of Elastomers and Plastics*, **12**, 3 (1980).
268. Connor J.J., Brebbia C.A., *Finite Element Techniques for Fluid Flow*, Newnes - Butterworths, London - Boston (1977).
269. Stevenson J.F., *Polym. Eng. Sci.*, **18(7)**, 577 (1978).
270. Richardson S.M., Pearson H.J., Pearson J.R.A. ,*Plastics and Rubber: Processing*, **5(2)**, 55 (1980).
271. Booy M.C., *Polym. Eng. Sci.*, **22(7)**, 432 (1982).
272. Spencer R.S., Gilmore G.D., *J. Colloid Sci.*, **6(1)**, 118 (1951).
273. Ballman R.L., Shusmun T., Toor H.L., *Ind. Eng. Chem.*, **51(7)**, 847 (1959).
274. Jackson G.B., Ballman R.L., *Soc. Plast. Eng. Journal*, **16(10)**, 1147 (1960).
275. Kamal M.R., Kenig S., *Polym. Eng. Sci.*, **12(4)**, 302 (1972).
276. Write J.L., Dee H.B., *Ibid.*, **14(3)**, 212 (1974).
277. Oda K., White J.L., Clark E.S., *Ibid.*, **16(8)**, 585 (1976).
278. Basov N.I., Lyubartovich V.A., Leonov A.I., Kazankov Yu.V., *Teoretich. osnovy khim. tekhnologii*, **7(1)**, 80 (1973).
279. Schmidt L.R., *Polym. Eng. Sci.*, **14(11)**, 797 (1974).
280. Schmidt L.R., *Ibid.*, **17(17)**, 666 (1977).
281. Gogos C.G., Huang C.-F., Schmidt L.R., *Ibid.*, **26(20)**, 1457 (1986).
282. Kruger W.L., Tadmor Z., *36th Annual Technical Conference Society of Plastics Engineers:* Technical Papers - Washington, P.87 (1978).
283. Sanou M., Chung B., Cohen C. *Polym. Eng. Sci.*, **25(16)**, 1008 (1985).
284. Coyl D.J., Blake J.W., Macosko C.W., *AIChE Journal*, **33(7)**, 1168 (1987).
285. Bhattacharji S., Savic P., *Proc. Heat Transfer Fluid Mech. Inst.*, 248 (1965).
286. Manzione L.T., *Polym. Eng. Sci.*, **21(18)**, 1234 (1981).
287. Amsden A.A., Harlow F.H., *J. Comput. Phys.*, **6**, 322 (1970).
288. Kim J.H., Kim S.C., *Polym. Eng. Sci.*, **27(16)**, 1243 (1987).
289. Manas-Zloczower I., Blake J.W., Macosko C.W., *Ibid.*, **27(16)** 1229 (1987).
290. Kamal M.R., Lafleur P.G., *Ibid.*, **22(17)** 1066 (1982).
291. Berezin I.K., Levina G.V., *Rheological Properties of Polymeric Systems,* Urals Brahch AN SSSR, Sverdlovsk, p.20 (1979).
292. Manzione L.T., Osinski I.S., *Polym. Eng. Sci.*, **23(10)**, 576 (1983).
293. Esteves S.R., Castro J.M., *Ibid.*, **24(6)**, 428 (1984).
294. Manas-Zloczower I., Macosko C.W., *Polym. Proc. Eng.*, **24(2-4)** 173 (1986).
295. Kolodzej P., Macosko C.W., Ranz W.E., *Polym. Eng. Sci.*, **22(6)** 385 (1982).
296. Castro J.M., Macosko C.W., Tackett L.P., Steinle E.C., Critchfield F.E., *Soc. Plast. Eng., Tech. Pap.*, **38**, 423 (1980).

SUBJECT INDEX